PROGRAM OF

The 107th Meeting of the Acoustical Society of America

Omni International Hotel Norfolk, Virginia 6-10 May 1984

MONDAY MORNING, 7 MAY 1984

EPPINGTON ROOM, 8:45 TO 11:55 A.M.

Session A. Noise I: Sound and Vibration Measurements at the Surface

Thomas H. Hodgson, Chairman

Center for Sound and Vibration, North Carolina State University, Raleigh, North Carolina 27695-7910

Chairman's Introduction-8:45

Invited Papers

8:50

A1. Application of the fiber optic lever in surface vibration and acoustic intensity measurements. Reginald O. Cook (National Institute of Environmental Health Science, P.O. Box 12233, Research Triangle Park, NC 27709)

Renewed interest in optic motion sensors has been prompted by the potential application of such techniques to surface vibration and acoustic intensity measurements. Optical sensors intrinsically possess one highly desirable attribute, that is, no loading of the structure, and possibly several others including high resolution and wide bandwidth. Of the available optic sensors, the fiber optic lever is perhaps the simplest practical approach. The characteristics of the fiber optic lever are such that the principal parameters, i.e., linear range, resolution, bandwidth, and working distance can be optimized to meet the constraints imposed by most surface vibration problems of interest. The key strategy in optimizing the lever is to obtain sufficient linear range to encompass low-frequency, high-amplitude vibrations while retaining sufficient resolution for small amplitude high-frequency motions. When sufficient reflected light is available to meet these requirements, wide bandwidth and excellent phase characteristics can be achieved by presently available electro-optic devices. The potential for a device permitting hand held "sweeps" of complicated noise radiators exists but is critically dependent on achieving extended linear range. The extent to which these requirements have been achieved in instruments optimized for acoustic intensity measurements close to the vibrating surface is described.

9:10

A2. Acoustic intensity measurements at the surface. Thomas H. Hodgson (Center for Sound and Vibration, North Carolina State University, Raleigh, NC 27695-7910)

A surface acoustic intensity meter is described for measuring acoustic intensity at a vibrating surface using a fiber optic lever as a displacement transducer and a condenser microphone to measure surface pressure. Digital signal processing using a two-channel FFT analyzer allows the calculation of surface intensity as a function of frequency. The technique has been tested in an anechoic chamber on a point monopole and a steel plate clamped at the edges. Calculated sound power levels are compared with results obtained by traditional techniques.

A3. Measurement of plate waves. Gunnar Rasmussen (Bruel & Kjaer, 18 Naerum Hovedgade, 2850 Naerum, Denmark)

Progressing waves in plates transport energy. The flow of energy will pass from the source of excitation to the damping mechanism. The flow may be measured using two accelerometers with a known spacing. The acoustic intensity flow, very near and parallel to the plate surface, follows closely the wave motion of the place. Theory of mechanical flow measurements in plates, and in the very near acoustic field, will be reported together with presentation of measurement results. The application of vibration intensity measurements is useful in the field of noise reduction as well as structural analysis. A4. Prediction of surface velocity of plate vibration using two microphones. Bjorn H. Forssen (Carrier Corporation, Syracuse, NY 13201) and Malcolm J. Crocker (Department of Mechanical Engineering, Auburn University, Auburn, AL 36869)

A theoretical derivation is presented for the spectral density of the acoustic velocity in terms of the autoand cross-spectral densities of the signals from two closely spaced microphones. This theory, a Fast Fourier Transform mini-computer, and a two-microphone probe, were used to measure the surface velocity of a vibrating flat panel. The surface velocity thus measured agrees quite well below the panel critical frequency with that measured by an accelerometer. Theory has also been developed to determine the difference between the sound pressure and intensity levels obtained with a two-microphone probe near to an arbitrary source distribution on a surface. The application of this theory to a point source and a rectangular radiator is discussed. An error analysis for these simplified cases is presented.

Contributed Papers

10:25

A5. Studies on acoustical field of vibrating pistons, J. K. Jiang and M. G. Prasad (Department of Mechanical Engineering, Stevens Institute of Technology, Castle Point, Hoboken, NJ 07030)

Studies on acoustic radiation from vibrating structures is of importance in machinery noise control. This paper reports studies on both the acoustical near and farfields of vibrating pistons. The boundary integral equation (BIE) method based on the Helmholtz integral formulation has been used. Three types of pistons are investigated: (1) a circular piston in an infinite baffle (baffled piston), (2) a circular piston at one end of a semiinfinite rigid pipe (enclosed piston), and (3) a finite thickness piston in space (free piston). The studies are aimed at investigating the boundary effects of the baffle, effect of the piston thickness, and directivity patterns in both acoustical near and farfields. The results from the BIE method are compared with the available classical results such as from the Rayleigh integral. The comparison of the results for the case of the baffled piston is very good in both near and farfield. It is intended that this method will be useful in investigating the acoustical fields of vibrating structures including the boundary effects. [Work supported by IBM Corporation, Poughkeepsie, New York.]

10:40

A6. Silator: A small volume resonator. E. Laudien and O. Bschorr (Messerschmitt-Bölkow-Blohm GmbH, Central Laboratories, BT 22, P.O. Box 80 12 20, 8000 Munich 80, West Germany)

The paper presents an experimental and analytical study of a newly developed small volume resonator element-called Silator-which can be used for sound attenuation wherever a free air passage is required. A Silator consists of two metal diaphragms-shaped like flat calotteswhich are joined together to form a single element. The enclosed space is evacuated. The diaphragm represents a spring-mass system which allows very low spring constants due to its nonlinear spring characteristic. Consequently, the resonance frequency of the system depends only on the shape of the Silator and not on its volume. The acoustic impedance becomes a minimum at resonance and can-depending on the amount of Silator damping-reach values which are lower than the characteristic impedance of air. An array of properly spaced Silators with preselected resonance frequencies constitutes an acoustic screen which nevertheless allows free airflow through it. Presented experimental data of Silators in intake and exhaust systems shows that noise reductions of more than 10 dB are obtainable not only for discrete frequencies but also for broadband noise.

10:55

A7. On validity of *in situ* sound intensity estimation. Gopal P. Mathur (Structural Dynamics R & D, Beech Aircraft Corporation, 9709 E. Central Avenue, Wichita, KS 67201)

In many noise control engineering applications, estimation of sound intensity in the nearfield of sound source under *in situ* measurement conditions is of considerable importance. This paper presents an analytical examination of statistical errors involved in estimation of sound intensity variables under *in situ* conditions. In view of the recent development of a stochastic theory for sound intensity method [G. P. Mathur, J. Acoust. Soc. Am. 74, 1752–1756 (1983)], results are first obtained for the new stochastic estimation procedures and a comparison is then made between finite difference based estimation procedures and stochastic estimation procedures of evaluating sound intensity variables. It is shown that unbiased *in situ* sound intensity estimates can be obtained from the two-microphone intensity probe conform to those typical of plane wave, periodic, or nonperiodic type stochastic processes. On the basis of results presented in this paper, a new stochastic criterion is thus evolved to check whether there will be significant errors in measuring sound intensity in a practical sound field.

11:10

A8. A model for the cross spectra between pressure and temperature downstream of a combustor. J. H. Miles and E. A. Krejsa (NASA Lewis Research Center, 21000 Brookpark Road, Cleveland, OH 44135)

Recently, measurements of pressure-temperature cross spectra were made in a duct downstream of a combustor to provide additional information beyond that available from pressure spectra and cross spectra measurements so that an appropriate source region model could be selected and to provide information on the physical mechanisms active at the combustion noise source. The model developed to interpret the measurements is presented and compared with the data. The results show good agreement with the data.

11:25

A9. Noise transmission loss of a rectangular plate in an infinite baffle. Louis A. Roussos (NASA Langley Research Center, Mail Stop 463, Hampton, VA 23665)

An improved analytical procedure has been developed that allows for an efficient solution of the finite plate noise transmission problem. The plate is modeled with classical thin plate theory and is assumed to be simply supported on all four sides. The incident acoustic pressure is modeled as a plane wave impinging on the plate at an arbitrary angle of incidence. Assuming the radiation damping is negligible compared to the structural damping, the incident, reflected, and transmitted pressures are approximated by the blocked pressure which allows the plate vibrations to be calculated by a normal-mode approach. A Green's function integral equation is used to link the plate vibrations to the transmitted farfield sound waves. The incident and transmitted acoustic powers are calculated by integrating the incident and transmitted intensities over their appropriate areas, and transmission loss is calculated from the ratio of incident to transmitted acoustic powers. The result is a versatile research and engineering analysis tool that not only enables the determination of which modes are dominating the noise transmission, but also allows for the problem to be broken down into its composite parts. This includes determining what the modal behavior is, such as, coupling between the incident noise and the plate vibrations; the plate resonance behavior; and the coupling between the plate vibrations and the transmitted noise. The effect of varying the angle of incidence and the farfield directivity can also be determined from the analytical model. The analysis approach was developed to study propeller noise transmission into aircraft and is seen to be equally applicable to sound transmission through building walls, floors, and windows.

11:40

A10. Effect of turbulent boundary layer flow on measurement of acoustic pressure and intensity. Gerald C. Lauchle (Applied Research Laboratory, The Pennsylvania State University, Post Office Box 30, State College, PA 16804)

Acoustic measurements performed with pressure sensors (microphones and hydrophones) can be subject to error if the sensors are in contact with a turbulent boundary layer flow. These errors are a result of the random pressure fields (flow noise) generated by the turbulent motions of the fluid. In this paper, a simple analysis is given whereby the flow noise response of a pressure sensor placed in a turbulent boundary layer flow can be estimated. If the purpose of the sensor is to measure the sound emitted from a source outside of the turbulent boundary layer, then a bias error for the measurement can be calculated. The error formula is equally applicable to intensity measurements made with the two-sensor technique, providing the mean flow Mach number is small. Example calculations are presented. [Work supported by NAVSEA 63R-31.]

MONDAY MORNING, 7 MAY 1984

GREENWAY ROOM, 9:00 TO 11:35 A.M.

Session B. Physical Acoustics I: Hyperthermia

Floyd Dunn, Chairman

Bioacoustics Research Laboratory, University of Illinois, 1406 W. Green Street, Urbana, Illinois 61801

Chairman's Introduction-9:00

Invited Paper

9:05

B1. Cell biology effects of ultrasound and microwave hyperthermia. Peter M. Corry (Department of Physics, University of Texas System Cancer Center, Houston, TX 77030)

Hyperthermia, or elevated temperature in the 41 °C to 50 °C range, in cancer treatment has been the subject of intense renewed interest over the past decade. This interest has come about primarily for three reasons: (1) conventional therapies such as ionizing radiation and chemotherapy have failed in several disease categories, (2) historical anecdotal reports of tumor responses after episodes of fever, and (3) the development of instrumentation systems for the controlled and reproducible administration of tumor temperature elevation such as ultrasound and microwaves. Until recently it was thought that cancer cells possessed an intrinsic sensitivity to these elevated temperatures, however, application of the ever more sophisticated techniques of modern cellular and molecular biology have demonstrated that solid tumor physiological factors, such as a lowered pH and nutrient deprivation appear to be the responsible factors rather than the transformation to malignancy. Other studies have demonstrated that hyperthermia can also result in dramatic enhancement of the more conventional therapies in addition to the heat-induced cytotoxicity. This latter enhancement comes about by the alteration of membrane permeabilities and the inhibition of subcellular repair mechanisms and in some cases, both effects. These observations have led to several studies to develop possible advantages of the various methods of tumor temperature elevation, however no specific effects of either ultrasound or microwaves have been documented other than those attributed to the elevation of tissue temperatures. [Supported in part by CA-17891 and CM-17524 from the NCI.]

Contributed Papers

9:50

B2. Ultrasonically produced hyperthermia in ophthalmology. Frederic L. Lizzi, Jack Driller, Michael Ostromogilsky, Angel Rosado (Riverside Research Institute, New York, NY 10036), D. Jackson Coleman, and Joan Torpey (Department of Ophthalmology, Cornell University Medical Center, New York, NY 10028)

A series of related experimental and theoretical studies have been conducted on lesions produced in various structures of the eye by ultrasonically induced hyperthermia. Results obtained in animal eyes have been used to plan clinical treatments of various diseases. Clinical treatments of medically nonresponsive glaucoma are now in progress, and an 81% success rate has been achieved. This paper will review a theoretical model of ultrasonically induced hyperthermia. The model has been applied to the study of lesions produced in thin ocular layers by focused beams exhibiting various frequencies and beamwidths. Empirical corrections for blood flow cooling have been incorporated using data reported for related laser experiments. The model has successfully predicted the threshold values and sizes of experimental chorioretinal and scleral lesions that are useful in treating ocular disorders. In addition, the paper will describe ultrasound and thermal parameters that have been used successfully in treating human tumor transplants in nude athymic mice. [Work supported by NIH.]

10:05

B3. Thermal dosimetry studies in ultrasonically induced hyperthermia in normal dog brain and in experimental brain tumors. Richard H. Britt, Douglas W. Pounds, Jeffrey S. Stuart, and Bernard E. Lyons (Division of Neurosurgery R155, Stanford University School of Medicine, Stanford, CA 94305)

S3

In a series of 24 acute experiments on pentobarbital anesthetized dogs, thermal distributions generated by ultrasonic heating using a 1-MHz PZT transducer were compared with intensity distributions mapped in a test tank. Relatively flat temperature distributions from 1 to 3 cm have been mapped in normal dog brain using "shaped" intensity distributions generated from ultrasonic emission patterns which are formed by the interaction between compressional, transverse, and flexural modes activated within the crystal. In contrast, these same intensity distributions generated marked variations in three malignant brain tumors presumably due to variations in tumor blood flow. The results of this study suggest that a practical clinical system for uniform heating of large tumor volumes with varying geometries is not an achievable goal. Our laboratory is developing a scanning ultrasonic rapid hyperthermia treatment system which will be able to sequentially heat small volumes of tumor tissue either to temperatures which will sterilize tumor or to a more conventional thermal dose. [Supported by NIH/NCI CA29731.]

10:20

B4. Application of a nonlinear layered model to hyperthermia. Michael E. Haran (Office of Science and Technology, National Center for Devices and Radiological Health, Rockville, MD 20857) and Peter A. Lewin (Department of Electrical and Computer Engineering, Drexel University, Philadelphia, PA 19104)

The use of ultrasound as a heating modality in cancer therapy gives rise to the need for delivering prescribed exposures of high-intensity ultrasound to deep tissue volumes. It is known that the attenuation coefficient of nonlinear media depends upon the local acoustic pressure amplitude for a given fundamental frequency. It is also known that such anomalous effects occur at biomedical frequencies and intensities [e.g., E. L. Carstensen *et al.*, Acustica **51**, 116–123 (1982) and F. Dunn *et al.*, Br. J. Cancer **45**, 55–58 (1982)]. In this presentation a series algorithm [M. E. Haran and B. D. Cook, J. Acoust. Soc. Am. **73**, 774–779 (1983)] is applied to study the propagation of plane finite amplitude waves through multiple layered media. It is shown that in some cases harmonic distortion and the resulting anomalous attenuation are sufficient to reduce the heat generation to a large degree. It is hoped that this elementary model will aid in the development of more effective acoustic sources and exposure protocols.

10:35

B5. Hyperthermia: Its role in the production of tissue damage induced by high intensity focused ultrasound. Michael J. Borrelli^(a) and Floyd Dunn (Bioacoustics Research Laboratory, University of Illinois, 1406 W. Green Street, Urbana, IL 61801)

Tissue damage resulting from irradiation of adult cat brain with varying exposure of focused 1-MHz, 300-W/cm² intensity ultrasound was examined with electron and light microscopy, and thermocouples were used to record the ultrasonically induced temperature changes. Identical exposures produced both more tissue damage and a higher peak temperature in white than gray matter. Cultured BHK cells were heated at temperatures corresponding to the peak temperatures recorded by the tissueembedded thermocouples. Electron microscope observations of the heated cells revealed that for temperatures less than 57 °C, the heating time required to elicit morphological changes was significantly longer than the ultrasonic exposure times which produced an identical peak temperature yet induced tissue damage within the cat brain. These results suggest that tissue damage resulting from the ultrasonic exposures shorter than 3-4 s was not strictly the result of the ultrasonic hyperthermia. The degree of hyperthermia apparently does, however, influence the degree of tissue damage, as evidenced by the differences observed between the damage in identically irradiated white and gray matter. [Supported in part by NSF and NIH.] * Present address: Radiation Oncology Res. Lab., Univ. of California, CED-200, San Francisco, CA 94143.

10:50

B6. The role of hyperthermia and cavitation in production of hind limb paralysis in ultrasonically irradiated mouse neonates. M. J. Borelli,^{a)} L. A. Frizzell, and F. Dunn (Bioacoustics Research Laboratory, University of Illinois, Urbana, IL 61801)

The third lumbar region of the neonatal mouse spinal cord was irradiated with 1-MHz ultrasound using intensities between 46 and 289 W/ cm² at hydrostatic pressures of 1 and 16 atm. It was previously reported that the threshold exposure duration necessary for production of hind limb paralysis of the neonates increased with hydrostatic pressure at 289 W/cm² but not at the lower intensities, although subharmonic and harmonic signals were observed at all intensities [Frizzell et al., J. Acoust. Soc. Am. 74, 1062-1065 (1983)], suggesting that acoustic cavitation is involved at 289 W/cm². Examination with electron and light microscopy reveals that permanent paralysis is always accompanied by altered spinal cord morphology and that the minimum tissue damage is altered synaptic morphology similar to that observed in the cat brain [Borrelli et al., J. Acoust. Soc. Am. 69, 1514-1516 (1981)]. Tissue damage was greatest at the perimeter of the spinal cord, possibly as a result of higher temperatures resulting from heat conduction from the more highly absorbing spinal column. This suggests that hyperthermia plays a role in development of tissue damage even when another mechanism is involved. [This work was supported in part by grants from the NSF and the NIH.] * Present address: Radiation Oncology Laboratory, Department of Radiation Oncology, University of California, CED-200, San Francisco, CA 94143.

11:05

B7. Radiation forces between small particles in a sound field. Wesley L. Nyborg (Department of Physics, University of Vermont, Burlington, VT 05405)

When ultrasound propagates through an aqueous suspension of particles, radiation forces exist between neighboring particles. This is a phenomenon of biophysical interest because, in suspensions of biological cells, it leads to aggregation of the cells into lines or sheets under some conditions. Considering a pair of identical spherical particles whose separation distance r is small, it is found that the interaction force can be expressed as $-\nabla W$, where W is a scalar function, which may be called the "acoustic interaction energy" for the pair. This energy is proportional to r^{-3} and to $(3 \cos^2 \phi - 1)$, where ϕ is the angle between the line of centers and the line along which motion occurs in the local ambient sound field. Also W is proportion to $a^6 u_{0}^2$, where u_0 is the acoustic velocity amplitude and a is the particle radius. A criterion for aggregation can be arrived at by setting a characteristic value of W equal to the thermal energy kT, as was done by Schwan in treating pearl-chain formation by electromagnetic waves. [Supported by NIH grant GM-08209.]

11:20

B8. Assessment of vibrational effects by ultrasound on biological targets at low temperatures Douglas E. Himberger, George L. Malinin, and Walter G. Mayer (Department of Physics, Georgetown University, Washington, DC 20057)

Biomedical applications of ultrasound are generally regarded to be reasonably safe. However, under certain conditions, the functional and structural integrity of biological targets can be severely impaired by ultrasound. Tissue damage by insonication can be brought about concurrently by thermal and by vibration-induced mechanisms. Whereas thermal effects have been characterized extensively, virtually nothing is known about vibration-induced damage. The problem is compounded by practical impossibility of separating the two effects at ambient temperatures. In order to assess only vibrational effects of ultrasound we have developed and tested a system for insonication of biological targets at 77 °K in liquid nitrogen. Isolated human erythrocyte membranes (ghosts) frozen in the presence of 10% dimethysulfoxide (DMSO) in phosphate buffered saline (PBS) were irradiated with ultrasound ranging in frequency from 3 to 7 MHz and intensities between 2 and 24 mW/cm². Thawed control and insonicated ghosts were then analyzed by sodium dodecylsulfate (SDS)polyacrylamide gel electrophoresis for changes of membrane protein components. Preliminary results are presented. [Work supported in part by the Office of Naval Research, U.S. Navy.]

Session C. Speech Communication I, Physiological Acoustics I, Psychological Acoustics I: Hearing Impairment

G. Richard Price, Chairman

U. S. Army Human Engineering Laboratory, Aberdeen Proving Ground, Maryland 21005

Chairman's Introduction-9:00

Contributed Papers

9:05

C1. Effects of filtering and hearing impairment on sensitivity to cues to initial stop voicing. Quentin Summerfield, Brendan Barker (MRC Institute of Hearing Research, University Park, Nottingham NG7 2RD, United Kingdom), Stewart Gatehouse, and George G. Browning (MCR Institute of Hearing Research, Southern General Hospital, Glasgow, United Kingdom)

The perception of stop voicing is relatively resistant to noise, filtering, and hearing impairment, partly because voicing cues are subsumed by robust amplitude patterning at low frequencies, but possibly also because listeners can compensate when listening is difficult by increasing the weight given to those cues that are audible. We measured the amount by which changes in F1, F0, aspiration amplitude, and syllable duration shifted the VOT boundary on a 'dole-toll' series bandlimited to 0-4250 Hz. Where σ_{μ} and μ_{μ} are the mean and standard deviation underlying the sigmoidal best fit to the identification function with value i of cue j, sensitivity was defined as $(1/\sigma_{ij})$ to VOT and otherwise as $[(\mu_{1j} - \mu_{2j})/(\sigma_{1j}^2 - \sigma_{2j}^2)^{1/2}]$. Compared to normal broadband performance, listeners with normal hearing (n = 12) showed increased sensitivity to F0 and F1 following abrupt low-pass filtering at 1600 Hz, demonstrating that compensation can occur. In contrast, overall, listeners with high-frequency sensorineural losses (n = 10) showed a reduction in sensitivity to VOT, but no change in sensitivity to the secondary cues. For some impaired listeners, reduced sensitivity to VOT allowed secondary cues to surpass the effect of VOT, demonstrating their potential for maintaining stable performance when cues co-vary naturally.

9:20

C2. The effects of duration adjustments of preceding vowels on fricative voicing perception by hearing-impaired listeners. S. G. Revoile, L. D. Holden-Pitt, and J. M. Pickett (Sensory Communication Research Laboratory, M. T. Building, Gallaudet College, Washington, DC 20002)

For /bæf/, /bæv/, /bæs/, and /bæz/, perception of the fricative voicing distinction was studied for 25 moderately to profoundly hearing-impaired undergraduates. The purpose was to discover whether some listeners might benefit from enhancement of the duration cue in the preceding vowel. Identification was tested for ten utterances of each syllable. These utterances were presented unedited or with their vowels adjusted for duration. The utterances of /bæf/ versus /bæv/ and /bæs/ versus /bæz/ had been selected to differ in the degree of contrast for the vowel duration cue. The unedited utterances best-perceived for fricative voicing contained vowels that were the most salient for the duration cue. The durations of these vowels were exemplars to be approximated among the other utterances that were adjusted for vowel duration. For /bæf/, and /bæs/ utterances, the vowels were shortened through pitch-period deletions; the adjusted /bæv/ and /bæz/ utterances contained vowels lengthened via iterated pitch periods. Preliminary analyses revealed that the utterances with duration-adjusted vowels yielded substantially improved fricative voicing perception for 15 of the listeners. The other listeners showed minimal changes in performance between the unedited versus vowel-adjusted syllables. These were listeners whose perception for the unedited syllables was either very good or very poor.

9:35

C3. Spectral tilt and burst duration as determinants of stop consonant identification accuracy for hearing-impaired listeners. Michael F. Dorman, Julie M. Lindholm, and Maureen Hannley (Departments of Speech & Hearing Science and Psychology, Arizona State University, Tempe, AZ 85287)

In a series of experiments we have manipulated the tilt of the onset spectrum and duration of the release burst in syllables with initial voiced stop consonants. In identification tests we have found that normal hearing listeners are largely unaffected by abnormal tilt or burst duration. Hearing-impaired listeners, on the other hand, are significantly affected. We speculate that when moderately and severely hearing-impaired listeners achieve normal recognition accuracy for stop consonants, they do so by giving greater-than-normal perceptual weight to the information provided by burst duration and spectral tilt. The results of identification tests in listeners with congenital severe to profound sensorineural hearing impairments are consistent with our speculation.

9:50

C4. Perception of vowels produced by the hearing impaired. Judith Rubin-Spitz (Graduate Center, C. U. N. Y., Speech and Hearing Sciences, 33 W. 42nd Street, New York, NY 10036)

Hearing and hearing-impaired talkers were compared with respect to the information used by listeners in decoding their vowels. Each vowel was produced in a fixed consonant context (/bVb/) within a carrier phrase. Experienced and inexperienced listeners were asked to identify the vowel and the hearing status of the talker when provided with the entire sentence, with the /bVb/ word only, or with a gated steady state vowel segment. Although there were no significant differences between sentences and words, there were between words and gated vowels. Results suggest, however, that listeners use the same acoustic sources of information in decoding vowels produced by the two groups of talkers. While the ability to identify the hearing status of the talker decreased as a function of condition, performance in the gated vowel condition was significantly above chance. There were no significant differences between experienced and inexperienced listeners in any perceptual task. Results are discussed in terms of current theories regarding the underlying deviant nature of speech production by the hearing impaired. [Work supported in part by NIH Grants NS-17764, NS-13617 and HD-01994, and also by C. U. N. **Y.1**

10:05

C5. Suppression within frequency regions of normal and impaired hearing. Daniel L. Weber (Boys Town National Institute, 555 North 30th Street, Omaha, NE 68131)

In psychophysical experiments, the reduction in the effect of one stimulus (the masker) due to the addition of a second stimulus (the suppressor) is attributed to the suppression of the masker by the suppressor. Kramer [reported by F. L. Wightman, T. McGee, and M. Kramer, in *Psychophy*sics and *Physiology of Hearing*, edited by E. F. Evans and J. P. Wilson (Academic, London, 1977)] measured "unmasking patterns" (signal threshold as a function of suppressor frequency) in listeners with highfrequency hearing loss. Although he observed normal suppression effects in a region of normal hearing, he found no evidence of suppression in regions of impaired hearing. One factor which might have contributed to this failure was an unlucky selection of the suppressor level. This experiment compares the effect of suppressor level in normal and hearing-impaired frequency regions. Thresholds for 10-ms signals (10-ms, cosinesquared ramps with no steady state) were obtained for signals at 1 and 4 kHz forward masked by 300-ms, narrow-band (50-Hz-wide) noise maskers centered at the signal frequencies. Masker levels were 50 and 70 dB (total noise power), respectively. Suppressor levels varied from 30 to 90 dB SPL; suppressor frequencies were 0.7 kHz for the 1-kHz masker and 2.8 and 5.0 kHz for the 4-kHz masker. As observed by Kramer, suppression effects appear to be absent in regions of hearing impairment. However, in this experiment, this absence does not appear to be correlated with an absence of a difference between simultaneous and forward masking. [Research supported by grants from NSF and NIH.]

10:20

C6. Hearing impairment and the masking-level difference in wideband and narrow-band masking noise. Joseph W. Hall (Department of Communicative Disorders, Northwestern University, 303 E. Chicago Avenue, Chicago, IL 60611), Mark P. Haggard, and Anthony D. G. Harvey (MRC Institute of Hearing Research, Nottingham, England)

The masking-level difference (MLD) was investigated for normalhearing and cochlear hearing-impaired listeners. A 500- or 2000-Hz signal was detected in wideband noise (spectrum level 50 dB/Hz) and in a 50-Hz-wide noise around the signal frequency (spectrum levels of 50 and 60 dB/Hz). At 500 Hz the hearing-impaired listeners had appreciably smaller MLDs than normal in wideband noise, but normal MLDs in narrow-band noise. At 2000 Hz, the only condition in which the impaired group had abnormally small MLDs was the narrowband noise condition at the 50-dB/Hz noise spectrum level. The diagnostic and theoretical implication of these results will be discussed.

10:35

C7. Intensity and duration effects in pure-tone frequency discrimination with normal-hearing and hearing-impaired listeners. Richard L. Freyman^{e)} and David A. Nelson (University of Minnesota, 2630 University Avenue SE, Minneapolis, MN 55414)

Moore [J. Acoust. Soc. Am. 54, 610-619 (1973)] has suggested that under the assumptions of a place or excitation-pattern theory of frequency discrimination, frequency DLs should be dependent on auditory excitation-pattern slopes only for long-duration tones with spectral slopes that are steeper than those of the excitation pattern. Otherwise, according to this theory, it is the slopes of the stimulus spectrum that limit the frequency DL. In this paper, we extend these ideas to evaluate the prediction that for very short, spectrally broad tones, frequency DLs obtained from hearing-impaired subjects should not differ systematically from those obtained from normal-hearing listeners. Frequency DLs were obtained as a function of intensity at 500, 1000, and 2000 Hz for 5- and 300-ms pure tones in normal-hearing and moderately hearing-impaired subjects. The DLs obtained from hearing-impaired subjects were larger than normal for long-duration but not short-duration pure tones; these results are consistent with the predictions of the excitation-pattern theory. However, an unexpected but consistent finding of nonmonotonic frequency DL-intensity functions in the 5-ms condition in normal-hearing subjects complicates interpretations of the results. * Present address: University of Massachusetts, Dept. of Communication Disorders, Amherst, MA 01003.

C8. Model for threshold shift following intense exposures. G. Richard Price (U. S. Army Human Engineering Laboratory, Aberdeen Proving Ground, MD 21005)

Hearing loss experiments with impulse noises at high intensities typically produce threshold shifts that have an extremely high variability. Price [Hearing and Other Senses: Presentations in Honor of E. G. Wever, edited by Fay and Gourevitch (Amphora, Groton, 1983), Chap. 20, pp. 335–346] proposed that at high intensities, loss was essentially mechanical in origin and that its growth might be a function of the number of stress cycles times the mechanical stress raised to a power. A model was constructed to embody this relationship as well as a normally distributed threshold of sensitivity to damage. Given a standard deviation of about 8 dB for the sensitivity and a power of 2 for the stress exponent, the model produces threshold shifts that look like those seen with both human and animal subjects exposed to intense impulses.

11:05

C9. Developmental and genetic differences of susceptibility to noise trauma. Kenneth R. Henry (Department of Psychology, University of California, Davis, CA 95616)

Mice of two genotypes were exposed, at one of eight ages, to 2 min of a 124-dB SPL, 8–16 kHz octave band noise. In both genotypes threshold shifts (TS) of evoked cochlear microphonics (CM) and action potentials (AP) were not observed when exposure occurred at 12 days of age, were maximal in 30–36 day exposed mice, and declined with increasing age. TS was greater for AP than for CM, with higher frequencies most severely affected. CBA mice were more severely affected than C57BL/6 mice. In CBA mice, susceptibility to TS paralleled susceptibility to acoustic priming for audiogenic seizures. Exposure at 30–36 days had no immediate observable behavioral effect. But re-exposing these mice 5 days later caused them all to convulse, with 87% of them dying. In contrast, susceptibility to acoustic priming for the C57BL/6 peaked sharply at 18 days of age, not corresponding to its age of peak cochlear susceptibility. Genetically determined differences of auditory brainstem function were hypothesized to account for these strain differences.

11:20

C10. Hearing losses in mongolian gerbil after 300 days of continuous exposure to noise. John H. Mills, Richard A. Schmiedt, and Larry F. Kulish (Department of Otolaryngology and Communicative Sciences, Medical University of South Carolina, Charleston, SC 29425)

As part of a large, long-term study of noise-induced hearing loss, presbyacusis, and the interactions of the two, groups of mongolian gerbils are being exposed for their entire life to a wideband noise. The A-weighted sound pressure level is 85 dB. Control groups are being raised in an acoustic environment where the average sound level is less than 35 dBA. Hearing is estimated from electrical potentials arising from the auditory nerve and brainstem and recorded with noninvasive electrodes. Now, we report results from a pilot group of gerbils during the course of 300 days of continuous exposure to noise. Estimated threshold shifts were largest, about 40 dB, between 2 and 8 kHz and decreased at lower and higher frequencies. Threshold shifts at 4.0 and 8.0 kHz did not appear to increase (\pm 5 dB) between 30 and 300 days of exposure whereas at other test frequencies threshold shifts increased by as much as 20 dB between 60 days and 180 days. Aging control animals appear to develop hearing losses first at 16 and 20 kHz whereas noise-exposed animals develop their hearing losses first at 4 and 8 kHz. [Work supported by NIEHS.]

The present study was designed to contribute information on kinematic details of the glottal abduction-adduction gesture in voiceless conso-

nant production. Transillumination was used to record glottal move-

ments. The linguistic material consisted of multiple repetitions of dental

stops and fricatives which differed in stress and were spoken at two differ-

ent rates. Two native American English speakers served as subjects. As

expected, glottal opening was larger for fricatives than for stops. Prelimi-

Session D. Speech Communication II: Laryngeal Articulation and Voice

Thomas Baer, Chairman

Haskins Laboratories, 270 Crown Street, New Haven, Connecticut 06510

Chairman's Introduction-9:00

Contributed Papers

9:05

D1. Methods for using a noninvasive technique for estimating glottal functions from oral measurements. Eva Holmberg (Department of Communication Disorders, Boston University, 48 Cummington Street, Boston, MA 02215), Joseph Perkell (Laboratory of Electronics, Speech Communication, M. I. T., Cambridge, MA 02139), and Robert Hillman (Department of Communication Disorders, Boston University, 48 Cummington Street, Boston, MA 02215)

A noninvasive technique is used to make acoustic and aerodynamic recordings in an ongoing study whose goal is the objective assessment of vocal function in normal and dysphonic speakers. Intraoral pressure, oral volume velocity (flow), and radiated sound pressure are recorded for strings of repeated productions of the syllable /pae/. A high time resolution pneumothachograph is used to record flow [M. Rothenberg, J. Acoust. Soc. Am. 53, 1632-1645 (1973)]. Transglottal air pressure, glottal air flow, and sound power for the vowel are estimated from the oral measurements, and glottal resistance and vocal efficiency are calculated. Initial results suggest that production mode (smooth versus interrupted) and rate (slow versus fast) may affect the reliability of the aerodynamic measures. An interaction between production mode and rate can result in unreliable pressures on one hand and unreliable flows on the other. Results from a separate, methodological study illustrate the importance of control over production mode and rate to obtain oral pressure and flow signals that allow for reliable estimates of glottal functions. [Work supported by The Voice Foundation.]

9:20

D2. Transillumination of the glottis during Hindi obstruents. R. Prakash Dixit (Department of Speech, Louisiana State University, Baton Rouge, LA 70803), Thomas Baer (Haskins Laboratories, 270 Crown Street, New Haven, CT 06510), and Kiyoshi Honda (Haskins Laboratories, 270 Crown Street, New Haven, CT 06510 and University of Tokyo, Tokyo, Japan)

The purpose of this study was to examine the degree of glottal opening and the temporal relationship between articulatory events and openingclosing gestures of the glottis during the production of Hindi obstruents which contain phonologically distinctive four manner categories of stops and affricates (voiceless unaspirated, voiceless aspirated, voiced unaspirated, and voiced aspirated) and two manner categories of fricatives (voiceless and voiced). To that end, we obtained glottograms, using transillumination technique, while a native speaker of Hindi produced disyllabic nonsense words of CVCVC form, where C was an obstruent and V was a high front unrounded vowel. All C positions in an individual word were occupied by the same obstruent. The vowel in the second syllable carried the stress. The glottograms, thus obtained, show a systematic relationship between articulatory events and opening-closing gestures of the glottis during various obstruents, which is fairly similar within the same category but quite dissimilar across different categories of obstruents. The degree opening also differs from one category of obstruents to another, however, within the same category of obstruents it is quite similar. The glottograms will be presented and discussed.

9:35

D3. Kinematic studies of laryngeal articulation. Anders Löfqvist^{a)} and Nancy S. McGarr (Haskins Laboratories, 270 Crown Street, New Haven, CT 06510)

⁸ nary kinematic results suggest a stable positive relationship between maximum displacement and peak velocity of glottal movements. That is, peak velocity of both abduction and adduction was positively correlated with peak glottal opening for both fricatives and stops. An increase in glottal opening was also associated with stress, with stressed voiceless consonants having a larger peak glottal opening than their unstressed counterparts. In general, peak velocity of glottal abduction was higher than that of glottal adduction. Results from laryngeal articulatory gestures are consistent with reports for other articulators. [Work supported by NINCDS and BRSG.] ^{al} Also Lund University, Sweden.
 ^{bl} **9:50 D4. Laryngeal adducation and tongue lowering movements in stopconsonant production.** Kevin G. Munhall and David J. Ostry (Department of Psychology, McGill University, Montreal H3A 1B1, Canada)

Phonetic segments are instantiated across the vocal tract as a whole and the various articulators that shape the production mechanism thus co-determine segmental properties. This requires that the activity of the speech articulators be related in a systematic fashion. Perhaps the simplest manner in which different articulators could be coordinated is by sharing some kinematic characteristics. The present study examines the similarities between tongue dorsum lowering and vocal fold adduction during the production of the intervocal stop consonant in a CVCVC. Lexical stress was manipulated with either the first or second vowel receiving the primary stress. The movements of the two articulators were measured separately within a single session with a computerized ultrasound system. Preliminary analyses indicate a similarity in the form of adjustment to the stress manipulation across the two articulators. The time to reach peak velocity was shorter for both articulators in the poststress context. Further, the movement onset times of the two articulators relative to oral implosion varied systematically with stress levels. The results are discussed in terms of inter-articulator timing.

10:05

D5. Active in vitro force-elongation response of canine vocalis muscle. Ingo R. Titze and Fariborz Alipour (Department of Speech Pathology and Audiology, University of Iowa, Iowa City, IA 52242)

Vocalis muscle tissue was dissected from live dogs and kept alive in Krebs-Ringer solution for several hours. The temperature of the tissue was maintained at approximately 37 °C by a circulating fluid around the sample holder. Force-elongation responses of the vocalis muscle under various levels of stimulated muscle activity were obtained through one-dimensional stretch and release. Both force and elongation were monitored electronically with a Cambridge Technology Dual Servo System (ergometer), while stimulation was applied to the muscle with fine-wire electrodes and a Grass stimulator. Families of force-elongation curves for various frequencies of stimulation and various relaxation times are given,

from which average elastic constants, such as Young's modulus, can be estimated. [Work supported by NINCDS.]

10:20

D6. Simulation of vocal fold tissue movement. Fariborz Alipour and Ingo R. Titze (Department of Speech Pathology and Audiology, University of Iowa, Iowa City, IA 52242)

A computer simulation for two-dimensional vibration of the vocal folds is presented. Free and forced oscillations are studied by imposing an impulse and time varying surface force. The solution is obtained by a semidiscrete numerical method. A finite element technique is used for the space-dependent solution and a Crank-Nicholson finite difference method is used for time integration. Horizontal and vertical displacements as a function of time, as well as x-y trajectories, are calculated for some points at the tip of fold. In addition, the response of the system due to a sinusoidally varying force was obtained and compared with experimental results of an excised larynx of similar loading. [Work supported by NINCDS.]

10:35

D7. Real-time extraction of vocal quality parameters from electroglottographic signals. Akira Hasegawa, James Mahshie, Eugene Herbert, Fred Brandt, Marguerite Mars, and James Pickett (Sensory Communication Research Laboratory and Department of Audiology, Gallaudet College, Washington, DC 20002)

This paper reports the second phase of our efforts to efficiently and effectively parametrize the electroglottographic (EGG) signal for monitoring and modification of deaf speech. The first phase [real-time extraction of the voice fundamental frequency (F0)] was reported at a previous meeting. Our EGG, pneumotachographic, and cinematographic observation of the vocal fold movement revealed systematic changes in the duration of the vocal fold contact with respect to characteristics of the individual movement cycle. Reduced contact typically reflects breathier voices, which are common among deaf speakers. The parameter extraction system under development consists of an EGG, a linear phase high pass filter, a custom-made signal conditioner/parameter extractor, and a PDP 11/ 34A computer. Additional hardware is used for display and storage of the extracted parameters. Details of the extraction scheme and the results of modification of vocal quality using the visual display will be presented. [Study supported by the National Institute of Handicapped Research and the Gallaudet Research Institute.]

10:50

D8. The validity of using phonatory jitter to detect laryngeal pathology. Christy L. Ludlow, Celia J. Bassich (Speech Pathology Unit, IRP-NINCDS, Bldg. 36, Rm. 5A-15, Bethesda, MD 20205), Young J. Lee (Office of Biometry and Field Statistics, NINCDS, Federal Bldg., National Institutes of Health, Bethesda, MD 20205), Nadine P. Connor, and David C. Coulter (Speech Pathology Unit, IRP-NINCDS, Bldg. 36, Rm. 5A-15, Bethesda, MD 20205)

A multiple regression model was developed to account for the variance in phonatory jitter among normal speakers and for predicting an expected jitter value and confidence interval for individual subjects. Jitter was measured with a system resolution capable of measuring a minimum perturbation of 2.15 μ s. Measures were made from maximum phonation lengths of 95 adults without laryngeal pathology. Seven factors were examined for contributions to the prediction of jitter: sex, age, smoking history, drinking habits, F_0 , vocal intensity, and length of phonation. A multiple correlation coefficient of determination of 97.6% was obtained for the normal subject pool with a three-factor model including: vocal intensity, F_0 and phonation length. For 20 patients with laryngeal pathology, individual predicted jitter values and 90% confidence intervals were computed using the normal regression model, for determining when patients' actual jitter values were outside of their expected confidence intervals. Only 30% of the patients with confirmed laryngeal pathology had jitter values outside of their predicted intervals, indicating that this measure would not be valid for use in screening for laryngeal pathology.

11:05

D9. Some relations between voice quality judgments and derived acoustic measurements. Robert A. Prosek, Allen A. Montgomery, Brian E. Walden, and David B. Hawkins (Army Audiology and Speech Center, Walter Reed Army Medical Center, Washington, DC 20307)

The use of extracted acoustic features as descriptors of abnormal voice quality was explored by correlating voice quality ratings with the measurements. Sixteen talkers with no history of speech problems and 52 talkers with documented laryngeal pathologies recorded the vowel / α / using their typical pitch and loudness. Estimates of the excitation for each vowel were obtained using the linear prediction technique of inverse filtering, and the acoustic measurements, known as residue features, were calculated from this waveform. Voice quality estimates were obtained from a panel of judges who rated each vowel on 11 voice quality scales that have been described in the literature. The residue features were used as predictors of average voice quality rating in multiple linear regression analyses. The results are discussed in terms of the voice quality scales that were used most reliably by the judges and the ability of the features to distinguish among various voice quality categories.

11:20

D10. Computer measurements of breathy voice quality. Peter Ladefoged and Norma Antonanzas (Phonetics Laboratory, Linguistics Department, UCLA, Los Angeles, CA 90024)

Most measures of phonation types analyze samples of steady-state vowels that last several seconds. Such segments do not occur in natural languages. The principle used in the current measure is that within a single period of a voiced speech sound, a waveform with no breathiness should be the same as the waveform produced by the previous glottal pulse. But when a sound is produced with a turbulent glottal flow there will be randomness. Hence an appropriate measure of breathiness is the variance of the difference between the points in a window with a length slightly less than one period and the points in the most similar window of equal length in one of the immediately following periods. The measure can be used on segments of speech lasting only about 150 ms. It is largely unaffected by the changes in glottal pulse frequency that correspond to the intonation, and by period to period jitter. The measure has been tested on two languages that use phonological contrasts dependent on the difference between breathy voice and modal (regular) voice. [Work supported by NINCDS.]

11:35

D11. Perceptual dimensions of dysphonic voices. Gail B. Kempster and Doris J. Kistler (Department of Communicative Disorders, Speech and Language Pathology, Northwestern University, 2299 Sheridan Road, Evanston, IL 60201)

The perceptual dimensions of dysphonic voices were derived through a multidimensional scaling algorithm (ALSCAL). Listeners responded to 1-s segments of the vowel / α / produced by 30 dysphonic female talkers in a triadic comparisons task. On each trial listeners were asked to select the two most similar stimuli. An acoustic analysis was performed to determine the fundamental frequency, intensity, pitch perturbation, amplitude perturbation, and harmonics-to-noise ratio of each vowel. The vowel stimuli were also rated by voice pathologists on six perceptual attributes (e.g., "breathiness"). Both the acoustic measures and the perceptual ratings were used to identify the dimensions of the perceptual space. Results are compared to a similar study by Murry, Singh, and Sargent [J. Acoust. Soc. Am. **61**, 1630–1635 (1977)]. D12. Fundamental frequency characteristics of deaf speakers. James Mahshie, Akira Hasegawa, Marguerite Mars, and Eugene Herbert (Sensory Communication Laboratory and Audiology Department, Gallaudet College, Washington, DC 20002)

Fundamental frequency (f0) characteristics of deaf speech appears to differ from normal, although the extent and nature of these differences is unclear. Fundamental frequency characteristics are dependent upon the way the speech sample is elicited (spontaneous or read). This study examined the /0 characteristics of 25 deaf and 10 normal-hearing adults during various speaking tasks, including spontaneous speech, oral reading, and declarative sentence and yes/no question production. Comprehensive descriptions of f0 were obtained by means of a computer based f0 measuring and analyzing system developed at Gallaudet College. These descriptions included: (1) f0 distribution, (2) measures of central tendency, (3) distribution variance, (4) estimates of f0 range, and (5) cycle-to-cycle f0 change. Results show that the f0 characteristics of the hearing-impaired subjects differed from normal, and that the hearing-impaired subjects tend to alter f0 characteristics among the different speaking tasks to a lesser extent than normal-hearing subjects. Implications of findings will be discussed. [Research supported by the National Institute for Handicapped Research and the Gallaudet Research Institute.]

D13. Investigating the voice quality dimension in Western Nilotic vowel harmony. Ian Maddieson (Phonetics Laboratory, Linguistics Department, UCLA, Los Angeles, CA 90024)

It has been suggested at least since 1936 (Tucker, 2nd International Congress of Phonetic Sciences, Cambridge) that the vowel harmony system in Western Nilotic languages includes a dimension of voice quality contrast. X-ray studies of Dho-Luo and Ateso have shown that there are generally differences in the superalaryngeal regions (e.g., in tongue height and/or pharyngeal volume) between vowels of the two vowel harmony sets. It has remained unclear whether these vowels are additionally distinguished by a voice quality difference between "hard" and "breathy" phonation types produced by different laryngeal settings. Techniques being developed at the UCLA Phonetics Laboratory for examining phonation types in natural languages have been applied to answering this question. These tend to confirm that there are differences in laryngeal setting, although this conclusion must remain tentative until these techniques are more fully developed and more data is available. [Work supported by NINCDS.]

MONDAY MORNING, 7 MAY 1984

CLAREMONT ROOM, 9:30 TO 11:50 A.M.

Session E. Musical Acoustics I: Tuning, Tones, and Technology

Edith L. R. Corliss, Chairman

Forest Hills Laboratory, 2955 Albemarle Street, N.W., Washington, DC 20008

Chairman's Introduction-9:30

Contributed Papers

9:35

E1. How loudly should you hear your colleagues and yourself? Sten Ternström and Johan Sundberg (Department of Speech Communication and Music Acoustics, Royal Institute of Technology (KTH), 100 44 Stockholm, Sweden)

A choir singer needs to hear both the sound of his/her own voice and the sound of the other choir members. If either of these signals becomes too loud, problems can be assumed to arise. The present study investigates the importance of the amplitude ratio between the sound of one's own voice and the sound of an external reference signal. Nine male choir singers were asked to sing in unison with synthetic reference vowel stimuli presented over earphones. In the earphones they also heard the sound of their own voice as picked up by a microphone in front of the mouth. The SPL of the reference stimuli was varied over a range of 40 dB, while the subjects were asked always to sing at a constant SPL, as indicated by a level meter. The fundamental frequency agreement between the reference and the subjects' responses was analyzed. The fundamental frequency of the responses depended strongly on the SPL of the reference in the case of the vowel /u/, presumably because of a pitch-amplitude dependence, which, however, was compensated for in the analysis. It was found that the fundamental frequency agreement between the reference vowels and the corrected responses was approximately constant over a dynamic range of 20 dB of the reference vowels. Outside this range, choir singers tended to fail in matching the pitch of the external reference.

9:50

E2. Critical band for frequency: A revision of the limits. J. Douglas Solowan (School of Music DN-10, University of Washington, Seattle, WA 98195) Numerous music acoustics and psychomusicology text books claim that it is not possible to hear the individual pitches when two simultaneous tones are separated by a half-step. Musicians, on the other hand, find that their day-to-day experience does not correspond well with this claim. Remarkably little research literature was found which tests this question in a musical situation. Because this task pits the information available in the frequency domain and that available in the time domain in opposition, it is important to determine who is right. The results of a test in which subjects used the method of adjustment to match a tone to either of two, simultaneous tones are presented. These subjects qualified to take the test by demonstrating fine-tune pitch matching ability to a single tone. In contrast to the previously accepted limit of frequency discrimination, the results indicate that the subjects were able to effectively analyze one of the pitches out of a two-tone stimulus whose frequencies were as little as onequarter step apart.

10:05

E3. Tonal scale step encoding and the recognition of octave-scrambled melodies. W. J. Dowling (Program in Human Development and Communication Sciences, UT/Dallas, Richardson, TX 75083-0688)

Octave-scrambled melodies, having their pitches randomly distributed over several octaves, are difficult to recognize. Such melodies do not preserve pitch-interval patterns of undistorted melodies, but only their sequences of chromas—that quality of pitch shared by tones an octave apart. It was shown previously [W. J. Dowling, J. Acoust. Soc. Am. Suppl. 1 64, S146 (1978)] that such melodies can be recognized if preceded by a title or a melody cue (an unscrambled version). Here melody cues preceded unfamiliar tonal or atonal, scrambled or unscrambled test melodies. Unscrambled repetitions of tonal melodies were easier to recognize than atonal ones for all subjects. Even inexperienced subjects encoded scale steps of tonal cue melodies more effectively than they encoded pitches of atonal cue melodies. Musically experienced (but not inexperienced) subjects found tonal scrambled melodies easier to recognize than atonal. Subjects apparently tested encoded cue patterns against chromas of comparison melodies. Experienced subjects used that information more effectively to evaluate the chroma patterns of octave-scrambled melodies.

10:20

E4. Rules for the performance of melodies. Origin, functions, purposes. Lars Frydén (Conservatory of the Swedish Radio, Edsberg, Sweden) and Johan Sundberg (Department of Speech Communication and Music Acoustics, Royal Institute of Technology (KTH), 100 44 Stockholm, Sweden)

In J. Acoust. Soc. Am. Suppl. 1 69, S103 (1981) a computer program was presented, which works as a musical version of a text-to-speech-conversion program. Thus, the input is the melody in musical notation, and the output is the melody played. The "pronunciation rules" in this program, which serve the purpose of improving the musical quality of the performance, have now been further developed. New rules have been formulated which work with a time window corresponding to one or several bars. In a formal test the musical effect of these rules have been approved by a group of professional musicians. The purpose and means of the rules are discussed. Some rules apparently serve the purpose of emphasizing unexpected notes or marking structural components of the melody such as chord shifts and phrases. The ways in which this is signaled in the performance often show a striking similarity with rules for speech suggesting that the rules refer to the listener's acquaintance with speech. Other rules seem to allude to the listener's previous experience of motion. In this way, the project seems to shed some light on some basic requirements for music communication.

10:35

E5. Synthesis of consonants in singing. Jan Zera (Chopin Academy of Music, Warsaw, Poland; guest researcher at the Department of Speech Communication and Music Acoustics, KTH, Stockholm, Sweden) and Johan Sundberg (Department of Speech Communication and Music Acoustics, Royal Institute of Technology (KTH), 100 44 Stockholm, Sweden)

In previous singing research hi-fi synthesis efforts have mainly aimed at long, sustained vowel sounds. The present paper reports on an attempt towards hi-fi synthesis of some consonants in singing. The synthesis is made by means of a formant synthesizer (MUSSE) complemented by two pole zero circuits, two noise generators, and a filter. Examples of the synthesis will be played.

10:50

E6. Four new scales based on nonsuccessive-integer-ratio chords. M. V. Mathews, L. A. Roberts (AT&T Bell Laboratories, 600 Mountain Avenue, Murray Hill, NJ 07974), and J. R. Pierce (Stanford University, Stanford, CA 94305)

Our previous work demonstrated that chords with frequency ratios 3:5:7: and 5:7:9: have many perceptual harmonic properties of major triads (4:5:6 ratios). The traditional diatonic scale can be constructed from three major chords, the tonic, the dominant, and the subdominant chords. Using analogous techniques with the new chords, we have constructed four new scales which we call the M579, M357a, M357b, and the P3579 scales. Pitches of the notes of these scales sound very different from the diatonic scale. All scales have clearly perceptable harmonic structure. All notes can be harmonized with consonant "major" chords. There are strong perceptual differences between consonant and dissonant chords. The M scales are based on an octave with a 2:1 frequency ratio. The P3579 scale has a 3:1 octave and was designed for timbres having only odd harmonics. In addition, P3579 is an equal tempered scale using a subset of 13 equal frequency divisions of the 3:1 octave. We believe these scales will be useful for nontraditional new music which has well defined and easily perceived harmonics. We also believe our techniques can be used to manufacture many additional scales.

11+05

E7. Effect of the inharmonicity of stiff strings on piano tuning. Hideo Suzuki (CBS Technology Center, Stamford, CT 06905)

The presently used tuning theory [A. A. Reblitz, *Piano Servicing, Tuning, and Rebuilding*, 5th Printing (Vestal Press, Vestal, NY, 1981)] uses the beat rates calculated from the ideal harmonics of notes in the temperament octave. Following this theory, the note F3 is tuned sharp to C4 (middle C) with a 0.59-Hz beat rate. Then, the note F4 is tuned to the note F3, beatless. Theoretically, assuming the ideal harmonic relationship of partials, the best rate between notes C4 and F4 (test interval) is 1.18 Hz with F4 sharp. This is not true, however, for real piano strings with some amount of inharmonicity. If the inharmonicity index B, which describes the degree of inharmonicity of a string [H. Fletcher, J. Acoust. Soc. Am. 36, 203–209 (1964)], is assumed to be 0.0004 for notes F3, C4, and F4, the beat rate between notes C4 and F4 becomes 0.696 Hz with F4 flat. This is a self-contradiction inherent in the present tuning theory. A method will be presented to calculate the beat rates when the inharmonicity indexes are known for all thirteen notes of the F3–F4 octave.

11:20

E8. Vibrational modes of a handbell. Robert Perrin (University of Technology, Loughborough LE 11 3TU, England), Richard W. Peterson (Bethel College, St. Paul, MN 55112), Thomas D. Rossing (Northern Illinois University, DeKalb, IL 60115), and H. John Sathoff (Bradley University, Peoria, IL 61606)

The vibrational modes of a small handbell tuned to C_5 (523 Hz) have been calculated by means of a finite element method, and also measured by means of holographic interferometry as well as by scanning the sound field close to the bell. The frequency ratios calculated for the various modes as well as the locations of the nodes are found to be in good agreement and also consistent with those previously reported [T. D. Rossing and H. J. Sathoff, J. Acoust. Soc. Am. 68, 1600 (1980)]. Only two flexural modes without nodal circles are observed; these have two and three complete nodal meridians, respectively (m = 2 and 3). For m > 3, the modes without nodal circles are replaced by a family of modes having a nodal circle near the mouth of the bell, similar to those observed for m > 4 in a large handbell [T. D. Rossing, Overtones 29 (1), 15 (1983)]. The finite element analysis also predicts several extensional modes and other modes that have not yet been observed experimentally.

11:35

E9. Chasing the lost chord with an Apple computer. Gary L. Gibian and Eric Harnden (Department of Physics and Audio Technology, The American University, Washington, DC 20016)

The twentieth century has seen the rapid growth of electronic synthesis and reproduction of music, to the point where "a major part of recent popular and commercial music would not exist without synthesizers and...the recording studio...has itself become a musical instrument..." [Gordon Mumma, in *Electronic Music* (Allen Strange, 1983)]. The Audio Technology Program at The American University includes a course in Digital Music Synthesis based in part on the Soundchaser system manufactured by Passport Designs for the Apple computer equipped with Mountain digital circuit cards. Measurements of performance parameters (e.g., the discrete nature of the attack, decay, and release) will be discussed and musical excerpts will be presented.

Session F. Physiological Acoustics II: Ear Canal, Drum, Acoustic Reflex

Edgar A. G. Shaw, Chairman

Division of Physics, National Research Council, Ottawa, Ontario, Canada K1A OR6

Chairman's Introduction-9:30

Contributed Papers

9:35

F1. Sound pressure distributions and resonances in the human ear canal in the presence of a measuring microphone. George F. Kuhn and Larry D. Greller (Vibrasound Research Corp., 10957 E. Bethany Drive, Suite J, Aurora, CO 80014)

The effect of measuring microphones on the acoustic pressure distribution in ear canals has been studied analytically and experimentally up to 20 kHz using scaled model ear canals and real ear canals molded from cadavers. These pressure distributions are a function of frequency, microphone size, microphone location, and ear canal geometry. The presence of the microphone causes not only a localized disturbance of the sound field, producing an erroneous pressure measurement, but also disturbs the pressure distribution across the eardrum, beginning in the mid-frequency range. Furthermore, the measuring microphone as well as the nonuniform canal geometry in the vicinity of the eardrum cause the longitudinal resonances of the ear canal to become anharmonic. This anharmonicity is analytically predictable for canals of sufficient crossectional uniformity and with sufficiently well behaved, but not necessarily uniform, crossectional canal-geometry near the eardrum. [Work supported by NIH.]

9:50

F2. A procedure for calibrating ear canals at high frequencies. D. M. Green, K. N. Stevens, R. Berkovitz, A. Derr, M. Krasner, and R. Pyle (Bolt Beranek and Newman, Inc. Cambridge, MA 02238)

A system for delivering a sinusoidal signal of known sound pressure to the ear at high frequencies (8-20 kHz) is explored. A high-frequency driver unit is coupled to the ear canal through a long tube, so that the acoustic source at the ear-canal entrance had an impedance close to ρc . The system is calibrated by applying an impulse of voltage to the source and measuring the response at a small microphone located in the coupling tube close to the ear-canal entrance. A signal-processing procedure detects the zeros in the spectrum of this response and uses these data to estimate the transfer function from the source voltage to the sound pressure at the inner end of the ear canal. The system has been calibrated for a number of different ears in this way, and data giving the range of characteristics of the ear the results are consistent with theoretical predictions based on the known average shape of the ear canal. [Supported by a contract from NINCDS.]

10:05

F3. Optical measurement of ear canal length. Jan Zemplenyi, Samuel Gilman, and Donald Dirks (Head and Neck Surgery Department, Center for the Health Sciences, UCLA School of Medicine, Los Angeles, CA 90024)

This paper reports an optical, noninvasive technique for measurement of both open and occluded ear canal length. The method is based on the use of an operating microscope set at a standard magnification. Initially the microscope is adjusted so that the umbo is sharply in focus when the body of the microscope is close to fully "down" position on its track. The microscopic support is then locked in all directions of motion and the microscope body position is measured. The microscope is then refocused on a reference point along the ear canal. The distance that the microscope

S11 J. Acoust. Soc. Am. Suppl. 1, Vol. 75, Spring 1984

body traveled along the track is then measured. This measurement is equal to the distance between the umbo and the previously chosen reference point. The length of an occluded ear canal can be measured by choosing the lateral plane of the earmold as the new reference and then subtracting the earmold length. The distance from umbo to the junction of the concha cavum and the ear canal can also be measured directly. The depth of focus of the microscope optics is selected to provide a maximum error no greater than ± 1 mm. Measurements obtained by this technique were compared to those made by invasive methods reported in the literature.

10:20

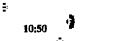
F4. Determination of eardrum reflectance using measurement of phase. Michael R. Stinson (Division of Physics, National Research Council, Ottawa, Canada K1A OR6)

At frequencies greater than 8 kHz the acoustic energy reflectance at the eardrum is not well established in living human subjects. This quantity is of interest, though, in high-frequency audiometry and in network modeling of the middle ear. In this paper a technique for measuring highfrequency reflectances is discussed that makes use of the phase component of a pressure signal, rather than its amplitude. In a section of ear canal having a constant cross section, or having a constant taper, the maximum rate change of phase with position is simply related to the energy reflectance at the eardrum. Experimentally the phase of the pressure signal is determined at several positions over a 2-mm distance, centered about an interference minimum. By choosing appropriate sound frequencies the measurements can be confined to a 6- or 7-mm region near the ear canal entrance; this avoids the deep penetration of probe microphones required by other techniques, and avoids the large variations in ear canal cross section that occur close to the eardrum. Preliminary results have been obtained, suggesting an eardrum energy reflectance of about 80% (25-dB equivalent standing wave ratio) at 15 kHz.

10:35

F5. Digital measurement of acoustic reflex response in normally hearing subjects. L. N. Robinette, D. J. Thompson, and D. F. Nalty (Audiology Research Program (151B), Dorn Veterans Hospital, Columbia, SC 29201)

Determination of acoustic reflex response morphology requires an aural acoustic immittance instrument capable of accurate measurement of complex immitance. Unfortunately, conventional analog instruments are either (1) incapable of measuring complex immittance or (2) do so inefficiently and with long time constants. Accurate data can be obtained, however, with a digital immittance instrument. Acoustic reflex response measurements were obtained using a digital acoustic immittance instrument (226-Hz probe tone) and a laboratory computer. Activating signals (1-s duration) were four tones and broadband noise presented in 5 dB increments (maximum 120 dB SPL) from -5 to +30 dB re: acoustic reflex threshold (ART). Ten subjects were tested per decade of age from 20 years through 79 years. Results for the 2-kHz tone and BBN at 20 dB re: ART indicated that (a) slope of onset increased with signal level, (b) response slope during signal presentation was greater for noise than for the 2-kHz signal, (c) baseline, attack time, onset latency, and amplitude of maximum response decreased for the oldest age group, and (d) release time and recovery time increased for the oldest age group. [Work supported by Rehabilitative Research and Development Service of Veterans Administration.]



ŵ

.

х 😜

÷

é

٠į,

۰

F6. The role of the acoustic reflex in modifying identification accuracy for vowels. Maureen Hannley, Michael F. Dorman, Julie Lindholm, and Ingrid Cedar (Departments of Speech & Hearing Science and Psychology, Arizona State University, Tempe, AZ 85287)

444

135

÷

÷.

÷

÷

"Rollover," poorer word identification accuracy at high than at low SPLs, is correlated with the absence of the acoustic reflex in individuals with lesions to c.n. VII and c.n. VIII. The increased number of word identification errors at high SPL is due largely to errors in vowel identification. Individuals with these types of lesions, however, are rare. In order to study rollover in a normal population, we constructed 10 vowels of 50ms duration. These were presented to normal hearing listeners at moderate and high SPLs. We reasoned that, since the latency to onset of the acoustic reflex, at the test levels, was longer than the total duration of the vowels, we should observe poorer vowel deputification at the higher SPL than at the lower. This was, in fact, the obtcome. Vowel confusions were usually with vowels with higher F2 and lower F1. This outcome was confirmed by the results of identification tests with stimuli along an $/i/-/\epsilon/$ continuum.



ı (in

÷

e.

- 64

٠Ï٢

· 8

٠Ű

Session G. Physiological Acoustics III: Auditory Pathway: Cochlea to Cortex

R. Bruce Masterton, Chairman

Department of Psychology, Florida State University, Tallahassee, Florida 32306

Chairman's Introduction-1:00

Contributed Papers

1:05

G1. A model of cochlear processing. Shihab Shamma, Richard S. Chadwick,⁴⁾ John Wilbur, and John Rinzel (Mathematical Research Branch, NIADDK, NIH, Bethesda, MD 20205)

A mathematical model is developed to describe the transformation from acoustic stimulus to intracellular hair cell potentials in the mammalian cochlea. The model incorporates a physiologically reasonable linear formulation of basilar membrane mechanics, a treatment of basilar membrane-cilia displacement coupling, and a simplified description of the inner hair cell nonlinear transduction process based on recently published data of intracellular recordings. The model at this stage is restricted to frequencies below 2000 Hz. The computed responses to single tone inputs display the major qualitative features of hair cell intracellular potentials and auditory nerve fiber activity (e.g., frequency tuning; rectified waveforms; saturating rate-level functions). The computed results also account for some subtle effects of stimulus intensity on frequency tuning of phase locked responses observed experimentally in both inner hair cells and auditory nerve fibers. For example, experiments reveal that (1) the bandwidth of the frequency selectivity increases with intensity, and that there are (2) downward (upward) shifts of the best frequency of units tuned above (below) approximately 1 kHz with increasing intensities. In the model, the computed ac outputs show both these trends. The first is primarily due to the saturating effect of the hair cell nonlinearity. The second results as a consequence of both the nonlinearity and the combined effect of the high-pass transfer function of basilar membrane-cilia coupling and the inner hair cell low-pass transfer function. In contrast to these shifts along the frequency axis, the model does not exhibit intensity dependent shifts of the spatial location along the cochlea of the peak response for a given single tone. The observed shifts, therefore, may not be disruptive to a stable tonotopic code. * Biomedical Engineering and Instrumentation Branch, Division of Research Services, NIH, Bethesda, MD 20205.

1:20

G2. A new model of an auditory nerve fiber. Blaise Donhouédé and J. Marc Dolmazon (Institut de la Communication Parlée, Laboratoire Associé au CNRS, ENSERG, 23 rue des Martyrs, 38031 Grenoble Cedex, France)

The main temporal characteristics of discharges observed in the primary auditory neuron are the phenomena of adaptation and synchronization of the responses on the phase of the stimulus. These phenomena play a major role in the mechanisms of speech coding [Delgutte, J. Acoust. Soc. Am. **68**, 843 (1980)]. We propose a stochastic threshold model which mainly asumes that the process of adaptation is additive. This model reproduces appropriately adaptation and its per-stimulatory effects. It simulates in the same way the locking of nerve discharge to the stimulus cycle up to about 5000 cycles/s, in accordance with experimental results (Anderson *et al.*, J. Acoust. Soc. Am. **54**(2) (1971)]. In comparison with other threshold models, the originality of ours lies in the fact that it includes the temporal evolution of graded potentials described by Furukawa *et al.* [J. Physiol. **276** (1978)].

1:35

G3. Auditory nerve responses following middle-ear disarticulation in kittens. Edward J. Walsh (Southern Illinois University, School of Medicine, Department of Surgery, 800 North Rutledge Street,

Springfield, IL 62702), JoAnn McGee (Southern Illinois University, School of Medicine, Department of Pharmacology, 800 North Rutledge Street, Springfield, IL 62702), and Eric Javel (Boys Town Institute for Communication Disorders in Children, Omaha, NE 68131)

The effects of partial acoustic deprivation during postnatal development of kittens were studied following the disarticulation of their malleoincal joints. Disarticulations were performed between birth and 10 postnatal days. Prior to 10 postnatal days, auditory thresholds are in excess of 100 dB SPL, and it can be assumed that these animals receive little, if any, acoustic stimulation prior to surgery. Following surgical manipulation of their middle ears, kittens were allowed to grow to adulthood at which time single auditory nerve fibers were studied extracellularly, from both operated and intact sides. Threshold differences between the operated and intact sides confirmed that a conductive lesion had been produced. Other indices of neuronal function, however, showed that most of the fibers from the operated side were normal with respect to their tuning, dynamic range, and phase-locking ability. There was a slight tendency for fibers on the operated side to exhibit higher than normal spontaneous discharge rates, as well as slightly reduced tip-to-tail ratios. Most neurons had normal appearing tuning curves, however, some displayed shallow low-frequency slopes near their best frequency. In general, middle ear disarticulation did not produce profound effects on auditory nerve responses.

1:50

G4. Adaptation and variability of spike discharge of auditory nerve. Larry A. Westerman and Robert L. Smith (Institute for Sensory Research, Syracuse University, Syracuse, NY 13210)

The response of afferent fibers in gerbil auditory nerve to constant intensity tone bursts was observed. The rapidly declining rate during the first 10 ms appears to have lower variability than the response during the steady state. That is, PST histograms appear smoother during the rapid adaptation phase than at later times. We tested this impression by calculating pulse-number distributions. Histograms of bin width T were constructed by dividing the response record of single fibers into N subsets. The mean and variance of the number of spikes in each bin of the subset PST histograms were calculated, for various values of N and T. We observed that the variance-to-mean ratio was relatively constant and independent of (declining) firing rate during the adapting response, except for the onset 1-ms bin. At high intensities the probability of firing approached unity during the onset 1-ms window, so that the variance approached zero. At all later times, the ratio was near unity, consistent with a Poisson process with a relative refractory period.

2:05

G5. Localized distribution of olivocochlear fibers. Phyllis E. Stopp (Neurocommunications, University of Birmingham Medical School, Birmingham, England B15 2TJ)

One of the problems the auditory system has to deal with is that of preserving the identity of a signal against a distracting background, a role in which the centrifugal pathway has been implicated. There are two ways in which this might act: (a) by adjusting the general threshold level of the hair cells to be below saturation level, (b) by inhibition at the boundary edges of the active-fiber array. The hypotheses were tested anatomically by studying the organization of the olivocochlear bundle using retrograde axonal transport. True Blue, (TB) a fluorescent dye, was introduced into discrete regions of the guinea pig cochlea. When TB contacted the whole cochlea labeling appeared throughout the whole ipsilateral lateral superior olive (LSO), together with some lesser labeling in the contralateral periolivary nuclei and trapezoid body. When TB was applied only to the apical turn labeling was confined to the dorsolateral region of the LSO, while basal turn treatment resulted in labeling restricted to the medial region. This cochleotopic organization corresponds to the tonotopic arrangement of the afferent cells (cat) and suggests that the OCB acts by a localized rather than a diffuse mechanism.

2:20

G6. Point process model of LSO unit discharges. Don H. Johnson, Darel Linebarger (Department of Electrical Engineering, Rice University, Houston, Texas 77251), and Chiyeko Tsuchitani (Sensory Sciences Center, University of Texas Graduate School of Biomedical Sciences, Houston, TX 77030)

A point process model for the responses of single auditory-nerve fibers to time-varying stimuli was extended to describe lateral superior olive (LSO) unit responses to monaural cf tones. In contrast to auditory-nerve fiber discharges, successive interspike-intervals of LSO unit discharges exhibit serial dependence. This dependence was found to be well described by a first-order Markov model of the underlying point process. The characteristics of this model were measured from the conditional interval histogram: the usual interspike interval histogram restricted to those intervals preceded by an interval of a specified duration. From this quantity, the conditional hazard function was derived. This computation revealed that the influence of the pentultimate interval was to shift the hazard function. This detailed description of the serial dependence cannot be derived from measurements of serial correlation coefficients. The cf tone burst responses of LSO units are characterized as "chopper"-type. Within the context of the point process model outlined above, the parameters of the model were measured from the sustained portion of the tone burst response. Using the model thus derived, the initial chopping portion of the response was predicted. [Work supported by NINCDS and NSF.]

2:35

G7. Two-tone interactions in the auditory cortex of the squirrel monkey. Shihab Shamma^a and David Symmes (Laboratory of Developmental Neurobiology, NICHD, NIH, Bethesda, MD 20205)

Two-tone interactions are recorded in the responses of single units in the superior temporal gyrus to contralateral acoustic stimulation of the awake squirrel monkey. Four response types are distinguished based primarily on the nature of the two-tone response, and secondarily on criteria such as the patterns of response to single tones and noise stimuli, thresholds, and spontaneous activity levels. Type A units (24/80) display strong lateral inhibitory influences which may extend up to two octaves on either side, or both sides, of the BF. They are sharply tuned at all intensities, and generally exhibit sustained response to single-tone stimuli at the BF. The units have nonmonotonic rate-level functions, and where tested, show little or no response to broadband noise. Most type A units have low spontaneous rates (<1 spikes/s), and relatively high thresholds (>30 dB SPL). Type B units (22/80) are characterized by relatively high spontaneous rates of activity (>20 spikes/s) and inhibitory responses to single-tone stimuli. Broadband noise is applied to a few type B units, and in all cases it evokes strong excitatory response. Type C units (17/80) summate the responses to the two-tone stimulus, and show little or no inhibitory influences. They have V-shaped tuning curves, monotonic rate-level functions, low thresholds (<30 dB SPL), moderate spontaneous rates (~10 spikes/s), and a strong and sustained response to noise and single tone stimuli. Type D units (17/80) show "temporal inhibition" to two-tone stimuli, in that an excitatory response to the first tone suppresses (adapts or inhibits) the response to the second tone. These units generally have moderate to broad frequency tuning and phasic responses to single tone stimuli. Histological examination of electrode tracks suggests that type A units are restricted to A1 (and possibly the rostral field) while other types are distributed over all auditory fields. ^a Present address: Mathematical Research Branch, NIADDK, NIH, Bethesda, MD 20205.

2:50

G8. Changes in human regional cerebral blood flow in response to pure tones. Judith L. Lauter (Central Institute for the Deaf, St. Louis, MO 63110), Peter Herscovitch, and Marcus E. Raichle (Washington University Mallinckrodt Institute of Radiology, St. Louis, MO 63110)

Last year we reported that changes in human cerebral blood flow, monitored with a positron emission tomography device (PET VI), could be demonstrated in response to auditory stimulation with synthetic syllables. Developments in image processing and schemes for anatomical localization have now made it possible to detect similar changes in response to pure tones. The topography of these changes seems to reflect: (a) ear of presentation, and (2) frequency of the stimulating tone. A number of presentation variables such as stimulus repetition rate affect the clarity of the response from individual to individual. Definition of these variables can help determine how best to proceed in our application of the PET scan to the study of human auditory perception.

3:05

G9. PET imaging during auditory stimulation. John J. Sidtis (Department of Neurology, Cornell Medical Center, 1300 York Avenue, New York, NY 10021), Jens O. Jarden, Kimberlee J. Kearfott, and David A. Rottenberg (Memorial Sloan-Kettering Cancer Center, New York, NY 10021)

Positron emission tomography (PET) provides a means of studying regional brain activity in vivo. PET measurements of regional cerebral blood flow (rCBF) were obtained in 3 subjects with normal hearing during the continuous inhalation of CO¹⁵O. A nominally unstimulated 3-min period, during which a moderate level of apparatus noise was present, was followed by the continuous binaural presentation of white noise (3 min). In addition, dichotic stop-consonant and complex pitch discrimination tests (3 min) were administered to two subjects. White noise produced 10%-15% and 15%-25% increases in rCBF in the temporal lobes and thalamus, respectively. Increases were also observed in nonauditory structures: 10%-25% in medial frontal cortex and 5%-10% in medial occipital cortex. In contrast, maximum changes in rCBF during speech and pitch discrimination were of smaller magnitude and occurred over more restricted cortical regions. These results suggest that continuous white noise produces significant increases in rCBF in both auditory and nonauditory areas. The relative magnitude of this effect compared to rCBF changes observed during auditory pattern discrimination suggests that regional brain activity associated with specific auditory functions is likely to be extremely focal and that the quantitation of such activity requires wellcontrolled within-subject studies. [Supported by NIH.]

Session H. Engineering Acoustics I: New Materials for Piezoelectric Transducers and Transducers

Geoffrey L. Wilson, Chairman

Applied Research Laboratory, Pennsylvania State University, P. O. Box 30, State College, Pennsylvania 16801

Chairman's Introduction-1:30

Invited Papers

1:35

H1. Materials used by industry for the production of piezoelectric transducers. The state of the art of research work performed in the field of PZT ceramics and ferroelectric polymers. Lucien Eyraud, Paul Eyraud (Institut National des Sciences Appliquées de Lyon, 69621 Villeurbanne Cedex, France), and François Bauer (Institut Franco-Allemand de Saint Louis, B.P. 301, 68301 Saint Louis Cedex, France)

For inorganic materials such as piezoelectric PZT ceramics, the phenomena of conduction and aging set severe limits to the development of some industrial applications. Various models, in particular that of a suggested structure model, allow one to get insight into these phenomena and to limit these effects by acting either on the manufacturing process or on the composition itself. For organic materials, in contrast, the phenomena are quite different and, from the outset, the problems are much less severe. A brief review will be given of the properties of the PVF2 homopolymer as well as of a few copolarized in a suitable manner. These organic and inorganic materials must be taken into account as strong candidates for the production of new transducers.

2:05

H2. Ceramic-polymer composite transducers. R. E. Newnham (Materials Research Laboratory, The Pennsylvania State University, University Park, PA 16802)

One of our major interests in the past few years has been in the development of diphasic transducer materials made from polymers and lead zirconate titanate (PZT) ceramics with high hydrostatic pressure sensitivity. The concept of phase connectivity, the manner in which the individual phases are interconnected, has been used to optimize the electric flux pattern and mechanical stress distributions in attaining remarkable improvements in the hydrostatic strain coefficient (d_h) and the hydrostatic voltage coefficient (g_h) over the corresponding values of solid PZT ceramics. Recent results on 0–3, 1–3, 1–3–2, 2–2, 3–1, 3–2, and 3–3 composites will be presented, and a comparison made with polyvinylidene fluoride and other hydrophone materials. When driven at high frequency the composite transducers exhibit a number of interesting modes of motions in which the component materials sometimes vibrate out of phase. Some of the proposed applications for composite transducers will be described.

2:35

H3. Piezoelectric response in trifluoroethylene copolymers of vinylidene fluoride. J. C. Hicks (Naval Ocean Systems Center, San Diego, CA 92152)

The copolymer system of polyvinylidene fluoride-trifluoroethylene, P(VDF-TrFe), has been shown to exhibit a Curie temperature Tc that is dependent upon the monomer ratio. Below this temperature the copolymer is in a ferroelectric phase similar to the stretched homopolymer, Polyvinylidene fluoride, PVDF. The piezoelectric response of this copolymer system for oriented, well-poled samples is very similar to and in some cases better than PVDF. Again the piezoelectric response may also depend upon the monomer ratio. However, when the copolymer with a monomer ratio of 3/1 for VDF/TrFE is poled above Tc and subsequently annealed it has an exceptionally high percentage crystallinity and an electromechanical coupling coefficient of 0.3. These values are for undrawn samples and can be used to predict a hydrostatic piezoelectric response approximately two to three times better than PVDF. These concepts and possible new data will be presented.

Contributed Papers

3:05

H4. The piezoelectric properties of some polar glass-ceramics. R. Y. Ting (Naval Research Laboratory, Underwater Sound Reference Detachment, P. O. Box 8337, Orlando, FL 32856) and A. S. Bhalla (Materials Research Laboratory, The Pennsylvania State University, University Park, PA 16802)

A completely new family of nonferroelectric polycrystal materials was recently developed. The samples were prepared by recrystallizing the glass of suitable composition in a very strong temperature gradient. The thermal gradient produced a driving force which gave strong preference to crystal nuclei of a given polarity, resulting in a highly oriented polar phase. The hydrostatic piezoelectric coefficient d_h and hydrostatic voltage coefficient g_h of this new class of transduction material were measured as functions of temperature, pressure, and frequency. The d_h and g_h values were found to be comparable to those of the state-of-the-art piezoelectric PVDF polymers, but independent of hydrostatic pressure up to 35 MPa. This effect may be attributed to the high stiffness of the glass and the firm polar character of the polarization. The advantages of glass-ceramics for hydrophone applications will be discussed.

3:20

H5. Pressure effects on the dynamic effective properties of perforated resonating elastomers. G. Gaunaurd, E. Callen, and J. Barlow (Naval Surface Weapons Center, White Oak, Silver Spring, MD 20910)

We quantitatively analyze the effect of hydrostatic pressures on the static and dynamic effective material properties of perforated visoelastic elastomers. A resonance methodology that we had developed earlier [i.e., G. Gaunaurd and J. Barlow, J. Acoust. Soc. Am. 75, 23-34 (1984)] is here extended to account for the distorting effect of added pressures. The distortion basically produces a broadening of the spectral plots and a shift in the resonance peaks/dips that are observed in the dynamic plots of all the effective properties of the pertinent composites. For the lossy, air-filled rubberlike materials considered here the pressure effect is quite noticeable but smaller than the viscous effect or than the effect of nonuniformity in the cavity size-distribution functions that we analyzed earlier. The model is implemented by a computer code and its numerical predictions are quantitatively displayed for some of the most important of the effective material properties of a given perforated elastomer up to applied pressures of 400 psi. These perforated elastomers have uses as underwater sound absorbers. [Work partially supported by NOSC, San Diego, CA and by NSWC, White Oak, MD.]

3:35

H6. Optimization of the transmitting characteristics of a tonpilz-type transducer by proper choice of impedance matching layers. Michel VanCrombrugge (Applied Research Laboratory, P. O. Box 30, State College, PA 16804) and William Thompson, Jr. (Applied Research Laboratory and Department of Engineering Science and Mechanics, The Pennsylvania State University, University Park, PA 16802)

Many attempts have been made to design wideband transducers. These attempts were concentrated on simple configurations such as a single piezoceramic disk with a limited number of impedance matching layers on its front and/or back faces. For the complex-structured tonpilz transducer, the methods described in the literature are no longer appropriate. Furthermore, trial-and-error attempts to choose matching layers to obtain better performance are time consuming. Consequently, a systematic procedure based on the Mason equivalent circuit representation of the transducer and the nonlinear goal programming algorithm has been implemented. This procedure allows one to design both broadband and high-power transducers. The mathematical implementation of this procedure produces excellent results. Moreover, it can easily be adapted for other design objectives such as minimization of weight, cost, size, etc. [Work sponsored by the Naval Sea Systems Command.]

3:50

H7. Preliminary design rationale for tonpliz transducer elements. Stephen C. Thompson and Stephen Hess (Gould Defense Systems, Inc., Ocean Systems Division, Department 721, 18901 Euclid Avenue, Cleveland, OH 44117)

Analysis methods for the prediction of performance parameters for tonpilz transducer elements are quite common. Given a physical design, the methods of equivalent circuit analysis, one-dimensional plane-wave modeling, or finite element modeling each gives useful approximations of increasing accuracy. However, none of these methods can provide a design from a given set of performance requirements. They are *analysis* methods rather than *design* methods. This paper presents a rationale for the development of a preliminary *design* method for tonpilz transducer elements. The algorithm requires input values for the transducer resonant frequency, 3-dB bandwidth, radiated power level, and beamwidth. The output is a simple tonpilz element consisting of a head mass, a tail mass, a ceramic stack with minimum volume, and a stress rod if desired. H8. A figure of merit for head mass materials for broadband transducer applications. John J. Gray (Gould Defense Systems, Inc., Ocean Systems Division, Department 721, 18901 Euclid Avenue, Cleveland, OH 44117)

In the past it has been proposed that the transducer designer use the specific rigidity as a figure of merit (FOM) for transducer head mass materials. This FOM places a premium on high flexural resonance frequency for a given head mass thickness, but it is not useful in selecting materials for broadband applications where a small value of mass is desired. Using the specific rigidity, steel would have a higher FOM than magnesium, despite the fact that for broadband applications magnesium is usually preferable. A new FOM is proposed which simultaneously places a premium on low mass and high-flexural resonance frequency. This FOM is the specific rigidity divided by the density.

4:20

H9. Fiber optic gradient hydrophone. G. B. Mills, S. L. Garrett, and E. F. Carome (Physics Department, Code 61Cm, Naval Postgraduate School, Monterey, CA 93943)

A laboratory study has been made of the characteristics of an interferometric type optical fiber pressure gradient hydrophone. The optical system is configured as an all fiber Mach–Zehnder interferometer excited by a single mode gallium arsenide diode laser. A pair of identical fiber coils, one in each arm of the interferometer, forms the sensing portion of the gradient hydrophone. Each coil consists of 8 m of polyethylene jacketed, single mode fiber, wound in a doughnut shaped element of mean diameter 5 cm and thickness 3 mm. The acoustic sensitivity of each coil was determined separately and then the pair was aligned coaxially and separated by 10 cm to operate as a pressure gradient device. Details of the construction of the system, calibration procedure, and hydrophone sensitivity data are presented. [Work supported by ONR.]

4:35

H10. Some possible novel configurations for optico-acoustic transducer arrays created by controlled motion of laser beams across water surfaces. Hsiao-an Hsieh and Allan D. Pierce (School of Mechanical Engineering, Georgia Institute of Technology, Atlanta, GA 30332)

Laser beams impinging on water surfaces will generate underwater sound if the beam intensity is modulated or if the beam is moving, although the optical-to-acoustical energy conversion efficiency is typically extremely low. Previous analyses have been confined to modulated beams impinging at a fixed point or moving rectilinearly at constant speed, but the present paper adopts a futuristic view that intricate moving and rotating mirror systems can be designed that will allow the entry point to move in any desired pattern (including skips and zig-zags) and with any velocity versus time profile; the only constraints are that the beam entry angle be fixed and that the exponential decay rate of beam intensity with depth be fixed. This latitude in beam configuration allows a systematic exploitation of the pumping principle, that local energy conversion efficiency is proportional to product of acoustic pressure and beam intensity, by placing the beam wherever and whenever the acoustic pressure is currently the highest. Directed acoustic waves pointed obliquely downwards can be created by moving an obliquely incident beam through a sequence of short parallel path segments, the first sequence pattern simulating a sinusoidal heat deposition wave of fixed wavelength and beam width, the next sequence causing this pattern to move at the sound speed in the desired propagation direction. [Work supported by ONR.]

4:50

H11. Interferometric measurement of the magnitude of acoustic transducer motion. Howard Fein (Gould Inc., Ocean Systems Division, 18901 Euclid Avenue, Cleveland, OH 44117)

Experiments have shown that the magnitude of the displacement of excited acoustic transducers can be simply and very accurately measured employing a technique called Speckle Field Interferometry. The application of a specially designed Speckle Field Displacement Interferometer to problems of motion measurement has resulted in the successful quantitative characterization of the behavior of certain transducers. These characterizations are part of a program, which includes holographic interferometry [H. Fein, J. Acoust. Soc. Am. Suppl. 1 73, S24 (1983)], to accurately evaluate the performance of transducer systems and are shown to be of great value in defining actual operating dynamics. Interferometric data, methods, and results are presented.

5:05

H12. Ratio of specific heat γ of humid air. G. S. K. Wong and T. F. W. Embleton (Division of Physics, National Research Council, Ottawa, Ontario, Canada K1A 0R6)

For primary microphone calibration (and in some thermodynamic applications) it is necessary to have a precise knowledge of γ . In national and international microphone calibration standards, a value of 1.402 is recommended for dry air, and there is no information on γ for humid air. Based on known theoretical and experimental thermodynamic data on the constituents and properties of humid air, the values of γ for various degrees of relative humidity h (dimensionless), and ambient temperatures t (degrees Celsius) have been computed for the first time. An empirical equation in terms of h and t has been obtained to fit the precisely calculated values for γ . By ignoring the effects of humidity on γ , the sensitivities of microphones calibrated in ambient air can be underestimated by approximately 0.01 dB, an amount which is greater than the currently attainable uncertainty in reciprocity calibration. A direct acoustical method to verify the variation of γ with humidity is discussed.

MONDAY AFTERNOON, 7 MAY 1984

CLAREMONT ROOM, 2:00 TO 3:50 P.M.

Session I. Musical Acoustics II: (A) Wind Instrument Qualities; (B) Sound for Those Who Cannot Hear

Arthur H. Benade, Co-Chairman Physics Department, Case Western Reserve University, Cleveland, Ohio 44106

Carleen M. Hutchins, Co-Chairman Catgut Acoustical Society, 112 Essex Avenue, Montclair, New Jersey 07042

Chairman's Introduction-2:00

Contributed Papers

2:05

11. Simulation of flow through a parametrized "reed-aperture." William J. Strong (Department of Physics and Astronomy, Brigham Young University, Provo, UT 84602)

In systems used to simulate wind instrument behavior the blowing pressure is often set to some constant value. This is equivalent to assuming that the blowing pressure source (lungs-bronchi-trachea-vocal tract) has an internal impedance that is small in comparison with reed-aperture plus tube impedance. A stylized pressure source plus reed-aperture plus tube is simulated to investigate the effects of source characteristics and tube characteristics. The pressure source is represented by one of four configurations: large cross-sectional area vocal tract, small cross-sectional area vocal tract, and an /i/-shaped tract. The rectangular "reed-aperture" is parametrized so that its time variation is independent of any source or tube loading. Four "tube" loadings are simulated: a zero impedance, a resistance, an inertance, and a section of uniform tubing. Waveforms and spectra are calculated for air flow through the reed-aperture, blowing pressure, and tube pressure for the $4 \times 4 = 16$ possible combinations to demonstrate the effects of source and tube characteristics.

2:20

12. Dynamical equations for sound generation in wind instruments. R. E. Davis and A. Tubis (Department of Physics, Purdue University, West Lafayette, IN 47907)

An exact set of coupled ordinary nonlinear differential equations is derived for the mouthpiece pressure in reed wind instruments for cases in which the mouthpiece impedance function is expressible as a series of pole terms in the complex frequency plane. The equations are applicable even in the "beating reed" regime. The integration of the equations to obtain transient and steady state behaviors of the instrument apepars to be a practical alternative to integral equation approaches.

2:35

I3. Semi-empirical formula for the clarinet spectrum. A. H. Benade and S. Kouzoupis (Physics Department, Case Western Reserve University, Cleveland, OH 44106)

A single formula is presented giving the normalized strengths (p_n/p_1) of the harmonics belonging to any note of a clarinet's scale. The formula is based on Worman's internal spectrum systematics, a transformation function connecting this with the external (room average) spectrum, plus the pipe-scaling relations for air column damping. Any note is characterized by the ratio F of its fundamental frequency f_1 to the instrument's essentially constant tone hole lattice cutoff frequency f_c . The playing level is specified by $L = (p_1/p_0)$ where p_0 is the value of p_1 when the reed just beats (L < 1). $(p_n/p_1) = L^n [1 + \alpha(nF)^6]^{-1/2} (1 + \beta F^{1/2} e^{-\gamma F} n)^c DN$. For $n \text{ odd}, e = \pm 1 \text{ and } D = 1$. For n even, e = -1 and D = nF/(1 + nF). Here N normalizes to unity at n = 1, $\alpha = 0.85$, $\beta = 8.5$, $\gamma = 3$, as fitted to the clarinet C_4 (where $F \simeq 1/6.5$) at L = 1. A fixed-parameter filter set can be built, which when driven by a constant-width pulse train having a repetition rate corresponding to any desired note, can well approximate the clarinet's spectrum for L = 1. A-B listening tests against a real clarinet show good matching over the entire scale. Analogous spectral formulas and filter sets for other wind instruments appear possible.

Invited Papers

2:50

14. Problems of the modern oboist that might be worthy of attack by acoustical engineers. Patrick A. Gainer (25 Sanford Drive, Newport News, VA 23601)

In its evolution through and beyond the shawm, the modern oboe has become, at least to some ears, a versatile instrument with a range of beautiful and expressive sounds. It has also become a very complicated

MONDAY PM

instrument. Whereas the baroque oboe had 11 holes (or 13 if double holes count) and three keys, only two of which could be used, the modern oboe is drilled with at least 21 holes and a plethora of keys joined by linkages that would make Rube Goldberg happy. While the extra hardware and holes do make it easier to play in keys with lots of sharps and flats, they also cause problems. The oboe is not so close an approximation to the simple conical-bored reed instrument that it was in former days. Not only are there more holes, but the bore of the oboe has been made smaller over the years, and the walls thicker. Each tone hole is more like a tube. The placement, diameter, and amount of undercutting of the holes and the actual shaping of the bore seem to be an art rather than a science. Even two oboes from the same maker are likely to have significant differences that are left to the player for curing. Some of the deficiencies of the modern oboe, oboe d'amore, and English horn will be demonstrated along with some "home cures" used by performing oboists.

3:20

15. Exploring the concepts of music and sound: Instructional methods and techniques. Norman Lederman (Model Secondary School for the Deaf, Gallaudet College, Washington, DC 20002)

Over the past five years, the author of this paper has developed a sound demonstration lab and taught interdisciplinary courses in sound and music at the Model Secondary School for the Deaf (M.S.S.D.), a precollege program of Gallaudet College. The courses have been unique in their approach to demonstrating auditory events (which the hearing impaired individual may not be able to detect) through multisensory (visual and tactile) means. By way of classroom demonstrations, hands-on experiments, a student workbook, and teacher's guide; the students gain an increased self-awareness and understanding of the physical/scientific concepts of sound, the hearing process, the speech mechanism, musical instruments, and associated technology (e.g., hearing aids, equipment used in testing hearing, etc.). In addition to its involvement with hearing impaired individuals, the M.S.S.D. sound lab has been visited by various professional organizations and other school programs. Upon experiencing the sound lab, these visitors (many from hearing schools) have cited the usefulness of the multisensory approach to teaching material of this nature. For the Acoustical Society meeting, the author intends to present an overview of the techniques used in the sound lab, show student response (videotape), and invite audience participation. There will be live demonstrations as well as slides and video.

MONDAY AFTERNOON, 7 MAY 1984

EPPINGTON ROOM, 2:00 TO 5:05 P.M.

Session J. Noise II: Legal and Economic Aspects of Engineering Noise Control

Edwin H. Toothman, Chairman Bethlehem Steel Corporation, Bethlehem, Pennsylvania 18016

Chairman's Introduction-2:00

Invited Papers

2:05

J1. The legal aspects and economic feasibility of engineering noise controls; origin and developments of cost/ benefit, Frank R. Barnako (Reed Smith Shaw & McClay, 1325 18 Street, Washington, DC.20036)

In Continental Can Company the respondent defended a citation for violation of the noise standard 29 C.F.R. 1910.95 raising the question of economic feasibility of technological controls as compared with an effective hearing conservation program. The Occupational Safety and Health Review Commission (OSHRC) in a two to one decision held that feasibility as used in the standard contemplates economic as well as technological feasibility; that the cost of engineering controls, loss of production or efficiency, if any, together with annual maintenance costs thereof and the reasonably expected noise reduction must be weighed against the cost of an effective hearing conservation program. The Commission held that under that test the cost of controls was excessive and vacated the citation. Subsequent Review Commission decisions in Turner Company, Samson Paper Bag Co., Inc., Carnation Co., Louisiana-Pacific, RMI, International Harvester, and Castle and Cook developed the application of that decision in various factual situations and following decisions of the United States Circuit Court of Appeal. The Centred to the Commission's expertise as a "independent adjudicator" and agreed that the Act and Standard required only those controls economically justified after analyzing costs of controls versus benefits obtained by effected employees from an effective hearing conservation program. The Court of Appeal to the program.

2:30

J2. Current case law of the Occupational Safety and Health Review Commission. Robert A. Rowland (Chairman, Occupational Safety & Health Review Commission, 1825 K Street, N.W., Suite 409, Washington, DC 20006)

The current Occupational Safety and Health Review Commission precedent on the feasibility of engineering noise controls is Sun Ship, Inc., a 1982 decision. In that case Commissioners Cleary and Cottine reached a consensus on the meaning of the term "feasible," on which they had not been able to agree earlier in Samson Paper Bag. Because Samson Paper Bag had not achieved a consensus on a new definition, the Commission there concluded that its original cost-benefit test (Continental Can) would remain in effect. Commissioners Cleary and Cottine now agreed to reject that test on the basis of the Supreme Court's 1981 decision in the "cotton dust case," American Textile Manufacturers Institute, Inc., vs. Donovan (ATMI). The Court's decision, however, interprets and is predicted on a different provision of the Occupational safety and Health act than that under which the noise standard was promulgated. In a subsequent appellate decision, Castle & Cook Foods, the Ninth Circuit specifically concluded that the ATMI decision does not control the interpretation of the noise standard and that the Commission's previous cost-benefit test was reasonable.

2:55

J3. The role of economics in compliance with the OSHA Noise Standard. Mark A. de Bernardo (Labor Law Section, U.S. Chamber of Commerce, 1615 H Street, NW, Washington, DC 20062)

The role that economic feasibility plays in employer compliance with (and OSHA enforcement of) health standards in general and the Noise standard in particular. Industries' problems with compliance with the Noise Standard and Hearing Conservation Amendment, particularly small business' problems. Preference for effective hearing conservation programs over government insistence of engineering controls. A comparison of the Reagan and Carter Administrations' Hearing Conservation Amendments. Industry objections to the current rule: (1) integration to 80 dBA; (2) inclusion of impulsive noise; (3) requirement of *annual* audiometric testing in all cases (instead of biennial or periodic); (4) qualification of the area sampling provision; and (5) general length and complexity (as unnecessary impediments to small business compliance). Support for OSHA compliance directive interpreting *Castle & Cooke Foods*, CPL 2-2.35. The cost-benefit issue in general, and the impact of the Supreme Court's 1981 cotton dust decision and Executive Order 12291 on cost-benefit analysis. Industry's position regarding further rule-making on the Noise Standard.

3:20

J4. Some practical aspects of OSHA noise litigation. Russell J. Thomas, Jr. (Pepper, Hamilton and Scheety, 100 Renaissance Center, Suite No. 3730, Detroit, MI 48243)

Abstract unavailable.

3:45

J5. The practical side of determining feasibility of engineering noise controls. Charles M. Chadd (Pope, Ballard, Shepard, and Fowle, Ltd., 69 W. Washington Street, Chicago, IL 60602)

As set out in *Continental Can Company, Castle & Cooke* and other noise cases decided by the Occupational Safety and Health Review Commission before its *Sun Ship* decision, determination of the economic feasibility of engineering controls is a practical matter which balances all costs and benefits of engineering and compares them to the costs of hearing conservation. Under OSHA's new instruction CPL 2-2.35, the agency has adopted this approach. Factors that must be considered in determining the costs of engineering controls include not only the costs of design, development, construction, and implementation, but also the continuing costs of living with the controls such as lost production or efficiency, decreasing product quality, increasing amount of rejects, maintenance of the equipment with which the controls are associated, and maintenance of the engineering controls. Because many purported engineering controls merely involve encasing or blocking the sound by some type of enclosure or barrier, or enclosing the employee, important factors in determining the feasibility are the effects of a control on employee's ability to perform his job and the acceptance level of the control as compared to ear protection.

4:10

J6. Legal issues arising under OSHA's noise standard. Robert D. Moran (Vorys, Sater, Seymour, and Pease, Suite 1111, 1828 L Street, NW, Washington, DC 20036)

At what level, if any, is noise a "harmful" physical agent subject to regulation under § 6(b) (5)? Only § 6(b) (5) standards can include requirements for noise monitoring and audiometric testing. Is the present noise standard such a regulation? Are employees exposed to hazard when they are wearing devices which attenuate surrounding noise to within permissible levels? Can OSHA impose engineering control requirements in such cases? Is a single 8-h exposure to excessive noise legally sufficient to trigger the standard's requirements? Can any part of an employer's obligation be based upon employee hearing loss not caused by that employer's noncompliance? Can OSHA impose any requirement on the basis of 80 and 85 dB noise levels which are admittedly well below the permissible 90 dB limit? Finally, is the imposition of administrative and engineering requirements to control workplace noise "reasonably necessary or appropriate" when hearing protectors are available which will achieve an equal or greater attenuation in such noise? No OSHA requirement is legally permissible unless it is reasonably necessary or appropriate to achieve a safe work environment.

J7. Feasible engineering noise controls in General Motors Corporation. James H. Pyne (Plant Engineering Programs, General Motors Corporation, General Motors Building A-290, 3044 West Grand Boulevard, Detroit, MI 48202)

The implementation of engineering noise controls on existing, rebuilt, and new equipment must take into account both technological and economic feasibility. Retro-fitting engineering controls to existing noisy equipment on the production floor, while desirable and in some instance necessary, can have serious negative economic consequences. Costs resulting from decreased productivity, increased maintenance, frequency of replacement, and possible increased floorspace requirements are all factors which must be considered. General Motors Corporation, (GM, while pursuing the investigation and implementation of feasible engineering noise controls on existing equipment, places special emphases on the purchase of new equipment. The "General Motors Corporation Sound Level Specification for Machinery and Equipment," Revision February 1979, specifies a maximum time-weighted average sound level of 80 dB (A). Measurements are taken at the operator's ear location and on the measurement envelope as specified in "NMTBA Noise Measurement Techniques" Second Edition dated January 1976. GM, working in conjunction with its suppliers, has experienced considerable success in achieving feasible engineering controls through the application of the GM Purchase Specification.

4:50

J8. The Singapore construction noise standard. Raymond B. W. Heng^a (Department of Mechanical Engineering, National University of Singapore, Kent Ridge Campus, Singapore, Republic of Singapore 0511)

With the construction boom presently being experienced in Singapore and further massive construction and demolition programs expected for the proposed new Mass Rapid Transit system, construction noise is now a major problem that has to be controlled with urgency. Studies for the development of a suitable Singapore Code of Practice for control of noise from construction and demolition sites began in 1978 with investigation of the standards of other countries available at that time. Local construction methods and equipment were surveyed and noise studies carried out at various sites. A survey was conducted among residents in different parts of the country, zoned according to differing local conditions and sensitivities. Laboratory studies were also carried out to determine subjective response of the local population to the noises expected during various stages of the construction works. From these, the L_{eq} equivalent energy level unit was chosen as an adequate noise descriptor but the L_{eq} (5 min) was adopted rather than the more usual daily or 12-h L_{eq} for prediction, measurement as well as control purposes. Considerable thought was given to establishing acceptable noise levels which continue to be economically realistic for the survival of the local construction industry. Some of the aspects involved in the implementation of noise control procedures as well as the extent to which public approval could be more effective than resorting to the usual legal actions are reviewed. " Present address: Department of Mechanical Engineering, University of Sheffield, Mappin Street, Sheffield S1 3JD, United Kingdom.

MONDAY AFTERNOON, 7 MAY 1984

BRANDON ROOM, 2:00 TO 4:35 P.M.

Session K. Physiological Acoustics IV and Psychological Acoustics II: Pitch Perception

Charles S. Watson, Chairman

Department of Speech and Hearing, Indiana University, Bloomington, Indiana 47405

Chairman's Introduction-2:00

Contributed Papers

2:05

 K1. Pitch-relevant patterns of discharge synchronization to twocomponent signals in cochlear nerve fibers of the cat. Steven Greenberg,
 C. Daniel Geisler, and L. Deng (Department of Neurophysiology, University of Wisconsin, 1300 University Avenue, Madison, WI 53706)

Over 40 years ago, Jan Schouten proposed that the pitch of complex tones is derived from the activity of peripheral auditory neurons synchronized to the temporal fine structure of the cochlea-filtered signal [J. F. Schouten, Proc. K. Ned. Akad. Wet. 43, 991-999 (1940)]. The present study sought to evaluate Schouten's model by recording the responses of low-frequency cochlear fibers from the cat during presentation of two (isoamplitude)-component signals which, in human listeners, produce a reliable sensation of low pitch [G. F. Smoorenburg, J. Acoust. Soc. Am. 48, 924-942 (1970)]. Signal frequencies, f_1 and f_2 , arithmetically centered around the fiber's characteristic frequency (CF), conformed to the equations (1) $f_1 = [2n/(2n + 1)]$ CF; (2) $f_2 = [(2n + 2)/(2n + 1)]$ CF, where $n = f_1/(f_2 - f_1)$ and assumed values between 2.5 and 8.5. A large proportion of cochlear fibers synchronize to both frequency components in approximately equal measure (thus implying synchronization to a half-wave recitified version of the signal's temporal fine structure), even when the signal components are as much as half an octave apart. These data are consistent with the basic tenor (if not the details) of the temporal fine structure model. However, it remains uncertain whether such pitch-relevant information is utilized by higher auditory centers. [Research financially supported by NIH.]

2:20

K2. Perception of complex-tone pairs mistuned from unison: Waveform relations determines whether pitch glides or iterated complex auditory patterns are heard. Richard M. Warren, Brad S. Brubaker, and Daniel A. Gardner (Department of Psychology, University of Wisconsin-Milwaukee, Milwaukee, WI 53201)

When a broad-spectrum complex tone (CT) (whether derived from a voice, musical instrument, pulse train, or randomly generated waveform), having a stable frequency and containing harmonics above the 7th or 8th, is mixed with itself after a slight (1 Hz or less) change in the waveform repetition frequency, listeners hear a rising glissando when fine structures of the correlated waveforms approach alignment and a falling glissando as they move away. If harmonics above the 8th are removed, multiple beats are heard (not glissandi) with the dominant repetition frequency equal to the difference (in Hz) between the CTs. When two broad-spectrum uncor-

MONDAY PM

related CTs mistuned slightly from unison are mixed, complex periodic patterns rather than glissandi are heard: Multiple beats dominate following removal of harmonics above the 8th (the dominant repetition frequency heard in each case equals the difference in Hz between the uncorrelation CTs). These observations provide information concerning the nature of spectral and periodicity analyses of iterated acoustic patterns. [Work supported by NSF.]

2:35

K3. Discrimination of binary tone sequences. Robert D. Sorkin (Department of Psychological Sciences, Purdue University, West Lafayette, IN 47907)

Subjects were presented with two sequences of tones, e.g., HLLHHHLL, HLHLHHLL. The tones were either 669 Hz or 1621 Hz. Subjects were instructed to respond "same" if the same serial pattern of high and low tones were repeated in the second sequence. They were to ignore any variation in the time between the tones. Performance was assessed in a variety of task conditions. The variables studied included: the number of tones, the mean time separation between tones, the magnitude of variability (jitter) in the time between tones, the correlation between the jitter pattern in the two sequences, the pattern variability in the sequences, and the serial position of pattern differences between the sequences. The results are interpreted using an extension of the auditory memory model developed by Durlach and Braida [J. Acoust. Soc. Am. 46, 372-383 (1969)]. This model postulates two independent memory modes, a trace (time-dependent) mode, and a context coding (set-size-dependent) mode. The data provide general support for the extension of the dual mode model to this task. [Work supported by NSF.]

2:50

K4. Pitch discrimination as a function of tone duration. W. M. Hartmann and T. N. Packard (Physics Department, Michigan State University, East Lansing, MI 48824)

Numerous experiments have studied pitch discrimination for sine tones as a function of the duration T of the two tones to be discriminated. All the data agree that as T decreases the uncertainty in pitch discrimination becomes larger, and the functional dependence of the uncertainty on T has been used to test various models of pitch perception. However, all simple models, whether temporal or spectral, predict that if the two tones have different durations, T_1 and T_2 , then the uncertainty should lie between the uncertainty obtained when both tones have duration T_1 and the uncertainty obtained when both tones have duration T_2 . To find out whether this is so we measured the variability in a pitch matching task where the tones to be matched had different durations. The matching task provides data on pitch uncertainty in the presence of large duration-dependent pitch shifts whereas a standard discrimination experiment does not. We studied seven different frequencies between 200 and 7000 Hz and all combinations of 12, 25, and 50 ms for T_1 and T_2 . Ninety percent of the data with $T_1 \neq T_2$ show a variability which is larger than would be expected based upon the variability in the data with $T_1 = T_2$. We believe that it is possible to understand these results in terms of an improved statistical decision theoretic model of pitch perception. [Work supported by the National Institutes of Health Grant 17917.]

3:05

K5. Frequency discrimination for conditions of roving standard and random interstimulus interval. Gerald Kidd, Jr., and Donna L. Neff (Laboratory of Psychophysics, Harvard University, 33 Kirkland Street, Cambridge, MA 02138)

A two-interval forced-choice adaptive tracking procedure was used to estimate the frequency difference limen (DL). In one condition, the frequency of the standard tone was constant for every trial with the frequency of the comparison tone varied according to the adaptive procedure. The interval between standard and comparison stimuli (ISI) was fixed. In contrast to this "fixed-standard fixed-ISI" condition, other conditions were tested in which the standard frequency and/or the ISI were chosen on each trial according to pseudo-random algorithms. The results indicate that the frequency DL may increase by as much as a factor of 2 for

some roving-standard and random ISI conditions. In addition, a trial-bytrial record of each run was used to assess discrimination performance as a function of frequency and ISI. The decay of the sensory trace with increasing ISI, and uncertainty about signal frequency and timing appear to account for the changes in discrimination. [Supported by NIH.]

3:20

K6. Two kinds of pitch: Matching and discrimination with complex signals. C. Douglas Creelman and Anthony Komar (Department of Psychology, University of Toronto, Toronto, Canada M5S 1A1)

With specially constructed harmonic stimuli, observers matched pitch neither to the period of the stimuli nor to the fundamental of components in the spectral "critical region." The lowest and highest components of the stimuli were multiples of three times the (missing) fundamental frequency, while the central components were multiples of twice the (missing) fundamental frequency. Matches were almost equally divided between the two secondary fundamentals, with very little variability. There were no matches to the fundamental. In a second experiment, observers discriminated between the frequencies of complex stimuli, including those used in the first study as well as more traditional "missing fundamental" stimuli. The data suggest that pitch-discrimination is based on the actual frequency components present in the stimuli, rather than on the apparent or perceived pitch. These findings imply at least two "pitch" mechanisms, one responsible for perceived pitch, and the other required for relative judgment and fine discrimination. [Work supported by NSERC.]

3:35

K7. Mechanisms in auditory discrimination: Ontogeny and phylogeny. Joan M. Sinnott (Psychology Department, Indiana University, Bloomington, IN 47405)

Previously reported data indicates that human adults, human infants, monkeys, and birds can all be easily trained to discriminate frequency increments, frequency decrements, and intensity increments in a pulsedtone stimulus using a repeating standard procedure and operant conditioning techniques. However, it is difficult, if not impossible, to train infants, monkeys, and birds to discriminate intensity decrements using the same methods, although human adults experience no difficulty with this task. An hypothesis to account for these results will be proposed: Discrimination of frequency increments, frequency decrements, and intensity increments implies a coding mechanism based on detecting rate increases in populations of peripheral auditory neurons, but discrimination of intensity decrements implies a mechanism based on detecting rate decreases. Therefore, the CNSs of human infants, monkeys, and birds may not be well adapted to monitoring rate decreases in peripheral auditory neurons. [Supported by Deafness Research Foundation.]

3:50

K8. Accuracy and perceptual asymmetry during dichotic pitch discrimination. John J. Sidtis (Department of Neurology, Cornell Medical Center, 1300 York Avenue, New York, NY 10021)

Dichotic listening studies with normal right-handed listeners and with patients who have suffered focal cortical lesions suggest that the right hemisphere plays an important role in complex pitch discrimination. The perceptual asymmetry observed in normal listeners was studied using a dichotic recognition test consisting of 500-ms square wave tones with fundamental frequencies corresponding to the 12 semitones in the octave 261.63-523.25 Hz. A diotic recognition probe followed the presentation of each dichotic pair. The probe was identical to one of the dichotic items on 50% of the trials. On the remaining trials, the probe differed from one of the dichotic items by 0.25, 0.50, 0.75, or 1.00 semitone. Subjects who demonstrated a left ear advantage on this test were significantly more accurate in their pitch discrimination than were subjects who demonstrated a right ear advantage. Within each group, left and right discrimination functions were similar. The right ear advantage for pitch discrimination may reflect a sub-optimal strategy for processing pitch or for selecting dichotic signals. [Supported by NIH.]

K9. The dependence of noise edge pitch and binaural edge pitch on the frequency width of the edge. W. M. Hartmann (Physics Department, Michigan State University, East Lansing, MI 48824, and Institut de Recherche et Coordination Accoustique/Musique, 31 rue Saint Merri, 75004, Paris, France)

A low-pass noise band with a sharp spectral edge produces a sensation of pitch, noise edge pitch (NEP), which matches a sine tone having a frequency below the noise edge frequency. Similarly a high-pass noise band results in a NEP above the edge frequency. Dichotic noise with an interaural phase shift varying rapidly with frequency at an edge frequency produces the binaural edge pitch (BEP). The BEP is bimodal and is normally equal to both the low-pass and the high-pass NEP. We performed pitch matching experiments to study both NEP and BEP as functions of the width of the edge. Edge center frequencies were between 150 and 1500 Hz, and the edge widths were 0%, 10%, 20%, and 40% of the edge center frequencies. Experimental variance increased with increasing edge width, but less than proportionally. The low-pass NEP increased systematically with increasing width, especially for edge frequencies above 300 Hz, where the NEP exceeded the edge center frequency for 30% and 40% widths. The high-pass NEP changed less predictably and it usually remained above the edge center frequency. The two modes of the BEP distribution changed less with increasing edge width than did either NEP. This difference in dependence challenges dichotic pitch perception models in which the BEP and the NEP have a common central origin. [Work partially supported by the NIH Grant 17917.]

K10. Binaural coherence edge pitch. W. M. Hartmann (Physics Department, Michigan State University, East Lansing, MI 48824)

The binaural coherence edge pitch (BICEP) is a dichotic broadband noise pitch effect similar to the binaural edge pitch. The noise is made by summing sine waves with equal amplitudes and random phases. The interaural phase angle is a constant for sine wave components with frequencies below a chosen frequency, and it is a random variable for components with frequencies above that frequency. The chosen frequency is a coherence edge because the signals to the two ears are mutually coherent within any band of frequencies below the edge and they are mutually incoherent in any band above the edge. Sine tone pitch matching experiments show that the BICEP exists for coherence edge frequencies between 300 and 1000 Hz and that it is always matched by a frequency above the edge frequency, by 5%-10%. The effect can be extended to higher edge frequencies, at least 2000 Hz, if the listener is appropriately cued. The results do not depend upon whether the coherent components are presented in phase or completely out of phase to the two ears. For the opposite case, coherence above the edge frequency and incoherence below, the BICEP can be reliably matched only for coherence edge frequencies between 300 and 600 Hz, and the matching frequency is invariably below the coherence edge frequency, by 10%-20%. [Work supported by the National Institutes of Health Grant 17917.]

MONDAY AFTERNOON, 7 MAY 1984

YORK HALL, 2:00 TO 5:20 P.M.

Session L. Speech Communication III: Speech Production

Fredericka Bell-Berti, Chairman

Department of Speech Communication and Theater, St. John's University, Grand Central and Utopia Parkways, Jamaica, New York 11439

Chairman's Introduction-2:00

Contributed Papers

2:05

L1. Relationships between articulatory and acoustic measurements from an x-ray microbeam study of variability in the production of the vowels /i/ and /a/. J. S. Perkell (Research Laboratory of Electronics, Massachusetts Institute of Technology, Cambridge, MA 02139) and W. L. Nelson (Bell Laboratories, Murray Hill, NJ 07974)

We have reported previously that midsagittal distributions of points on the dorsal tongue surface for multiple repetitions of the vowels /i/ and /a/ show more variation along a direction parallel to the vocal tract midline than perpendicular to the midline. This finding was interpreted as support for a hypothesis based on articulatory-to-acoustic modeling: the programming of movements towards the vowel targets is sensitive to nonlinear relationships between articulatory displacements and formants [J. S. Perkell and W. L. Nelson in Speech Motor Control, edited by S. Grillner, A. Persson, B. Lindblom, and J. Lubker (Pergamon, New York, 1982)]. Statistics on formant values for one subject have been calculated, and pairwise regressions of displacement and formant data have been run. An articulatory synthesizer [P. Rubin, T. Baer, and P. Mermelstein, J. Acoust. Soc. Am. 70, 321-328 (1981)] has been manipulated through displacements similar to the subject's articulatory variation. The range of formant variation for the subject is comparable to the range of formant values produced by the synthesizer. However, there were only very weak correlations between the subject's articulatory displacements and his formant data. Possible reasons for the lack of correlations will be discussed. [Work supported in part by NIH Grant No. NS04332.]

2:20

L2. From sagittal distance to area. A study of pharyngeal cross-sectional area of computer tomography. Carina Johansson, Johan Sundberg (Department of Speech Communication and Music Acoustics, Royal Institute of Technology (KTH), 100 44 Stockholm, Sweden), and Hermann Wilbrand (Department of Diagnostic Radiology, University Hospital, Uppsala, Sweden)

In studies of the articulation in speech, data on the pharynx are scarce. Still the pharynx is an important part of the vocal tract. The present paper reports on an attempt to use computer technology. Tomograms were taken at four levels in the pharynx of a male and a female subject sustaining the vowels /u, i, o, ce/. From the tomograms, the lateral width and the cross-sectional area are measured and their relations to the sagittal distance from the back pharynx wall to the midline of the tongue are examined and compared with previously published data. The results suggest relevant interindividual differences.

2:35

L3. Articulatory synthesis from underlying dynamics. Catherine P. Browman, Louis Goldstein, J.A.S. Kelso, Philip Rubin, and Elliot Saltzman (Haskins Laboratories, 270 Crown Street, New Haven CT 06510)

We are testing a model of articulatory coordination and control over time using an articulatory synthesizer (ASY) that converts time-varying

MONDAY PM

specifications of articulator positions into speed [Rubin, Baer, and Mermelstein, J. Acoust. Soc. Am. 70, 321–328 (1981)]. These articulator specifications are now generated from an underlying dynamical model that defines a particular linguistic event. Coordination among individual articulators emerges from this model, as does the time course of the event. No point-by-point temporal control is required. Synthesis will allow perceptual evaluation of different underlying dynamical models. [Work supported by NIH and ONR.]

2:50

L4. A dynamic analysis of reiterant speech production. J. A. S. Kelso (Haskins Laboratories, 270 Crown Street, New Haven, CT 06510 and University of Connecticut, Storrs, CT 06268), E. V. Bateson (Haskins Laboratories, 270 Crown Street, New Haven, CT 06510 and Indiana University, Bloomington, IN 47401), E. L. Saltzman (Haskins Laboratories, 270 Crown Street, New Haven, CT 06510), and B. Kay (Haskins Laboratories, 270 Crown Street, New Haven, CT 06510), and B. Kay (Haskins Laboratories, 270 Crown Street, New Haven, CT 06510), and B. Kay (Haskins Laboratories, 270 Crown Street, New Haven, CT 06510 and University of Connecticut, Storrs, CT 06268)

Speaking, like other biological activities, emerges from a neuromuscular basis of high dimensionality as a coherent pattern of articulator motions. What form, if any, does such coherence take and how might it be rationalized? Conventional analyses of articulatory motion are not always informative. Here we use the tools of qualitative dynamics, particularly phase portrait techniques [cf. J. A. S. Kelso and E. V. Bateson, J. Acoust. Soc. Am. Suppl. 173, S67 (1983)] to analyze articulatory gestures from an experiment in which speaking rate and stress are naturally varied. We show that the strong relationship between a gesture's amplitude and peak velocity may be accounted for when movements are analyzed in an action (energy imes duration) versus amplitude performance space. The action for a given gesture (associated with consonant-vowel and vowel-consonant transitions) and for a given speaker scales to (amplitude)². This finding suggests (1) that stiffness is a key dynamic parameter of the articulatory system, and (2) that an elastic similarity principle may underlie the articulatory behavior of different speakers. [Work supported by NIH, BRSG, and ONR.]

3:05

L5. Characterization of tongue shape during normal speech. Kathleen A. Morrish (Department of Diagnostic Radiology, National Institutes of Health, Bethesda, MD 20205), Maureen Stone, Thomas H. Shawker, and Barbara C. Sonies (Department of Rehabilitation Medicine and Diagnostic Radiology National Institutes of Health, Bethesda, MD 20205)

Averaged tongue shapes and polynomial equations were computed for five phonemes in order to determine aspects of tongue curve which distinguish between phonemes. Five repetitions of each of the phonemes /i/, /u/, /o/, /x/, and /a/ were produced by a normal volunteer using the carrier phrase "I can say /dVd/again." An ultrasound sector scanner was used to obtain midsagittal pictures of the posterior section of the tongue from vertical to 85° back into the throat. The pictures were digitized, and the resulting points were used to generate average tongue shapes and average quadratic and cubic fits for each phoneme. While both techniques provide information which allows the researcher to distinguish between the five phonemes used, only the averaged tongue shapes adequately reflect certain details of tongue shape.

3:20

L6. Temporal organization of muscle activity in simple disyllables. Michèle Gentil (Centre Scientifique IBM-France, 36 Av. Raymond Poincare, 75116 Paris, France), Katherine S. Harris, Satoshi Horiguchi (Haskins Laboratories, 270 Crown Street, New Haven, CT 06510), and Kiyoshi Honda (Research Institute of Logopedics and Phoniatrics, Faculty of Medicine, University of Tokyo, Tokyo, Japan)

In an earlier paper, Tuller and her associates have shown that the onsets of consonant and vowel related activity in several articulatory muscles tend to maintain a constant relationship over changes in stress and speaking rate [Tuller *et al.*, J. Exp. Psychol. Percept. Perf. **8**, 460–472

(1982)]. Similar results are found for analogous kinematic events [Tuller *et al.*, J. Exp. Psychol. Percept. Perf. 9, 829–833 (1983)]. The present study confirms and extends the results of the original electromyographic study, for a speaker of a different language (French rather than English), for a somewhat extended consonant and vowel inventory /p VC p a p/, where V = /i, a, or u/, and C = /p, t, s/; and for a somewhat broader range of muscles, five associated with tongue movement, and two others associated with lip and jaw movements. The constancy of the relative timing is compatible with a model of speech production in with coordinative structures are specified. [Research supported by NINCDS.]

3:35

L7. Electromyographic and kinematic measures of articulatory coordination in a deaf speaker. Nancy S. McGarr, Noriko Kobayashi, and Kiyoshi Honda⁴ (Haskins Laboratories, 270 Crown Street, New Haven, CT 06510)

Variability in production and disruption of interarticulator timing is reported for a deaf speaker. Acoustic, electromyographic, and movement records were obtained from a deaf subject and a hearing control, producing multiple repetitions of nonsense syllables (e.g., a bib a b) with stress on either V_1 or V_2 . Electromyographic recordings were obtained from genioglossus, geniohyoid, and anterior belly of digastricus. Temporal patterns of lip closure were recorded using an electrical conductance technique. Infrared LEDs were attached to the jaw and monitored using a modified SELSPOT optical tracking system. Tokens were sorted into perceptually correct versus error patterns according to listener judgments, and formant frequency measures obtained. The deaf speaker differed from the normal control in several ways. She was unable to consistently execute changes in stress across different syllables and did not differentiate high versus low vowels in either genioglossus or relative jaw position. Timing of geniohyoid was variable and did not accompany stress changes. While activity of digastricus paralleled jaw movement, the duration of muscle activity continued well beyond maximum displacement of the jaw, perhaps contributing to laryngeal instability. [Work supported by NINCDS.]^{a)} Also: University of Tokyo, Japan.

3:50

L8. Contribution of mandible movement to lower lip and tongue blade movements. Jan Edwards (Haskins Laboratories, 270 Crown Street, New Haven, CT 06510 and The Graduate Center, City University of New York, New York, NY 10036) and O. Fujimura (AT&T Bell Laboratories, Murray Hill, NJ 07974)

Apparent violations of the sequential organization of phonetic gestures in the observed time series of constrictive positions were reported by Fujimura [Phonetica (1980)]. Using data collected by the x-ray microbeam system [Kiritani et al., J. Acoust. Soc. Am. (1975)], we have found that the temporal structure of lip and tongue blade movement patterns can be interpreted more straightforwardly if the jaw component of lip and tongue blade movements is subtracted. Previously observed violations of segmental sequencing are largely interpretable as the superposition of mandible gestures onto lip or tongue blade gestures. This suggests that apparent complexities and variabilities of the observed movement patterns may be reduced by distinguishing between stress-related syllabic gestures and place-related consonantal gestures. Different functions assigned to the articulators can be implemented via articulatory subsystems with different dynamic characteristics. This implies that in speech perception the interpretation of acoustic signals involves the undoing of these temporal complications in order to identify the "correct" sequential patterns. [Supported in part by NINCDS.]

4:05

L9. Remote and autogenic articulatory adaptation to jaw perturbations during speech: More on functional synergies. Eric V. Bateson and J. A. S. Kelso (Haskins Laboratories, 270 Crown Street, New Haven, CT 06510)

The present research is a continuation of a program devoted to understanding the cooperative behavior among neuromuscular elements during speech. In an earlier study, we found functionally specific electomyographic and kinematic evidence of compensation in remote articulators (upper lip and tongue) to perturbations of the jaw [J. A. S. Kelso, B. Tuller and C. A. Fowler, J. Acoust. Soc. Am. Suppl. 1 72, S103 (1982)]. Here we extend the earlier work to include additional subjects and phonetic contrasts and to test for phase dependent perturbation effects on the extent and style of compensation. We observe in this case that compensation in perturbed productions of /bæb/ and /bæp/ is primarily autogenic, that is local to the perturbed structure itself, the lower lip-jaw complex. We also find that contrasts not involving different articulators, e.g., between final /b/ and /p/, differ only in the degree to which compensation is achieved; the paterns are kinematically similar. The phase at which the jaw cycle is perturbed does not seem to affect either the position to which the system recovers following perturbation or the style of compensation. There are, however, phase dependent acoustic differences which suggest that compensation of a largely autogenic kind is not sufficient for complete compensation. [Work supported by NINCDS and ONR.]

4:20

L10. Modeling the source for fricative consonants. Christine H. Shadle (Research Laboratory of Electronics, 36-521, Massachusetts Institute of Technology, Cambridge, MA 02139)

Turbulence noise in the vocal tract, which plays a role in the production of fricative and stop consonants, is usually modeled by placing one or more sound-pressure sources with smooth spectra in series with a onedimensional model of the vocal tract [G. Fant, Acoustic Theory of Speech Production (Mouton, 1960)]. In this paper it is shown that this model is consistent with the sound generated when a jet of air impinges on an obstacle. Theoretically, the sources at the obstacle are dipoles, and thus are equivalent to a pressure source. Experimentally, the power spectrum of the sound generated by a mechanical model corresponds closely to the transfer function simulated for a tube with identical area function and a pressure source at the location of the obstacle. When no obstacle is present downstream of the constriction in the model, no such correspondence is observed, indicating that for this case a distributed source is a better model of the sound generation mechanism. Analysis of spoken sustained fricatives shows a similar division between stridents (with obstacle) and nonstridents (without an obstacle). [Work supported by NIH.]

4:35

L11. Asymmetries in placement and timing of alveolar tongue contact patterns for /s/ and /l/. Sandra L. Hamlet and T. Bunnell (Department Hearing and Speech Sciences, University of Maryland, College Park, MD 20742)

The "central groove" of the tongue for /s/, and the alveolar tongue contact pattern of /l/ frequently show left-right asymmetries. These articulatory asymmetries are highly consistent within an individual, but do not seem to bear a clear relationship to other type of sidedness, such as hand preference. Left-right differences in alveolar and palatal contour have been suggested as a causal factor. The present study employed dynamic palatography with five subjects. Tongue contact for /s/ was initiated earlier on one side, as if to anchor the tongue. Subsequently, a more anterior groove formation followed. Contact and release in a VCV environment were similar, with the side touched first at onset of /s/ being the side to be released later. The side with greater (and usually earlier) contact for /s/ was generally also more widely contacted for /l/, such that the lateral margin of the tongue appeared at times to be free only on one side. Since sidedness was similar for /s/ and /l/, /sl/ blend articulation was simplified. Preliminary results of an experiment in altering the oral contour with a dental appliance, thicker on one side, and the resulting palatographic changes will also be discussed. [Work supported by NIDR.]

4:50

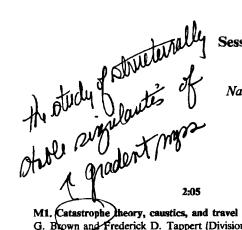
L12. Coarticulation in lateral pharyngeal wall movements. Avraham Parush and David J. Ostry (Department of Psychology, McGill University, Montreal, H3A 1B1, Canada)

Medial movements of the lateral pharyngeal wall (LPW) at the level of the velopharyngeal port were examined using a computerized ultrasound system. Subjects produced CVNVC sequences with all combinations of the vowels /a/ and /u/, and the nasal consonants /n/ and /m/. The flanking consonants were always /p/. The effects of either vowel upon the CVN or NVC gestures (opening or closing of the velopharyngeal port, respectively) were assessed in terms of displacement, duration, and movement onset time. Both CVN and NVC gestures were primarily affected by the initial vowel: movements had less displacement when the initial vowel was /a/. The onset of the CVN (opening) gesture was affected by the final vowel: the movement started earlier, during initial consonant closure, when the final vowel was /a/. In addition, the duration of this gesture was longer when the final vowel was /a/. Finally, no consistent carryover effects of the initial vowel were found upon the onset time or duration of the NVC gesture. The findings are discussed in terms of the role of LPW movements in the operation of velopharyngeal port.

5:05

L13. Velar position and port size: Spectral and perceptual effects. F. Bell-Berti (Department Speech Communication and Theater, St. John's University, Jamaica, NY 11439 and Haskins Laboratories, New Haven, CT 06510), T. Baer (Haskins Laboratories, New Haven, CT 06510), and L. J. Raphael (Lehman College, City University of New York, Bronx, NY 10468 and Haskins Laboratories, New Haven, CT 06510)

We have used an articulatory synthesizer to study the effects of independent and systematic changes in velar position and velar port size on vocal tract transfer functions of vowels. We have also examined the acoustic and perceptual effects of combining these components of natural nasalizing gestures. Lowering the velum, in the absence of nasal coupling, has small effects, primarily on F_2 and F_3 frequencies. On the other hand, opening the port without lowering the velum has the greatest influence on F_1 frequency, shifting it upward or downward, as necessary, to produce a concentration of spectral energy at about 400 Hz. As expected, the combined effects of lowering the velum and opening the velar port are more heavily influenced by nasal coupling than by changes in velar position. We have also found differences in the degree of perceived nasality associated with velar port areas from 0 to 84 mm², as a function of the oral vowel (0 mm²) quality. [Work supported by NINCDS.]

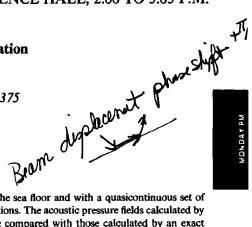


Session M. Underwater Acoustics I: Propagation

Ralph Baer, Chairman Naval Research Laboratory, Washington, DC 20375

Chairman's Introduction-2:00

Contributed Papers



M1. Catastrophe theory, caustics, and travel time diagrams. Michael G. Brown and Frederick D. Tappert (Division of Ocean Engineering, Rosenstiel School of Marine and Atmospheric Science, University of Miami, Miami, FL 33149)

A commonly used technique in the analysis of broadband underwater acoustic wave data is to display the times of arrival of geometric rays as a function of position (typically range or depth). When caustics are present these travel time diagrams are multivalued functions of the position coordinate. Catastrophe theory may be used to classify these caustics. When the ocean properties vary as a function of depth or depth and range only and the waves are excited by a compact source then all of the caustics formed belong to the cuspoid family. The following result, which pertains to this situation, is proved: the locus of travel times of the geometric rays which form a cuspoid caustic of codimension n form a surface in the n + 1dimensional space $(t, x_1, x_2, ..., x_n)$ which is identical (after a stretching of coordinates) to the locus of singular points (the caustic surface) of the cuspoid caustic of codimension n + 1 in the (n + 1)-dimensional space $(x_1, x_2, \dots, x_{n+1})$. A consequence of this result is that any structurally stable travel time diagram corresponding to a one-dimensional ocean model must be a two-dimensional slice of one of the cuspoid caustics. Some of the implications of this result are discussed including how constraints imposed on travel time diagrams by catastrophe theory might be exploited in the inverse travel time problem.

2:20

M2. The effect of a cyclonic ring on 3-D ray geometry. R. Pitre and T. L. Foreman (Applied Research Laboratories, The University of Texas at Austin, Austin, TX 78712-8029)

A 3-D ray trace model has been constructed and employed in an examination of horizontal deflection effects due to a cyclonic ring. The ring examined had a radius of 125 km, a maximum flow rate of 100 cm/s, and a maximum isotherm uplift of 300 m. Effects of fluid motion on ray geometry were found to be negligible; but horizontal gradients of the index of refraction caused significant deflection. The maximum deflection of 0.75° occurred for a ray traveling along the SOFAR channel axis. Rays which oscillate about the SOFAR axis experience less horizontal deflection. An examination of deflection versus impact parameter indicates that the rays which encounter the eddy with an impact parameter of roughly one-half of the eddy radius experience maximum deflection. A group of rays launched in the same vertical plane experiences an azimuthal angle dispersion of 0.5° in crossing the eddy. [Work supported by the Office of Naval Research.]

2:35

M3. Ray theoretic modeling applied to low-frequency interaction with the sea floor. Martin W. Lawrence⁴⁾ (Woods Hole Oceanographic Institution, Woods Hole, MA 02543)

A computer model has been developed which uses ray theory, with various corrections, to provide calculated acoustic pressure fields for a given geoacoustic model of the sea floor. This computer model has been used to provide acoustic pressure fields for comparison with those measured in the deep ocean using a harmonic source located near the sea floor, with receivers also near the sea floor and with a quasicontinuous set of source-to-receiver separations. The acoustic pressure fields calculated by the ray theory model are compared with those calculated by an exact technique (using the Hankel transform). The decomposition of the acoustic field into components generated by different ray families is used to assist in understanding the results of the exact technique. The effect of variation of some experimental parameters can be more easily studied using this model than the Hankel transform model. For example, the effect of source height variation may be addressed.^{a)}The author is on exchange from the Royal Australian Navy Research Laboratory, P. O. Box 706, Darlinghurst, Australia 2010.

2:50

M4. Inversion of shallow water reciprocal transmission data to determine current profiles. H. A. DeFerrari, N. J. Williams, and D. S. Ko (Rosenstiel School of Marine and Atmospheric Science, University of Miami, FL 33149)

Acoustic reciprocal transmission geometries have been used to remotely measure fluctuations of ocean current and temperature. Usually, the travel time of a pulse is used as a measure of the integrated sound speed or current along a ray path. Reciprocal transmission experiments in the Florida Straits are characterized by refracted, bottom reflected rays making multiple bottom reflections resulting in a continuum of multipath arrivals. Owing to interference, distinct arrivals cannot be identified and used for travel time measurements. As an alternate method, we are comparing the phase differences for the upstream and downstream pulse arrival patterns. Modeling the sound channel with a linear sound speed profile, sloping bottom, we find that arrival time is linearly related to the average height of the rays above the bottom. Thus phase differences for upstream and downstream transmissions are proportional to depth average currents making possible a simplified inversion to obtain current profiles. At the time of this writing, we are attempting to demonstrate the method with existing data from recently completed experiments in the Florida Straits. Results of the data analysis will be presented along with the details of the models.

3:05

M5. A comparison of parabolic equation predictions with reciprocal transmission measurements in the Florida Straits. L. Nghiem-Phu (Daubin Systems Corporation, Miami, FL 33149) and H. A. DeFerrari (Rosenstiel School of Marine and Atmospheric Science, University of Miami, Miami, FL 33149)

A parabolic equation model has been developed to study transmission in the Florida Straits and to interpret the results of reciprocal transmission experiments. The model source is both broadband and narrow beam. The bandwidth makes possible prediction of pulse arrival patterns and travel times. The narrow beam shows the path of sound energy between source and receiver. Both arrival times and sound paths are necessary to invert acoustic measurements to give oceanographic measurements of currents and water temperatures. Color graphic displays are used to demonstrate ray-type paths through the medium, using environmental data as inputs; model results are compared with results of pulse reciprocal transmission experiments for several geometries and range-dependent soundspeed profiles and bottoms.

M6. Low-frequency sound propagation across a bathymetric ridge in the Strait of Juan de Fuca. David G. Browning, Ding Lee, George Botseas, and Paul D. Scully-Power (Naval Underwater Systems Center, New London Laboratory, New London, CT 06320)

In the deep ocean, bathymetric ridges have been shown to have a significant effect on low-frequency sound propagation [R. W. Bannister *et al.*, J. Acoust. Soc. Am. **62**, 847–859 (1977)]. These results may be further enhanced in the relatively shallow Strait of Juan de Fuca where a bathymetric ridge forms a sill across the Strait running north-south between Victoria, British Columbia and Port Angeles, Washington. This ridge not only significantly changes the bottom contour but also is the boundary between two distinctly different oceanographic domains. The implicit finite difference (IFD) model is used to determine the relative importance of changing bottom slope and oceanographic conditions across the ridge as factors affecting low-frequency (10–200 Hz) sound propagation. [Research supported by NUSC.]

3:35

M7. A high-speed, compact, and interactive Parabolic Equation SOlution GENerator (PESOGEN) system. Lan Nghiem-Phu, Scott C. Daubin (Daubin Systems Corporation, Miami, FL 33149), and Fred Tappert (University of Miami, DSC, Miami, FL 33149)

A special purpose microcomputer to solve the parabolic approximation to the acoustic wave equation using the split step Fourier algorithm has been developed. The Parabolic Equation SOlution GENerator (PE-SOGEN) is a dedicated, fast, compact, and interactive computer system consisting of a host processor, a high-speed array processor, a graphic processor, and a color display monitor. PESOGEN is able to compute the acoustic field in a fully range dependent environment for both deep and shallow water scenarios with computational speed an order of magnitude faster than current mainframes such as the UNIVAC 1108. Transmission loss values are color contoured and are available as the solution is being generated, providing almost real time interaction with the acoustic modeler. Additional graphic capability includes transmission loss displayed as a function of range at any depth, bathymetry, and sound speed profiles superimposed on TL color contoured field. Typical throughput time for a deep ocean environment to cover 14 CZs ranges from 16 to 100 s. Sample outputs from the PESOGEN that clearly demonstrate acoustic energy distribution in the acoustic field are presented.

3:50

M8. The numerical modeling of underwater acoustic wave propagation using finite element or finite difference methods. Charles I. Goldstein (Applied Mathematics Department, Brookhaven National Laboratory, Upton, NY 11973), Alvin Bayliss, and Eli Turkel^a) (Exxon Research and Engineering Corporate Research Science Labs, Annandale, NJ 08801)

The Helmholtz equation with wavenumber K in vector and scalar form describes a wide range of acoustic phenomena. As one example, the propagation of sound waves underwater in the presence of strong lateral variations in topography and sound speed must often be described by the Helmholtz equation since approximate propagation models can be inadequate. If the equation is discretized by a numerical scheme with mesh size h, the accuracy of this discretization is generally measured by the number of points/wavelength, $2\pi(Kh)^{-1}$. We show that Kh is not a good indicator of the accuracy of the discretization. If a scheme of order m is used, then we show that mean square errors depend on $KL(Kh)^m$, where L is a measure of the size of the computational region. Thus for a standard secondorder scheme, $h \sim (KL)^{-3/2}$ is required in order to maintain a fixed accuracy as K or L increases. This is a much more stringent requirement than the behavior $h \sim (KL)^{-1}$, which follows from using a fixed number of points/ wavelength. Several practical consequences of this result will be enumerated. The result will be justified mathematically and illustrated by numerical examples for a model of underwater acoustic wave propagation. The numerical results will be obtained using an efficient iterative technique we have recently developed for solving the discrete equations. *) Permanent address: University of Tel-Aviv, Tel-Aviv, Israel.

M9. Acoustic reflection from Arctic ice cover. Diana F. McCammon and Suzanne T. McDaniel (Applied Research Laboratory, Penn State University, University Park, PA 16802)

The ice canopy that covers large areas of the Arctic in winter is acoustically a very complex structure. It is a layered, anisotropic solid containing brine drainage channels as well as inclusions of brine and precipitated salts. Because of this complexity, it is desirable to ascertain those ice characteristics that play a dominant role in the reflection process. To this end, the plane-wave reflection coefficient for reflection process. To this end, the plane-wave reflection coefficient for reflection from smooth ice and snow cover has been modeled using a matrix approach. Results are presented for frequencies of 1 to 5 kHz, showing the effect of layers of ice chosen to conform to a measured sound velocity profile in floe-ice. The reduction in reflectivity due to the absorption of shear and compressional waves in ice are displayed and the effect of the addition of a 30-cm snow layer is demonstrated. [Work supported by ONR.]

M10. Possible effects of snow layer absorption on under ice reflectivity. Orest Diachok, Stephen Wales, and Tran Ngoc (Naval Research Laboratory, Washington, DC 20375)

4:20

Sea ice, which consists of relatively flat plates (nominally 2.5-m thick), randomly interrupted by ridges (rubble piles of broken ice), is generally coverged by a thin layer (nominally 0.2 m) of snow. The reflection coefficient from snow-covered sea ice plates, computed with the FFP, reveals generally large losses at frequencies higher than 100 Hz and grazing angles greater than 10°. Losses are maximum for frequency-angle combinations that permit conversion to Lamb modes in the ice plate. Loss magnitudes are particularly sensitive to the snow layer absorption coefficient. Computed results are consistent with reflectivity versus frequency and grazing angle ($\Theta > 14.3^{\circ}$) measurements reported by Yang and Votaw [J. Acoust. Soc. Am. (1981)], assuming their estimates of plate thickness and historical ice and snow velocity, density, and absorptivity data. At grazing angles less than 10° computations suggest that snow effects on the reflection coefficient are small, a result which is consistent with the hypothesis that long-range under-ice propagation loss is dominated by ridges [Diachok, J. Acoust. Soc. Am. (1976).]

4:35

M11. Model for Arctic propagation loss using scattering integrals and empirical reflection losses. D. F. Gordon and H. P. Bucker (Naval Ocean Systems Center, San Diego, CA 92152)

A normal mode program for under ice propagation has been developed. To permit rapid computation, eigenvalues are determined for lossless boundaries and attenuation is then added for reflection losses. Scattering from nonspecular angles is included by integration over ray paths from the surface to the source and receiver. Various published shot data were assembled and compared with computed propagation losses, using graphical methods, to determine ice reflection losses. Losses for ranges greater than 100 km gave the most definitive values for ice loss. Losses for shorter ranges, with greater dependence on grazing angles from 0° to 10°, were less definitive. Therefore, a linear function in decibels with 0-dB loss at 0° was assumed for the ice loss. The slope was then determined by comparison with the data. For Central Arctic data this slope is $1.125 \times 10^{-3} f \, dB/deg \, (f \text{ is frequency in Hz}) \, \text{for frequencies from 0 to 400} \, \text{Hz}$ and a constant 0.45 dB/deg above 400 Hz. [Work supported by NORDA, Code 110 A.]

4:50

M12. Generalized parabolic wave equation and field-moment equations for random media having spatial variation of mean sound speed. Reginald J. Hill (U.S. Department of Commerce, 325 Broadway, R/E/WP1, Wave Propagation Laboratory, Boulder, CO 80303)

The wave equation for propagation of sound waves through random oceanic inhomogeneities is expressed in a special coordinate system that follows the ray path of the deterministic wave that would propagate in the absence of randomness. The ratio of the full wave field in the presence of random inhomogeneities to the deterministic wave field is shown to satisfy the parabolic wave equation with acoustic wavelength depending on position along the ray. This approximation requires that the local sound speed be only slightly perturbed from its local deterministic value, although it may be very much different from the sound speed at a distant point on the deterministic ray. No matter how tortuous the path of the deterministic field, this parabolic equation holds provided that the angles between the rays of the full field and rays of the deterministic field are small. The equations for moments of the field (mean field, mutual coherence function, fourth moment) have a form very similar to the case of uniform mean sound speed. The numerical solution of these randommedium propagation equations is conceptually simple.

MONDAY AFTERNOON, 7 MAY 1984

GREENWAY ROOM, 3:30 TO 5:00 P.M.

Session N. Physiological Acoustics V and Psychological Acoustics III: Animal Communication

Richard R. Fay, Chairman

Parmly Hearing Institute, Loyola University of Chicago, 6525 North Sheridan Road, Chicago, Illinois 60626

Chairman's Introduction-3:30

Contributed Papers

3:35

N1. Extraction of acoustic signatures from animal signals using a set of pattern discrimination techniques. Leslie A. Wheeler, Jacques Lefebvre, and Michel Wimitzky (Laboratoire de Physiologie Acoustique, I. N. R. A.-C. N. R. Z., Jouy-en-Josas, France, and Laboratoire de Génètique Factorielle, I. N. R. A.-C. N. R. Z., Jouy-en-Josas, France 78350)

Acoustic recognition of individuals has been demonstrated experimentally in most, if not all, birds and mammals studied from this point of view. The investigator trying to identify the "acoustic signatures" on which recognition is based invariably finds what he seeks, sooner or later, depending on the degree of intra-individual variation in vocalizations compared to inter-individual variation. However, acoustic signatures brought out using analytical methods are not necessarily those used by the animals themselves. Such is the case for peach-faced lovebirds (Agapornis roseicollis). In an attempt to overcome this problem, we designed a set of pattern discrimination techniques which are based on previous psychoacoustic and neurophysiological data and whose validity could be tested experimentally. Our techniques exploit temporal evolution of energy spectrum density and comprise Fourier analysis, various standardization procedures, and three multivariate statistical analyses. Use of these techniques in further psychoacoustic and neurophysiological investigations, particularly those concerning the functioning of "complex" neurons, is discussed.

3:50

N2. Acoustic analysis of the budgerigar vocal repertoire. Cynthia A. Kline and Robert J. Dooling (Department of Psychology, University of Maryland, College Park, MD 20742)

Previous ethological studies of the budgerigar (*Melopsittacus undulatus*) have provided a functional description of the vocal repertoire [B. F. Brockway, Anim. Behav. 23, 294–324 (1964)]. The present study describes the acoustic structure of each of these complex vocalizations with an emphasis on the contact call. Acoustic features of each vocalization were measured from standard sonograms. Most of the vocalizations of the budgerigar are short, discrete calls varying in duration between 20 and 200 ms. A long, rambling courtship vocalization is also described which varies in duration from 10 s to 1 min. This vocalization is composed of many different elements and is performed primarily by males. This courtship vocalization may be functionally similar to the song of oscine song birds. The acoustic properties of these vocalizations are discussed in relation to the hearing capabilities of the budgerigar. [Work supported by NICHHD and NINCDS.] 4:05

N3. Discrimination of natural vocalizations by budgerigars (*Melopsittacus undulatus*) using operant techniques. Thomas J. Park and Robert J. Dooling (Department of Psychology, University of Maryland, College Park, MD 20742)

Budgerigars (*Melopsittacus undulatus*) were trained by operant techniques on a GO-NOGO discrimination task requiring the classification of complex species specific acoustic signals. Budgerigars began training on one pair of contact calls. After reaching a criterion of 85% correct, a third stimulus was added to the classification task. This procedure was reported each time budgerigars reached criterion on the current set of calls. By 70 sessions (days) budgerigars demonstrated the capacity for correctly identifying/classifying ten contact calls. Responses to probe stimuli indicate that the budgerigars were relying on the features of each call, not a rule or rules, in making a correct classification. Canaries (*Serinus canarius*) trained on the identical task failed to reach criterion on a single pair of budgerigar contact calls. These data suggest species differences in the perception and learning of complex vocalizations. [Work supported by NINCDS and NICHHD.]

4:20

N4. Critical band analysis of avian vocalizations. Robert J. Dooling (Department of Psychology, University of Maryland, College Park, MD 20742), H. Timothy Bunnell (Gallaudet College, Washington, DC 20002), and Christopher Clark (Rockefeller University, Millbrook, NY 12545)

In searching for the basis of information encoding in avian vocalizations, conventional analysis techniques fail to take into account what is known about peripheral auditory processing in the avian ear. A spectral analysis of the entire vocal repertoire of the budgerigar is described based on the threshold of hearing and acoustic transformations derived from psychoacoustic studies of masking in this species. Some vocalizations of the budgerigar are matched to the region of best absolute sensitivity and smallest critical bandwidth in this species while others are not. The unusual shape of the critical band function for the budgerigar provides a considerably different view of the spectral differences normally observed between categories of vocalizations and between the vocalizations of other species. These results will be discussed in relation to the probable function of budgerigar vocalizations and the acoustic cues facilitating individual recognition. [Work supported by NICHHD and NINCDS.] N5. Discrimination of frequency-modulated sounds by the frog Kassina senegalensis. R. R. Capranica, G. D. Harned (Section of Neurobiology and Behavior, Cornell University, Ithaca, NY 14853), and N. I. Passmore (Department of Zoology, University of the Witwatersrand, Johannesburg 2001, South Africa)

Male South African running frogs (Kassina senegalensis) produce a pronounced frequency modulated (FM) mating call during the breeding season which serves to attract conspecific females. The call typically

sweeps upward from 750 to 2250 Hz in 140 ms. Behavioral phonotaxis studies were conducted with 73 female frogs. Results from 475 two-choice playback discrimination trials, using natural and synthetic mating calls, verify that females can readily discriminate among a variety of FM signals based on sweep direction, duration, rate, and frequency range. Concomitant electrophysiological results indicate that these animals afford an opportune model for neurobehavioral studies of encoding of FM sounds in the vertebrate peripheral and central auditory system. [Work supported by N. I. H. Grant NS-09244, South African Council for Scientific and Industrial Research, and Animal Communication Research Program, University of the Witwatersrand.]

X

Session O. Underwater Acoustics II: High Frequency I

Herman Medwin, Chairman

Physics Department, Naval Postgraduate School, Monterey, California 93940

Chairman's Introduction-8:00

Invited Papers



8:05

01. Surface and volume backscattering of broadband acoustic pulses normally incident on the sea floor: Observations and models. D. J. Dodds (Huntec (70) Limited, 1750 Brimley Road, Scarborough, Ontario, Canada—M1P 4X7)

When a broadband (1–10 kHz) impulsive (0.2-ms duration) acoustic source is directed vertically at the sea floor, the resulting echo contains a significant proportion of energy which does not remain coherent during horizontal translations of the acoustic system. This indicates that scattering is taking place. The scattering effects are a function of frequency, and the interaction of the source beam function with the bottom produces a time dependence as the expanding wave front encounters the sea floor at an increasing distance off the axis of the source. These effects can be displayed in a contour diagram of signal power as a function of time and frequency, called a sonogram. By using models of surface and volume scattering, a synthetic sonogram can be calculated from parameters of volume scattering and surface roughness. Such a synthetic sonogram can be fitted to an actual sonogram, yielding estimates of the parameters. These parameters promise to be useful in characterizing sediments, their acoustic properties, and their surfaces.

8:30

O2. Acoustic volume scattering: 100 kHz to 10 MHz. D. V. Holliday (Tracor, Inc., 9150 Chesapeake Drive, San Diego, CA 92123) and R. E. Pieper (Institute of Marine and Coastal Studies, University of Southern California, Los Angeles, CA 90089-1231)

High resolution profiles of acoustic volume scattering strength were made to a depth of 100 m at 18 frequencies spaced approximately logarithmically in a band between 100 kHz and 10 MHz. Stations were located in a complex marine environment extending offshore from Los Angeles, CA. High resolution temperature, conductivity, and chlorophyll fluorescence data were also collected and comparisons are made with the acoustic profiles. Interpretations of the data are made in relation to size and abundance of zooplankton collected at selected depths during the same cruise. Comparisons are also made to data collected in different seasons in the same geographic area. [Work supported by ONR and NSF.]

8:55

O3. Bubbles near the surface of the ocean and their influence on wind-generated ambient noise. David M. Farmer (Institute of Ocean Sciences, P. O. Box 6000, Sidney, British Columbia, Canada) and David D. Lemon (Arctic Sciences Ltd., Sidney, British Columbia, Canada)

Bubbles of radius 40–400 μ m are formed by breaking wind waves and are known to influence significantly air-sea gas exchange. Do they also modify wind generated ambient noise? For frequencies greater than 500 Hz, wind-generated noise typically has a constant spectral slope, but a layer of bubbles will scatter and absorb the sound, changing its spectral and directional properties at high wind speed. Observations in Queen Charlotte Sound, B. C., in bands centered at 4.3, 8.0, 14.5, and 25.0 kHz illustrate these effects; at sufficiently high wind speeds noise at 14.5 and 25.0 kHz actually decreases with increasing speed. The changes in spectral slope as a function of wind speed and frequency allow bubble populations and size distribution to be inferred. These were found consistent with previous photographic and bubble trap measurements, but the range of wind speeds encountered permits determination of a more complete relationship. Scattering and absorption by the bubble layer has implications for the use of ambient noise in passive remote sensing of wind speed and precipitation.

9:20

O4. Hybrid ray-mode methods for underwater acoustic propagation. L. B. Felsen (Department of Electrical Engineering and Computer Science/Microwave Research Institute, Polytechnic Institute of New York, Farmingdale, NY 11735)

Ray fields and guided mode fields form alternative and complementary building blocks for modeling highfrequency acoustic propagation in the ocean environment. Since the ocean waveguide is large compared to the local wavelength, a mode formulation requires many modes. In the presence of surface ducts and submerged ducts, a ray formulation at long ranges requires many rays. Since either formulation is therefore inconvenient, a hybrid combination in terms of rays and modes can introduce efficiencies and greater physical clarity. The

S29

foundation for the hybrid scheme is the ray-mode equivalent that permits a finite spectral interval of continuously distributed local plane-wave fields to be filled either with rays or with modes plus a truncation remainder. The equivalent can then be used to eliminate troublesome ray or mode spectral intervals and replace these by troublefree modes or rays, respectively. Exact for range-independent environments, including those with elastic layers where P–SV coupling may occur and ray species proliferate in consequence, the equivalent can also be formulated approximately for weak range dependence through use of adiabatic invariants. These concepts are developed, quantified, and illustrated on examples involving modal substitution for ray clusters in caustic forming surface ducts, for bottom glancing and refracting ray transitions, for collective treatment of ray fields in elastic layers, and for ocean channels with sloping penetrable bottom. Alternatively, rays are efficient for tracking interference maxima of groups of modes. Implications of these concepts for time-dependent propagation are also discussed. [Work supported by ONR, Ocean Acoustics Branch.]

9;45

O5. Scale-model studies of normal mode field. E. C. Shang^a (Ocean Acoustics Laboratory, NOAA/AOML, Miami, FL 33149), C. S. Clay, and Y. Y. Yang^a (Department of Geology and Geophysics, University of Wisconsin-Madison, Madison, WI 53706)

In recent years scale-model studies of normal mode fields in waveguides have been conducted by the authors both in the Institute of Acoustics, Academia Sinica, the Institute of Oceanography in China, and in the Department of Geology and Geophysics, University of Wisconsin-Madison in the United States. Some results concerning the implementation of mode filtering and some new techniques of signal processing in waveguides are summarized. The results of the study of source location-source ranging, source depth estimation, and source bearing in waveguides are presented. ⁴¹On leave from the Institute of Acoustics, Academia Sinica, Peking, People's Republic of China.

Contributed Papers

10:10

O6. High-frequency propagation modeling using HYPER. Fred Tappert (University of Miami, Miami, FL 33149), Ding Lee, and Henry Weinberg (Naval Underwater Systems Center, New London, CT 06320)

The hybrid parabolic equation-ray (HYPER) model previously described [J. Acoust. Soc. Am. Suppl. 1 74, S96 (1983)] has been further developed both theoretically and numerically. The small-angle Newtonian ray equation that is consistent with the parabolic approximation has been integrated numerically through strongly range-dependent ocean environments and compared to the exact rays with satisfactory agreement. The modified parabolic equation that correctly describes amplitude and phase within a ray bundle has been integrated numerically at kHz frequencies through strongly range-dependent ocean environments and the caustic structure at convergence zones has been examined. Comparisons to available caustic theories show that the HYPER model provides fully diffractive results that are uniformly valid.

10:25

O7. Acoustic backscattering at low grazing angles from the ocean bottom. **I.** Bottom backscattering strength. H. Boehme, N. P. Chotiros, L. D. Rolleigh, S. P. Pitt, A. L. Garcia, T. G. Goldsberry, and R. A. Lamb (Applied Research Laboratories, The University of Texas at Austin, P. O. Box 8029, Austin, TX 78712-8029)

Acoustic backscattering measurements on a sand bottom were made at grazing angles in the range of about $2^{\circ}-10^{\circ}$ in water depth of approximately 15.5 m near San Diego, CA [T. G. Goldsberry, S. P. Pitt, and R. A. Lamb, J. Acoust. Soc. Am. Suppl. 1 72, S74 (1982)]. Data from these measurements have been analyzed to determine the mean value and standard deviation of the bottom backscattering strength per m² as a function of grazing angle, insonified area, transmit signal type, and frequency. A curved ray path propagation model and measured sound speed profiles were used to determine grazing angle versus time. The mean value followed Lambert's law for the range of grazing angles measured and for all frequencies used. No significant differences in mean value were observed when the insonified area and transmit signal type were varied. The observed frequency dependence of the bottom backscattering strength per m² falls in the range from $f^{1.5}$ to $f^{1.8}$ for this relatively flat, sandy bottom. [Work supported by NAVSEA 63R and NORDA Code 113.]

10:40

O8. Acoustic backscatter at low grazing angle from the ocean bottom. II: Statistical characteristics of bottom backscatter at a shallow water site. N. P. Chotiros, H. Boehme, T. G. Goldsberry, S. P. Pitt, R. A. Lamb, A. L. Garcia, and R. A. Altenburg (Applied Research Laboratories, The University of Texas at Austin, P. O. Box 8029, Austin, TX 78712-8029)

Analyses of the statistical characteristics of bottom backscatter, measured in shallow water off San Diego, CA [T. G. Goldsberry, S. P. Pitt, and R. A. Lamb, J. Acoust. Soc. Am. Suppl. 1 72, S74 (1982)] are presented. An experimental sonar, operating at 30 kHz, mounted on the sea bottom was used to gather data over a wide sector of the bottom within its operating range. The bottom was comprised of areas of coarse and fine sand. The distribution function and probability of false alarm function of the detected envelope of a "widebeam" and a "narrowbeam" signal were measured. Some spatial and temporal correlation functions of the signal amplitudes were measured. A limited attempt was made to compare the results with existing theoretical models. [Work supported by NAVSEA 63R and NORDA Code 113.]

10:55

O9. A semi-empirical model for high-frequency bottom backscattering. Darrell R. Jackson (Applied Physics Laboratory, College of Ocean and Fishery Sciences, University of Washington, 1013 Northeast 40th Street, Seattle, WA 98105)

Expressions have been developed for bottom scattering strength as a function of frequency and four bottom parameters. These parameters are rms roughness, sound speed, mass density, and a volume scattering parameter. Procedures have been developed for assigning best values to these parameters for poorly characterized sites, e.g., for sites at which mean sediment grain size or porosity is the only known quantity. This model is based upon the composite roughness and Kirchhoff approximations, but empirical adjustments have been made to fit data that lie outside the region of applicability of these approximations. [Work supported by NAVSEA.]

chargenetts 3-4 2 11:10

O10. Angle spreads of broadband high-frequency signals reflecting from a random surface. Michael H. Brill (Science Applications, Inc., 1710 Goodridge Drive, McLean, VA 22102) and Xavier Zabal (TRW, 7600 Colshire Drive, McLean, VA 22102)

A simple geometric-acoustic model (appropriate for high frequencies) has recently been used to compute time and frequency spreading of a broadband acoustic signal reflecting from an ocean bottom [M. H. Brill, X. Zabal, and S. L. Adams, J. Acoust. Soc. Am. Suppl. 1 73, S11 (1983); also 74, S76 (1983)]. In that model, the expected power received from a bottom facet dxdy at (x,y,0) is computed as a function of the x and y coordinates of the reflecting point on the bottom. A ray arriving from any reflecting point has a well-defined travel time, relative frequency shift (for a given source and receiver motion), polar arrival angle, and azimuthal arrival angle. In the present work, the received power from a grid of facets is histogrammed in the two arrival angles. The resulting histogram, called the angle-spread function, is a measure of the spatial coherence of the reflected signal. Computed angle-spread functions will be presented for various source/receiver geometries, and implications for sonar signal processing will be discussed.

11:25

O11. High resolution bottom backscatter measurements, W. I. Roderick, R. K. Dullea, and J. M. Syck (Naval Underwater Systems Center, New London, CT 06320)

Acoustic bottom backscattering measurements and the corresponding geoacoustic properties of the ocean bottom are presented for an experiment conducted in the shallow waters of the North Atlantic. The bottom scattering strength data, which were obtained with a high resolution (nar-

Sand E PARMA

TUESDAY MORNING, 8 MAY 1984

Session P. Physiological Acoustics VI and Psychological Acoustics IV: Tinnitus, Audiometry, and Aids for the Deaf

James M.Pickett, Chairman

Sensory Communication Research Laboratory, Gallaudet College, Washington, DC 20020

Chairman's Introduction-8:30

Contributed Papers

8:35

P1. Electrical tinnitus control. Abraham Shulman and Juergen Tonndorf (Audimax Corporation, 200 Holt Street, Hackensack, NJ 07606)

Tinnitus can be suppressed electrically in various ways: Grapengiesser (1801), Wreden (1887), Aran (1981), and Chouard (1981). The present portable instrument uses a new technique: audio frequencies that vary continuously but slowly between 0.2 and 20 kHz modulate a 60-kHz carrier. The combined signal (1.77 V rms, 5-6 mA) is applied to stainless-steel electrodes placed on both mastoids. Exposure starts with 1 h/day, increasing up to 5 h/day. It may be reduced again, once supression is achieved. This mode of control is currently tested on a number of patients, who complain of severe tinnitus. If results continue to be favorable (50%-60% success), this method appears to be superior to acoustic masking because (1) patients have no sensations during exposure, the signals being much below auditory or tactile thresholds, (2) simultaneous auditory inputs are neither masked nor attenuated, (3) the ear canals remain free, without irritation, and (4) "residual inhibition" (continued suppression after cessation of stimulation) lasts for several hours or even days, instead of minutes or a few hours, although suppression is not immediate, taking 2-5 h to take effect.

row beamwidth) parametric sonar, were measured as a function of frequency (5-20 kHz), grazing angle (4°-10°), azimuthal angle (\pm 55°), and pulse length (0.4-10 ms). The supporting environmental measurements included box cores for determining the acoustic properties of the sediment and stereo photography for calculating the two-dimensional roughness spectrum of the sea floor. [Work supported by NAVSEA 63R.]

11:40 from Chester O12. High-frequency acoustic backscatter from the sea surface. W. I. Roderick, R. K. Dullea, and J. B. Chester (Naval Underwater Systems Center, New London, CT 06320)

A high resolution acoustic surface scattering experiment was conducted in the shallow waters of the North Atlantic. A narrow beam parametric array, which was rotatable in both azimuth and elevation, was utilized as a broadband high-frequency acoustic projector. Acoustic surface scattering data were obtained at normal incidence and low grazing angles (less than 10°) as a function of acoustic transmit frequency and sea state conditions. Meteorologic and oceanographic data were obtained in concert with the acoustic measurements and included wind speed and direction, ocean surface wave spectra and currents, and ocean sound speed. Surface backscattering strength, Doppler spectra (shift and spread), and envelope statistics were some of the measured parameters. It will be shown that the Doppler spectra are approximately Gaussian and the spectral shift could be predicted from Bragg diffraction theory modified by the induced Doppler due to surface currents. At normal incidence, the surface loss varied 20 dB as the frequency changed from 5 to 80 kHz, under nearly constant sea surface conditions. [Work supported by NAVSEA 63R.]

BRANDON ROOM, 8:30 TO 11:20 A.M.

8:50

P2. Tinnitus occurence and modification-A case study. Angelo J. Campanella (ACCULAB, 3201 Ridgewood Drive, Columbus, OH 43220)

In July 1982, a brief exposure to 133-dB 400-Hz sounds to the author caused a mild case of tinnitus to erupt that evening. Ancillary circumstances included insufficient earplug attenuation, fatigue, and hot weather. No significant TTS was noted at the time of exposure, though the environmental noise was sufficient to mask mild TTS. Tinnitus tones were generally above 4 kHz and occasionally of narrowband (versus tonal) quality at an SPL estimated to be about 35 dBA. Audiograms taken a few days after the exposure indicated no notable PTS, though personal experience indicated a slight loss of response in the 4-, 5-, or 6-kHz region. Lack of sleep was relieved by medication and tinnitus masking for a few weeks. Long-term acclimatization is now more or less complete. Recent measurements indicate that permanent tinnitus tones lie in the 10 to 13 kHz region. Mild exposure to noise (vis, a 60-mile automobile trip without earplugs) incites lower tones in the 5- to 8-kHz region which persist for a few hours. Mechanical pressure on certain skull locations will increase the 10/13-kHz tinnitus tone level by 10 to 20 dB. Still another pressure point will stop the tone as long as the pressure is applied. Blood pressure pulses

individually modulate the 10/13-kHz tinnitus by an estimated 10 dB. Acoustical measurements pertinent to these observations will be presented. Such observations suggest that tinnitus can be altered by such mechanisms as pressure, stresses, or dislocations in the cochlear region. It is also possible that the damage mechanism (in this case) would include mechanical stress induced in the cochlear assembly and its attachments by intense sound vibrations.

9:05

P3. High-frequency audiometry. Juergen Tonndorf and Barbara Kurman (Audimax Corporation, 200 Holt Street, Hackensack, NJ 07606)

High-frequency hearing was routinely, although not very precisely, tested with the monochord, but this was no longer done after the advent of electronic audiometers. For many disorders, high-frequency losses were recently shown to precede losses in the speech frequencies. At f > 6-8kHz, precalibrated earphones become increasingly unreliable. Replacing the air conduction input by bone conduction, generated by electrical inputs (fixed carrier signal of 60 kHz, modulated by audio signals) overcomes these difficulties. Electrodes, placed on the mastoid and on the forearm, are Mylar-coated to provide capacitive coupling, the subject becoming part of a tuned circuit. The nontest ear was being masked. Input voltage was kept constant at 1.77 V rms, since signal magnitude is mainly determined by current. For normal-hearing subjects, thresholds varied with frequency between 1 and 25 mA. The current required rose with about 130 dB/oct near the upper frequency limit, which for young adults was found at about 18 kHz, with testing limited at 30 mA for safety reasons. However, some subjects with upper limits as low as 11 kHz still showed "normal" air-conduction thresholds at 8 kHz.

9:20

P4. Detection of frequency modulation by normally hearing and severelyto-profoundly hearing-impaired listeners. Ken W. Grant (Central Institute for the Deaf, St. Louis, MO 63110)

Listeners with a severe to profound hearing loss often perceive changes in loudness when the frequency of a stimulus is changed. As a result, researchers who have studied frequency discrimination in impaired listeners may have underestimated the extent of the frequency impairment. In this study, we compare normal and impaired listeners in three frequency modulation detection experiments, in which the amplitudes of the test signals were either fixed, sinusoidally modulated at a constant rate of 3 Hz, or randomly modulated at rates of 3 Hz and below. Results for listeners with normal hearing showed that modulation of signal amplitude yielded Δ FMs that were 2-3 times larger than those obtained with fixed amplitude. Results for one impaired listener tested thus far show abnormally large Δ FMs for all conditions, and, in addition, that Δ FMs obtained with random amplitude modulation are as much as 45 times larger than those found for listeners with normal hearing. [Work supported by NIH.]

9:35

P5. Loudness discomfort level measurements and their implications for the design and fitting of hearing aids. Harvey Dillon, Robyn Chew, Margaret Deans, and William Tonisson (National Acoustic Laboratories, 5 Hickson Road, Sydney, 2000, Australia)

If the maximum power output (MPO) of a hearing aid is set at too high a level, then the aid wearer experiences discomfort from the intense sounds produced. This paper presents measurements of the loudness discomfort level (LDL) of 120 hearing-impaired individuals. As well as large differences between the average LDLs of the subjects, there are large differences in the shapes of the LDL curves. For subjects with severe to profound losses, the shape of the LDL curve is closely related to the shape of the threshold curve. Some of these individuals have as little as 5-dB dynamic range available between their threshold and LDL at some frequencies. The extreme range of shapes, especially when combined with narrow dynamic ranges implies that a similar range of shapes should be available in the MPO curves of hearing aids if aid wearers are to have an audible, comfortable signal present in each frequency region. This feature can be readily arranged in aids incorporating compression limiting. **P6. Improved frequency-lowering technique.** M. P. Posen, C. M. Reed, L. D. Braida, and N. I. Durlach (Research Laboratory of Electronics, Massachusetts Institute of Technology, Cambridge, MA 02139)

Frequency lowering is a form of signal processing intended to make high-frequency speech cues available to those who cannot hear high-frequency sounds. We have evaluated a frequency-lowering technique studied by Lippmann [J. Acoust. Soc. Am. Suppl. 1 67, S78 (1980)]. In this system speech levels in high-frequency bands modulate 1/3 octave bands of noise at low frequencies, which are then added to unprocessed speech. We found, in agreement with Lippmann, that processing improved the recognition of stop and fricative consonants when the listening bandwidth is restricted to 800 Hz. However, we also found that processing degrades the perception of nasals and (particularly) semivowels, consonants not included in Lippmann's study. We modified Lippmann's signal processing by reducing the level of the modulated noise when low-frequency components dominate the speech signal. Preliminary results indicate that the modified system does not degrade nasals and semivowels, but maintains the processing advantage for stops and fricatives. [Work supported by NIH.]

10:05

P7. Hearing aid signal processing for noise and nonsense syllables. David A. Preves (Starkey Laboratories, 6700 Washington Avenue South, Minneapolis, MN 55344)

Transfer function magnitude and phase, coherence, cross power spectrum, and cross correlation measurements for vented hearing aid fittings worn *in situ* near onset of acoustic feedback oscillation were obtained with linear system identification techniques utilizing a FFT spectrum analyzer. These measurements were repeated for various methods of suppressing the oscillation tendency. Time segments containing formant transitions of selected CV and VC nonsense syllables found to be difficult to perceive by hearing-impaired persons were passed through the vented hearing aid fittings worn *in situ*. The ability of the hearing aids to process difficult-toperceive speech stimuli is discussed in light of interpreting the cross correlation and cross spectrum measurements.

10:20

P8. Visual speech display for the deaf. Stephen A. Zahorian and James R. Holland (Department of Electrical Engineering, Old Dominion University, Norfolk, VA 23508)

In this paper, the results of the preliminary development of a visual speech display as a speech training aid for the hearing impaired will be presented. The training aid consists of analog electronics for extracting speech parameters and a microprocessor-based system for converting the speech parameters to color parameters and for controlling the display parameters. The speech parameters consist of six spectral shape factors, similar to speech spectral principal components and a pitch signal proportional to voice fundamental frequency. The spectral shape factors are computed by appropriately combining the low-pass-filtered logarithmically scaled outputs of a bank of 16 bandpass filters. The spectral shape factors will be used to control the color of the display. The results of a vowel discrimination experiment for steady-state vowels will be presented. [Work supported by the Whitaker Foundation.]

10:35

P9. The evaluation of speech-to-tactile transformations utilizing two training paradigms. Matt Fluster (Department of EE & CS, Johns Hopkins University, Baltimore, MD 21218)

Two distinct training paradigms, building block and holistic, were used to evaluate two speech-to-tactile transformations, vocoder and flowed spectrographic. A separate group of subjects was used for each of the four conditions in the 2×2 (transformation \times training) experimental design. The building block subjects were taught first to identify a small set of vowels and consonants, followed by CVs and VCs, nonsense words, small phrases, and finally, small phrases in conjunction with a simple, visually presented game. Each level used elements from the preceding level. With the holistic paradigm, the subjects were only presented with the final task. No significant difference in the overall effectiveness of the vocoder versus the flowed spectrographic transformation was seen. However, in the initial level of the building block paradigm, vocoder subjects relied more heavily on durational cues. The stimuli were constructed following simple phonological, syntactic, and semantic rules. This stimulus structure was seen to have specific effects on the types of confusions found with the building block paradigm, and on the manner in which the subjects learned the tactile patterns in the holistic paradigm. Results of these experiments have implications for the evaluation of communication aids. [Work supported by NSF and NIH training Grant 5T32GM07057.]

10:50

P10. Categorical perception of vibrotactile signals. M. J. Collins and R. R. Hurtig (Department of Speech Pathology and Audiology, University of Iowa, Iowa City, IA 52242)

Hearing-impaired children's successful use of vibrotactile devices as a substitute for audition may be dependent on the wearability of the device and the transmission of phonemically recognizable information. The present study was carried out to determine the extent to which categorical perception of voiced-voiceless cognates could be achieved with a commercially available, wearable, single-channel, vibrotactile device. Stimuli were computer-generated pairs of syllables differing only in voice onset time (ka-ga). Adult subjects with normal hearing were trained to identify tactile signals at the extreme of the continuum prior to collection of discrimination data. Peaks in discrimination functions were observed to mark voiced-voiceless boundaries for both acoustic and tactile stimulation modes. These peaks occurred at consistently longer voice onset times for tactile stimulation than for auditory stimulation. The results indicate that although categorical perception of speech sounds can be learned in the tactile mode, because of the shift in the boundary, voiced-voiceless confusions may occur with voice onset times commonly observed in real speech. Thus for effective use of the tactile modality for speech, specialized signal processing may be required.

11:05

P11. Consequences of audiovisual asynchrony for speech perception: Implications for signal processing in aids to lipreading. Matthew McGrath^{a)} and Quentin Summerfield (MRC Institute of Hearing Research, University Park, Nottingham NG7 2RD, United Kingdom)

Audiovisual identification of sentences was measured as a function of audio delay in untrained listeners with normal hearing; the sound track was replaced by rectangular pulses originally synchronized to the closing of the talker's vocal folds and then subjected to delay. Although groupmean performance declined monotonically with delay, systematic decrements occurred only when delay exceeded 80 ms. A similar tolerance of delay was found in judgments of audiovisual onset time when observers determined whether a 120-Hz triangular wave started before or after the opening of a pair of liplike Lissajou figures. Group-mean 70% DLs were -78 ms (sound leading) and +137 ms (sound lagging). This result suggests, first, that most observers possess insufficient sensitivity to intermodal timing cues in audiovisual speech for them to be used analogously to VOT in auditory speech perception, and, second, that the effects found in the first experiment derive from syllabic rather than phonemic interference. However, the best lipreaders, who also gained most from the audio signal in that experiment, were affected by delays shorter than 80 ms. Accordingly, we suggest that signal processing in aids to lipreading should be allowed no more than 40 ms to do its work. ^{a)} Supported by a studentship from the TWJ Foundation.

TUESDAY MORNING, 8 MAY 1984

GREENWAY ROOM, 8:30 A.M. TO 12:20 P.M.

Session Q. Physical Acoustics II: Absorption, Relaxation, and Physical Effects of Sound

Allan D. Pierce, Chairman

School of Mechanical Engineering, Georgia Institute of Technology, Atlanta, Georgia 30332

Chairman's Introduction-8:30

Invited Paper

8:35

Q1. Sound speed and attenuation in thin polymer films in the frequency range 0.2-1 GHz. G. M. Sessier, R. Gerhard-Multhaupt (Technical University, Merckstrasse 25, D-6100 Darmstadt, West Germany), and J. E. West (AT&T Bell Laboratory, Murray Hill, NJ 07974)

Pressure pulses or pressure steps with rise times on the order of 0.2 ns can be generated in dielectric films by application of laser pulses to a specially coated surface of the dielectric [G. M. Sessler, J. E. West, and R. Gerhard-Multhaupt, Phys. Rev. Lett. 48, 563 (1982)] or by excitation with a quartz crystal [W. Eisenmenger and M. Haardt, Solid State Commun. 41, 917 (1982)]. The acoustic phenomena propagate in the thickness direction of the films and are reflected at its surfaces. If the samples are electrically biased or charged, electrode signals are generated upon each reflection. The sound speed may be obtained from the relative delays of these signals while the sound attenuation can be evaluated by comparing their spectra. A modification of the laser method consists in the generation of double (or multiple) pulses by splitting the laser beam into two (or more) components and delaying one component relative to the other by a time T. This results in a boost of the spectrum at the frequency f = 1/T. Measurements on PETP, PI, PVDF, and FEP yield sound speeds close to the values determined for bulk material with other methods and sound attenuation coefficients that rise almost linearly with frequency in the range 0.2–1 GHz. The attenuation data can probably be explained by a hysteresis-type absorption process.

Q2. Sound absorption by inhomogeneous porous layers. Shawn Burke (Acoustics and Vibration Laboratory, Room 5-021, Massachusetts Institute of Technology, Cambridge, MA 02139)

A three-dimensional governing equation is derived from first principles that describes the effect of an inhomogeneity of acoustical parameters in rigid, porous sound absorbers. The equation contains a scattering term expressed in terms of the gradient of the material's complex fluid density. An expansion of the equation for weak inhomogeneities yields a source component containing the perturbations, giving rise to a secondary scattered acoustic field in the material. The analysis is then specialized to the exact solution of the oblique incidence problem for plane waves striking a layer of such a material with arbitrary (but continuous) inhomogeneity in the direction normal to the layer's surface. This analysis is applicable to the description of wicking (or fouling) of porous absorptive treatments in industrial or aircraft applications. The transformed governing relation is solved numerically assuming the acoustical parameters vary linearly with space in a 2.54-cm layer of fiberglass. These results imply that the inhomogeneity degrades the layer's absorptive characteristics, as expected.

9:20

Q3. The effect of viscous relaxation on sound propagation in porous materials. M. v. Haumeder (SACLANT ASW Research Centre, La Spezia, APO New York, NY 09019)

The Biot theory treats a porous, fluid-filled material as a composite of two, interpenetrating elastic continua. In the theoretical description this composite nature is reflected by a set of two equations of motion which are coupled via a flow term. It can be shown that this formulation includes viscous relaxation due to a local flow of the pore fluid relative to the frame. This local flow is strongly frequency-dependent because the geometry of the pores supports flow only for a certain wavelength range in which the fluid flow can follow the excitation by the elastic wave. Accordingly we derive a relaxation time τ which is partly determined by geometrical factors. τ is expressed in terms of permeability, porosity, viscosity, and effective modulus. The viscous relaxation in a porous material can result in a local minimum in the frequency dependence of the reflectivity and a corresponding step in the sound velocity. These and other unusual features predicted by the Biot theory are explained in terms of a viscous relaxation process.

9:35

Q4. Theoretical study of the acoustical resistance of small orifices. R. J. Donato (Division of Physics, National Research Council, Ottawa, Canada K1A OR6)

The power dissipation produced by small holes to an incident sound field is important, for instance, in the design of hearing defenders and mufflers. No satisfactory theory for the acoustical resistance of a small hole in a thin plate appears to have been developed. A possible approach to the problem, using a variational technique, is presented for the linear region of small amplitudes.

9:50

Q5. Hydroacoustic analysis of multiple relaxation kinetics. Timothy S. Margulies and W. H. Schwarz (Department of Chemical Engineering, Johns Hopkins University, Baltimore, MD 21218)

This investigation presents a hydroacoustic theory which accounts for sound absorption and dispersion in a multicomponent mixture of reacting fluids (assuming a set of first-order acoustic equations without diffusion) such that several coupled reactions can occur simultaneously. General results are obtained in the form of a biquadratic characteristic equation (called the Kirchhoff- Langevin equation) for the complex propagation variable $\chi = (\alpha + \omega i/c)$ in which α is the attenuation coefficient, c is the phase speed of the progressive wave, and ω is the angular frequency. Computer simulations of sound absorption spectra have been made for three different chemical systems each comprised of two-step chemical reactions using physico-chemical parameter data available in the literature. The chemical systems studied include (1) water-dioxane, (2) glycine-water, and (3) cobalt polyphosphate water mixtures. Explicit comparisons are made between the biquadratic characteristic solution and the approximate equation (sometimes referred to as a Debye equation) previously applied to interpret the experimental data for the total chemical absorption versus frequency. The relative chemical reaction and classical viscothermal contributions to the sound absorption are also presented. Several discrepancies that can arise when estimating thermodynamic data (i.e., chemical reaction heats or volume changes) for multistep chemical reaction systems when making dilute solution or constant density assumptions are discussed.

10:05

Q6. Low-frequency sound absorption in air. Allan J. Zuckerwar (NASA Langley Research Center, M/S 238, Hampton, VA 23665) and Roger W. Meredith (Old Dominion University Research Foundation, Norfolk, VA 23502)

An extensive set of sound absorption measurements was taken in air over a range of frequency from 20–2500 Hz, of temperature from 20°– 50 °C, and of relative humidity from 0.3%-100%. Over the lower portion of this frequency range, where relaxation in N₂ is prominent (except in very dry air), prior measurements are scanty. This study yielded the following conclusions: (1) The humidity dependence of the relaxation frequency of N₂ differs in air from that in binary N₂-H₂O gas mixtures (246-Hz/atm. mole % in air vs 184-Hz/atm. mole % in binary mixtures at 20 °C). (2) The temperature dependence of the relaxation frequency of N₂ is the same in air as in binary mixtures. (3) At low humidities (~0.01% mole ratio), where relaxation in O₂ agree with those reported by Harris and Tempest [J. Acoust. Soc. Am. 36, 2390–2394 (1964)] and lie substantially lower than specified by ANSI Standard S1.26-1978.

10:20

Q7. Acoustic characterization of changes in viscoelastic properties of epoxy during cure. William P. Winfree and F. Raymond Parker (NASA-Langley Research Center, Mail Stop 231, Hampton, VA 23665)

The transformation of an epoxy during cure from a viscoelastic liquid to a viscoelastic solid is characterized by the change in the shear and longitudinal ultrasonic velocities and attenuations. The measurement of these ultrasonic properties is reported for several different resins cured at room temperature. The velocities are used to calculate the bulk and shear moduli as a function of cure time. The results indicate a parallel development during cure of the shear and bulk moduli. Measurements of the longitudinal attenuation at several different frequencies indicate the viscoelastic response can be characterized by a single relaxation time which increases as the cure progresses.

10:35

Q8. Pressure dependence of sound absorption in synthetic seawater at 0 °C. C. C. Hsu, A. G. Dickson, and F. H. Fisher (University of California, San Diego, Marine Physical Laboratory of the Scripps Institution of Oceanography, San Diego, CA 92152)

Measurements have been made of sound absorption in Lyman and Fleming seawater at 1 and 307 atm. Results for maximum absorption per wavelength $(\alpha\lambda)_{max}/10^6$ are 45.8 ± 0.4 at 1 atm and 28.9 ± 0.6 at 307 atm. The relaxation frequency of ~39 kHz appears to be independent of pressure as had been observed earlier at 25 °C. Our results are in excellent agreement with the predictions of Francois and Garrison for 0 °C for both sound absorption and relaxation frequency. Based on these results together with the earlier ones at 25 °C reported by Hsu and Fisher [J. Acoust.

Soc. Am. 74, 564–569 (1973)], we find a temperature dependence for both absorption and relaxation frequency different from that reported by Francois and Garrison. These differences will be discussed. The following equation represents our results for absorption ($s = \pm 0.8$): ($\alpha\lambda$)_{max}/10⁶ = 45.6 + 0.652(t/°C) - 0.0533(P/atm). [Work supported by the Office of Naval Research, Code 400R.]

10:50

Q9. The influence of the dissolved ion concentration on the acoustic cavitation threshold of water. A. A. Atchley, L. A. Crum, J. R. Reidy, and R. A. Roy (Department of Physics and Astronomy, University of Mississippi, University, MS 38677)

The variation in the transient acoustic cavitation threshold of water was measured as a function of the dissolved ion concentration of various salts. The measurements were made with a resonant sphere system in which solid particle size, water temperature, and dissolved gas content could be controlled within a closed circulating system. The normal criterion used for a cavitation event was the detection, by a photomultiplier tube, of sonoluminescence produced by a collapsing cavity. Water with a specific conductance of about $1 \mu S \text{ cm}^{-1}$ was assigned zero concentration for the first data point. Measurements were then made at successively higher concentrations, up to 10 mmoles 1^{-1} . The salts were chosen to check and extend the measurements of a previous researcher [V. A. Akulichev, Sov. Phys. Acoust. 12, 144-149 (1966)], who first detected a dependence of the cavitation threshold on dissolved ion concentration. The results of our measurements show that the threshold increases with ion concentration, reaching saturation at concentrations of 2 mmoles 1⁻¹ or less. This dependence is in the opposite direction to that observed by Akulichev. Our results will be analyzed with regard to the standard models of cavitation nucleation. [Work supported in part by the Office of Naval Research and the National Science Foundation.]

11:05

Q10. Discrepancy between experiment and theory for magneto-acoustic fields in salt water. Allan D. Pierce (School of Mechanical Engineering, Georgia Institute of Technology, Atlanta, GA 30332)

Moose and Klaus [J. Acoust. Soc. Am. 74, 1066-1068 (1983)] report results of novel and carefully controlled fundamental experiments in which a rectangular Plexiglas container filled with saturated salt solution was between the poles of a strong electromagnet. When the solution was driven at an acoustic resonance frequency an oscillating electric potential difference developed between electrodes placed on container sides parallel to magnetic field lines. The potential difference was nearly ten times larger than magneto-acoustic theory predictions. This abstract and proposed talk is with belief that such a discrepancy should not be ignored by the acoustics research community. Present author suggests that Moose and Klaus's assumption that electric field inside cavity has factored form f(x)g(y)h(z) may be an inappropriate approximation. A more nearly complete theory should take into account continuity conditions across container walls to the surrounding air, boundary conditions that require quasistatic electromagnetic disturbance to vanish at large external distances, and the presence of the electrodes. Simple estimates suggest the elaborated model will yield predictions more in accord with experiment.

11:20

Q11. Gain and efficiency of a short traveling wave heat engine. Peter H. Ceperley (Department of Physics, George Mason University, Fairfax, VA 22030)

Gain and efficiency equations are derived and evaluated for a traveling wave heat engine having a regenerator of short length compared with an acoustic wavelength. A traveling wave heat engine is a modified Stirling engine in which acoustic waves replace the usual pistons and energy is transferred between thermal and acoustic forms, depending on the wave direction [P. H. Ceperley, J. Acoust. Soc. Am. 66, 1508–1513 (1979)]. This paper is similar to another paper on gain and efficiency [P. H. Ceperley, J. Acoust. Soc. Am. 72, 1688–1694 (1982)] except that the present paper assumes that the wave impedance is not determined by the regenerator's properties, but instead by the acoustic circuit exterior to the regenerator. For acoustic impedance of freely propagating traveling waves in air, the efficiency is limited to 11% of Carnot efficiency due to visious heating in the regenerator. This can be greatly increased by going to higher impedances; e.g., 79% is possible at ten times greater impedance.

11:35

Q12. Force on a sphere associated with nonuniform temperature distribution in an acoustic resonance chamber. Emily W. Leung and Taylor G. Wang (Jet Propulsion Laboratory, California Institute of Technology, Pasadena, CA 91109)

In an acoustic resonance chamber, the force on a hollow heated sphere is investigated. The temperature of the sphere is controlled by a heater inserted inside its shell. The heating of the sphere produces a nonuniform thermal gradient in the resonance chamber. During the heating and the cooling process, the resonance condition is maintained by an analog tracking technique. The force on the sphere in a direction perpendicular to the direction of gravity is measured. Steady and nonsteady forces were observed under various conditions.

11:50

Q13. Ultrasonic flaw detection in rubber composites. J. F. Covey (Sachs/ Freeman Associates, 14300 Gallant Fox Lane, Bowie, MD 20715) and R. D. Corsaro (Code 5135, Naval Research Laboratory, Washington, DC 20375)

Sonar dome rubber windows are constructed much like steel-belted automobile tires, in that they are composed predominantly of rubber reinforced with wire cords. The use of convention ultrasonic flaw detection techniques to locate voids and disbonds in such a media is complicated both by the high attenuation in the rubber media and the layered construction technique used in its fabrication. This paper describes laboratory research efforts leading to the development of a simple reliable portable ultrasonic flaw detection system designed specifically for use in this complicated media. The potential benefits of using high-speed digital signal processing equipment in this application is also demonstrated and discussed.

12:05

Q14. Response to ultrasound of a Cheng-type liquid crystal cell. W. Hamidzada and S. V. Letcher (Department of Physics, University of Rhode Island, Kingston, RI 02881)

We reported earlier on the ultrasonic response of a bistable twisted nematic cell [W. Hamidzada and S. V. Letcher, J. Acoust. Soc. Am. 72, 561 (1982); Appl. Phys. Lett. 42, 785–787 (1983)]. We now report on similar properties of an untwisted nematic cell that can have two different types of bistability [G. D. Boyd, J. Cheng, and P. D. T. Ngo, Appl. Phys. Lett. 36, 556–558 (1980)]. Sensitivity is quite good, but depends rather strongly on the state of the cell and on the angle of incidence of the sound. Ultrasonically induced switching from the so-called vertical to horizontal state (or vice versa) is difficult because of the disclination motion that is required, but it is possible to induce switching between two similar, but optically distinguishable, states that exist in the horizontal state with a holding voltage.

Session R. Noise III: Propagation of Sound Outdoors

Frank H. Brittain, Chairman

Bechtel Group, Inc., 50 Beale Street, San Francisco, California 94105

Chairman's Introduction-8:55

Invited Papers

9:00

R1. Review of conventional methodology used for predicting the propagation of sound outdoors. F. H. Brittain (Bechtel Group, Inc., 50 Beale Street, San Francisco, CA 94105)

Many factors affect the outdoor propagation of sound, some of which remain roughly constant and others vary considerably with time. For example, the variable propagation characteristics of the atmosphere can cause noise from an industrial source to be annoying at one time and inaudible at another, as perceived in a community. As an introduction to the special session on outdoor propagation of sound, this paper will cover various phenomena that affect propagation of sound through the atmosphere, including spherical spreading, atmospheric absorption, turbulence, terrain/barriers, foliage, and ground effects. The quantization of these phenomena, and conventional methodology used for predicting their effect on noise in the community, will be discussed. Other factors that affect the variability of propagation characteristics of the atmosphere will be briefly reviewed.

9:25

R2. Sound propagation phenomena relevant to prediction schemes. Tony F. W. Embleton (Division of Physics, National Research Council, Ottawa, Ontario K1A OR6, Canada)

Interference between direct and reflected waves can produce a shadow region near the ground because most ground surfaces have a detectably finite acoustic impedance. In a steady isotropic atmosphere this region is penetrated at low frequencies by a ground wave, especially at short ranges, or by a trapped surface wave, significant at longer ranges. The thickness and flow properties of surface layers, (e.g., snow) also affect the propagation of low frequencies near the surface. For ground having impedance discontinuities (e.g., asphalt/grass) diffracted waves originated at the interface. Diffraction theory allows prediction of sound pressures in the shadow region behind thin barriers and has been applied to thick barriers, multiple barriers, and ground surfaces of various shapes. In a downward-refracting atmosphere, such as propagation downwind or in a temperature inversion, the shadow region is diminished: conversely, in upward refraction, a refractive shadow reinforces the ground impedance shadow region: Wind and temperature fluctuations (turbulence) cause sound energy to be redirected by scattering or variable refraction: this occurs most noticeably at high frequencies and where coherent theory would otherwise predict reduced sound pressure levels. For most of these phenomena quantitative agreement has been achieved between measurements and predictions of the relevant theory: however, the situation in real life is complicated by the fact that several effects usually coexist.

10:05

R3. Outdoor propagation models with and in the absence of barriers. Sabih I. Hayek (The Applied Research Laboratory and the Department of Engineering Science and Mechanics, The Pennsylvania State University, University Park, PA 16802)

Analytic models for predicting the propagation of noise outdoors over uniform, flat terrain covered by a variety of ground covers have been proposed by the author and other researchers. These mathematical models are compared analytically and numerically for few ground cover impedances. Furthermore, when the terrain is partly covered by a hard pavement and partly by an absorbent ground, the models must take account of this discontinuity in the ground impedance. A review of the few analytic models developed by the author and other researchers is given and compared analytically and numerically. If a noise barrier is erected on a uniformly covered ground or over a pavement-absorbent ground, then the barrier performance is affected by the ground absorption. Various empirical analytic models based on geometrical acoustics and diffraction, which account for multiple diffraction by barriers located on an absorbent ground, are reviewed. [Work supported by FHWA.]

10:25

R4. Sound propagation over the ground. Lee N. Bolen (Acoustics Laboratory, University of Mississippi, University, MS 38677)

The intensity of sound propagating outdoors is reduced by spreading losses and absorption losses. Absorption losses are due to atmospheric absorption and absorption by the ground and ground cover. At low frequen-

cies, the major factor reducing intensity is reflection and interference and absorption by the surface of the earth. This paper will review the theoretical predictions of sound propagation losses over various ground covers. The prediction of sound intensity at some distance from an outdoor source near the surface requires a solution for a spherical spreading wave near a boundary. That boundary can be characterized by its impedance. Several models will be described which simplify the characterization of the surface in terms of a single parameter determined by the flow resistance of the surface. Several techniques to measure this parameter will be discussed, and a description of the calculation needed to predict the surface effects on the acoustic intensity will be presented. The effects of interference of the reflected wave and absorption by the ground surface will be described for a variety of surfaces. Effects of diffraction from barriers and atmospheric turbulence will be neglected in this review. [Work supported by ARO.]

10:45

R5. Sound propagation through the atmosphere near the ground. G. A. Daigle (Division of Physics, National Research Council, Ottawa, Canada K1A OR6)

Within the first meter above the ground there are strong gradients of temperature and wind velocity. For sources or receivers on the ground these gradients produce significant refraction of sound, even at distances as short as 15 m. The refractive shadow is penetrated by energy diffracted via a creeping wave and good agreement is obtained between point source measurements and simple theory. In additon to their gradients, the temperature and wind fluctuate rapidly about their mean. Close to the ground, the spectrum of these fluctuations is dominated by eddies having a characteristic size of about 1 m. The resulting phase fluctuations of the sound increase with increasing distance, frequency, and strength of turbulence. Good agreement is obtained between measurements and simple theory that approximates the eddy spectrum by a Gaussian. However, the amplitude fluctuations are substantially smaller than predicted and, in addition, show clear evidence of saturation. Both experiments and theory are starting to show how and to what extent the acoustical shadow regions predicted by coherent theory are reduced by the effects of atmospheric turbulence, even at short distances.

11:05

R6. Refractive effects on sound propagation in a nonturbulent atmosphere. Richard Raspet (United States Army Construction Engineering Research Laboratory, P. O. Box 4005, Champaign, IL 61820)

Atmospheric refraction due to temperature and wind variations with altitude can produce large changes in sound level from day to day and during the course of a day. Scientific studies performed during the day in low wind conditions may not be representative of average conditions. This paper will review empirical and theoretical studies of the effects of meteorological variables on sound propagation. The results and applicability of empirical studies will be discussed with the aim of identifying data sets useful for estimating refractive effects. Theoretical solutions for specific and general sound velocity profiles will also be covered. Examples from the literature will be used to illustrate the concepts.

Contributed Papers

11:25

R7. Abstract withdrawn.

\$37

11:40

R8. Quantitative sound exposure level spectra of some sonic booms. Robert W. Young (Naval Ocean Systems Center, San Diego, CA 92152)

The spectrum of a continuing sound pressure waveform often supplied by a digital spectrum analyzer can be interpreted as a spectrum of timemean-square sound pressure during a sample time window T, within a succession of "bins" whose frequency width is b = 1/T. But a time-meansquare sound pressure during a time window that is not filled by a transient, is not an appropriate measure of the transient. The quantity needed is the time integral of squared, somehow frequency-weighted, sound pressure; this time integral is called sound exposure. Sound exposure per unit bandwidth (sound exposure spectral density) can be calculated by multiplying by T the time-mean-square sound pressure during T in bin b, and dividing by b. The practical form of this is sound exposure spectrum level (1-Hz SEL). Sound exposure per unit bandwidth can be integrated over the wide passband of the transient; the practical form of the integral is flat sound exposure level (TSEL). Frequency weightings such as A can be applied before integration; the practical form of the integral is A-weighted sound exposure level (ASEL). Quantitative spectra of more than a dozen sonic booms are here reported, which have been measured by procedures just described. For example, the 150-ms wave of an F-15 aircraft maneuvering at Mach 1.1, at a slant range of 35 km caused TSEL = 116.1 dB; ASEL = 82.9 dB. Reference sound exposure is $E_0 = (20 \,\mu Pa)^2 \cdot 1$ s. The

T JESDAY AM

96-ms N wave of an F-15 aircraft maneuvering at Mach 1.2, at a slant range of 9 km caused TSEL = 120.5 dB; ASEL = 93.6 dB.

11:55

R9. Relating fluctuations of propagating acoustic signals to vertical heat flux. S. David Roth (103 Van Buskirk Avenue, Stamford, CT 06902)

The atmospheric boundary layer is said to be convectively unstable when the sun heats the earth's surface causing a positive temperature lapse rate to have developed near the surface. The surface layer (SL) of the convective boundary layer (CBL) has been studied for many years by meteorologists. The dynamics and structure of the convective SL have relatively recently become of interest to acousticians. The effects on propagating signals of mean temperature and wind velocity profiles as well as scatter from small scale eddies are fairly well understood. However, larger scale eddies known as "thermal plumes" which transcend the SL and in fact scale with the CBL have not been considered by the acoustics community. Thermals act as large scale discontinuities in the surface layer and their passage may cause variation of signals propagating over a 100-m path by about 30 dB. The transport of heat in the atmosphere is mainly accomplished by thermals [D. H. Lenschow and P. L. Stevens, Boundary Layer Meteorol. 19, 509–532 (1980)]. We therefore can expect that, to some extent, large scale fluctuations of propagating acoustic signals in the surface layer of the convective boundary layer will be related to the heat flux. Theoretical and experimental results are presented supporting this hypothesis.

12:10

R10. Acoustic propagation in a lapse temperature gradient. William K. Van Moorhem (Mechanical and Industrial Engineering Department, University of Utah, Salt Lake City, UT 84112)

The propagation of acoustic waves in the atmosphere with a realistic lapse temperature gradient has been modeled analytically. The atmosphere is assumed to be bounded by a ground surface described by a finite normal impedance. Two cases will be discussed: the plane wave solution, where plane waves are assumed to originate at infinite heights above the ground; and the point source solution. In both cases numerical evaluation of the solution has been carried out. The solution yields the unexpected result of weak refracted waves. [Work supported by NASA Langley.]

TUESDAY MORNING, 8 MAY 1984

MONTPELIER ROOM, 9:00 A.M. TO 12 NOON

Session S. Architectural Acoustics I: Robert B. Newman Tribute Session (Sponsored by the Technical Committee on Architectural Acoustics)

M. David Egan, Chairman

College of Architecture, Clemson University, Clemson, South Carolina 29631

Chairman's Introduction-9:00

Robert Bradford Newman (1917-1983)

Robert B. Newman-acoustical consultant, teacher, and author-was a founding partner of the Cambridge, Massachusetts research and development firm of Bolt Beranek and Newman, Inc. (BBN). For nearly four decades he served as professor of architecture at the Harvard University Graduate School of Design and at the Massachusetts Institute of Technology. He was a fellow of the Society and an honorary member of the Institute Brasileiro de Acustica. His consulting projects at BBN involved buildings of all types including numerous concert halls throughout the world. Four recent projects were the Joseph Meyerhoff Hall in Baltimore, Davies Hall in San Francisco, Roy Thomson Hall in Toronto, Canada, and Victorian Arts Centre in Melbourne, Australia. In 1966, for contributions to the building industry, he received on behalf of BBN the Brown Medal from the Franklin Institute in Philadelphia and in 1977 for his significant contributions to building science, a Quarter Century Citation from the U.S. National Research Council. Many of his former students have become leading educators and consultants throughout the world. He wrote the acoustics chapter in McGraw-Hill's Time-Saver Standards for Architectural Design Data, the acoustics section in Encyclopedia Britannica, and numerous papers on architectural acoustics. In addition, he presented and coauthored many papers at ASA meetings and lectured on architectural acoustics at nearly every school of architecture in the U.S. and at many universities abroad. Today's program will honor Bob Newman and his contributions to education and to the field of architectural acoustics by presenting recollections of colleagues who knew him well.

Invited Papers

9:05

S1. The Early Years. Richard H. Bolt, Adjunct Professor of Acoustics (Department of Architecture, Massachusetts Institute of Technology, Cambridge, MA 02138)

9:20

S2. Four Decades as a Teacher at MIT and Harvard. William J. Cavanaugh, Lecturer (Division of Architectural Studies, Rhode Island School of Design, Providence, RI 02903)

S3. Consulting Achievements at BBN. Ewart A. Wetherill (Bolt Beranek and Newman, 21120 Vanowen Street, Canoga Park, CA 91305)

9:50

S4. Outreach to the Architecture Profession. John H. Spencer, Chairman (Department of Architecture, Hampton Institute, Hampton, VA 23668)

S5. A Student's View. Mark E. Schafer (Biomedical Engineering and Science Institute, Drexel University, Philadelphia, PA 19104)

10:05

10:20

S6. Coordination of Architecture and Acoustics. Jack B. C. Purcell (Purcell + Noppe + Associates, 21408 Devonshire Street, Chatsworth, CA 91311)

10:35

S7. Application of Modern Room Acoustics to Design of Concert Halls. Theodore J. Schultz (Theodore J. Schultz Associates, 7 Rutland Square, Boston, MA 02118)

10:50

S8. The Later Years. Leo L. Beranek (7 Ledgewood Road, Winchester, MA 01890)

11:05

Open Discussion Period

TUESDAY MORNING, 8 MAY 1984

YORK HALL, 9:00 A.M. TO 12:20 P.M.

Session T. Speech Communication IV: Speech Prosody and Timing

Emily A. Tobey, Chairman

Kresge Hearing Research Laboratory, LSU Medical Center, 1100 Florida Avenue, Building 124, New Orleans, Louisiana 70119

Chairman's Introduction-9:00

Contributed Papers

9:05

T1. On the perception of intonation from sinusoidal signals: Tone height and contour. Robert E. Remez (Department of Psychology, Barnard College, New York, NY 10027) and Philip E. Rubin (Haskins Laboratories, 270 Crown Street, New Haven, CT 06510)

Our recent investigations of intonation have employed signals that consist of three or four time-varying sinusoids. Each tone reproduces the changes in formant center frequencies from a natural utterance. Such sentences produce a clear impression of intonation though there is no fundamental frequency common to the sinusoids composing the pattern. We find that the tone corresponding to the first formant is the basis for sinusoidal intonation, much as signal periodicity in the region of the first formant (not coincidentally, the *dominance* region) provides the information for pitch in natural speech. A series of differential similarity tests was used to determine whether listeners represent sinusoidal intonation as patterns of specific tone heights or as patterns of relative pitch changes. The results are discussed in terms of auditory frequency coding of the speech signal, intonation, whispered speech, and musical pitch. [Supported by the National Institute of Child Health and Human Development.]

9:20

T2. Sentence intonation is context/discourse oriented: Evidence from Mandarin Chinese. Chiu-yu Tseng (Institute of History and Philology, Academia Sinica, Taipei, Taiwan 115, Republic of China)

Analysis of a corpus of simple declarative sentences extracted from natural spontaneous fluent speech in Mandarin Chinese (Tseng, 1981) shows that only 20% of the data can be accounted for in the declination theory (Maeda, 1976; Pierrehumbert, 1979; Sorensen and Cooper, 1980). In this study, the same corpus of sentences produced as unrelated utterances in read form are being examined in comparison with their spontaneous natural fluent counterparts. Results of intonation analysis from this set of production data appear to be adequately characterized by the "topline" rule (Sorensen and Cooper, 1980), thus supporting one version of the declination theory to a certain extent. However, further analysis of those sentences whose natural spontaneous fluent versions cannot be characterized by the declination pattern shows the influence of contextual as well as discourse information, as noted by Umeda (1982). It appears that having the same syntactic structure does not provide much explanation or support for having the same intonation pattern. Furthermore, the intonation pattern of sentences appears to be governed by information beyond the scope of sentential information. The present investigation thus provides support for a context/discourse oriented theory of intonation.

9;35

T3. Anchor line theory of fundamental frequency variation in speech. Karen L. Landahl (Department of Linguistics, The University of Chicago, 1010 East 59th Street, Chicago, IL 60637) and Philip Lieberman (Department of Linguistics, Brown University, Providence, RI 02912)

We propose a theory that appears to characterize quantitatively those aspects of the temporal pattern of fundamental frequency (F_0) variation that delimits the constituent structure of speech, most notably sentences. The anchor line frequency theory we propose provides a major refinement of the breath-group theory [P. Lieberman, Intonation, Perception and Language (MIT Press, Cambridge, MA, 1967); J. E. Atkinson, J. Acoust. Soc. Am. 63, 211-222 (1978)]. We will present an analysis of data that is consistent with the hypothesis that the F_0 contour (1) provides continuity across voiced-unvoiced segmental boundaries, (2) that local F_0 minima tend to fall on anchor lines, (3) that the anchor lines are linear level, falling, or rising, and (4) that the level anchor is most characteristic for normal, nonemphatic declarative sentences of American English and English. We further propose that the F_0 continuity inherent in the anchor lines may play a crucial function in the perception of speech by "tagging" a speaker's voice so that we may track it in an environment of noise and competing voices.

9:50

T4. Stop voicing, intonation, and the F_0 contour. Arthur S. Abramson and Leigh Lisker (Haskins Laboratories, 270 Crown Street, New Haven, CT 06510)

The F_0 contour of an utterance is likely to show perturbations correlated with the voicing states of syllable-initial consonants. Thus the F_0 after the release of a voiceless stop will be higher than after a voiced stop. Research has shown that such differences can play a minor perceptual role in voicing distinctions. This phenomenon has also figured in arguments about the rise of phonemic tones in certain language families. We are concerned here with how the robustness of the feature might be affected by sharply contrasting intonations and the presence of a voicing break in the preceding carrier. We composed pairs of sentences with the words bark and park preceded by [s] in one pair and a vowel in the other. Three native speakers of American English recorded them ten times each, with a rising intonation and a falling intonation. Data are presented to show the extent to which the effect persists across the several contextual conditions, and inferences are drawn as to its availability for a role in speech communication. [Work supported by NICHD.]

10:05

T5. Prosodic rules for speech synthesis from Japanese text. Yoshinori Sagisaka and Hirokazu Sato (Musashino Electrical Communication Laboratory, Nippon Telegraph and Telephone Public Corporation, Musashino, Tokyo, Japan)

Three prosodic rules are proposed to realize Japanese text-to-speech conversion system. The first prosodic rule groups words into accent phrases and breath groups, using both the grammatical relationship among adjacent words or phrases by local dependency analysis and the restriction of breath group length. The second prosodic rule decides the accent position in each accent phrase, using accent attributes of constituent words. Accentuation rules are applied to constituent words in an accent phrase according to its structure. These two kinds of information, accent (or breath) group boundaries and accent positions, are utilized to generate a sentence fundamental frequency pattern. The third segmental duration control rule decides segment temporal patterns, which are used to lengthen or to shorten prestored syllabic multiphone units such as CVC and CV segments. These prosodic rules enable one to produce speech waveform with natural prosody using ECL's speech synthesis system.

10:20

T6. On the phonetics of rhythm: Evidence from Swedish. Gösta Bruce (Bell Laboratories, 600 Mountain Avenue, Murray Hill, NJ 07974)

Rhythmic alternation among sequences of unstressed syllables in Swedish utterances was examined from phonetic starting points. The results of a series of pilot experiments using both reiterant nonsense speech and original sense speech can be summarized as follows. The rhythmic alternation among unstressed syllables is reflected in the temporal domain as an alternation in syllable duration. This alternation between longer and shorter syllables can be seen as a reflex of the postulated alternation between strong and weak syllables forming rhythmic subgroups within stress groups. It appears to be quite systematic, although the size of this difference is considerably less than for a corresponding comparison of stressed versus unstressed syllables. The temporal relations also seem to be in accord with the hypothesis that the alternation is governed from the upcoming stress, so that the prestress syllable is relatively shorter, the preceding one is relatively longer, and so on by way of alternation.

10:35

T7. Rhythm in poetry and in prose. Ilse Lehiste (Department of Linguistics, Ohio State University, Columbus, OH 43210)

The paper describes an attempt to compare the rhythm of poetry with the rhythm of prose. Two poets read a number of their own poems in two modes, "poetry mode" and "prose mode." The recordings were analyzed acoustically; segmental durations were measured from broadband spectrograms, while the duration of longer utterances and pauses was measured from oscillograms produced on a Honeywell model 1858 Visicorder. It was expected that the rhythm of read poetry would be more regular than that of materials read as prose. This was expected to be reflected in durational variability. Specifically, it was anticipated that the duration of metric feet contained in texts read as poetry would be less variable than the duration of the same verbal material read as prose. This expectation was not met: for both speakers, the variability of the durations of metric feet in texts read as poetry was greater than the variability found in texts read as prose. The difference was nonsignificant in the materials produced by one of the speakers; in the materials read by the other speaker, the durations of metric feet read in the poetic mode were significantly more variable than the durations of the same verbal material read as prose.

10:50

T8. The perceived rhythm of English and French as assessed by the tapping task. Stephen D. Isard, Donia R. Scott (Laboratory of Experimental Psychology, University of Sussex, Brighton BN1 9QG, United Kingdom), and Benedicte de Boysson-Bardies (Laboratorie de Psychologie, 54, bvd. Raspail, F-75006 Paris, France)

Pike [Intonation of American English (UMP, Ann Arbor, 1945)] and many others have claimed that English is a stress-timed language, having equally spaced interstress intervals (ISIs), as opposed to French which is said to be syllable-timed. Although measurements of ISIs in English show equally spaced ISIs to be the exception rather than the rule, it is the generally accepted view that there is a tendency for more-or-less equally spaced ISIs. Darwin and Donovan [Proceedings of NATOASI, edited by J. C. Simon (Reidel, Dordrecht, 1980)] found that when English listeners were asked to tap out the rhythm of stressed syllable onsets of English utterances, the rhythm of their taps was more isochronous than that of the stress beats of the target utterances, and conclude from this that English is perceptually isochronous. Using the same task, we have replicated their results, but have found that English listeners also tap more isochronously to French targets. Moreover, so do French listeners. We conclude that the results of the tapping task cannot be used to support the distinction between stress-timed and syllable-timed languages.

T9. Rhythmic processes in Spanish. Ana M. B. de Manrique and M. I. Massone (Laboratorio de Fonética Experimental, Universidad Católica Argentina, Bartolomé Mitre 1869, 1039 Buenos Aires, Argentina)

In a recent paper [A. M. B. de Manrique and A. M. Signorini, J. Phonet. 11, 2 (1983)], experimental evidence was obtained about the nature of Spanish rhythm. The measurement of vowel, consonant, and syllable duration showed that segments vary according to several factors. The measurement of interstress intervals showed some regularity in the occurrence of stress. From these results it was concluded that Spanish has a tendency towards stress-timed rhythm. The present work was undertaken in order to examine the processes by which regular intervals are achieved. The material consisted of two sets of three sentences. The sentences differed from each other in one word so as to increase the number of syllables of one interval, the other intervals having a fixed number. Results showed shortening and lengthening processes by which intervals, both fixed and variable, adjust the duration of their segments in accommodation to each other. It was also observed that a secondary stress becomes stronger in some variable intervals as another mechanism to attain regularity.

11:20

T10. Effects of accent on vowel amplitude in Japanese. Mary E. Beckman (Phonetics Laboratory, Morrill Hall, Cornell University, Ithaca, NY 14853)

It has long been known that accent (i.e., lexical stress) is a major factor contributing to variations in both vowel duration and vowel amplitude in English. An earlier experiment [Beckman, J. Acoust. Soc. Am. Suppl. 1 71, S1 (1982)] showed that, by contrast to English, Japanese accentual patterns have only a minimal effect on duration patterns. The present experiment compared accentual effects on amplitude in the two languages. It measured vowel amplitudes in a smaller subset of the minimally contrasting Japanese word pairs used earlier, as well as in a set of comparable English pairs. Three measures of vowel amplitude were obtained; namely, peak amplitude, average amplitude, and total amplitude. All three measures performed substantially worse as criteria for accent in Japanese than in English.

11:35

T11. Vowel-to-vowel coarticulation in English and Japanese. Harriet Magen (Haskins Laboratories, 270 Crown Street, New Haven, CT 06511-6695 and Department of Linguistics, Yale University, New Haven, CT 06520)

Vowel-to-vowel coarticulation was investigated by analysis of formant trajectories in VCV utterances. Two sets of English utterances were analyzed, one with initial stress and one with final stress. The VCV utterances consisted of all combinations of the labial consonants /b/, /p/, and /m/ and the vowels /a/ and /i/. Preliminary acoustic analyses indicate: (i) There are substantial vowel-to-vowel coarticulatory effects in both English stress patterns not only in transitions but also in steady state portions, and (ii) Stressed vowels in English are more resistant to coarticulation than are unstressed vowels. The effects of transconsonantal vowel are present for the duration of an unstressed vowel, but are small or absent at the beginning of a stressed VC and the end of a stressed CV. A pilot study on Japanese VCV utterances with low pitch accent on initial and final vowels suggests that the magnitude of coarticulation is greater in Japanese than in English throughout the duration of the vowel. [Work supported by NICHD.]

11:50

T12. Physical acoustic information for magnitude estimation of rate of speech. Keith R. Kluender (Department of Psychology, University of Texas, Austin, TX 78712)

Several studies have demonstrated that the phonetic identity of a segment can be altered by the rate of a precursive sequence. While this rate normalization effect has been shown for both consonants and vowels [J. L. Miller, Phonetica 38, 159-180(1981)] it has never been clear what the physical acoustic basis of the rate information is. In these experiments, subjects' magnitude estimations of rate for a short passage are used to assess the physical acoustic parameters used by the listener to perceive rate of speech. From earlier experiments [F. Grosjean and N. Lass, Lang. Speech 20(3), 198-208(1977)] it appears likely that the source of information for rate is not based upon any higher information including words or word boundaries. In the first experiment, subjects give rate estimations for a passage, spoken at five rates by a female English speaker that has been low-pass filtered at 300 Hz. Estimates for these filtered stimuli, in which energy for F1 and higher formants is deleted leaving only pitch and amplitude information, are indistinguishable from those for intact passages. It appears then that not even phonetic perception is necessary for perception of rate in this paradigm. Data for estimates of rate for passages with only pitch or only amplitude information will also be presented. [Work supported by NINCDS.]

12:05

T13. Temporal speech characteristics and vocal pleasantness in the aging voice. Herbert J. Oyer and Michael D. Trudeau (Speech and Hearing Science, The Ohio State University, 154 N. Oval Mall, Columbus, OH 43210)

Previous work by the authors emphasized temporal characteristics of speech as critical cues in age estimation. The present study assessed the role of the same temporal cues in listener perception of vocal pleasantness (PL). Twenty-four speakers (12 male), ages 41–82 years, read the passage "My Grandfather" and prolonged /aeiou/. With the first two sentences of "My Grandfather" as the stimulus, 22 college-age naive listeners (11 male) judged speaker PL on a five point scale. The times to initiate and to terminate /aeiou/, the time to articulate /mai grændfaðə/, reading rate, pause time within the passage, and speaker sex were regressed against PL. The single best predictor for PL was reading rate (*R*-square = 0.48) and the best significant model (12 variables) for PL yielded *R*-square = 0.77. Similar to age estimation, the perception of PL appeared to be strongly influenced by temporal characteristics of speech. While the contributions of individual variables differ, the results suggest that estimations of age and pleasantness involve closely related perceptual processes.

Session U. Musical Acoustics III: Violins: Old Instruments and New: Methods for Analysis

Thomas D. Rossing, Chairman

Department of Physics, Northern Illinois University, DeKalb, Illinois 60115

Chairman's Introduction-9:30

Invited Paper

9:35

U1. Accustical dilemmas for modern violin makers. Lance G. Bellamy (Bellamy's Violin Shop, 318 West 21st Street, Norfolk, VA 23517)

This paper will discuss the dilemmas of a maker of violins with regard to three important factors. The first is the selection of wood, where density must be balanced against the resonant frequency required for a piece of a given size. The second is the choice of the degree of arching with regard to the main resonant frequencies for the back and the top. The third is the graduation (thickness as a function of position on the surface). This situation will be compared to the choices available to violin makers in Golden Period, 1650–1750. There will be a demonstration of period and modern violins.

Contributed Papers

10:05

U2. Objective: Evaluation of violin tone quality. Norman C. Pickering (The Norman Pickering Company, 23 Culver Hill, Southampton, NY 11968)

A method has been developed for comparing violins by computer processing of the long-term one-third octave spectrum obtained while bowing the instrument in a rigidly prescribed program. At the same time, the sound pressure level of each semitone for the lowest three octaves is recorded. All the data obtained are analyzed by a program which assigns a figure of merit, derived from correlation with subjective evaluation of many instruments over several years of data accumulation. Results will be shown for some old Italian instruments, nineteenth century French and German violins, and some contemporary work.

10:20

U3. Physical parameters of Chinese and Australian woods in relation to their use in violin making. Morton A. Hutchins (Catgut Acoustical Society, Inc., 112 Essex Avenue, Montclair, NJ 07042) Report covers strip tests showing physical parameters of native woods from China and Australia used in construction of string instruments of the violin family or considered of potential use in such instruments. Results are compared with those obtained on European and American woods conventionally used in violin making.

10:35

U4. Air modes in the violin. Carleen M. Hutchins (Catgut Acoustical Society, Inc., 112 Essex Avenue, Montclair, NJ 07042)

In 1972 the higher air modes of the violin, which radiate very little through the f-holes, were explored by Erik Jansson [E. V. Jansson, "On Higher Air Modes in the Violin," Catgut Acoust. Soc. Newsletter #19 (May 1973)]. He studied the standing wave patterns of these modes in a violin shaped cavity with rigid walls, and then recorded the first (A1) air mode frequency for six normal violins. The present study extends this work to include the A1-A2 and A3 higher air modes in more than 50 violins of a wide variety of styles ranging from 1595 to the present. The test method will be described and mode frequencies reported with selected examples discussed in detail, particularly in relation to evidence of coupling between the wood and these higher air modes.

Session V. Underwater Acoustics III: Signal Processing

Samuel W. Marshall, Chairman

Naval Ocean Research and Development Activity, NSTL Station, Mississippi 39529

Chairman's Introduction-1:30

Contributed Papers

1:35

V1. A new normalization algorithm for detection systems. William A. Struzinski (Naval Underwater Systems Center, New London Laboratory, New London, CT 06320)

Normalization is a critical function in detection systems. Without proper normalization, the detection algorithm will suffer a severe performance degradation. To date, several normalization schemes have been developed. These include the Two Pass Mean, the Split Three Pass Mean, the Modified Median, and the Order Truncate Average normalizers. However, all these normalizers have a deficiency that will cause a performance degradation in detection systems (susceptibility to strong signals, excessive execution time, sensitivity to the noise probability distribution, etc.). In an effort to minimize the performance degradation, a new normalization scheme has been developed. The new approach, Split Average Exclude Average, was developed by combining the desirable features of the Two Pass Mean and the Order Truncate Average schemes. The new normalization scheme is examined in this paper, and the potential performance of this approach is demonstrated. [Work supported by NAVSEA.]

1:50

V2. A method employing OR-ing for treating dynamic signals. William A. Struzinski (Naval Underwater Systems Center, New London Laboratory, New London, CT 06320)

In a previous study [W. A. Struzinski, IEEE Trans. Acoust. Speech Signal Process. ASSP-31, 651–656 (1983)], OR-ing loss data were provided for a system composed of electrical integrators followed by an ORing device and a display. This analysis was for static signals. In this paper, consideration is given to a sinusoidal frequency modulation signal. For this type of signal, we examine an alternative processor where this is no pre-OR-ing device. The performance of the alternative processor is evaluated and compared with the previously analyzed system. An experimental performance comparison of the two processors was also conducted on the NUSC Acoustic Display Research Facility. Based upon the results of the subject analysis, it is concluded that for a sinusoidal frequency modulation signal, there should be no electrical integration prior to OR-ing. [Work supported by NAVSEA.]

2:05

V3. Bayesian weight estimation for adaptive arrays. S. L. Earp and L. W. Nolte (Department of Electrical Engineering, Duke University, Durham, NC 27706)

Adaptive arrays are used in many underwater sound applications. Although there are algorithms available for updating the adaptive weight vector, most of them are obtained by considering the heuristics of a given application. In this work, an algorithm derived from a formal optimization procedure is presented. The algorithm is a recursive realization of a Bayes estimate for the weighting vector, and is in this sense optimal. Initialization of the algorithm, governed by prior knowledge of the problem, is also shown. Performance for selected situations is obtained by computer simulation, and the behavior of the algorithm as a function of several adjustable parameters is discussed in detail. [Sponsored by ONR Code 411SP.]

2:20

V4. Detection performance in non-Gaussian environments. Karen Zeferjahn and L. W. Nolte (Department of Electrical Engineering, Duke University, Durham, NC 27706)

The detection performance of optimal processors in non-Gaussian environments is examined. A numerical method for computing likelihood ratios and the corresponding processor performance is developed with minimal restrictions on the probability density of the independent noise. This enables one to obtain the ROC rapidly for a wide range of non-Gaussian noise types. Results are presented for two different impulsive noise environments: (1) the Middleton Class A narrow-band noise model, and (2) a mixture model of normal and Laplacian noise. In addition to the ROCs the detector nonlinearities are presented. Finally, a suboptimal processor (cross correlator) is compared to the optimal processor. [Sponsored by ONR Code 411SP.]

2:35

V5. Signal detection for mixed multichannels. Kai-Kuang Ma and L. W. Nolte (Department of Electrical Engineering, Duke University, Durham, NC 27706)

In this paper the detection performance is presented for a signal received over M different channels. Two situations are considered; (1) the signal has uncertain parameters, and (2) the channels have a mixture of uncertainties, such as stable and rapidly varying phase channel types. This can occur in the ocean where the propagation characteristics are such that one channel may be quite stable over long periods of time and another may not. The effects of channel uncertainties on optimum performance are presented on the ROC. The sensitivity to knowledge of the channel types is also discussed. [Sponsored by ONR Code 411SP.]

2:50

V6. Ahead look sonar performance prediction via FFT, A. D. Matthews (Naval Coastal Systems Center, Panama City, FL 32407)

It is desired to predict the probabilities of detection and false alarm for an ahead look sonar providing N echoes from a cylindrical target. The signals are detected noncoherently and the targets are assumed to be bounded by, but not restricted to, the four Swerling cases. The clutter is assumed to be Rayleigh distributed. A computer algorithm is developed whose inputs are the number of echoes, the number of degrees of freedom, the multiple correlation of the echoes, and the average single-ping signalto-noise ratio. The outputs will be graphic representations of clutter and target probability density functions and a log-log representation of their corresponding false alarm and detection probability distributions. The process is accomplished by calculating the characteristic function reversing and conjugating, and performing an FFT to obtain an estimate of the probability density functions.

Session W. Psychological Acoustics V: Loudness and Intensity

Jack B. Kelly, Chairman

Department of Psychology, Carleton University, Ottawa, Ontario, Canada K1S 5B6

Chairman's Introduction-1:30

Contributed Papers

1:35

W1. Profile information improves Weber fraction. David M. Green and Christine R. Mason (Laboratory of Psychophysics, Harvard University, 33 Kirkland Street, Cambridge, MA 02138)

We measured the ability of observers to detect an increment in the intensity of a 100-ms 1000-Hz sinusoid under two conditions. In the first condition, the observer heard single 1000-Hz sinusoids-either the standard or the standard plus the increment. In the second condition, ten other sinusoids were added to the 1000-Hz sinusoid with frequencies ranging from 200 to 5000 Hz. These additional components were equal in intensity to the standard and the frequency ratio between successive components of the 11-component complex was 1.38. The basic task for each condition was the same, to detect an increment in the 1000-Hz component. The increment was easier to detect in the complex spectrum or "profile," presumably because the additional components allow one to make simultaneous comparisons among the different components. Only a successive comparison between the 1000-Hz components was possible in the single sinusoid condition. The improvement is as much as 10 dB for some observers and conditions, when expressed in terms of the signal relative to the standard. [Work supported by NIH.]

1:50

W2. Factors affecting descending binaural loudness balance. I. M. Young and L. D. Lowry (Department of Otolaryngology, Jefferson Medical College of Thomas Jefferson University, Philadelphia, PA 19107)

The control continuous tone (1000 Hz) was presented in one ear starting at an intensity of 100 dB SPL with an attenuation rate of 1 dB per second by descending manner. The balancing comparison continuous tone (1000 Hz) was presented in the opposite ear also starting at 100 dB SPL with an attenuation rate of 5 dB per second. Three trained subjects with normal hearing were instructed to release the Bekesy switch to increase the loudness and to push the switch to reduce the loudness of the comparison tone. While there were inter-subject variations, our data indicated that there was continuous decrease in the ratio of balanced loudness levels between tones with attenuation rates of 5 dB per second and 1 dB per second as the functions of time and decreasing intensity. This is considered a manifestation of normal adaptation. Present results were compared with our previous reports for the threshold differences produced by different attenuation rates at the suprathreshold starting intensities.

2:05

W3. Perceived magnitude of two-tone-noise complexes. Rhona P. Hellman (Communication Sciences Laboratory, Boston University, Boston, MA 02215)

Overall perceived magnitude (loudness, annoyance, and noisiness) of two-tone-noise complexes was measured by absolute magnitude estimation. The stimuli were tone pairs added to a low-pass noise that was attenuated by 5 dB/oct above 600 Hz. The low-frequency tonal component remained at 250 Hz, while the high-frequency component was set, in separate sessions, at 275, 350, 500, 1000, and 3000 Hz. Listening was binaural through earphones. Within a session, the experimental variables consisted of the SPLs of the added tones, the SPL of the noise, and the tone-to-noise ratios relative to the appropriate 1/3-octave-band pressure levels. Data analysis showed that perceived magnitude is a complex function of the overall SPL of the noise-tone-complex, the frequency separation (ΔF) between the tonal components, and tone-to-noise ratio. The results are related to underlying mechanisms governing loudness and masking. The possible role played by consonance and dissonance effects described by Plomp and Levelt [J. Acoust. Soc. Am. 38, 548–560 (1965)] is also discussed. [Work supported by NASA Langley Research Center.]

2:20

W4. Comparative redundancy as an influence on loudness. Ernest M. Weiler (Mail Location #379, University of Cincinnati, Cincinnati, OH 45221), David Sandman, Frederick Cobb (Psycho-Acoustics Lab, University of Cincinnati, Cincinnati, OH 45221), and James M. Davis (Department of Communication Disorders, Northern Michigan University, Marquette, MI 49855)

Adaptation to a stimulus environment often implies suppression of the redundant features in favor of stimuli carrying more information. Study of auditory adaptation of a continuing (redundant) stimulus, also requires consideration of the less redundant "comparison" stimulus. A magnitude estimation loudness adaptation study (1 kHz, 60 dB) designed to parallel the steps of the SDLB technique, yielded the following: (a) no loudness adaptation occurred during the pre-test baseline when binaural simultaneously intermittent stimuli were presented, (b) immediately afterward, 7 min. of continuous redundant monaural stimulation yielded negatively accelerated adaptation, (c) finally, restoration of intermittent stimulation in the contralateral ear, resulted in apparent binurally "induced" adaptation of the continuous tone, but not of the less redundant intermittent tone. Previously, monaural heterophonic balances (Weiler and Friedman, 1973, etc.) resulted in the decline of the continuous (redundant) tone in the presence of an intermittent comparison tone. In summary, adaptation occurs in the more redundant stimulus when the two are competitive, similar, and in the same frame of reference.

2:35

W5. Intensity discrimination in chinchillas. Bhagyalakshmi G. Shivapuja, Samuel S. Saunders, and Richard J. Salvi (University of Texas at Dallas, Callier Center, Dallas, TX 75235)

Previous research using amplitude modulated noise has suggested that the intensity discrimination thresholds of the chinchilla would be larger than those of humans. Consequently, intensity discrimination thresholds (ΔI) were measured in the chinchilla using a positive reinforcement technique. Intensity discrimination thresholds were obtained at several different frequencies over a range of sensation levels. In general the intensity discrimination thresholds improved as the sensation level in-

creased. The smallest intensity discrimination thresholds obtained were approximately two to three times larger than those for humans. Furthermore, the effect of sensation level on intensity discrimination threshold was more pronounced in the chinchilla than in man. Results and their implications will be discussed.

TUESDAY AFTERNOON, 8 MAY 1984

YORK HALL, 1:40 TO 3:15 P.M.

Session X. Speech Communication V: Development and Disorders of Speech

Winifred Strange, Chairman

Department of Communicology, University of Florida, Tampa, Florida 33620

Chairman's Introduction-1:40

Contributed Papers

1:45

X1. Features of infant vocalization at successive age levels. Rachel E. Stark, Jennifer L. Bond, Lynne E. Bernstein, and John M. Heinz (John F. Kennedy Institute 707 N. Broadway, Baltimore, MD 21205 and Johns Hopkins University, Baltimore, MD 21205)

It has been suggested that speech motor abilities in infants emerge within an invariant sequence of levels. The present study was designed to describe the articulatory-acoustic features of infant vocalization and thus, to identify those that may be characteristic of infant utterances at different age levels or developmental levels. The vocalizations of five infants were studied on a limited longitudinal basis. The age ranges of these infants were 2-10, 12-23, 26-36, 40-55, and 72-88 weeks, respectively. Forty to 50 vocalizations were selected randomly from each infant's output at the first and at the last recording session for a total of ten recordings. These vocalizations were analyzed acoustically by means of computer-assisted spectral analyses. Measurements of duration and frequency were made from the resulting displays, which also provided information to listeners as they judged voicing and vocalic and consonantal features. Analyses of these preliminary data suggest that three classes of features may provide useful indices of development of infant speech motor abilities: namely, (1) pitch contour; (2) vocalic features; and (3) consonantal features. The relative importance of each will be discussed. [Work supported by Bureau of Community Health Services, Maternal and Child Health.]

2:00

X2. A neuroethologic hypothesis of speech development. Harold R. Bauer (Speech and Hearing Science, 324 Derby, Ohio State University, 154 N. Oval Mall, Columbus, OH 43210)

The relation between phonetic contrast and individual differences in infants was noninvasively measured to operationally state a hypothesis of speech development. Four 13-month-old infants were recorded interacting with their mothers at home. Continuous f0 and amplitude displays were used in analyses made by two observers from each 1-h, time coded session of all vocalizations. Acoustic-phonetic data were lumped into front, central, and back vocants and bilabial, apical, palatal, and velar closants to emphasize motor contrast. These seven categories of speech sounds were graphed by each minute in the Phonetic Record, and then multiplied within each minute sample to yield a Phonetic Product, as a production/contrast measure. Individual Phonetic Record and Phonetic Product populational differences in production and contrast were found in the temporal analyses that are hypothesized to be predictive of speech-language development. [Supported by NINCDS Grants NS 16763 and 5T32 NS 07147.]

2:15

X3. Developmental speech perception of three acoustic cues associated with place of articulation, J. E. Sussman (Department of Curriculum and Instruction, Louisiana State University, Baton Rouge, LA 70803) and A. E. Carney (Department of Speech and Hearing Science, University of Illinois, Champaign, IL 61820)

In this experiment, 30 children and 10 adults participated in three speech perception tasks: discrimination, labeling, and adaptation. Stimuli were four sets of synthetic CV syllables, varying along a bilabial-to-alveolar, place-of-articulation continuum. The primary acoustic cue in each continuum was the change in slope of the F2-F3 transitions. The continua were constructed so that two had transition lengths of 45 ms, and two of 95 ms. Two continua contained a 5-ms burst, and two were burstless. The discrimination task was a change-no change procedure, in which subjects indicated whether a set of four stimuli remained the same or changed. Results indicated a complex developmental pattern. For discrimination, there was a progression in response strategy and sensitivity with increasing age. In contrast, labeling performance was similar for all subjects. Finally, only the adult subjects showed significant adaptation effects. Children's responses were essentially unchanged after adaptation. Further, transition length affected all three tasks, while the presence of a burst was nonsignificant. Results will be discussed with respect to implications for the study of children's speech perception.

2:30

X4. Acquisition of the English voicing contrast by Arabic children. Joann Fokes, Z. S. Bond, and Marcy Steinberg (School of Hearing and Speech Sciences, Ohio University, Athens, OH 45701)

Children are typically more proficient than adults in learning the phonetic detail of a second language. The purpose of this study was to investigate the acquisition of the English voicing contrast as cued by voice onset time in syllable-initial position comparing the performance of children whose native language is Arabic with that of American English speaking children and of adult speakers of Arabic learning English as a second language. Twelve children, 24 to 135 months in age, were recorded producing 11 minimal pairs differing in the voicing of the initial stop consonant, such as *pea/bee* and *cab /gab*. Voice onset time (VOT) was measured from spectrograms for labial, apical, and velar stops. Children were highly variable in their mastery of the voicing contrast; neither a child's age nor his experience with English could predict his phonetic proficiency.

S45

X5. Organization and timing of prephonatory movements in mild and severe stutterers. Ben C. Watson (Haskins Laboratories, 270 Crown Street, New Haven, CT 06510) and Peter J. Alfonso (Department of Communication Sciences, University of Connecticut, Storrs, CT 06268 and Haskins Laboratories, 270 Crown Street, New Haven CT 06510)

In a previous paper [J. Acoust. Soc. Am. Suppl. 1 73, S16 (1983)], we reported a composite foreperiod and stuttering severity effect on stutterers' acoustic laryngeal reaction time (LRT) values. That is, mild, but not severe, stutterers' LRT values approach nonstutterers' values as foreperiod increases. This observation lead to the formulation of the differential deficit hypothesis, which suggests that mild and severe stutterers execute qualitatively different prephonatory movements. In the study reported here, the differential deficit hypothesis was tested directly by examining movement and acoustic data obtained simultaneously from mild and severe stutterers and nonstutterers. The acoustic data replicated our previous results with respect to the composite foreperiod and stuttering severity effect on stutterers' LRT values. More importantly, movement data reveal that mild and severe stutterers can be differentiated on the basis of the organization, frequency of occurrence, and timing of prephonatory laryngeal and respiratory movements. That is, movement data both support the differential deficit hypothesis and account for the composite foreperiod and stuttering severity effect on stutterers' acoustic LRT values. [Work supported by NINCDS grant NS13870 to Haskins Laboratories.1

X6. Detecting and correcting mispronunciations: A note on methodology. Larry H. Small and Z. S. Bond (School of Hearing and Speech Sciences, Ohio University, Athens, OH 45701)

Two different techniques were employed to investigate subjects' ability to detect mispronounced words in continuous speech. Twenty twosyllable words were mispronounced in each of three prose passages, changing either the stress pattern, the voicing of obstruents, or the frontback dimension of vowels. Each passage contained only one mispronunciation type; the mispronounced words were equated for predictability from context and for frequency of occurrence in English. Subjects were tested under two conditions. In the first, subjects indicated mispronounced words on a script while listening to the passages. In the second, subjects were instructed to stop the tape when they detected a mispronounced word and to say what the word was. The subjects' spoken responses were recorded on tape. The first condition provides information regarding subjects' ability to detect mispronunciations under optimal conditions. The second condition provides detection information as well as information about the subjects' ability to correct the mispronounced words and the location of the detection in the stream of speech. The subjects' responses to stress mispronunciations were different from those to the other two mispronunciation types, in both test conditions.

MONTPELIER ROOM, 1:55 TO 3:15 P.M.

TUESDAY AFTERNOON, 8 MAY 1984

Session Y. Musical Acoustics IV and Architectural Acoustics II: Performance and Lecture Hall Acoustics

Samuel A. Elder, Chairman

Department of Physics, U. S. Naval Academy, Annapolis, Maryland 21402

Chairman's Introduction-1:55

Invited Paper

2:00

Y1. Compensating for the hall. Peter Zaret (Norfolk State University, Norfolk, VA 23504)

The performer and conductor must adjust their performance to compensate for the characteristics of the concert hall. A very different style of playing is required for an acoustically damped recording studio as compared with a live concert hall. In each case, the tonal balance must be adjusted by the performers because what they hear differs from that heard by the audience. The difference is a strong function of the hall or studio acoustics.

Contributed Papers

2:30

Y2. Loudness discrimination in the sound field of a room, I. M. Lindevald and A. H. Benade (Physics Department, Case Western Reserve University, Cleveland, OH 44106)

Subjects moving freely in the reverberant field of a room $(T \simeq 1 \text{ s})$, were presented with alternating pairs of 1-s soft-switched signals from loud-speakers differing in input level by |z| < 6 dB. The fraction of subjects perceiving pairs as equally loud were fitted to the curve $P(z) = A / [1 + (z/J)^C]$. A is the population fraction expected to perceive equal-level sources as equally loud, J is the 50% jnd, while $\delta (= 4J/C)$ measures the width of the transition region. Similar experiments using headphones give very

small values of $J(\simeq 0.5 \text{ dB})$ and $\delta(\simeq 0.1 \text{ dB})$. This precision for signals specified at the ear predicts chance performance in the Rayleigh-distributed sound field typical of rooms. The experiment was done with 400-Hz signals. (1) sinusoid; A = 0.44, J = 3.57 dB, $\delta = 3.45$ dB: (2) bandlimited tone with first five harmonics strong; A = 0.58, J = 2.79 dB, $\delta = 2.91$ dB: (3) tone with five equal amplitude harmonics; A = 0.60, J = 2.97 dB, $\delta = 3.45$ dB: and (4) a related "tone" having five nearly harmonic equal-amplitude sinusoids; A = 0.61, J = 2.87 dB, $\delta = 4.10$ dB. The observed (A, J, δ) sets lie between the values obtained in headphone experiments and those predicted via the Rayleigh distribution. Increasing the number of components reduces J, as it does the SD of the overall physical signal in the room. The values of A are nearly equal for all room signals except (1). The transition region δ is smallest for signal (2) which is most similar to musical tones and largest for the least musical signal (4).

Y3. An investigation of sound pressure level predictions in large lecture halls. David W. Kahn (Peter George Associates, 34 W. 17th Street, New York, NY 10011) and Jiri Tichy (Graduate Program in Acoustics, The Pennsylvania State University, University Park, PA 16802)

Measurements of steady-state sound pressure levels above the audience in large lecture halls show that the classical equation for predicting the sound pressure level is not accurate. The direct field above the seats was studied on a 1:10 scale model of a large lecture hall using the removable audience from the scale model. It was found to be dependent on the incidence angle and direction of sound propagation across the audience. The reverberant field above the seats was studied by subtracting the direct field from the measured field in the model. It was found to be dependent on the magnitude and particularly on the placement of absorption in the room. The decrease of sound pressure level versus distance in the total field depends on the angle (controlled by absorption placement) at which the strong reflections are incident upon the audience area. Sound pressure level decreases at a fairly constant rate with distance from the sound source in both the direct and reverberant field, and the decrease rate strongly depends on the absorption placement. The lowest rate of decay occurs when the side walls are absorptive, and both the ceiling and rear wall are reflective. The consequences are discussed with respect to prediction of speech intelligibility, and modifications are suggested for three current speech intelligibility prediction schemes.

3:00

Y4. Image method predictive acoustic: Shortcuts to computational time and infinite summation accuracy. Gilles Lemire and J. Nicolas (Mechanical Engineering Department, Université de Sherbrooke, Sherbrooke, Quebec, Canada J1K 2R1)

The image method can be used to predict the noise levels within rectangular halls. One of the drawbacks of this method is the lengthy computational time involved to reach a reasonable accuracy. Although the commonly used Allen and Berkley algorithm [J. Acoust. Soc. Am. 65, 943– 950(1979)] is excellent, we thought that an algorithm which would permit us to evaluate the sound level produced by each of the sources order would be useful. So we derived one, and information on each order contribution showed that, at high enough orders, the contribution of each order is independent of receiver location and that it varies linearly with the order number. It will be explained how these two findings can be used to reduce the computational time and yet approach the infinite summation accuracy. [Work supported by the Institut de Recherche en Santé et Sécurité du Travail.]

TUESDAY AFTERNOON, 8 MAY 1984

EPPINGTON ROOM, 1:55 TO 3:15 P.M.

Session Z. Noise IV: Some Thoughts on Noise Criteria

Ronald L. Bannister, Chairman

Westinghouse Electric Corporation, The Quadrangle, Orlando, Florida 32817

Chairman's Introduction-1:55

Contributed Papers

2:00

Z1. Guidelines for noise exposure: An analysis of 100-dB vs 90-dB ambient levels. John Erdreich (National Institute for Occupational Safety and Health, Robert A. Taft Laboratories, 4676 Columbia Parkway, Cincinnati, OH 45226)

Among the various techniques available to reduce noise exposure, personal protective devices may be used to reduce worker exposure from 100-dB TWA to 90-dB TWA. From an analysis of risk statistics for workers exposed between 80 and 100 dB the effect of relying on personal protection in this range rather than to require source reduction to 90 dBA is shown to be a 20% increase in attributable risk of hearing loss and a doubling of the odds that an exposed worker will suffer an occupationally produced hearing loss.

2:15

Z2. The exchange rate and noise-induced hearing loss. Alice H. Suter (Consultant, 1501 Red Oak Drive, Silver Spring, MD 20910)

Scientists and policy makers have debated the subject of the exchange rate (3, 4, or 5 dB per doubling or halving of duration) for many years. A recent historical review of this topic in the U.S. reveals that early criteria were based on temporary threshold shift (TTS) studies, and it is well known that TTS is not always a valid predictor of permanent hearing impairment. OSHA's 5-dB exchange rate is founded on TTS experiments and therefore is of dubious validity. Data from experiments of noise-induced cochlear damage support the use of the 3-dB exchange rate for single exposures within an 8-h day. There is some evidence that intermit-

S47 J. Acoust. Soc. Am. Suppl. 1, Vol. 75, Spring 1984

tency can be beneficial, at least in the laboratory, which may support a correction to the daily "dose" as calculated by the 3-dB rule. Data from most field studies support the 3-dB exchange rate, with the exception of some (but not all) studies of hearing loss due to intermittent noise in outdoor occupations. Because any adjustment to the daily, average exposure level for outdoor occupations will be fraught with complication, a more satisfactory and protective approach is simply to use the 3-dB exchange rate for all conditions.

2:30

Z3. Intermittence and the equal-energy theory. W. Dixon Ward (2630 University Avenue, SE, Minneapolis, MN 55414)

The "equal-energy" theory of noise-induced damage to the auditory system caused by habitual daily exposure postulates that the degree of damage depends only on the total amount of energy absorbed by the ear during the workday, and not on the temporal pattern of the noise. To test this hypothesis, two groups of chinchillas were exposed to 700–2800-Hz noise at 102-dB SPL. Monday through Friday, for 9 weeks. One group received a single daily 48-min continuous exposure; the other was given 40 1.2-min exposures, one every 12 min. The intermittent exposure produced significantly less temporary threshold shift, permanent threshold shift, and histological damage. Comparison with other chinchilla data indicates that the degree of reduction in hair-cell destruction, for this pattern of intermittence, is consistent with the trading relation of 5 dB per halving of exposure duration still used in the USA for assessing daily exposure, rather than the 3 dB required by the equal-energy-based ISO recommended standard R-1999. [Work supported by NIH Grant NS 12125.]

Z4. Reported outdoor speech interference and event L_{AX} . Fred L. Hall, Susan Birnie, and S. Martin Taylor (Department of Geography, McMaster University, Hamilton, Ontario, Canada L8S 4K1)

One plausible interpretation of annoyance at noise is that the annoyance arises primarily because of speech and sleep interference caused by the noise. If this is true, then it is sensible to look for relationships between activity interference and indicators of the noise from specific noisy events. Such an analysis could provide the first step toward a better understanding of the relationship between noise and annoyance. This paper describes the results of such an analysis for reported speech interference due to aircraft noise in residential areas. The event noise levels are derived from data collected during the summer of 1983 by Transport Canada's automatic monitoring system at ten locations around Toronto International Airport. For each location, this data set provided the maximum L_{AX} and average L_{AX} by aircraft type. The analysis relates the outdoor speech interference reported by respondents at each site to the worst case and average L_{AX} for aircraft operations at their location, by means of a nonlinear regression. The results are compared with a similar analysis for road traffic data, to see if the same equation can serve for both types of noise source.

Z5. Impulse noise: Comparison of dose calculated by 5-dB rule and 3-dB rule. John Erdreich (National Institute for Occupational Safety and Health, Cincinnati, OH 45226)

In the past several years, there have been many proposals concerning incorporation of impulse noise into total worker exposure. This is a problem of particular concern in the United States as a consequence of the 5dB trading rule mandated by regulation. The alternative approaches to integrating impulse noise are to use a direct integration with a 5-dB trading rule, to use a 3-dB rule SLOW integration according to ISO 1999 and the proposed ANSI standard for high level signals above 120 dBA or to use a 5-dB SLOW integration as performed by the ANSI Standard (S1.25) personal noise dosimeter. Simulation of each of these approaches with industrial noise data was performed. The effect of integrating high level transients with a 3-dB rule (p^2) integration compared with a 5-dB rule $(p^{1,2})$ integration is that the calculated dose is 3 to 15 times greater than the 5-dB rule dose. We would infer from this that substantially greater numbers of workers would be protected (or more sites would be in noncompliance) by using a 3-dB rule for impulse noise. Because of this, it is critical that a rigorous scientific basis be established for impulse noise dose prior to defining procedures for such dose determination.

TUESDAY AFTERNOON, 8 MAY 1984

GREENWAY ROOM, 2:00 P.M.

Meeting of Standards Committee S2: Mechanical Shock and Vibration

to be held jointly with the

Technical Advisory Group (TAG) Meeting for ISO/TC 108 Mechanical Vibration and Shock

P. H. Maedel, Jr. Chairman S2⁴

Westinghouse Electric Corporation, Lester Branch, P.O. Box 9175, Lester, Pennsylvania 19113

G. Booth, Chairman Technical Advisory Group for ISO/TC 108 220 Clark Avenue, Branford, Connecticut 06405

Standards Committee S2 on Mechanical Shock and Vibration. Working group chairpersons will present reports of their recent progress on writing and processing various shock and vibration standards. There will be a report on the interface of S2 activities with those of ISO/TC 108 (the Technical Advisory Group for ISO/TC 108 consists of members of S2, S3, and other persons not necessarily members of those committees). Plans for the ISO/TC 108 meeting, to be held during September 1984 will be discussed.

Plenary Session

Frederick H. Fisher, Chairman President, Acoustical Society of America

Presentation of Awards

Presentation of the Gold Medal to Robert T. Beyer

Presentation of the Biennial Award to Peter N. Mikhalevsky

The Navy in Space

Address by Commodore Richard H. Truly, United States Navy Commander of the Space Shuttle Columbia on its second space flight and Commander, Navy Space Command

Session AA. Underwater Acoustics IV: High Frequency II

R. Martin, Chairman

Naval Ocean Research and Development Activity, NSTL Station, Mississippi 39529

Chairman's Introduction-8:00

Invited Papers

8:05

AA1. Sea surface reverberation. Suzanne T. McDaniel (Applied Research Laboratory, The Pennsylvania State University, University Park, PA 16802)

Reflection and scattering from the sea surface have been extensively studied both experimentally and from a theoretical standpoint. This paper focuses on reverberation processes because, due to the relative case of measurement, a vast store of experimental data has been amassed. Measurements have been performed to study the dependence of the strength and Doppler spread of monostatic backscatter on acoustic frequency, incidence angle, sea state, windspeed, and heading with respect to the mean wind direction. In this paper, reverberation measurements and the accompanying development of theories to explain the experimental results are reviewed from a historical perspective. The theoretical effort is traced from the application of the Kirchhoff approximation in the geometrical optics limit, to the use of composite-roughness theory along with a treatment of scattering from the layer of wind generated microbubbles that exist below the surface. Our present ability to characterize sea surface reverberation is demonstrated using recent measurements of ocean wave spectra and bubble densities as inputs to the theory. [Research supported by NORDA.]

8.30

AA2. Progress in our understanding of forward acoustic scattering. T. E. Ewart (Applied Physics Laboratory and the School of Oceanography, University of Washington, Seattle, WA 98105) and B. J. Uscinski (Department of Applied Mathematics and Theoretical Physics, University of Cambridge, Cambridge, England CB3 9EW)

Recent solutions of the parabolic fourth moment equations, pioneered by Shishov have led to good predictions of the power spectral density of temporal intensty fluctuations as meaured in the Cobb71 and MATE experiments for a wide range of scattering parameters. Comparison of Monte-Carlo solutions of the parabolic wave equation with the above predictions for the vertical spatial fluctuations of intensity produces excellent agreement between simulations and theory. The discrepancies between experiment and theory which remain appear to be due to our lack of understanding of the index of refraction field itself. The intensity moments m_a , q > 2 of a propagating wavefield in a random medium exhibit log-normal behavior at short ranges when observed as a function of m_{2} ; subsequently they rise to a maximum in the second moment and then drop back at long ranges to the exponential moments. The shape of the moment curves and their point of departure from lognormal are dependent on the specific correlation function of the index of refraction. Prediction of the higher moments using a model which spans the regime between log-normal and exponential, and is based on the m_2 and m, moments as parameters, has proved quite successful at explaining the Cobb71, MATE, AFAR, and SW Bermuda results. Thus, if a theoretical prediction of m_3 can be obtained, the probability distribution and the spectral decomposition of the lower moments of intensity fluctuations due to forward scattering should be predictable in the parabolic approximation. The development of the theory-experiment comparisons will be presented and so will the authors views on what else needs to be measured for a complete test of the current theories.

8:55

AA3. Survey of high-frequency bottom reverberation. T. G. Goldsberry (NATO SACLANT ASW Research Centre, Viale San Bartolomeo, 400, La Spezia, Italy I-19026)

High-frequency sonars are almost always reverberation limited and the most important contributor to this reverberation is backscattered energy from the ocean bottom. This has been long recognized; however, until recently the status of knowledge about this important subject was reflected in the classic paper of McKinney and Anderson [J. Acoust. Soc. Am. 36, 158–163 (1964)]. In recent years there has been a revival of interest in acoustic scattering from the ocean bottom at high frequencies, including measurements at sites on the East, West, and Gulf coasts. This paper presents a survey of recent and historical work in the area.

9:20

AA4. Environmental bottom characterization required for modeling and prediction of high-frequency acoustic bottomscattering. Michael D. Richardson (Naval Ocean Research and Development Activity, NSTL, MS 39529)

Modeling and prediction of acoustic bottom scattering require characterization of sediment geoacoustic and bottom roughness properties. Data, from five recent shallow-water acoustic experiments, are presented on the temporal and spatial variability of values of those bottom parameters thought to be important to bottomscattering. The importance of hydrodynamic and biological processes in controlling relevant sediment geoacoustic and roughness properties is also discussed. An improved understanding of which physical scattering processes dominate bottom scattering at different frequencies, beamwidths, pulse lengths, and grazing angles is required to predict bottomscattering from environmental properties. [Work supported by NORDA.]

Contributed Papers

9:45

AA5. Two-scale solutions for intensity fluctuations in strong scattering. Shimshon Frankenthal, Alan M. Whitman, and Mark J. Beran (Department of Interdisciplinary Studies, Faculty of Engineering, Tel-Aviv University, Tel-Aviv, Israel)

An exact integrodifferential equation is derived for a certain transform of the 4-point coherence function, using a two-scale embedding procedure. The solution is expanded in an asymptotic series in the inverse strong scattering parameter, whose terms are solutions of a hierarchy of simple first-order partial differential equations. Further approximations simplify the retransformation, and display the 4-point coherence in a useful, numerically convenient form. Results compare favorably with existing numerical computations of the scintillation index and the covariance in two-dimensional plane-wave propagation. Results for three-dimensional plane-wave propagation are also presented.

10:00

AA6. High-frequency acoustic scattering from stratified turbulence. Andrew Lintz and C. M. Dube (Dynamics Technology, Inc., 22939 Hawthorne Boulevard, Torrance, CA 90505)

A laboratory study of high-frequency acoustic scattering from stratified turbulence was performed in order to test the theories and techniques used for the prediction of acoustic scattering. Scattering predictions were made with a computer simulation code which incorporates Lane's hydrodynamic model of stratified turbulence with the relevant aspects of linear scattering theory. Laboratory acoustic measurements were made for a range of acoustic system parameters, including forward scatter in the vertical and horizontal planes, and vertical backscatter. Hydrodynamic characterization of the sound speed spectrum was made with trayersing conductivity probe arrays and with quantitative optical shadowgraphs; the data were then used to define the turbulence model parameters. The analytical techniques used to extract the hydrodynamic model parameters from both conductivity and shadowgraph data gave consistent results, and verified the Lane model as a valid descriptor of stratified turbulence. Theoretical acoustic scattering level predictions made with the simulation code are in good agreement with the laboratory acoustic measurements. These results verify the laboratory measurement techniques and validate our implementation of linear scattering theory and Lane's turbulence model for predicting acoustic scattering from stratified tubulence. [Work supported by Navy SSPO and Dynamics Technology internal R&D funding.]

10:15

AA7. High-frequency propagation through a turbulent thermal plume. Joe W. Posey and Coleman Levenson (Naval Ocean Research and Development Activity, NSTL, MS 39529)

High-frequency acoustic signals were propagated in a large water tank over a fixed range which included a turbulent thermal plume of variable thickness. The signals were 1-ms cw pulses in the frequency range 0.8 to 2.0 MHz. The repetition rate was one pulse per second, and the propagation range was 10.4 m. The thermal plume was created by activating all or part of an array of heating elements which ran the full length of the propagation path about 1.5 m below it. Five different heating configurations were investigated by energizing portions of the heat array: (1) the one third nearest the projector, (2) the one third nearest the receiver, (3) the two thirds nearest the projector, (4) the two thirds nearest the receiver, and (5) the entire array. It was found that the incoherent energy fraction of the received signals (measured over 2-min intervals) did not depend upon the position of the plume along the propagation path. Furthermore, observed fluctuations are in good agreement with the Wenzel theory if the length of the propagation path through the plume is used as the range.

10:30

AA8. Volume scattering: Echo peak PDF. T. K. Stanton (Marine Studies Center, 1225 West Dayton Street, University of Wisconsin-Madison, Madison, WI 53702)

The probability density function (PDF) of the maximum echo value achieved in a depth gate has been analytically derived, computer simulated, and measured in the field-all in cases where clouds of scatterers are involved. The clouds of interest are plankton, nekton, bubbles, etc. or a combination and are sufficiently dense so that echoes from the individual scatterers overlap. We show that this echo peak PDF is quite different than the Rayleigh PDF of the envelope, even for gate lengths smaller than one transmission pulse length. We have employed measured PDFs by (1) estimating the abundance of occasional large scatterers that are within the clouds (for example large fish feeding on plankton) since their occurrence is differentiable from the rest of the cloud in the PDF, and (2) clearly differentiating between conditions where the echoes overlap and do not overlap. Once it is determined whether or not they overlap, lower or upper bounds in scatterer density (number per unit volume) may be calculated. We have utilized both of these techniques in situ at the Gulf Stream Boundary near Cape Hatteras, NC where we observed continuous distributions of plankton and nekton. [Work supported by the ONR.]

10:45

AA9. Acoustic surveys for marine mammals using a towed hydrophone array. Jeanette A. Thomas, Sheldon R. Fisher, and Lisa M. Ferm (Hubbs Sea World Research Institute, 1700 South Shores Road, San Diego, CA 92109)

For the purposes of identifying and locating marine mammals by their sounds, we designed a broadband linear array of hydrophones that is towed from a survey vessel. This array is a modification of the low-frequency arrays currently used by the military and the geophysical industry. The array has been used during four studies: one offshore California, two in the eastern tropical Pacific, and one on a circumnavigation of Antarctica. Comparisons of visual and acoustic detections of marine mammals will be discussed. During one cruise as many as 32% of the marine mammals encountered were detected by the array, but not by observers. Factors affecting reception and detection of marine mammals will be discussed. We conclude that combining visual and acoustic surveys may produce more accurate species identifications and estimates of abundance for marine mammals.

11:00

AA10. Autoregressive modeling of pulse-to-pulse incoherent Doppler sonar data. D. Scott Hansen (Marine Physical Laboratory, A-005, Scripps Institution of Oceanography, La Jolla, CA 92093)

An innovative approach to modeling the range evolving spectral structure of pulse-to-pulse incoherent Doppler sonar data is presented.

This approach is demonstrated on a unique multifrequency, parallel beam oceanic data set. The approach is motivated by the desire to determine the parameters of the oceanic velocity field. Under a set of assumptions the mean frequency of the Doppler spectrum can be used to infer the velocity field of the oceanic water mass on a range evolving basis. If the Doppler spectrum is symmetric and unimodal, this mean freqency may well characterize the Doppler shift from which the relative radial velocity between the sonar platform and a dense "cloud" of scatterers may be derived. However, the Doppler spectrum may be multipeaked and/or asymmetric due to the nonhomogeneous nature of the reverberation process, instrumental effects, or beam pattern structure. In this case the mean frequency may have little relation to the Doppler shift associated with the true scatterer-platform velocity. To aid in interpretation, the data are modeled spectrally on closely spaced range intervals via autoregressive (AR) techniques. Interpretation of these AR spectra may lead to a determination of the velocity field and/or to the causative mechanism of anomalous spectral structure. In the case anomalous spectral structure is found, careful interpretation of the spectra is necessary to determine the velocity field. Two regions of the multifrequency, parallel beam data set are analyzed to demonstrate the relationship between the mean frequency and AR techniques. The first of these regions is shown to possess a unimodal, symmetric spectral structure on a range evolving basis. In this region the mean frequency profiles are shown to agree closely. In the second region, which is shown to possess an asymmetric spectral structure, the mean frequency velocity profiles are shown to agree poorly. Interpretation of the spectra leads to closer agreement between the velocity field as seen by the two parallel beam sonars.

11:15

AA11. Coherent acoustic Doppler measurement of estuarine internal waves. T. L. Clarke, J. F. Craynock, and J. R. Proni (Ocean Acoustics Division, AOML/NOAA, 4301 Rickenbacker Causeway, Miami, FL 33149)

A bottom-mounted 200-kHz narrow beam coherent acoustic Doppler system was used to observe profiles of vertical water velocity in Chesapeake Bay (17-m water depth) near the mouth of the Patuxent river in August 1982. Internal wave induced vertical water motion was up to 2 m as shown by observation of biological scattering layers. Coherent Doppler measurements gave vertical water velocities of several centimeters per second. The scattering layer motion and the velocity were in phase quadrature and the amplitudes were consistent with propagating internal waves. Of several types of internal waves seen, the most common were simple interfacial waves on the pycnocline, but some instances of higher mode waves were observed, <u>Soliton wave packets were also seen</u>. Problems of signal processing and of removing the aliasing resulting from the

WEDNESDAY MORNING, 9 MAY 1984

use of pulse-to-pulse coherent Doppler processing are also discussed. Fairly simple modifications to standard scientific echo sounders make it possible to extract vertical velocity profiles from recorded signals using coherent signal processing.

11:30

AA12. Doppler spread and temporal coherence of high-frequency volume reverberation. F. D. Tappert (University of Miami, Miami, FL 33149)

The wave kinetic technique of radiation transport theory has been used to derive a theoretical expression for frequency spread, and hence temporal coherence, of high-frequency volume reverberation from particulate matter entrained by oceanic turbulence. The following effects are taken into account: intrinsic Doppler spread due to turbulent motion, Doppler due to platform motion, transit-time broadening due to transmitter and receiver beam patterns in both nearfield and farfield, and broadening due to finite transmitted pulse length. With additional simplifying assumptions (Gaussian beam patterns, Gaussian velocity distribution, etc.), explicit results are obtained for estimating temporal coherence of volume reverberation.

11:45

AA13. A point-scatterer model for the spatial-temporal covariance of reverberation. Gary R. Wilson (Applied Research Laboratories, The University of Texas at Austin, Austin, TX 78712-8029)

A point-scatterer model of reverberation was developed to predict the spatial and temporal covariance of surface reverberation for both horizontal and vertical receiver separations. The point scatterers are modeled as perfect point reflectors with no frequency spreading. The distribution of scatterers was chosen to be representative of a sub-surface bubble layer, which is appropriate for high-frequency scattering at high wind speeds. Comparison to experimental measurements of reverberation covariance at 80 kHz indicates that projector (and receiver) beamwidths are the primary factors determining the horizontal spatial coherence, and not waveheights or sub-surface bubbles. However, it was found that to adequately model the vertical spatial covariance the bubble layer distribution was required, suggesting that the dominant scattering mechanism was subsurface bubbles rather than the air-water interface, at least at the high wind speeds associated with the vertical covariance measurements. The temporal covariance was also predicted and found to be in excellent agreement with the measured temporal covariance for the short pulse lengths used in the experiments. The pulse length and transfer functions of the projector and receivers were found to be the dominant factors affecting

his the temporal covariance for short pulse lengths. his the temporal covariance for short pulse leng

Session BB. Physical Acoustics III and Engineering Acoustics II: Radiation and Scattering

Susan K. Numrich, Chairman

Naval Research Laboratory, Code 5132, 4555 Overlook Avenue, Washington, DC 20375

Chairman's Introduction-8:00

Contributed Papers

8:05

BB1. Diffraction of pulsed ultrasonic waves in lossless and absorbing media. Daniel Guyomar and John Powers (Department of Electrical Engineering, Naval Postgraduate School, Monterey, CA 93943)

A theoretical model is presented for computing the transient acoustical field radiated by a baffled transducer in a lossless or absorbing medium. Attenuation is introduced by the addition of a term to the wave equation, simulating the absorption of biological tissue. The method is based on a time generalization of the angular spectrum theory. It shows that diffraction of the pulse is equivalent to the time-varying spatial filter that reduces the high spatial frequency components. The effect of attenuation is to enhance the low-frequency components even more than in the lossless case, while exponentially attenuating the wave amplitude. The method is valid for any planar velocity souce distribution with arbitrary time excitation. Neither the Fresnel nor the Fraunhofer approximations are used, consequently no restrictions on the propagation distance are required. The effects of a finite receiver are easily incorporated in the formulation as an additional spatial filter. Computer simulations of results both with and without attenuation are included.

8:20

BB2. Computer-aided backscattering measurement of ultrasonic waves. Antal Csakany, Shiao Wang, and Laszlo Adler (Department of Welding Engineering, Ohio State University, 190 19th Avenue, Columbus, OH 43210)

A system based on two microcomputers was developed to increase the precision and repeatibility of ultrasonic measurements. The first microcomputer controls the mechanical movements (resolution: $40 \mu m$ in linear distance; $1/40^{\circ}$ in angle) and data collection, the second one is used for data processing and interactive data presentation. The system was applied to measure leaky Rayleigh and leaky Lamb wave velocities from critical angles with an increased precision in different materials. A method was also developed to measure the loss of leaky Rayleigh waves from several materials in water. This system has been especially advantageously used where a large number of inhomogeneities are the sources of the ultrasonic scattering, i.e., grains, pores. Examples will be given to present the various displays of complex measured data.

8:35

BB3. Scattering of Rayleigh waves by an arbitrarily oriented sub-surface crack. J. H. M. T. van der Hijden (Schlumberger-Doll Research, P. O. Box 307, Ridgefield, CT 06877) and F. L. Neerhoff (Delft University of Technology, Department of Electrical Engineering, Laboratory of Electromagnetic Research, P. O. Box 5031, 2600 GA Delft, The Netherlands)

The diffraction of acoustic waves by a crack in an unbounded elastic medium has been extensively discussed in the literature. For practical purposes the problem in a semi-infinite solid is a more realistic one. A rigorous theory of the diffraction of time-harmonic elastic waves by an *arbitrarily* oriented, cylindrical, stress-free crack of finite width embedded in a semi-infinite elastic medium has been developed. The incident wave is taken to be either a P wave, an SV wave, or a Rayleigh wave. The resulting boundary-value problems for the unknown jump in the particle displacement across the crack are solved by employing the integral-equation method in combination with the Galerkin method. Numerical results are presented in the form of normalized power scattering characteristics, dynamic stress intensity factors, and Rayleigh-wave transmission and reflection coefficients, for a range of geometrical parameters. The most striking feature in the scattering characteristics are the sharp peaks that occur for scattered shear waves, for which an explanation will be given.

8:50

BB4. The transition matrix in prolate spheroidal coordinates. Roger H. Hackman (Naval Coastal Systems Center, Panama City, FL 32407)

At the 105th meeting of the Acoustical Society of America, a preliminary calculation of the acoustic scattering from a solid elastic prolate spheroid in water was presented. This calculation, which was based on a separation of variables technique in prolate spheroidal coordinates, can now be shown to be incorrect. In a recent paper [Hackman, J. Acoust. Soc. Am. 75, 35–45 (1984)], Betti's third identity was used to establish a spheroidal coordinate based transition matrix. This approach succeeds where the earlier work failed. Since this latter work is a true *T*-matrix approach, scattering by arbitrarily shaped bodies can be described. This work possesses a distinct advantage over the standard spherical coordinate based *T* matrix in that the formalism can be explicitly tailored to the aspect ratio requirements of the scatterer. Calculations are presented by the two *T*matrix approaches and their rates of convergence are compared. The reasons for the failure of the earlier work is also discussed.

9:05

BB5. A comparison of acoustical scattering from fluid loaded elastic shells and sound soft objects. Michael F. Werby (Naval Ocean Research and Development Activity, Numerical Modeling Division, NSTL, Code 221, MS 39529) and Larry H. Green (Naval Coastal Systems Center, Panama City, FL 32407)

Comparisons are presented for acoustical scattering from fluid loaded prolate spheroidal sound soft scatterers and elastic shells of the same shape ranging in thickness from 0.1% to 2.5% of the semi-major axis. The Ka region being studied varies from 3-12 where K is the wavenumber of the incident wave and a is one-half the length of the major axis. Exact theoretical calculations are performed using a modified T-matrix approach which allows one for the first time, to perform calculations on very thin nonspherical elastical shells. The calculations show that with the exception of the very thin shell, one does not observe a sound soft background. Furthermore, resonances for these objects are very broad and tend to dominate the form function plots. Of particular interest is the fact that by the time one reaches a thickness of 2.5% the background begins to appear rigid with a shift in resonance nulls which is related to the fact that rigid scattering is out of phase with sound soft scattering by 180°.

9:20

BB6. An orthonormalization method for solving the time harmonic acoustic scattering from finite, smooth, solid, elastic bodies. Alan Dallas (Sachs/Freeman Associates, Bowie, MD 20715) and C. F. Gaumond (Naval Research Laboratory, Washington, DC 20375)

The null field integral equations [P. C. Waterman, J. Acoust. Soc. Am. 45, 1417-1429 (1969); A. Bostrom, J. Acoust. Soc. Am. 67, 390-398 (1980)] are solved using orthonormalization in the appropriate Hilbert Space. An interior limiting amplitude principle is developed to identify the unique interior elastic field in the long time limit. The result is an algorithm for computing the scattered acoustic and interior elastic field which requires no matrix inversions.

9:35

BB7. Numerical implementation of the orthonormalization method for acoustic scattering from a rigid prolate ellipsoid. C. F. Gaumond (Naval Research Laboratory, Washington, DC 20375) and Allan Dallas (Sachs/ Freeman Associates, Bowie, MD 20715)

The orthonormalization method was used to derive the solution for a smooth rigid body. The scattering from a prolate ellipsoid was described using spherical harmonics on basis functions. The form function was found for low values of ka, where a is the semi-major axis, and for various length/width ratios. The effects of including various numbers of basis functions will be shown.

9:50

BB8. Resonance scattering of acoustic waves from air-filled cylinders in water. P. P. Delsanto, J. D. Alemar, E. Rosario (Department of Physics, University of Puerto Rico, Mayaguez, Puerto Rico 00708), A. Nagl, and H. Überall (Department of Physics, Catholic University, Washington, DC 20064)

A general theory for the scattering of plane elastic waves obliquely incident on an infinite cylindrical solid obstacle has been developed. In the present paper, this is specialized to the acoustic case for the example of an air-filled cylinder in water. We study the resonances of the scattering amplitudes, and determine their poles in the complex frequency plane (SEM poles) and mode number plane (Regge poles). The motion of the poles upon variation of the angle of incidence is investigated. The pole diagrams lead to a determination of the dispersion curves of helical surface waves generated by the incident wave, as well as their refraction and attenuation, all as a function of the angle of incidence. This includes both external (Franz type) and internal surface waves propagating in the water and air medium, respectively. [Work at Puerto Rico supported by the U.S. Army Research Office.]

10:05

BB9. Pulse response and the pole structure of elastic-body scattering amplitudes. S. K. Numrich (Naval Research Laboratory, Washington, DC 20375), W. E. Howell, and H. Überall (Department of Physics, Catholic University, Washington, DC 20064)

The interference features appearing in acoustic scattering amplitudes of elastic targets, when plotted versus frequency, are largely governed by the complex-frequency poles of the amplitudes. Unitarity entails the existence of a zero accompanying each pole. The dependence of interference features on the pole and zero structure of the scattering amplitude *S* can be strikingly visualized by plotting contour maps of |S| over the complex frequency plane. We further studied the influence of the pole structure on the scattering of long sinusoidal wave trains for tungsten carbide, aluminum, and lucite spheres and cylinders. Both quasi-stationary and transient portions of the echo are affected, as physically explained by the phase relationships between specularly reflected and circumferential pulses. [H.Ü. was partly supported by ONR.]

10:20

BB10. Complex eigenfrequencies of rigid and soft spheroids. J. M. D'Archangelo, P. Savage (Department of Mathematics, U.S. Naval Academy, Annapolis, MD 21402), H. Überall, K. B. Yoo (Department of Physics, Catholic University, Washington, DC 20064), S. H. Brown, and J. W. Dickey (David M. Taylor Naval Ship R&D Center, Annapolis, MD 21402)

The complex eigenfrequencies of impenetrable or penetrable target objects form a pattern which is characteristic for a given target, as far as its shape and/or composition is concerned. They manifest themselves as poles (resonances) in the amplitude of waves scattered from the object. We here obtain the eigenfrequency patterns of acoustically rigid and soft prolate spheroids in the complex frequency plane, and study their displacement when the eccentricity of the spheroids is varied. The eigenfrequencies were obtained numerically by subjecting spheroidal wavefunctions to the Neumann or Dirichlet boundary condition, respectively. Poles of both m = 0 (axial vibrations) and $m \neq 0$ (vibrations with azimuthal components) were obtained, and axes ratios of 1:1 (sphere), 1.33:1, 2:1, 3:1, 5:1, and 10:1 were considered. Increasing axes ratios lead to increasing splittings between poles with different m values. [Supported in part by the David W. Taylor Naval Ship R&D Center, Annapolis, MD 21402.]

10:35

BB11. A solution of multiple scattering problem by method of spatial stochastic systems. I. Discrete scatterers with arbitrary shape. II. Discrete scatterers and random interface. III. Two random irregular interfaces. K. C. Liu, V. K. Varadan, and V. V. Varadan (Department of Engineering Science and Mechanics, Pennsylvania State University, University Park, PA 16802)

This paper is an application of the "Spatial stochastic system theory" [K. C. Liu, J. Sound Vib. **79**(3), 321–339 (1979); **80**[4), 473–498 (1982)] to the problem of multiple scattering. It consists of three parts: (1) multiple scattering of randomly distributed discrete scatterers with arbitrary shape, (2) multiple scattering between discrete scatterers and a random irregular interface, and (3) multiple scattering between two random irregular interfaces. For these cases, a general expression for the space correlation function and intensity of the multiple scattered field is derived under very weak constraints. By means of these expressions, the space correlation functions and intensities of the multiple scattered fields caused by any kind (plane or spherical or others) of monochromatic incident wave can be calculated as long as the scattering property of each scatterer (for the first

case) or each scatterer and the random interface (for the second case) under plane monochromatic incident wave and the density function and the probability distribution of orientation of the scatterers are given. This calculation consists of only a single integration, a single summation, and some convolution operation. Some examples are considered and results will be presented for a uniform distribution of spherical particles in the presence of random irregular interfaces.

10:50

BB12. Iterative approaches in overcoming the instabilities of the *T*matrix method for scattering by nonspherical objects. Akhlesh Lakhtakia, Vijay K. Varadan, and Vasundara V. Varadan (Department of Engineering Science and Mechanics, Pennsylvania State University, University Park, PA 16802)

The T-matrix method, although very popular to examine single-particle scattering, becomes very unstable for highly nonspherical objects and/ or at high frequencies. In this paper we show how two different iterative schemes can be used to reduce these instabilities significantly. The first scheme is suitable for nondissipative objects and utilizes *a priori* the properties of the T-matrix and orthogonalization procedures to generate a stable T matrix for the computation of the scattered field. In the second scheme an initial "aproximate" solution is used to reduce the size of the resulting matrices and the field on the object surface is computed iteratively until it stabilizes. Numerical results pertaining to acoustic, electromagnetic, and elastic scattering phenomena are presented to illustrate the strengths of these two schemes.

11:05

BB13. Acoustic wave scattering by 3-D finite axisymmetric shells in water. S. Baskar, Vasundara V. Varadan, and Vijay K. Varadan (Department of Engineering Science and Mechanics, Pennsylvania State University, University Park, PA 16802)

In this paper, the scattering of acoustic waves by 3-D finite axisymmetric shells immersed in a fluid is analyzed. The governing equations for axisymmetric shells are derived by including the effects of rotary inertia terms and the dynamic impedance of the shell is then evaluated numerically and incorporated into the T-matrix formalism. Using the T matrix thus computed the farfield scattering is evaluated. Numerical results will be presented for the backscattered amplitude as a function of frequency for a finite cylindrical shell with hemi-spherical endcaps for different angles of incidence. This new semi-analytical method will be compared with the finite element method for incidence along the axis of the shell.

11:20

BB14. Image reconstructions from the applications of the ramp response signatures. S. J. Tsao, Vijay K. Varadan, and Vasundara V. Varadan (Department of Engineering Science and Mechanics, Pennsylvania State University, Hammond Building, University Park, PA 16802)

The ramp response signatures have been shown to relate well to the profile functions of various objects in the acoustic, electromagnetic, and elastic scattering problem. A modified method to reconstruct the scatterer image using the ramp responses at a finite number of look angles is introduced in this paper. The idea of synthetic scatterer image generation comes from a 3-D "approximate limiting surface" which has been well applied by Moffatt and Young in the image processing of perfectly conducting scatterers. The difficulty in getting good ramp responses by using the analytical frequency spectrum is resolved by modifying the T-matrix method to a wider bandwidth. The generated images of spherical, and oblate and prolate spheroidal voids in elastic solids, and those of rigid scatterers immersed in an acoustic field are presented. Some images of various shapes of scatterers in 2-D problems are also shown. Finally, an attempt to get the image of an elastic body and/or shell in an acoustic medium is discussed.

Session CC. Noise V and Architectural Acoustics III: Acoustic Intensity and Architectural Noise Control

Alfred C. C. Warnock, Chairman

Division of Building Research, National Research Council, Ottawa, Ontario, Canada K1A OR6

Chairman's Introduction-9:00

Contributed Papers

9:05

CC1. Fundamental relationships for the active and reactive acoustic intensity and their relationship with the acoustic energy density. Jiri Tichy and G. W. Elko (Graduate Program in Acoustics, P. O. Box 30, State College, PA 16801)

This paper will discuss the physical meaning of the active and reactive components of the acoustic intensity and the mathematical relationship with other sound field quantities, mainly, potential and kinetic energy. Examples of intensity fields for simple and complex sources will be presented and the interpretation and applications on some radiation and propagation problems will be shown.

9:25

CC2. Measurement of the complex acoustic intensity, the kinetic energy, and the potential energy in a reflective environment. G. W. Elko and Jiri Tichy (Graduate Program in Acoustics, P.O. Box 30, State College, PA 16801)

A four microphone intensity probe array has been designed and used to measure two components of the active and reactive acoustic intensity vector. The probe is also used to measure two components of the kinetic energy and the potential energy. Measurements of a point source above a reflecting plane and near the edge of two large reflecting planes were made. These results will be presented and the effects of sensor spacing, probe rotation, proximity of probe to source and boundary, and sensor phase error will be shown and the results will be compared to theoretically predicted values.

9:45

CC3. Measurement of energy flow and acoustic absorption. Gunnar Rasmussen (Brüel & Kjær, 18 Nærum Hovedgade, 2850 Nærum, Denmark)

The measurement of energy flow in rooms may be conveniently carried out using a real time intensity analyzer allowing one to plot the flow in the planes of interest. Supplemented with absorption measurements carried out with the same setup, a thorough knowledge of the important parameters, such as local absorption, controlling the acoustics of a room may be obtained over a wide frequency band in a very short time. Comparison with data obtained by conventional methods will be reported.

10:05

CC4. The two-microphone transfer function method for measuring absorption coefficients and impedance: Some limitations and precautions. Matthew A. Nobile (IBM Acoustics Laboratory, C18/704, P. O. Box 390, Poughkeepsie, NY 12602)

The transfer function (TF) method described by Chung and Blaser [J. Acoust. Soc. Am. 68, 907–921 (1980)] is an attractive alternative to the conventional, and tedious, standing wave ratio technique. Many laborato-

ries have already implemented the new method and are obtaining useful results. However, several problems are being encountered that have not been satisfactorily addressed in the literature. This paper discusses some of these problems, points out the limitations of the TF method as it is currently implemented, and suggests some necessary precautions. In addition, the importance of calibration is stressed and demonstrated through some examples (here, unlike two-microphone intensity measurements, the relative phase match between the microphone channels is just as critical at the higher frequencies as at lower frequencies). The results of measurements with the TF method, using two impedance tubes (100- and 30-mm diameters) to cover a frequency range of 90–6300 Hz, will be discussed.

10:25

CC5. A review of the in-duct method for measuring acoustic intensity and acoustic properties of materials and systems. A. F. Seybert (Department of Mechanical Engineering, University of Kentucky, Lexington, KY 40506-0046)

The decomposition theory [Seybert and Ross, J. Acoust. Soc. Am. 61, 1362–1370 (1977)] is reviewed and some new results applicable to problems in measuring acoustic intensity and acoustic properties in planewave ducts are presented. Specifically, it is shown that formulations for the net acoustic intensity and for the so-called transfer function approach of measuring acoustical impedance proceed directly from the general decomposition theory. Potential sources of signal processing and instrument errors are discussed, as are methods for instrumentation phase calibration. Experimental data showing the application of the decomposition technique to acoustic intensity and property measurement are presented.

10:45

CC6. Applications and experience with a portable microcomputer system controller and programmable sound level meter/frequency analyzer. George F. Hessler, Jr. (Hessler Associates, Inc., 6400 Wishbone Terrace, P. O. Box 77, Cabin John, MD 20818)

Today's availability and affordability of small truly portable, transportable, and desktop model microcomputers, with the power of recent minicomputers, make them ideal system controllers. The fundamental advantage of such a system is the ability to acquire massive amounts of measured data, perform complex and custom analysis, and format and present useful engineering results, all in near real time. A typical data acquisition and analysis system for sound level applications would consist of a computer controller interfaced with a programmable sound level meter and optional printers/plotters/noise sources, etc. This paper discusses experience and applications with a system comprised of a Hewlett-Packard transportable computer model HP 85 interfaced with a Larson-Davis laboratories model 800 programmable type 1 precision and sound level meter and 1/3-1/1 oct analyzer. Areas discussed are interface types and basic programming language routines for setting up the measurement and acquiring data on command. Application examples are routine steady-state and time varying sound level data acquisition, individual and cumulative aircraft flyover recording, and measurement of transmission loss and noise reduction in building wall structures.

CC7. Sound transmission through honeycomb stiffened panels. Ferdinand W. Grosveld (The Bionetics Corp., NASA Langley M.S. 463, Hampton, VA 23666) and John S. Mixson (NASA Langley Research Center, Hampton, VA 23666)

If the fundamental vibrational modes of the sidewall fuselage panels of a propeller driven aircraft coincide with highest excitation levels (at the propeller blade passage frequency and its harmonics), interior noise levels are adversely affected. To investigate experimentally how the increase in stiffness relates to the change in resonance frequency, various configurations of honeycomb stiffened panels have been tested in the NASA Langley Transmission Loss Apparatus. From the test results the effects of core thickness and the thickness of the facing material could be established. The change in resonance frequency was accurately determined by a modal analysis employing an impulse hammer and an accelerometer. The test results indicate that stiffening a panel with honeycomb material can shift the fundamental panel resonance frequency such that it no longer coincides with the frequencies of highest excitation. At low frequencies, this provides a potential noise control technique for propeller driven aircraft with a smaller weight penalty than encountered with conventional noise control methods.

WEDNESDAY MORNING, 9 MAY 1984

BRANDON ROOM, 9:00 TO 11:05 A.M.

Session DD. Psychological Acoustics VI: Masking

David R. Soderquist, Chairman

Department of Psychology, University of North Carolina, Greensboro, North Carolina 27412

Chairman's Introduction-9:00

Contributed Papers

9:05

DD1. Transition from simultaneous to forward masking. Daniel L. Weber (Boys Town National Institute, 555 North 30th Street, Omaha, NE 68131)

A stimulus condition in which the signal presentation partially overlaps the end of the masker presentation is intermediate between a simultaneous masking condition (complete overlap) and a forward masking condition (no overlap). The question is, "What process underlies signal detection in this condition?" To answer this question, this experiment examines the masked threshold for a 20-ms, 1-kHz sinusoidal signal (20ms cosine-squared ramps with no steady state) as a function of the temporal position of the signal with respect to a 400-ms, 1-kHz, 70-dB SPL sinusoidal masker (quadrature phase, 0-ms ramps). These thresholds are compared to those obtained for the portion of each signal which occurred after the masker; these "partial" signals had 1-ms onset ramps which rose during the final 1 ms of the masker; the beginning portion of the 20-ms signal (the portion which overlapped the masker) was eliminated. When the threshold for the whole signal equals the threshold for the partial signal (which necessarily is determined by the process of forward masking), one may easily argue that the "simultaneous" portion of the signal did not measurably influence signal detection. The data show that signal thresholds in transition conditions are determined by forward masking for stimulus overlaps as great as 90%. [Research supported by NSF and NIH.]

9:20

DD2. Masking period patterns: presentation of a model consistent with an enlarged set of experimental results. Jean-Luc Schwartz and Pierre Escudier (Institut de la Communication Parlée, Laboratoire associé au CNRS, ENSERG, 23 rue des Martyrs, 38031 Grenoble Cedex, France)

Masking period patterns (MPP) have been proposed by Zwicker as psychoaoustic equivalent of period histograms (PSTH) measured in auditory neurons. A large set of results have been obtained and represented on a model for predicting MPP [E. Zwicker, Biol. Cybern. 23, 49–60 (1976)]. We have already used this technique for studying PSTH when the basilar membrane is stimulated by trapezoidal patterns of excitation [P. Escudier *et al.*, J. Acoust. Soc. Am. Suppl. 1 67, S102 (1980)]. Our results cannot be completely interpreted on the basis of Zwicker's model. We present a new model, using a peripheral auditory system simulation previously elaborated in our group [J. M. Dolmazon *et al.*, Speech Commun. 1, 52–73 (1982)] and some simple additional hypotheses. This model is shown to be able to predict the whole set of available MPP results.

9:35

DD3. Forward masking by two sequential sinusoidal maskers. Donna L. Neff (Laboratory of Psychophysics, Harvard University, 33 Kirkland Street, Cambridge, MA 02138)

Two temporally distinct maskers of 300 and 30 ms were used to forward mask a 10-ms signal. The signal was a 1000-Hz sinusoid. The maskers were either 900- or 1000-Hz sinusoids and all four combinations of the masker frequencies were tested. From growth-of masking functions for individual maskers, levels were chosen to produce 5, 10, or 15 dB of masking for the first masker and 5, 10, 15, or 20 dB of masking for the second masker. When the two maskers were combined, the amount of additional masking, relative to that produced by the more effective masker, ranged from 0-24 dB across listeners and conditions. The smallest amount of additional masking was observed when both maskers were 1000 Hz. The remaining frequency combinations produced roughly similar amounts of additional masking. The results will be discussed in terms of models of additional masking. [Work supported by NIH.]

9:50

DD4. Presentation-order effects in the discrimination of rapidly presented short intervals. Gregory J. Fleet and Brian R. Shelton (Department of Psychology, University of Western Ontario, London, Ontario, N6A 5C2 Canada)

We previously reported a forward masking effect in a duration discrimination task [G. J. Fleet and B. R. Shelton, J. Acoust. Soc. Am. Suppl. 1 74, S10 (1983)], suggesting that the restriction of performance in the discrimination of rapidly presented brief durations was peripheral. This would predict a presentation-order effect, where a long-short discrimination would be easier than short-long. Two experiments examined this idea. The first study was two-interval forced-choice paradigm, with the thresholds for the long-short and short-long presentations adapted separately. A second experiment examined these same discriminations in a same-different paradigm. Signals were 80-dB SPL noise bursts fast gated in a continuous 60-dB noise background. Base durations of 25, 50, 100, and 200 ms were used, with ISI values of 25, 50, 100, 200, 400, 800, and 1600 ms. Counter to expectations, thresholds were much lower for the short-long presentations. These data are discussed in terms of their relation to the proposed peripheral limitation thesis, as well as the arguments that this presentation-order effect is the result of perceptual or assimilation effects. [Work supported by NSERC.]

10:05

DD5. Duration and rise-decay time in the masking-level difference obtained in pulsed masker conditions. William A. Yost and R. Dye, Jr. (Parmly Hearing Institute, Loyola University, 6525 N. Sheridan Road, Chicago, IL 60626)

The MLD (masking-level difference) is small when the signal and masker are pulsed together. The addition of a forward "masker fringe" to the pulsed signal-puls-masker can increase the pulsed MLD to that obtained when the masker is on continuously. The masker fringe must be at least 500 ms in order for the MLD to be as large as that obtained in the continuous masker condition. A parametric study of masker-plus-signal duration in the pulsed conditions and signal rise-decay time in the continuous masker conditions were investigated. Masked thresholds in the NoSo and NoS π conditions were obtained at 500 Hz from two-point psychometric functions determined in a single-interval procedure. The study was designed to test predictions of the equalization-cancellation model for the MLD and to test the assumption that the small pulsed MLD is due to a lack of change in interaural parameters at signal onset. [Work supported by NSF.]

10:20

DD6. Effects of masker level on binaural masking patterns. Janet Koehnke (Research Laboratory of Electronics, 36-730, MIT, Cambridge, MA 02139) and Marion F. Cohen (University of Connecticut, Storrs, CT 06268)

This study investigated the effects of masker level on the shape of masking patterns for binaural detection. Specifically, detection thresholds of a 700-Hz sinusoidal signal were measured as a function of the center frequency of a narrow-band masking noise. Thresholds for the 350-ms tone were measured twice at four masker levels, once with the signal presented diotically and once with the signal interaurally phase reversed. The masker was a continuous, diotic 80-Hz-wide noise that varied in frequency over a range of four critical bands above and below the signal frequency. Results show that the shape of the masking pattern varies as a function of masker level: with low-level maskers there is a downward spread of masking; with a moderate-level masker, masking is symmetrical; and with a high-level masker there is an upward spread of masking. This dependence is comparable to that observed in monaural masking patterns [E. Zwicker, Audiology 19, 330–334 (1980); E. Zwicker and A.

Jaroszewski, J. Acoust. Soc. Am. 71, 1508–1512 (1982)]; this similarity suggests that frequency analysis in the monaural and binaural auditory systems is similar. [Work supported by NIH grant ROI NS16802 and 2T32 NS07099-06.]

10:35

DD7. Effects of noise and cubic-difference-tone behavior. Susan J. Norton, Theresa Langer, and Walt Jesteadt (Boys Town National Institute, 555 North 30th Street, Omaha, NE 68131)

It has been suggested that external noise maskers, like sensorineural hearing loss, have a linearizing effect on cochlear function and that external noise maskers can be used to simulate sensorineural hearing loss. To test these hypotheses, cubic-difference-tone (CDT) behavior was measured in normal hearing listeners using a forward-masking paradigm for sinusoidal primaries presented in quiet and in the presence of low-pass, high-pass, and broadband noise. The noise was presented only during the primaries and could be considered as an additional forward masker. None of the noises used affected CDT behavior in a way that would support the hypothesis that noise has a linearizing effect on cochlear function. The range over which cubic difference tones could be measured was shifted by the amount that the thresholds for the primaries were shifted, but otherwise CDT behavior was similar to that observed in quiet. In contrast with results reported for persons with high-frequency sensorineural hearing loss, high-pass noise above the primaries had no effect on CDT behavior. Low-pass noise also had no effect on CDT behavior. Broadband noise added with the CDT much like external sinusoids and noise add. [Work supported by NIH.]

10:50

DD8. The prediction of masking in helicopters. R. D. Patterson (MRC Applied Psychology Unit, 15 Chaucer Road, Cambridge, England), M. Lower, P. Wheeler (Institute of Sound and Vibration Research, The University, Southampton, England), and G. Rood (Royal Aircraft Establishment, Farnborough, Hants, England)

The spectrum of the noise in helicopters is complicated because the rotor and blades produce intense low-frequency noise components, and the gears and transmission produce narrow-band peaks in the mid-frequency range. Thus the helicopter provides an excellent proving ground for theoretical models of auditory masking. The rounded exponential model of masking [Patterson *et al.*, J. Acoust. Soc. Am. **57**, 1788–1803 (1982)] has been extended to predict threshold at low frequencies and high levels by incorporating the results of recent laboratory studies. Two experiments were then performed to test the model's ability to predict masked audiograms gathered in the presence of helicopter noise. In one experiment the masker was presented via headphones in sound attenuating chambers to 12 listeners, in the other the masker was presented via lowspeakers in a Lynx helicopter simulator to six listeners. The results show that a very simple auditory filter, Roex (p), and mild asymmetry (upper side sharper) can predict the data well.

Session EE. Shock and Vibration I: Internal Fluid Generated Vibrations

Louis A. Herstein, Chairman

Naval Sea Systems Command, Washington, DC 20362

Chairman's Introduction-9:00

Contributed Papers

9:05

EE1. Point source excitation of cylindrical elastic shells filled with fluid. C. R. Fuller (Department of Mechanical Engineering, Virginia Polytechnic Institute and State University, Blacksburg, VA 24061)

The vibrations of a cylindrical elastic shell filled with fluid containing a monopole acoustic source are theoretically studied using the spectral equations of motion. The modal response of the shell wall is examined for different radial locations of the source and explained in terms of wave behavior. The distribution of vibrational energy between the shell and the fluid is evaluated at various axial locations and source positions. An interchange of energy of vibration between the shell and the fluid as the wave field propagates along the shell-fluid system is uncovered.

9:20

EE2. Resonant frequencies and modes of ribbed cylindrical shells. Courtney B. Burroughs and Sabih I. Hayek (Applied Research Laboratory, The Pennsylvania State University, P. O. Box 30, State College, PA 16804)

Measured data on resonant frequencies and modes of a ribbed cylindrical shell in air and immersed in water are presented. The ends of the shell are closed with caps so that the interior remains dry during immersion. An outer thin shell is added and resonant frequency and mode measurements repeated for the concentric shells in air and in water. The two shells are structurally coupled via annular plates between the two concentric shells. The volume between the shells is water-filled. The effects of the water-loading and the concentric outer shell on the resonant frequencies are discussed. Results from analytic models are used to assist in interpretation of the measured data.

9:35

EE3. Anomalous recovery of damped radial modes in a circular-sector duct with locally heated flow. J. R. Mahan (Department of Mechanical and Aerospace Engineering, West Virginia University, Morgantown, WV 26506) and S.-Y. Yeh (Link Simulation Systems Division, Singer Company, Silver Spring, MD 20904)

It is often desirable to predict acoustic propagation in a circular duct carrying a locally heated flow. Common examples include jet engines and certain industrial and commercial burners whose combustion-related noise can be an environmental problem if allowed to penetrate into the surroundings. In these cases axial gradients in the steady flow variables, established as a result of local combustion heating of the flowing gas, lead to important modifications of the usual linearized equations expressing conservation of mass, momentum, and energy in the acoustic variables. Thus the classical three-dimensional wave equation no longer applies and a new wave equation must be formulated. In the present work the appropriate modified wave equation is derived for and applied to a duct whose cross section is a sector of a circle of sufficiently small included angle to preclude the existence of circumferential modes in the frequency range of interest. This two-dimensional geometry, though somewhat artificial, has been chosen to allow the first radial mode to be isolated and studied separately. The analysis reveals that the first radial mode, when damped near the inlet to the duct, may under certain circumstances recover and even grow in amplitude as it passes through the heating region. [Work partially supported by NASA under Grant NAG3-124.]

S58

9:50

EE4. Signaling along elastic plates with wideband acoustic pulses. James E. Barger (Bolt Beranek and Newman, Inc., 10 Moulton Street, Cambridge, MA 02138)

High data-rate signaling with acoustic pulses along an elastic plate must contend with resolution of the launching pulse into many component pulses that arrive separately over a time span that is longer than the travel time of the first component to arrive. Computations of travel times (group velocities) and amplitudes (transfer admittances) for the first 12 modes are presented as functions of frequency. At frequencies below the cutoff frequency of about the fourth propagating mode, it is shown that a single mode can dominate the propagating signal. At higher frequences, up to the cutoff frequency of about the ninth mode, there are always at least four important modes that cluster between both faster and slower modes having low amplitudes. At higher frequencies the dominant modes cluster to form the Rayleigh wave, which travels at a speed intermediate to the remaining low-amplitude mode speeds. Measurements made in each of the three frequency regimes are presented to illustrate the propagation of third-octave-band pulses in a steel plate.

10:05

EE5. Measuring the transition to turbulence in oscillatory pipe flow. Martin Manley (MAR Inc., Suite 410, 6110 Executive Boulevard, Rockville, MD 20852) and Charles Thompson (Department of Engineering Science and Mechanics, Virginia Polytechnic Institute and State University, Blacksburg, VA 24061)

Acoustically induced turbulence, AIT, has recently become a topic of increasing interest. Research in AIT has been directed toward developing processes for aglomerating suspended particles using the nonlinear properties of the host fluid. However, the conditions governing the stability of the oscillatory or Stokes boundary layer have not been investigated. An experimental scheme for investigating the transition to turbulence in oscillatory flows will be presented.

10:20

EE6. Hermite-Beranek representation of acoustical transfer function. Richard H. Lyon (Department of Mechanical Engineering, Massachusetts Institute of Technology, Cambridge, MA 02139)

The advent of digital processing of acoustical (vibration and sound) transmission data has diminished interest generally in functionably based methods of system representation. Nonetheless, such methods continue to have a place because they offer certain economies when only a few terms of the expansion are able to represent the system and because they may provide physical models for the system under study. The Laguerre representation is an example which provides both a set of orthogonal functions for expansion of time domain behavior and a set of physical systems for modeling at the same time. Unfortunately, Laguerre expansions are inappropriate for the modeling of continuous systems with large numbers of degrees of freedom. A more appropriate expansion in this case is in Hermite (or Hermite/Gaussian) functions. When these functions are used to represent causal or minimum phase systems, it may also be useful to expand a part of the transfer function in Beranek functions which are Hilbert transform of the Hermite function. Beranek functions have orthogonality and recursion relations very similar to the Hermite functions. An example of the use of these expansions is presented.

Session FF. Speech Communication VI: Computer Analysis, Synthesis by Rule, Quality Measurement

Mark A. Clements, Chairman

School of Electrical Engineering, Georgia Institute of Technology, Atlanta, Georgia 30332

Chairman's Introduction-9:00

Contributed Papers

9:05

FF1. Block encoding of speech spectral principal components. James R. Holland and Stephen A. Zahorian (Department of Electrical Engineering, Old Dominion University, Norfolk, VA 23508)

A Karhunen-Loeve (KL) series expansion was used to block encode speech spectral principal components as a function of time. Each of ten principal components was first obtained as a linear combination of 20 speech spectral band energies. Using a fixed block length of ten frames (0.128 s), the KL basis vectors were computed separately for various speakers for each principal component. However, the optimal KL basis vector set was essentially the same for each principal component and for the different speakers. The basis vector set also closely resembled a cosine basis vector set. Approximately 94% of the variance of the principal components was accounted for by five (out of ten) basis vectors. Speech was synthesized using the KL basis vectors for block encoding of ten-frame blocks of principal components. Informal listening tests indicate that very little information is lost using five basis vectors. These results indicate that speech spectral principal components, particularly the low-ordered ones which reflect the overall spectral shape, are highly correlated in time. [Work supported by NSF.]

9:20

FF2. On the use of a perceptual distance with speech vector quantization. René Carré, Christian Lacoste, and Denis Tuffelli (Institut de la Communication Parlée, Laboratoire Associé au CNRS, ENSERG, 23 rue des Martyrs, 38031 Grenoble Cedex, France)

A vector quantization using perceptual data has been studied. The frequency and bandwidth scales of the poles computed by LPC methods were quantized according to perceptual difference limen. The small sensitivity of the hearing system to the formant amplitude was thus taken into account. A spectrum dictionary was then obtained. One spectrum is a set of quantized poles and the inter-spectrum distance is either 1 or 0. Good results are expected in the case of multi-speaker applications: low bit rate transmission and speech recognition. The method is well adapted for controlling all the steps of the processing and thus for improving the obtained results. For instance, the evolution of the dictionary can be easily studied with an increasing number of speakers and the statistical importance of each spectrum can be measured. First synthesis are quite good and comparable with those obtained by classical vector quantization. A phonetic labelling of the signal will lead to a dictionary spectrum labelling and a pointer giving the number of each successor permits to study the coarticulation effects at the level of the spectra. [Work supported by DRET.]

9:35

FF3. Optimum coding of formant speech synthesis parameters. S. S. Awad and B. Guerin (Institut de la Communication Parlée, Laboratoire Associé au CNRS, ENSERG, 23 rue Martyrs, 38031 Grenoble Cedex, France)

An optimum coding of the parameters of a formant speech synthesizer has been found. The optimization procedure is based on statistical and subjective criteria. The synthesizer is a parallel formant synthesizer. The utterances chosen for experimentation are groups of French high-quality synthetic vowel-consonant sounds (voiced stops and voiced fricatives). The proposed procedure consists of three principal steps. The first step is a statistical study on the parameters in order to find the effective range of variation of each parameter. The second step is to determine by subjective evaluation the minimum number of bits and type of quantization (linear or logarthmic) needed to quantize each parameter. The third and final step is to optimize the sampling interval depending on the nature of speech events. In fact a variable sampling interval is proposed. We have applied the proposed procedure in order to minimize the total bit-rate necessary for encoding the parameters of the synthesizer and in the same time obtaining synthetic utterances indistinguishable from original utterances obtained from nonoptimized parameters. Finally, throughout this study we have emphasized the different characteristics of each type of the utterances.

9:50

FF4. Abstract withdrawn.

10:05

FF5. Automatic alignment of phonetic transcriptions with continuous speech. Victor W. Zue and Hong C. Leung (Room 36-549, Department of Electrical Engineering and Computer Science, and Research Laboratory of Electronics, Massachusetts Institute of Technology, Cambridge, MA 02139)

The alignment of a speech signal with its corresponding phonetic transcription is an essential process in speech research, since the time-aligned transcription provides direct access to specific phonetic events in the signal. Traditionally, the alignment is done manually by a trained acoustic phonetician. The task, however, is prone to error and is extremely time consuming. This paper describes a system that performs the time alignment automatically. The alignment is achieved using a standard pattern classifiction algorithm and a dynamic programming algorithm, augmented with acoustic-phonetic constraints. The speech signal is first segmented into six broad phoentic classes using a sequence of nonparametric pattern classifiers arranged in a binary decision tree. The output of this initial classification is then aligned with the transcription using a knowledgebased dynamic programming algorithm. The aligned broad class segments provide "islands of reliability" for more detailed segmentation and refinement of boundries. Acoustic-phonetic knowledge is utilized extensively in the system during feature extraction for pattern classification, specification of constraints for path searching in dynamic programming, and subsequent knowledge-based segmentation labeling. The system was evaluated on sixty sentences spoken by three speakers, two male and one female. Aproximately 93% of the segments were mapped into only one phoneme. Over 70% of the boundaries found by the automatic system were within 10 ms of those determined manually by an acoustic phonetician. [Work supported by the Office of Naval Research under contract N00014-82-K-0727 and by the System Development Foundation.]

FF6. Some techniques for controlling distinctive contours of speech parameters in experimental manipulation. David Graff and Franz Seitz (Department of Linguistics, University of Pennsylvania, Philadelphia, PA 19104)

All acoustical properties which contribute to signaling phonemic contrasts are, to some extent, "time-varying." However, some properties, e.g., formant trajectories in diphthongs and fundamental frequency trajectories in tones, rely for their distinctiveness on time-varying contours which are quite complex. These complex contours are composites of two or more parameters, e.g., duration, rate of change, and relative values of extrema. Experiments concerned with the contribution of particular aspects of the contours' patterns to the perception of phoneme categories face the following problem: How are such composites of parameters to be controlled and modified to produce a synthetic continuum of variants for the basic ceteris paribus experimental paradigm? This report presents some techniques that we have devised which address this problem, and evaluates their effectiveness in LPC and terminal analog synthesis. The contours of formant trajectories in varieties of English, and the contours of fundamental frequency trajectories in Vietnamese tones, have been systematically modified using these techniques in order to produce stimulus sets. The central problems were time-warping and interpolating smooth curves through data points.

10:35

FF7. The Delta System for synthesis rules. Susan R. Hertz (Phonetics Laboratory, DMLL, Cornell University, Ithaca, NY 14853), James Kadin, and Kevin Karplus (Department of Computer Science, Upson Hall, Cornell University, Ithaca, NY 14853)

The Delta System is a computer system for developing synthesis rules. Building on nine years of experience with Hertz's SRS synthesis system [J. Acoust. Soc. Am. 72, 1155 (1982)], it gives users more flexible rule-development facilities and enables them to produce considerably more practical rules. The Delta System provides a high-level structured pattern matching language called Delta. The system achieves compact, efficient, and portable rule sets by compiling rules from Delta into a pseudo-machine language. With Delta, rule-writers can easily define and manipulate a broad class of utterance representations, ranging from linear strings to multi-level structures. An utterance consists of multiple synchronized steams of user-defined symbols and associated attributes. The symbols can represent phrases, words, morphs, demisyllables, phonemes, subphonemic units, etc. Delta's control structures and sophisticated pattern matching ease the writing of efficient rule sets. Symbols and attributes from all levels can be freely mixed in the patterns to be matched. When completed, the Delta System will accomodate almost any synthesis scheme, will support rule development for any language, will be extremely portable, and will produce compact, efficient rule sets.

10:50

FF8. Acoustic-phonetic analysis of Japanese. Chieko Aoki, Dennis Klatt, and Haruko Kawasaki (Room 36-511, Massachusetts Institute of Technology, Cambridge, MA 02139)

How difficult would it be to convert a synthesis by rule program for English (DECtalk) to speak Japanese? What is the ideal, hopefully minimal, corpus of recorded materials that would have to be spectrally analyzed in order to derive sufficient information for a first order approximation to Japanese? We have recorded three male speakers reading a list of a little over 100 nonsense syllables, which exhaust the CV(C) syllable inventory of Japanese, and provide information about segmental contrasts. One of the speakers then read a 500-word text to provide information on sentence-level phenomena. We have measured segmental durations, formant motions, and deletion phenomena in broadband spectrograms of this recording, and are beginning to formulate rules for synthesis on the basis of computer analyses of the data. The approach now appears far less unreasonable than it did when we began. Some results of the analysis will be presented. [Work supported in part by an NIH grant.]

11:05

FF9. Identifying familiar talkers over a 2.4 kbps LPC voice system. Astrid Schmidt-Nielsen (Code 7526, Naval Research Laboratory, Washington, DC 20375)

A commonly cited drawback of narrow-band digital voice communication systems such as the DoD standard LPC algorithm is that talker recognition is poor. Yet is is the opinion of many users that they frequently recognize the talker. Tape recordings of 24 talkers conversing over an unprocessed channel and over an LPC voice processing system were subjected to listening tests. The listeners were 24 co-workers who listened to the tapes and attempted to identify each talker from a group of about 40 people working in the same branch. Prior to the recognition test, each of the listeners also rated his or her familiarity with each of the talkers and the distinctiveness of each talker's voice. There was some loss in voice recognition over LPC, but the recognition rate was still quite high. Unprocessed voices were correctly identified 88% of the time, whereas the same people talking over the LPC system were correctly identified 69% of the time. Talker familiarity was significantly correlated with correct identifications. There was no significant correlation between the rated distinctiveness of the talker and correct identifications. However, familiarity and distinctiveness ratings were highly correlated. This suggests that people consider a familiar voice to be distinctive regardless of other characteristics that might make that particular voice stand out in a crowd. [Work supported by NAVELEX.]

11:20

FF10. Evaluating LPC-coder performance using voice quality analysis. R. J. Hanson (AT&T Bell Laboratories, Rm 6D-329, Naperville Road, Naperville, IL 60566) and J. Laver (Phonetics Laboratory, Department of Linguistics, University of Edinburgh, Edinburgh, Scotland EH8 9LL)

A system for characterizing individual voice quality has been developed and used successfully to describe normal voice, pathological voice, and paralinguistic affect. In this study, voice quality analysis is used to evaluate the distortion introduced by LPC-based speech coding. Vocal profiles of speakers are obtained by having trained judges rate the extent to which 21 phonetically based features deviate from the "neutral" setting. Profiles for original and coded material from the same speaker are compared and a distortion measure is derived that quantifies the change in voice quality attributable to the coder. Results indicate that voice quality analysis is sensitive to many characteristics of LPC: types of source coding, quantization of spectral parameters, and pole frequency and bandwidth accuracy.

11:35

FF11. Objective speech quality measures based on human audition. Mark A. Clements (Department of Electrical Engineering, Georgia Institute of Technology, Atlanta, GA 30332-0250)

To accurately assess the quality of a speech transmission or coding system generally requires subjective ratings obtained by experiment. An alternative measurement procedure which would be highly desirable would involve an objective assessment automatically performed by computer. Using a large data-base consisting of many distortions as well as the corresponding quality ratings, we have attempted to predict subjective quality based on psychoacoustic models. Such properties as intensity perception, frequency resolution, and time integration were incorporated. One of the most interesting results involves the fact that quality of distortions involving waveform coding and additive noise were well modeled by psychoacoustic parameters. However, the quality of more complex distortions, such as those produced by linear predictive coding, was best predicted using parameters (e.g., growth of loudness) at substantial variance with psychoacoustic test results. One conclusion is that complex distortions are not well characterized by simple measures. However, many of our measures outperformed more traditional measures by a large margin. [Work supported by the Defense Communications Agency.]

FF12. Pilot preferences, intelligibility, and learnability of two types of computer generated speech. Carol A. Simpson and Teresa Navarro (Psycho-Linguistic Research Associates, 2055 Sterling, Menlo Park, CA 94025)

Two types of computer speech were compared to obtain helicopter pilots' preference judgments and to determine if intelligibility, learnability, and/or confidence ratings would vary as a function of speech type, sex of listener, or whether the listener was a pilot. The two speech types were direct synthesized speech—generated by a Votrax ML-1 synthesizer, and an LPC-encoded version of the direct synthesized speech using the TMS-5220 speech chip. Stimuli for the preference study were sentence length helicopter voice warnings. Stimulus material for the second study was a PB word list. The direct synthesized speech was preferred by the pilots in the first study and, in the second study, was significantly more intelligible than the LPC-encoded synthesized speech. A significant interaction between speech type and runs indicated that intelligibility improved with exposure to PB words for direct synthesized speech. Confidence ratings agreed with the intelligibility data. Spectrograms of the two speech types reveal differences which might explain the differential learnability. [Funded by NASA-Ames.]

WEDNESDAY MORNING, 9 MAY 1984

EPPINGTON ROOM, 9:30 A.M.

Meeting Of Standards Committee S12 On Noise

to be held jointly with the

Technical Advisory Group for ISO/TC 43/SC1 Noise

K. M. Eldred, Chairman S12 P.O. Box 1037, Concord Massachusetts 01742

H. E. von Gierke, Chairman, Technical Advisory Group for ISO/TC 43/SC1 Director, Biodynamics & Bioengineering Division, AFAMRL/BB U.S. Air Force, Wright-Patterson AFB, Dayton, Ohio 45433

> Working group chairpersons will report on their progress under the plan for the production of noise standards. The interaction with ISO/TC 43/SC1 activities will be discussed.

WEDNESDAY AFTERNOON, 9 MAY 1984

EPPINGTON ROOM, 1:30 P.M.

Joint Meeting of Standards Committees S3 and S1

The activities of S3 will be discussed first, proceeding to matters of interest to both S3 and S1, and concluding with S1 activities.

Meeting of Standards Committee S3 on Bioacoustics

W. A. Yost, Chairman S3

Loyola University of Chicago, Parmly Hearing Institute, 6525 N. Sheridan Road, Chicago, Illinois 60626

Standards Committees S3, Bioacoustics. The current status of standards under preparation will be discussed. In addition to those topics of interest including hearing conversation, noise, dosimeters, hearing aids, etc., consideration will be given to new standards which might be needed over the next few years.

Meeting of Standards Committee S1 on Acoustics

T. F. W. Embleton, Chairman S1

National Research Council, Division of Physics, Montreal Road, Ottawa, Ontario, K1A OR6, Canada

Standards Committee S1, Acoustics. Working group chairpersons will report on their progress in the preparation of standards, methods of measurement and testing, and terminology in physical acoustics, electroacoustics, sonics, ultrasonics, and underwater sound. Work in progress includes measurement of noise sources, noise dosimeters, integrating sound-level meters, and revision and extension of sound level meter specifications. Open discussion of committee reports is encouraged.

 -0.130 s^{-1} to a sound channel axis of 150 m and a positive gradient of $+0.016 \text{ s}^{-1}$ to a critical depth of 1825 m. The resulting propagation was RR and RSR with losses of between 90 and 100 dB. These results show that for these environmental-acoustic conditions the synthetic apertures can be formed by the coherent summation of phase corrected subaperture beams over successive time samples as long as the synthetic aperture length is less than the single path coherence length and the synthetic aperture length. The results presented represent an extension of earlier work [R. Fitzgerald, J. Acoust. Soc. Am. 60, 752–753 (1976); R. Williams, J. Acoust. Soc. Am. 60, 60–73 (1976)] by the demonstration that coherent gain can actually be achieved with resolution such that multipath vertical arrival angle differences can be resolved.

3:05

GG7. Receiver directivity modeling in three dimensions. Fred Tappert and Lan Nghiem-Phu (Daubin Systems Corp. and University of Miami, Miami, FL 33149)

A technique has been developed to compute the quantity that is represented in the passive sonar equation as $TL' = TL - AG_s$, where TL is transmission loss and AG_s is receiver signal array gain. In full-wave theory these two quantities are not logarithmically additive because beam deviation loss is not separable, and hence TL' must be computed directly. It is required to compute TL' as a function of source coordinates x,y,z for given receiver location, given frequency, and given farfield beam pattern (depending on steering angle). Making use of reciprocity, we have used our PE model to compute TL' in realistic range-dependent ocean environments. Results are displayed as contours of TL' in the vertical x,z plane at various azimuths, and as contours of TL' in the horizontal x,y plane at various depths.

3:20

GG8. Properties of the beam noise distribution function for horizontal arrays in ship-induced noise fields. Richard M. Heitmeyer (SACLANT ASW Research Centre, I-19026 La Spezia, Italy)

An analysis is presented of the environmental and array system factors governing the fluctuations in the beam noise of a horizontal array in a ship-induced noise field. A model is used that relates the cumulative distribution function to the directivity and side-lobe characteristics of the system and the strength and anisotropy of the shipping distribution. The results are threefold. First, for a given environment, an increase in the array length results in a large increase in the prevalance of low noise periods at the expense of a modest increase of high noise periods. Second, for sufficiently large apertures, a "noise floor" develops in that noise values larger than the noise floor occur with high probability, whereas values less than the noise floor occur only rarely. Finally, the noise floor level is essentially independent of the noise anisotropy and of further increases in aperture length, and it increases with degradation in side-lobe level.

3:35

GG9. Vertical directionality and depth dependence of wind-generated noise. William W. Renner and William D. Kirby (Science Applications, Inc., 1710 Goodridge Drive, McLean, VA 22102)

For highly directive sensors, the spatial coherence of the background noise can be an important consideration in estimating system performance. An isotropic vertical-noise field, as often assumed, is typically an unrealistic characterization of the true field. In this paper we present a vertical-noise model for high-frequency, wind-generated noise based on the earlier work of Talham [J. Acoust. Soc. Am. **36**, 1541–1544 (1964)] extended to include the volume absorption model more recently developed by Fisher and Simmons [J. Acoust. Soc. Am. **62**, 558–564 (1977)]. The impact of various environmental factors upon both the directivily and the depth dependence of high-frequency noise is addressed. Limitations of existing boundary loss models and their implications for noise modeling are discussed. GG10. The theoretical response of a vertical array to wind noise in shallow water. Rachel M. Hamson (SACLANT ASW Research Centre, I-19026 La Spezia, Italy)

A wave theory model for the propagation of noise from a surface source layer has been used to investigate the response of a vertical array to shallow water wind noise. The model assumes an infinite layer of sources radiating sound with pressure directionality of the form $\cos^{m} \alpha$, where m > 1 and α is an angle measured from the downward vertical. The field incident on the array is inhomogeneous and directional responses have been calculated from the (non-Toeplitz) spatial correlation matrix for various bottom types, sound-speed profiles, and values of m up to 3. Results show that both components of the noise field, the discrete normal modes and the continuous spectrum, can contribute significantly to the array response. Furthermore the mode arrivals give much higher responses for near-horizontal steered directions than those predicted by a simple correlation model for a semi-infinite medium. Finally calculations using an approximated Toeplitz matrix result in large errors under certain conditions, and demonstrate that a one-dimensional correlation function is not a sufficient descriptor of noise in shallow water.

4:05

GG11. Low-frequency ambient noise mechanisms: A comparison of openocean and under-ice data. D. G. Browning, F. R. DiNapoli, R. J. Nielsen, N. P. Fisch (Naval Underwater Systems Center, New London Laboratory, New London, CT 06320), and R. H. Mellen (B-K Dynamics. Inc. 247 Shaw Street, New London, CT 06320)

A large increase in ambient noise spectrum level is observed in the open ocean at low frequencies. Most investigators have suggested wind and wave induced (surface coupled) mechanisms. [Kibblewhite *et al.*, J. Acoust. Soc. Am. Suppl. 1 74, S121 (1983)]. Our analysis of recent underice ambient noise data shows no large increase at low frequencies thus indirectly supporting the hypothesis of a surface coupled mechanism in the open ocean. The general level and frequency dependence of the spectrum suggests, however, the existence of a locally generated noise threshold which may be due to internal waves or seismic activity. [Work is funded by ONR Code 425-AR.]

4:20

GG12. Generation of uniform progressive periodic plane waves within a volume near an array of randomly positioned point sources. Bruce O. Moses (Applied Research Laboratories, The University of Texas at Austin, P. O. Box 8029, Austin, TX 78712)

A method is presented for computing complex shading coefficients for a specified array of randomly positioned point sources to produce an arbitrarily designed steady-state uniform progressive periodic plane wave. The coefficients are designed to produce the plane wave within a specified volume in the nearfield of the projecting array. The coefficients have been modeled on a computer, and contour plots of the resulting pressure field have been produced. The direction of propagation of the plane wave can be controlled by changing the shading coefficients for the elements of the array. The complete farfield equivalent beam pattern of an unknown transducer positioned within the controlled volume can be accurately measured while holding both the unknown transducer and the array fixed in position without rotation. The method opens many possibilities for improved acoustical calibration techniques.

4:35

GG13. Development of a new underwater acoustic test and calibration center. G. A. Zets (National Underwater Acoustics Centre, P. O. Box 181, Simon's Town 7995, Republic of South Africa)

A new underwater acoustics test and calibration center has recently been established in Cape Town, South Africa. With the 2.5 million liter main test tank measuring $20.2 \times 11.2 \times 11.2$ m and a second tank measuring $20.7 \times 3.5 \times 4.2$ m, the facility is amongst the largest in use today. Designed to meet the requirements of users involved in military, industrial, and research activities, the facilities incorporate some special features such as vibration isolation mounting of the tanks and the capability of supporting marine life for fisheries research. This paper presents details of this new facility and illustrates some interesting aspects of the design and construction of the tanks. The choice of instrumentation and signal processing techniques will be discussed as well as proposed methods for handling and positioning large transducers.

4:50

GG14. Underwater-nearfield acoustical holography using a robotic controlled scanner, Earl G. Williams, Henry D. Dardy (Naval Research Laboratory, Code 5133, Washington, DC 20375), and Richard G. Fink (Sachs/Freeman Associates, Bowie, MD 20772)

A computerized, experimental facility has been developed to implement nearfield acoustical holography in a large underwater tank. The

WEDNESDAY AFTERNOON, 9 MAY 1984

facility contains a robotic controlled hydrophone arm which allows the precise positioning and motion of a hydrophone in the tank completely under computer control. Automated scanning is done close to the surface of a radiating/scattering object and the resulting pressure data are stored digitally. The frequency range of operation is dc to above 30 kHz. Using the principles of nearfield acoustical holography [Williams and Maynard, Phys. Rev. Lett. **45**, 554 (1980)] this data are forward and backprojected to study the radiated/scattered acoustic fields. Forward projection provides directivity patterns, and intensity and vector-velocity field mappings. Backward projection provides surface velocity and pressure (fluid loading)—reconstructing the field in the extreme nearfield. Experimental results are shown providing a complete description of the field radiated underwater from a point-driven rectangular plate. Shown are its surface velocity, intensity vectors in the extreme near field, fluid loading effects, radiation efficiency, and directivity patterns.

YORK HALL, 1:30 TO 5:20 P.M.

Session HH. Speech Communication VII: Consonant and Syllable Perception

Richard Pastore, Chairman

Department of Psychology, State University of New York, Binghamton, New York 13901

Chairman's Introduction-1:30

Contributed Papers

1:35

HH1. Effects of intensity and filtering on identification of nonsense syllables. Gerald A. Studebaker and Edward L. Goshorn (Department of Audiology and Speech Pathology, Memphis State University, Memphis, TN 38105)

The identification of nonsense syllables was investigated under various conditions of filtering, noise, and intensity level. The syllables were filtered and recorded simultaneously as two separate bands in a background of speech spectrum noise. The low-pass band (200-400 Hz) was recorded at a nominal signal to noise ratio of 20 dB, the high-pass band (1-5 kHz) at 7 dB. The low-pass band was presented at 60, 80, and 96 dB SPL, the high-pass band at 60 and 80 dB SPL (nominal levels represent coupler level prior to filtering). Each band was presented alone and in every possible combination of intensity level with the other band to four normal hearing subjects. The best performance resulted when both bands were at 60 dB. Increasing the level of the high-pass band by 20 dB and of the low-pass band by 20 and 36 dB relative to the best condition resulted in a reduction in performance. Poorest performance resulted when the low-pass band was at the high-pass band was at the lowest level (60 dB).

1:50

HH2. Range effects for speech and nonspeech judgments of sine wave stimuli. Michael Studdert-Kennedy (Queens College, CUNY, Flushing, NY 11367 and Haskins Laboratories, 270 Crown Street, New Haven, CT 06511-6695), and David R. Williams (Haskins Laboratories, 270 Crown Street, New Haven, CT 06511-6695)

In a previous paper [Williams et al., J. Acoust. Soc. Am. Suppl. 1 74, S66 (1983)], we demonstrated that an influence of consonantal context on vowel perception [B. Lindblom and M. Studdert-Kennedy, J. Acoust. Soc. Am. 42, 830-843 (1967)] is obtained for sine wave as well as for formant stimuli. We showed further that a similar influence is not apparent when the sine wave stimuli were judged in terms of pitch rather than speech categories. Category boundaries for pitch judgments fell at the midpoint of the continua while those for isolated vowels and vowels in consonantal context were arrayed to the left and right of the midpoint, respectively. In the present set of experiments, we sought to assess the stability of the speech and nonspeech category boundaries by testing an effect of stimulus range on listeners' categorizations. To do this, we removed the lower one-third from each of the continua used in our previous experiment. Pilot results replicate our earlier findings: once again, pitch boundaries divided the continua in half and speech boundaries fell to either side of the midpoint. Nonetheless, these data show that speech as well as pitch judgments are subject to range effects. [Work supported by NICHD.]

2:05

HH3. Formant frequency lowering during acquisition of the French /r/. Walter H. Manning (Memphis State University, 807 Jefferson Avenue, Memphis, TN 38105)

Four adult males, all native speakers of English, were trained to produce the French /r/ during ten training sessions. Formant frequency values for /r/ were spectrographically analyzed based on the subjects' production of ten test words in each training session. In order to observe the importance of auditory feedback during the acquisition of /r/, subjects produced the ten test words under conditions of no masking and 100 dB (SPL) binaural competing speech masking. Formant values were plotted as F_1 - F_2 and F_2 - F_3 relationships. A decrease in formant frequencies across training was observed during both unmasked and masked conditions. F_2 values showed the greatest change across training. Formant values were consistently lower during the masked conditions. One explanation for the decrease in formant values appeared to be an increase in tongue height combined with a lowering of the velum. Results are contrasted with perceptual judgments of /r/ across training.

2:20

HH4. Perception of "modulation" in speechlike signals III: A psychoacoustic or phonetic dimension? R. J. Porter, Jr. (Kresge Hearing Research Laboratory of the South, Departments of Otorhinolaryngology

and Biocommunication, and Psychology, LSU Medical School, 1100 Florida Avenue, New Orleans, LA 70122) and C. J. Miller (Kresge Hearing Research Laboratory of the South, Department of Otorhinolaryngology and Biocommunication, LSU Medical School, 1100 Florida Avenue, New Orleans, LA 70122)

We have proposed that a "modulation sensation" may accompany second-formant variations like those found in speech [Porter and Miller, J. Acoust. Soc. Am. Suppl. 1 73, S3 (1983); Miller and Porter, J. Acoust. Soc. Am. Suppl. 1 74, S66 (1983)]. Unlike some other psychoacoustic attributes of formant variations, modulation sensations appear to be preserved when the transitions are presented either within or without first formant context. Modulation might, therefore, serve as a psychoacoustic basis for some phonetic decisions. On the other hand, the modulation sensation might be as phonetically irrelevant as, for example, a signal's loudness. To examine these alternatives, single haversine-cycle modulations of second formants were presented in the context of an F1. Systematic variations in the direction and extent of F2 modulation were coupled with variations in the amount of a simultaneous haversine modulation of F1 amplitude. The resulting set of signals define an acoustic space which casual listening suggests might be perceptually divided along phonetic dimensions as well as along psychoacoustic dimensions of modulation magnitude and quality. Comparisons between listeners' judgments of modulation magnitude, discrimination of signals, and phonetic labeling will be presented and discussed in terms of the alternatives presented above. [Supported in part by The Lousiana Eye and Ear Foundation, The Lousiana Lions, and the Kresge Foundation.]

2:35

HH5. Trading relations in nonspeech. Ellen M. Parker, Keith R. Kluender, and Randy L. Diehl (Department of Psychology, University of Texas, Austin, TX 78712)

Two acoustic features shown to be sufficient in specifying the distinction between intervocalic /b/ and /p/ are closure duration and the presence or absence of a low-frequency voicing pulse during the closure interval. These features of the signal can be considered to exhibit a trading relation [B. Repp, Psych. Bull. 92, 81-110 (1982)] to the extent that a longer closure is required to perceive the consonant as voiceless when the pulse is present than when it is not. This study addressed the issue of whether a trading relation of the type found in speech can be demonstrated for nonspeech as well. Two types of square wave analogs, modeled after a speech series ranging from "rabid" to "rapid," were constructed. One set of nonspeech stimuli contained frequency transitions into and out of the silent interval while frequency for the other nonspeech stimuli remained constant. Preliminary (AXB) identification results indicate that in the speech condition, the presence of the pulse affects a shift in the ID boundary between "rabid" and "rapid" relative to the no-pulse condition. A comparable shift is observed between the pulse and no-pulse series in the nonspeech transition condition; no shift is apparent for the nonspeech no-transition condition. The implications of these results for the notion that speech perception requires a "special" mode of processing will be discussed. [Work supported by NINCDS.]

2:50

HH6. The role of F1 cutback in the perception of voicing contrasts. Richard E. Pastore, Rosemary Szczesiul, Karen Nowikas, and Robert Logan (Department of Psychology, State University of New York, at Binghamton, Binghamton, NY 13901)

Recent research has convinced us that limitations on temporal order judgments (TOJ) do not provide an adequate acoustic basis for voicing contrast. Our correct research focuses on F 1 cutback, a second major cue in voicing contrasts. F 1 cutback exhibits categorical perception and at least some of the parameter dependencies found for voicing contrasts, but not found with TOJ. These results will be described. The possibility that F 1 cutback, acting alone or in conjunction with temporal order cues, may serve as a major acoustic cue for contrasts will be discussed.

3:05

HH7. VOT, /s/-noise duration and silent interval as trading cues; stops after /s/. George P. McCasland (School District of Philadelphia, 4045 Baltimore Ave., C3, Philadelphia, PA 19104) In the results of the writer's previous perceptual experiment [Phonetica 34, 218–228 (1977)] which was based on stimulus materials edited from spoken utterances, the minimally contrasting test utterances *it's dill*, *it still*, *it's still* were perceptually distinguished by appropriate values of /s/-noise duration and silent interval in the context of short delayed VOT. The utterance *it's till* containing a voiceless aspirated stop after /s/ was heard in 75% of the judgments of otherwise similar stimuli containing long delayed VOT. A recent reanalysis of the other 25% of the judgments suggests that the potency of the long delayed VOT in these tokens had been weakened in trading with /s/-noise duration and silent interval. These findings have been replicated in perceptual data from a new group of subjects. Lisker's work [Haskins Final Report 11, B-11, 1–9 (1965)] based on spectrographic measurements of similar utterances has been an important resource. For the stop after /s/ at word boundary, VOT as a voicing cue appears to be involved in a three-way trading relationship.

3:20

HH8. Effects of temporal stimulus properties on perception of the [sl]-[spl] distinction. Bruno H. Repp (Haskins Laboratories, New Haven, CT 06511-6695)

Two studies investigated the independent influences of the durations of preceding and following signal portions on the amount of closure silence needed to perceive "splash" rather than "slash." The durations of the [s] and [l] acoustic segments had opposite effects which canceled when the silence was short (Exp. 1) but yielded a net effect due to [s] duration when the silence was long (Exp. 2). These findings, which resolve a conflict between earlier results in the literature, are interpreted as reflecting a perceptual compensation for coarticulatory shortening of [s] before stop consonants, in conjunction with (possibly psychoacoustic) contrastive interactions between the perceived durations of adjacent acoustic segments. [Research supported by NICHD.]

3:35

HH9. Influence of following context on perception of the voicedvoiceless distinction in syllable-final stop consonants. David R. Williams and Bruno H. Repp (Haskins Laboratories, New Haven, CT 06511-6695)

The duration of the vowel preceding a syllable-final stop consonant (as defined by some acoustic criterion) generally is a potent cue to the perception of the stop as phonologically voiced or voiceless. We show that the absolute vowel duration that characterizes the voiced-voiceless boundary in a monosyllable is reduced considerably when a second syllable beginning with a different stop consonant is added to form a disyllabic word. We also show that this contextual effect declines with increasing temporal separation between the two syllables, and we examine this decline in relation to listener's judgments of whether they hear the stimulus as one disyllabic context, apart from introducing closure duration as an additional voicing cue, may reflect listeners' tacit knowledge of the temporal compression that occurs in speech production as the number of syllables in a word is increased. [Research supported by NICHD.]

3:50

HH10. Are selective adaptation and contrast effects really distinct? Randy L. Diehl, Keith R. Kluender, and Ellen M. Parker (Department of Psychology, University of Texas, Austin, TX 78712)

Despite evidence [e.g., R. L. Diehl *et al.*, J. Exp. Psych: Hum. Percept. Perform. 6, 24–44 (1980)] that selective adaption and contrast effects are produced by the same mechanisms, Sawusch and Jusczyk [J. Exp. Psych: Hum. Percept. Perform. 7, 408–421 (1981)] reported a dissociation between the effects and concluded that adaptation and contrast occur of separate processing levels. Specifically, they found that a VOT test stimulus near the [b]/[p] boundary was more likely to be labeled "b" following adaptation with [p^h a] and more likely to be labeled "p" following adaptation with [ba] or [spa] (the latter consisting of [ba] preceded by [s] noise). In the contrast session, where the long adaptation sequence was replaced by a single context stimulus occurring before or after a single test item, the [ba] and $[p^h a]$ contexts had contrastive effects similar to those of the [ba] and $[p^h a]$ adaptors, but the [spa] context produced an increase in "b" responses to the test stimulus, an effect opposite to that of the [spa] adaptor. One interpretation of this difference is that the rapid repetitive presentation of the [spa] adaptor gave rise to "streaming," whereby the [s] was perceptually segregated from lower-frequency [ba] component. In our experiment, we first replicated the results of Sawusch and Jusczyk, using procedures similar to theirs. Next we increased the interadaptor interval to remove the likelihood of stream segregation and found that the adaptation and contrast effects converged. [Work supported by NINCDS.]

4:05

HH11. Revisiting stop-consonant perception for two-formant stimuli. Ralph N. Ohde (Bill Wilkerson Hearing and Speech Center and Vanderbilt University School of Medicine, Nashville, TN 37212) and Kenneth N. Stevens (Research Laboratory of Electronics and Department of Electrical Engineering and Computer Science, Massachusetts Institute of Technology, Cambridge, MA 02139)

The aim of this study was to re-examine the factors leading to stop consonant perception for consonant-vowel stimuli with just two formants over a range of vowels, using stimuli and test procedures somewhat different from those used in earlier studies. Five two-formant CV stimulus continua were synthesized, each covering a range of second-formant (F2) starting frequencies, for vowels corresponding roughly to [inæau]. Listeners identified the beginning of the syllable under two different instructions: a forced-choice response of b, d, or g, and an open response set. The stimuli with the most unanimous responses were those with substantial F2transitions, i.e., [bi b du]. There were few consistent g responses. Under open response instructions, stimuli with straight or small transition ranges were identified as beginning with no consonant. The results are compared with those of other studies, particularly with regard to differences in stimulus characteristics, and are discussed in relation to theories of invariance. [Supported in part by grants from NIH.]

4:20

HH12. Coarticulation effects on fricative consonants across languages. Jonas N. A. Nartey (Remote Information Access Systems Group, IBM T. J. Watson Research Center, Yorktown Heights, NY 10598)

Previous studies (e.g., Nartey, 1981, 1982, and Soli, 1981) indicate that there is reliable vowel coarticulation effects on fricatives produced in the environments of [i], [a], and [u]. The present study further explores the notion of vowel coarticulation effects on fricatives both within and between languages. Critical band analysis was performed on the fricative consonants of 12 genetically diverse natural languages. These were recorded in the intervocalic environments of the three peripheral vowels i-i, a-a, and u-u. The resulting auditory spectra were compared for fricatives both within and between languages. Results indicate, among other things, that coarticulation rules are language specific. Furthermore, it appears that synchronic coarticulation rules can serve as a window by which we can observe diachronic sound changes such as Proto Slavic /x/ to modern Polish /[/.

4:35

HH13. More on the /t/:/d/ distinction in American alveolar flaps. Donia R. Scott (Laboratory of Experimental Psychology, University of Sussex, Brighton BN1 9QG, United Kingdom)

In American English, alveolar stop consonants occurring in intervocalic position tend to be articulated as a flap (or tap). It has long been claimed that the duration of the vowel immediately preceding the flap is a primary cue to its underlying voicing status. Evidence will be presented to show that listeners can discriminate between naturally produced minimal pairs containing flaps (e.g., coating, coding) based on cues other than preceding vowel duration or the acoustic properties of the flap itself. Consistent differences in phonetic quality and overall quantity between such word pairs will be discussed.

4:50

HH14. Stop CV duration and dichotic temporal order judgment. E. Rafferty (Department of Psychology, Tulane University, New Orleans, LA 70118), L. F. Hughes, and C. J. Miller (Department of Otorhinolaryngology and Biocommunication, Kresge Hearing Research Laboratory of the South, Louisiana State University Medical Center, 1100 Florida Avenue, New Orleans, LA 70119)

At a previous meeting of the Society we presented data which showed that sensitivity for dichotic temporal order judgment decreased with increases in intensity disparity between channels. Further work indicated that overall presentation level (whether 50 or 66 dB) did not affect performance as long as both channels were of equal intensity. In this study we varied the duration (40, 60, 90, and 180 ms) of naturally produced stop CVs having stimulus onset asynchronies of 2, 4, 8, 16, 32, and 64 ms. Seven subjects indicated the ear stimulated first. The difference between normal deviates for hits and false alarms was measured. Results contrasted with data from studies using monaural or binaural presentation in that sensitivity increased with increasing stimulus duration. In addition, plots of each duration condition revealed performance to be a monotonic function of stimulus onset asynchrony. Further testing on two subjects showed that at higher intensities the decrement in performance for 40-ms stimuli was attenuated. Results are discussed in terms of duration-intensity tradeoffs in dichotic temporal order judgment.

5:05

HH15. Memory modes and perceptual anchors in categorical perception. Neil A. Macmillan (Department of Psychology, Brooklyn College, Brooklyn, NY 11210 and Research Laboratory of Electronics, MIT, Cambridge, MA 02139)

A theory of intensity perception developed by Durlach and Braida [J. Acoust. Soc. Am. 46, 372-383 (1969), et seq.] is applied to data from categorical perception experiments. According to the theory, two memory modes are used in processing perceptual continua. In the trace mode, observers compare stimuli with the memory traces of other stimuli, and performance is limited by the inter-stimulus interval. In the context mode, observers compare stimuli to perceptual anchors, and performance is limited by the stimulus range. Analysis of existing speech and nonspeech data reveals that stimulus domains differ in (a) the amount of trace variance, (b) the amount of context-coding variance, and (c) the existence and location of anchors; but no single parameter captures the categorical/ continuous distinction. Memory variances and anchor locations can be estimated from experiments in which fixed-level discrimination, as well as identification and roving-level discrimination, is measured. Among the few experiments with categorically perceived continua that have used the critical fixed-level condition are some in which discrimination peaks arise from anchors, and others in which they reflect regions of high basic sensitivity. [Work supported by NIH.]

Session II. Shock and Vibration II: Reduction of Shock and Vibration Levels in Industrial Machinery

Ronald L. Bannister, Chairman

Westinghouse Electric Corporation, The Quadrangle, Orlando, Florida 32017

Chairman's Introduction-2:00

Invited Papers

2:05

II1. Vibration signature analysis in power plants. S. P. Ying (Gilbert/Commonwealth, 209 Washington Avenue, Jackson, MI 49201)

In order to reduce noise and vibration levels in power plants, vibration signature analysis was utilized as a diagnostic technique. Accelerometers, strain gauges, pressure transducers, or a combination thereof were used to monitor the vibration signatures and pressure pulsations. The signals from the sensors were analyzed by using a dual channel fast Fourier transform (FFT) analyzer to obtain cross-correlation functions in time domain and coherence functions in frequency domain. These techniques can pinpoint the source of vibration and have been successfully applied to turbine-generators, pumps, and fans in power plants to prevent trip-out and fatigue damage. Vibration signature interpretations for rotating machinery, cracked components, and structural resonant vibration are discussed for several case histories. Recommendations which have been implemented for the elimination of excessive vibration problems are also presented.

2:30

II2. Detuning a large turbine generator stator endwinding. Ben T. Humphries (Generator Development, Westinghouse Steam Turbine Generator Division, The Quadrangle MC 100, Orlando, FL 32817)

From experience with similar steam turbine generators it was predicted that the stator coil endwinding, a truncated cone shaped structure attached to the stator core, would have an elliptical mode natural frequency near, 120 Hz, its excitation frequency. A new support bracket was designed to lower this natural frequency 15 Hz. The turbine generator was built in its original form, and was excited using impact and random noise shakers. The impact tests were quick and excited all modes while the diametrical shaker tests were designed to simulate actual excitation forces and tended to accentuate the problem mode. The new support bracket was installed and the natural frequencies were measured again. Natural frequencies were then rechecked under simulated operating temperatures and decreased as expected. The new support bracket detuned the coil endwinding as expected.

2:55

II3. Passive isolation of industrial shock. Francis J. Andrews (Barry Controls, 700 Pleasant Street, Watertown, MA 02172)

Passive shock isolation can frequently be analyzed using a shock nomogram. However, for nonlinear isolation systems, this approach will result in low estimates of transmitted force for a stiffening system or low estimates of dynamic deflection for a softening (buckling) system. In such cases, energy methods are used to improve the accuracy of estimated performance characteristics. This presentation will discuss use of the shock nomogram and energy methods for each isolator type, as well as performance advantages of each isolator type. Shock test results will be included.

3:20

II4. Flexural vibration of printing cylinders on rotary web offset printing presses. John W. Evans (Publication Press, Harris Graphics Corp., Westerly, RI 02891)

Analytical and experimental studies on a flexural vibration problem characteristic of rotary web offset printing presses are described. This problem results in a printing defect referred to in the industry as "streaking." Applications of finite element analysis and vibration measuring instrumentation system to reduce vibration levels are described.

Contributed Papers

II5. A model for wing vibrations excited by a propeller wake. Rudolph Martinez (Cambridge Acoustical Associates, Inc., 54 Rindge Avenue Extension, Cambridge, MA 02140)

3:45

Predictions are made of unsteady airloads induced on a wing by the near wake of an upstream propeller. The forced infinite-beam equation is then solved and levels of structureborne sound at the cabin position obtained. The propeller wake is modeled as a system of infinite, straight vortices in rotary motion cutting through the wing at the two sparwise positions given by $y = \pm R$, where R denotes the propeller radius. The vortex arrangement is assumed rigid and therefore unaffected by the presence of the solid surface, or by mutual induced motions. Velocities induced on the wing plane yield time and spanwise variations of the effective angle of attack, from which the unsteady running lift driving the wing structure is computed using locally two-dimensional, quasisteady aerodynamics.

4:00

II6. Noise propagated into a fluid by sliding contacts. Michael A. Tucchio (Naval Underwater Systems Center, New London Laboratory, New London, CT 06320)

The noise propagated into a fluid associated with the relative motion and rubbing of two surfaces, one of which is in contact with the fluid, is investigated. The method presented in this report uses the finite element method to account for the fluid-structure interaction. The friction forces are calculated using the nonlinear equations of motion as derived from rigid body mechanics. Verification of the technique is provided with an experiment. A weight is abruptly moved over the surface of a simply supported beam which is in contact with the water. The pressure-time response of the resulting noise in the water is compared to the calculated pressure-time response from the finite element method. The correction applied to the plane strain finite element solution to convert it to spherical spreading in a semi-infinite medium uses the relationship between cylindrical and spherical spreading in an infinite medium. This area is in need of additional work. [Research supported by NUSC.] II7. Asymptotic modal analysis and statistical energy analysis of dynamical systems. Earl H. Dowell (School of Engineering, Duke University, Durham, NC 27706)

The well known text by Lyon on Statistical Energy Analysis (SEA) [R. H. Lyon, Statistical Energy Analysis of Dynamical Systems: Theory and Applications (MIT Press, Cambridge, MA, 1975)] is the standard reference on the subject. As originally conceived SEA was based upon several plausible hypotheses. Various authors have considered the underlying basis for SEA and thereby advanced our understanding of it. In the present paper, the relationship between classical modal analysis (CMA) and SEA is studied. It is shown how the results of SEA may be obtained as an asymptotic limit of CMA. The present work only considers the response of a single general linear structure under a random or sinusoidal load. However future plans will consider (a) the structural acoustic response of an enclosure bounded by a flexible wall and excited by external forces and (b) two (or more) coupled structural systems. Here the emphasis is on (1) a new derivation of the SEA results from CMA for a single structure under a random load, (2) the generalization of the usual SEA result to show that, asymptotically, all points on the structure have the same response. In the literature this is sometimes invoked as an assumption. Here the result is derived as part of the asymptotic limit of CMA. (3) A numerical example which displays the manner in which the asymptotic limit is approached for random loading and (4) an extension of the usual SEA result for sinusoidal loading. In view of the above, the present results might be called more appropriately Asymptotic Modal Analysis (AMA) rather than SEA.

WEDNESDAY AFTERNOON, 9 MAY 1984

MONTPELIER ROOM, 2:00 TO 4:10 P.M.

Session JJ. Physiological Acoustics VII: Cochlear Nucleus

Joseph E. Hind, Chairman

Department of Neurophysiology, University of Wisconsin Medical School, Madison, Wisconsin 53706

Chairman's Introduction-2:00

Invited Papers

2:05

JJ1. Physiology, morphology, and pharmacology of neurons in the anteroventral cochlear nucleus of the mouse studied in brain slices. Donata Oertel and Shu Hui Wu (Department of Neurophysiology, University of Wisconsin, Madison, WI 53706)

Intracellular recordings from brain slice preparations of the anteroventral cochlear nucleus show that the two major cell types, bushy and stellate cells, have different intrinsic membrane properties. To correlate physiological properties with morphology, cells were injected with horseradish peroxidase after their electrical properties were studied. Bushy cells have nonlinear current-voltage relationships around the resting potential; stellate cells have linear current-voltage relationships. Both bushy and stellate cells respond to electrical stimulation of the auditory nerve with early excitatory and later inhibitory postsynaptic potentials. The properties of bushy cells allow them to preserve the temporal firing pattern of excitatory synaptic inputs. To learn what neurotransmitters might mediate synaptic inputs onto stellate and bushy cells, bath applications were made of presumptive neurotransmitters and their antagonists. Inhibitory synaptic responses to stimulation of the auditory nerve stump are blocked by 10^{-6} M strychnine. The input resistance of cells dropped in the presence of glycine and gamma-aminobutyric acid at 0.1 to 5 mM. All cells tested were completely insensitive to L-glutamate and L-aspartate at concentrations up to 10 mM. [Work was supported by NIH, NS 17590.]

2:55

JJ2. Responses to amplitude modulation in the cochlear nucleus: A hierarchy of enhancement. Robert D. Frisina (Center for Brain Research, University of Rochester Medical School, Rochester, NY 14642), Robert L. Smith, and Steven C. Chamberlain (Institute for Sensory Research, Syracuse University, Syracuse, NY 13210)

Dynamic changes in sound amplitude are prominent features of naturally ocurring auditory stimuli. The neural responses to amplitude-modulated sounds may play important roles in speech encoding, pitch perception, and high-frequency sound localization. Here we report the results of a single unit study of the cochlear nucleus and auditory nerve of the anesthetized gerbil. We find that units of the ventral cochlear nucleus exhibit an enhanced response to amplitude modulation (AM) relative to units of the auditory nerve. This confirms and extends Møller's [Acta Physiol. Scand. 98, 157–167 (1976)] findings in the rat cochlear nucleus. Our results indicate that the amount of response enhancement is commensurate with a unit's rank in a hierarchy based on departure from a primarylike response. Onset units show the strongest phase locking to AM, followed by chopper, primarylike-with-notch, and primarylike units, respectively. A comparison of three-dimensional plots of response modulation versus average intensity and modulation frequency illustrates that the enhancement occurs over a range of AM frequencies between 40 and 1000 Hz, at intensities up to 90 dB above a unit's threshold.

Contributed Papers

3:25

JJ3. Intracellular studies in cat cochlear nucleus: Physiological responses of morphologically identified neurons. Richard H. Britt, Glenn T. Rossi (Division of Neurosurgery R155, Stanford University School of Medicine, Stanford, CA 94305), D. Kent Morest, and Michael Ostapoff (Department of Anatomy, University of Connecticut Health Center, Farmington, CT 06032)

Intracellular recording techniques were used to study the physiological responses of cochlear nucleus neurons in 32 pentobarbital anesthetized cats. Electrodes were filled with 2% to 4% horseradish peroxidase (HRP) in 0.5 M KCl. Each neuron was studied extracellularly by obtaining a tuning curve, determining the characteristic frequency (CF), and generating a peristimulus time histogram (PSTH) at the CF. After intracellular penetration, the PSTH at the CF was repeated to determine if any change in response had occurred. HRP was then iontophoretically injected intracellularly. Serial transverse frozen sections were incubated using a diaminobenzidine reaction intensified by preincubation with cobalt chloride. In the anteroventral cochlear nucleus (AVCN), three HRP-filled neurons were physiologically characterized. A bushy cell located in the AA region had a primarylike response at its CF of 4 kHz. An elongated stellate cell in the PD region of the AVCN had a primarylike response at its CF of 10 kHz at 90 dB, but at lower intensities (80-60 dB) the unit showed a progressive change to a chopperlike response. A small stellate cell along the medial border of PV in the AVCN showed an onset response at its CF of 4 kHz. In the dorsal cochlear nucleus (DCN), a horizontal giant cell showed a change from an onset pattern below its CF to an onset-sustained pattern at its CF of 10.5 kHz. The second HRP-marked cell in the DCN was a small broadly tuned (7-18 kHz) granule cell recorded in the molecular layer which showed a primarylike response at its CF of 14 kHz. [Support: NIH/NINCDS NS15860.]

3:40

JJ4. Putative amino acid neurotransmitters in cochlear (CN) and vestibular (VN) nuclei of guinea pig. Ruediger Thalmann and Thomas H. Comegys (Department of Otolaryngology, Washington University, St. Louis, MO 63110)

We reported that aspartate (asp) and glutamate (glu) are significantly reduced in the ventral CN after surgical destruction of the organ of Corti, corresponding to the pattern of primary innervation [Thalmann *et al.*, J. Acoust. Soc. Am. Suppl. 1 67, S77 (1980)]. More recently, we confirmed and extended Wenthold's finding [Brain Res. 143, 544 (1978)] that these substances decline similarly, although on a faster time scale, after VIIIth nerve section-no decline in molecular and fusiform layers of dorsal CN, but significant declines (p < 0.001) in deep dorsal CN (asp 29%, glu 24%) and in posteroventral CN (asp 48%, glu 45%). Analogous declines occurred in the phylogenetically older VN following VIIIth nerve section. In the heavily innervated central part of superior VN asp and glu decreased by 21% and 37%, respectively (p < 0.001), with no decline in the sparsely supplied peripheral part. In lateral VN, asp and glu declined significantly (35% and 21%, respectively) in the heavily innervated ventral portion, while in the sparsely innervated dorsal part, only asp declined (26%). The behavior of asp and glu after lesion (as well as their resting distribution) is consistent with the involvement of either or both in neurotransmission at the primary auditory and vestibular terminals. [Supported by NIH.]

3:55

JJ5. Effect of neonatal conductive hearing loss on neuronal size in the ventral cochlear nucleus of guinea pigs. Nancy A. O'Connell^e (Kresge Hearing Research Laboratory of the South, LSU Medical Center, New Orleans, LA 70119)

The left ear of newborn guinea pigs was closed by removing the skin and cartilage of the external auditory meatus and pulling the surrounding tissue over the opening with silk sutures. At 60 days of age the animals were anesthetized with chloral hydrate and auditory brainstem responses (ABR) were measured before and after destroying the intact right ear. After ABR testing the animals were killed and their cochleas were examined histologically. Right and left brainstems were embedded in paraffin, serially sectioned and stained with cresyl violet. The cross-sectional area of four different cell types was measured, using a total of 210 cells of each type from each side. For all four groups; large spherical cells, small spherical cells, pale globular cells, and octopus cells, soma size was significantly smaller (P < 0.01) on the left side. This result for guinea pigs, a precocial animal, agrees with earlier findings for an altrical animal the mouse [D. B. Webster, Exp. Neurol. 79, 130-140 (1983)]. [Supported by NIH training grant NSD-07058 and the Louisiana Lions Eye Foundation.] *) Present address: Dept. of Biological Sciences, Loyola University, New Orleans, LA 70118.

Session KK. Physical Acoustics IV and Engineering Acoustics III: Scattering and Holography

Gerhard M. Sessler, Chairman

Technical University Darmstadt, Merckstrasse 25, Darmstadt, West Germany

Chairman's Introduction-2:00

Contributed Papers

2:05

KK1. Plane-wave multiple-scattering approach to acousto-optic diffraction by adjacent ultrasonics. P. P. Banerjee, M. R. Chatterjee (Department of Electrical and Computer Engineering, The University of Iowa, Iowa City, IA 52242), and T. C. Poon (Department of Electrical Engineering, Virginia Polytechnic Institute and State University, Blacksburg, VA 24061)

Plane-wave multiple-scattering theory has been used to analyze the diffraction of light by adjacent ultrasonic beams of frequency ratio 1:m. The novelty of the method lies in the fact that it provides a better physical insight into the actual coupling process involved in the generation of various diffracted orders than earlier, more conventional analtyical techniques; hence the resulting equations may be arrived at by simply inspecting the geometry of the problem and incorporating the appropriate phase factors contributing to each order. The analyses of acousto-optic diffraction by adjacent ultrasonic beams of frequency ratio 1:2 in the Raman-Nath and near Raman-Nath regimes are presented as illustrative examples. To compare with the work of earlier investigators, the variations of the scattered intensities are obtained numerically, for equal sound pressures in both columns, as a function of the phase difference between the beams and the strength of the sound fields for the first and second cases, respectively. The principle may readily be extended to more complicated sound-light configurations.

2:20

i

KK2. Accustic scattering from a pair of rigid spheres. A. F. Seybert (Department of Mechanical Engineering, University of Kentucky, Lexington, KY 40506-0046) and B. Soenarko (Engineering Science Department, Bandung Institute of Technology, Bandung, Indonesia)

Scattering of a plane acoustic wave from a pair of rigid spheres is considered for the case where the spheres lie on a line perpendicular to the incident wave. Our primary interest is in the effect the second sphere has on the scattered field in the vicinity of the first sphere. The scattered field is computed by two methods. The first method is based on a numerical solution of the Helmholtz integral formula. The second method is an approximate solution formed by adding the scattered field of each sphere without the presence of the other. Comparison data are presented for the two methods as a function of frequency, distance between the spheres and the ratio of the spheres' radii.

2:35

KK3. The structural and acoustic response of a submerged infinite cylindrical shell in the presence of hydrostatic pressure fields. Richard F. Keltie (Department of Mechanical and Aerospace Engineering, Center for Sound and Vibration, North Carolina State University, Raleigh, NC 27650)

The dynamic response of an infinite circular cylindrical shell submerged in an acoustic medium was formulated using Flugge's thin shell theory. The effects of a uniform hydrostatic pressure field were modeled by including constant initial stress terms in the shell equations of motion. The driving point impedance of the shell was examined and characterized in terms of the *in-vacuo* shell impedance and the additional fluid impedance. The effects of the hydrostatic pressure on both were determined and examined as a function of frequency. The surface acoustic intensity field resulting from a localized harmonic driving force was formulated and integrated numerically over the surface of the shell in order to determine the radiated acoustic power. The relative effects of the fluid loading and the hydrostatic pressure field on the acoustic response were subsequently examined as a function of the frequency of the excitation.

2:50

KK4. Exterior surface acoustic waves scattered by impenetrable cylinders. G. Gaunaurd (Naval Surface Weapons Center, R-43, Silver Spring, MD 20910) and D. Brill (U.S. Naval Academy, Annapolis, MD 21402)

We study the scattering of acoustic waves by impenetrable (i.e., rigid and soft) cylinders by means of the poles of scattering amplitude that are present in the (nondimensional) complex-frequency plane, k_1a . These are analogous to the poles that in electromagnetism are studied via the Singularity Expansion Method (SEM) of radar scattering. These poles correspond to external eigenvibrations of the medium surrounding the scatterers, which cause the external creeping waves that revolve around the targets, as we have already explained in detail [i.e., G. Gaunaurd et al., Nuovo Cimento 76B, 153-175 (1983)] for spherical scatterers. We have developed a formulation that permits the computation and display of the dispersion plots for the phase and group velocities and for the phase and group attenuations of the various orders of external creeping (Franz) waves revolving round these targets, directly from the positions of the SEM poles in the k_1a plane. We show many such dispersion plots here as examples. We already showed [i.e., G. Gaunaurd et al., J. Acoust. Soc. Am. Suppl 1 72, S98 (1982)] how to compute the distortion of scattered δ function pulses, incident on impenetrable spheres, by means of the stationary phase method, and we tie it all together here.

3:05

KK5. Power scattered by a fixed point on a fluid-loaded plate. R. V. Waterhouse and F. S. Archibald (David Taylor Naval Ship R&D Center, Code 194, Bethesda, MD 20084)

When rectilinear bending waves on a thin plate encounter an obstacle in the form of a fixed point, some energy is scattered to the farfield. This scattered energy is the sum of two components, one traveling in the plate and the other in the fluid. The sum can be calculated from the real part of the driving point impedance imposed on a point-force driving the fluidloaded plate. This impedance has been computed at various frequencies below the coincidence frequency, for a steel plate, 1 cm thick, loaded with water on one side. The impedance for the plate *in vacuo* is real and independent of frequency, but for the fluid-loaded plate, it is complex and frequency dependent. At each frequency, an integral representing a Hankel transform is evaluated numerically to yield the complex impedance.

3:20

KK6. Active sound intensity precision in a progressive and nonprogressive field. J. Nicolas and G. Lemire (Mechanical Engineering Department, Université de Sherbrooke, Sherbrooke, Quebec, Canada J1K 2R1)

The work is mainly dedicated towards the precision of the measurement of active sound intensity. The object is to describe the basis used to understand what is happening when measuring the sound power via the active part of sound intensity whatever the field is. The effects of acoustic center variation, of the phase mismatch, of the proximity of the source, of finite approximations, and of angle of incidence of the incoming wave are all combined in a general formulation, valid for the progressive field. The nonprogressive field is studied by calculating the estimated active sound intensity due to two monopoles. The case of coherent and incoherent monopoles are examined. A general formulation of the resulting amplitude and phase is developed and emphasis is put on a systematic parametric study of the theoretical phase gradient. The parameters are mainly the sound power ratio between the two sources, distance ratio, propagation difference, angle of incidence, and frequency. A formulation which allows us to calculate the precision between the estimated active sound intensity and the exact one is proposed. A criteria for evaluating the degree of nonprogressivity of the field will be discussed. [Work supported by the "Institut de Recherche en Santé et Sécurité du Travail."]

3:35

KK7. Holographic reconstruction of odd-shaped 3-D sources. William A. Veronesi and J. D. Maynard (Department of Physics and the Applied Research Laboratory, The Pennsylvania State University, University Park, PA 16802)

As previously described [J. D. Maynard, J. Acoust. Soc. Am. Suppl. 1 74, S37 (1983)], nearfield acoustical holography can reconstruct the surface velocity and pressure over a level surface in a separable coordinate system from measurements of the radiated pressure field over a parallel level surface. This study investigates the feasability of reconstructing the surface pressure and normal velocity over surfaces which do not conform to a level surface. Such a reconstruction involves numerically determining a distribution of surface pressure and velocity which satisfies the surface Helmholtz integral equation and which is consistent with the Helmholtz integral equation for the pressure field measured on the level surface. Details of the algorithm and results of computer simulations for a uniformly pulsating sphere and a piston set in a sphere (measurements simulated over a planar surface) are presented. [Work supported by ONR and NASA.]

3:50

KK8. Advances in nearfield acoustical holography (NAH) algorithms I. Green's functions. William A. Veronesi and J. D. Maynard (Department of Physics and the Applied Research Laboratory, The Pennsylvania State University, University Park, PA 16802)

For efficiency, the spatial processing algorithms of NAH, based on Rayleigh's integrals, utilize the fast Fourier transform (FFT). In NAH, the FFT has been treated as an approximation to the continuous Fourier transform, and with this view, work has been done to reduce the errors introduced by the finite and discrete FFT. In this paper, it is shown that, by using the exact discrete convolution capabilities of the FFT and inverse FFT, as opposed to its approximate correspondence to the continuous Fourier transform, algorithms yielding more accurate results are obtained. The essential step is to replace the continuous field over the surface from which the data was gathered with a piecewise constant field, each patch having the constant field value as at a contained, measured point. With the field so replaced, Rayleigh's integral is reduced to a finite, discrete convolution of the measured data with the integrals of the kernel, or Green's function, over each path. Most importantly, this proces totally eliminates the effects of image sources. Conditions for validity of this model are presented, and results for a baffled piston source demonstrate the accuracy of this approach. [Work supported by ONR and NASA.]

4:05

KK9. Advances in nearfield acoustical holography (NAH) algorithms II: Zoom imaging. Yanmin Huang, William A. Veronesi, and J. D. Maynard (Department of Physics and the Applied Research Laboratory, The Pennsylvania State University, University Park, PA 16802)

In NAH, it is often desirable to increase the density of points in the transform space beyond the density produced by a simple 2-D discrete Fourier transform of the input data array. Two equivalent methods of increasing the density of points are presented. The two methods are: augmenting the original data with zeros before transforming, or convolving the transform of the unaugmented data array with the transform of a twodimensional square unit step function. Augmenting with zeros and the equivalent convolution approach are based on the assumption that the field is negligible beyond the measured region of the hologram surface. Although the hologram and its transform are two dimensional, the density increasing schemes can be cast ih a one dimension at a time form resulting in a great reduction in computation time. This technique has great utility when restricted to increasing the density of points inside the radition circle. When the radiation circle originally contains relatively few points, the direct convolution is faster, also this method is not limited to power of two increases indensity. Results for propagating the pressure field from a baffled piston source are given. [Work supported by ONR and NASA.]

4:20

KK10. The implementation of nearfield acoustic holography with an array processor. Yongchun Lee and J. D. Maynard (Department of Physics and Applied Research Laboratory, The Pennsylvania State University, University Park, PA 16802)

The data reduction capabilities of our nearfield acoustic holography (NAH) system have been greatly enhanced through the development of efficient computer algorithms utilizing an array processor with a minicomputer. The array processor accelerates not only the FFT computation, but also the Green's function calculation, data windowing, graphics display generation, and zoom imaging. In this paper, the various techniques, which have reduced the NAH processing time by a factor of ~ 20 , will be discussed. This new processing system speeds data collection and processing and will permit measurement of radiation from wideband noise sources with a large number of frequency components. [Work supported by ONR and NASA.]

4:35

KK11. Experimental studies of acoustic radiation for unbaffled complex planar sources with nearfield acoustic holography. Yongchun Lee and J. D. Maynard (Department of Physics and Applied Research Laboratory, The Pennsylvania State University, University Park, PA 16802)

Design data for the evaluation of the acoustic radiation coupling loss factor for complex planar sources, such as ribbed plates, nonuniform plates, damped plates, and aircraft panels, etc. is still fairly scarce. This work presents a broad survey of complex vibrating planar sources. These results were obtained using nearfield acoustic holography (NAH) to illuminate the effects of stiffness, mass, and damping on radiation loss factor. [Work supported by ONR and NASA.]

4:50

KK12. Nearfield holography for wideband sources. Donald J. Bowen and J. D. Maynard (Department of Physics and Applied Research Laboratory, The Pennsylvania State University, University Park, PA 16802)

Nearfield acoustical holography (NAH), a process developed at the Pennsylvania State University, has proved itself to be a powerful research tool in the study of single-frequency sound sources. A new high-speed data aquisition system has been developed which permits extension of the nearfield acoustical holography technique to the study of wideband noise sources. Using a partially parallel, partially sequential sampling network, near simultaneous sampling is achieved for 256 microphones in the holographic measurement plane, for acoustic frequencies up to 1500 Hz. Special problems encountered during the development of the high-speed data aquisition system are discussed. [Work supported by ONR and NASA.]

Session MM. Underwater Acoustics VI: Scattering

Suzanne T. McDaniel, Chairman

Applied Research Laboratory, Pennsylvania State University, University Park, Pennsylvania 16802

Chairman's Introduction-8:00

Contributed Papers

8:05

MM1. Rough surface boundary wave attenuation due to incoherent scatter, Ivan Tolstoy (Knockvennie, Castle Douglas, SW Scotland)

The incremental energy loss $\Delta E / E$ per unit path length for a boundary mode traveling along a rough surface may be calculated from elementary low-frequency scattering approximations, using previously published results [I. Tolstoy, J. Acoust. Soc. Am. 74, 1068-1070 (1983) and 72, 960-972 (1982)]. This allows one to calculate explicitly the attenuation factor $\exp(-\delta r)$, where r is the range, with $\delta = \frac{1}{2} \frac{E}{E}$ for rough two-fluid interfaces with arbitrary impedances, constraints, and roughness shapes. It is shown that $\delta = Af^6$, where f is the frequency and A a parameter which depends upon the size, spacing, and form of the roughness (for closepacked roughness elements A is proportional to the fifth power of the mean roughness height). Given a point source of sound and a receiver on rough interface the boundary wave amplitude p_B the $\propto r^{-1/2} f^{3/2} \exp(-\delta r)$ and exhibits, for fixed r, a well-defined maximum in the frequency domain at $f_M = (4Ar)^{-1/6}$ and falls off rapidly for higher frequencies, i.e., it displays a bandpass behavior with slow roll-off at low frequencies. The predictions of this theory agree with recently reported model work [G.L.D'Spain et al., J. Acoust. Soc. Am., in press]. [Work supported by ONR.]

8:20

MM2. Low-frequency, grazing propagation above randomly rough surfaces. Gerald L. D'Spain,* Emily H. Childs,* and Herman Medwin (Physics Department, Naval Postgraduate School, Monterey, CA 93943)

Previously we have summarized laboratory studies of the acoustic boundary wave due to coherent scattering at grazing propagation over surfaces with periodic roughness elements. Here we extend our study of low-frequency propagation for surfaces with three-dimensional, randomly rough elements [J. Acoust. Soc. Am. Suppl. 1 71, S24 (1982)]. The dependence of the boundary wave amplitude on scattering parameter, wavenumber, and range, $\epsilon k^{3/2} r^{-1/2}$, predicted by Tolstoy for hemispheres, is found again for stochastic surfaces. However, the inferred scattering parameter can be an order of magnitude greater for sharp-edged than for spherical protuberances of the same volume/area. The empirical dependence of ϵ on the volume/area, rms slope, and rms curvature of the surface is examined. The maximum boundary wave amplitude again suffers catastrophic attenuation at a range and frequency given approximately by $kr = 2\pi/(k\epsilon)^2$ as in the case of rigid spherical protuberances. The dispersion approaches 1%-2% at high frequencies and follows an approximate k^2 dependence. [Research supported by the Office of Naval Research.] *) Ocean Acoustics Associates.

8;35

MM3. Double refraction near a rough bottom in isothermal waters. Herman Medwin and Jorge C. Novarinia) (Physics Department, Naval Postgraduate School, Montercy, CA 93943)

The occurence of a boundary wave during low-frequency grazing scatter from rough rigid surfaces has been described by Tolstoy and experimentally verified by Medwin et al. [J. Acoust. Soc. Am. 66, 1131-1134 (1979)] for a homogeneous medium overlying the surface. Tolstoy [J. Acoust. Soc. Am. 69, 1290-1298 (1981)] has also shown that, when the velocity in the medium decreases away from the ocean bottom, tunneling into the shadow zone takes place, for source and receiver on the bottom. We re-examine this case but for the source and receiver near the ocean surface and for bottoms of lesser roughness. It is predicted that, under certain conditions of velocity gradient, frequency, and bottom roughness, the boundary wave mode causes a splitting of the limiting ray above the rough bottom. As a result, two refracted rays would reach the ocean surface: a primary ray (classical limiting ray for smooth bottom), and a secondary ray with a significantly greater skip distance. This double refraction phenomenon should be detectable at sea, under suitable experimental conditions. [Research supported by ONR.] a) Ocean Acoustics Associates.

kbcc1 4/b~.5 MM4. An assessment of second-order perturbation theory as applied to the scattering of sound by statistically rough surfaces. A. Tolstoy, D. Berman, O. Diachok (Naval Research Laboratory, Code 5160, Washington, DC 20375), and I. Tolstoy (Knockvennie, Castle Douglas, SW Scotland) Second-order perturbation theory is one of few theories presently ca-

8:50

pable of describing scattering of low-frequency acoustic plane waves by statistically rough surfaces. In order to assess this theory we have compared its predictions of the magnitude of the reflection coefficient |R| with known near exact solutions, in particular, for surfaces which consist of identical, hard, ellipsoidal bosses sparsely and independently distributed on a hard plane by means of a uniform probability law. In order to apply perturbation theory to such a surface we needed to compute its correlation function, operate on that function, and compute an effective boundary admittance. Finally we compared that admittance with (farfield) nearexact results for spherical and oblate ellipsoidal bosses with eccentricity e. Calculations of |R| are presented showing that discrepancies decrease as grazing angle increases and are less than 10% for e > 0.99, and approximately 70% for $e \approx 0$. We conclude that perturbation theory is excellent in the case of oblate spheroids and not to be used for prolate spheroids. [This work was supported by ONR and NRL.]

9:05

MM5. Perturbation theory for scattering from random rough surfaces using the extended boundary condition. Dale Winebrenner and Akira Ishimaru (Department of Electrical Engineering, University of Washington, Seattle, WA 98195)

Scattering from surfaces with roughness small relative to the wavelength of the incident radiation has most often been calculated using the perturbation method developed by Rice. This method uses the Rayleigh hypothesis, i.e., the assumption that the scattered field on the surface can be represented as a sum of up-going plane waves. This assumption is known to be invalid when slopes of the rough surface are sufficiently large. A way of treating scattering using a perturbation theory based on the extended boundary condition has been given by several authors. This method appears to avoid the Rayleigh hypothesis. We will compare the results of the two methods and discuss the connection between them. [Work supported by ONR.]

9:35

MM7. The T-matrix approach to scattering of waves by rough surfaces. Akhlesh Lakhtakia, Vijay K. Varadan, and Vasundara V. Varadan (Department of Engineering Science and Mechanics, Pennsylvania State University, University Park, PA 16802)

In this paper, we use the extinction theorem to compute a T matrix which characterizes a given rough interface between two media. In particular, we concentrate on multiple-layered geometries. Thus we consider an elastic rough infinite slab interfaced with different fluids on either side. This case serves as a model for studying water/ice plate/air systems. Numerical results illustrating the cases of longitudinal or shear wave incidence, as applicable, shall be presented.

9:50

MM8. Acoustic intensity from manganese nodule deposits, Y. Ma. V. K. Varadan, and V. V. Varadan (Department of Engineering Science and Mechanics, Pennsylvania State University, University Park, PA 16802)

Abundant information on manganese nodules in the deep ocean can be obtained from remote acoustic intensity measurements. The previously suggested low-frequency reflectivity measurements, neglecting the incoherent part of the backscattered acoustic signals, are quite good in predicting the presence of these nodules. However, in order to judge the effect of the size distribution on the acoustic response and to get the mean nodule size information, a wider frequency range is required. The contribution of the incoherent part of the acoustic response to the backscattered intensity becomes increasingly important as the sounding frequency gets higher. One may actually under-, or over-, estimate the amount of, and the average size of, the manganese nodules by carelessly neglecting the incoherent acoustic intensity. The intensity calculation based on the energy principle for nonabsorbing scatterers will be discussed, and the results will be presented for different concentrations of nodules with uniform as well as Rayleigh size distributions. All results presented shall be for sparsely distributed nodules made using the single scattering theory. The future extension to highly concentrated nodule fields by using the multiple scattering theory will also be discussed.

10.05

Tom Min det an Sub bits MM9. Backscattering from sub-bottom microlayers. Ronald J. Wyber (on long-term attachment from RAN Research Laboratory, P.O. Box 706, Darlinghurst, Australia 2010) and Thomas G. Muir (Applied Research Laboratories, The University of Texas at Austin, P.O. Box 8029, Austin, TX 78712-8029)

Vertical profiling measurements of the bottom in the frequency band from 1-5 kHz showed the variance of the reflected signal to be proportional to the frequency and the horizontal correlation length to be in the order of 10 m. This indicated that the variance in the backscattered signal is a function of the sonar beam pattern and the pulse shape, frequency, and grazing angle of the incident wave. For a pulse length of 25 ms and a grazing angle of 10°, the predicted backscattering strength was found to be independent of frequency at a level of $-40 \, dB$. This behavior agreed with

X CArlatin Levetty of How \$74 J. Acoust. Soc. Am. Suppl. 1, Vol. 75, Spring 1984 Declaration rodependent of f

data measured at this angle. As the classical theory of backscattering assumes that the bottom reverberation is due to independent scatterers which add incoherently, this theory will become invalid if the dimensions of the area ensonified on the bottom are less than the correlation length. Thus, for sonars with a short pulse or a narrow beam, the backscattered power will no longer be proportional to the ensonified area. [Work supported by the Office of Naval Research.]

43.30. - k

10:20

MM10. Acoustic differential scattering cross section for internal waves. Bruce J. Bates (Naval Underwater Systems Center, Bldg. 1171/1, Code 3513, Newport, RI 02841)

The Garrett and Munk internal wave field is a second-order process. It is also stationary, homogeneous, and anisotropic. Acoustic fields propagating through the internal waves are scattered by the internal wave sound speed fluctuations. The differential scattering cross section is derived employing the Born approximation and the "on frequency shell" condition. For comparison, the internal wave sound speed fluctuation is approximated by an anisotropic Gaussian correlation function and the resulting differential scattering cross section is evaluated for typical horizontal and vertical correlation lengths. Both differential scattering cross sections are compared as a function of scattering angle for selected angles of incidence and acoustic frequencies.

10:35

MM11. Acoustic propagation with an oceanic sound-speed model including a random field of internal waves. Susan M. Bates (SYSCON Corporation, 10 John Clarke Road, Middletown, RI 02840)

Flatté and Tappert [J. Acoust. Soc. Am. 58, 1151-1159 (1975)] have shown that internal waves cause significant fluctuations in the transmission of acoustic energy through the ocean volume, comparable in size and frequency to the fluctuations observed in field experiments. They use the parabolic equation method to propagate acoustic signals. The random component of the sound-speed field is modeled by a linear superposition of internal wave eigenmodes. Each eigenmode amplitude is selected independently from a complex Gaussian distribution. Using an improved version of their simulation, range versus loss data are generated for up to 100 h of simulated time at 0.5-h intervals. The source of 100 Hz is located on the axis of the canonical profile. The ensemble average and variance of the acoustic signal, as a function of receiver location, are computed. [Work supported by NUSC.]

10:50

MM12. Sound scattering in a turbulent medium. Richard J. Lataitis (NOAA/ERL/WPL-R/E/WP1, 325 Broadway, Boulder, CO 80303), Greg Crawford (Institute of Ocean Sciences, Victoria, BC, Canada V8L 4B2), and Steven F. Clifford (NOAA/ERL/WPL-R/E/WP1, 325 Broadway, Boulder, CO 80303)

Tatarski [V. I. Tatarski, Wave Propagation in a Turbulent Medium (McGraw-Hill, New York, 1960)] has derived an expression for the effective scattering cross section of an acoustic wave incident on a remote volume of atomospheric turbulence. His result is subject to the single scatter approximation and the restriction that both transmitter and receiver be in the farfield of the large scale inhomogeneities within the volume. We derive an expression for the effective scattering cross section. valid in both the near and farfield and extend these results to include the scatter of acoustic waves from underwater turbulence.

11:05

MM13. Near-range scintillations in a nonisotropic scattering medium. Shimshon Frankenthal (Faculty of Engineering, Tel Aviv University, Ramat Aviv, Israel)

Using the Rytov approximation, an expression is derived for the logamplitude correlation function of weak fluctuations induced in a plane wave propagating in a forward-scattering medium. The expression is valid at any range where weak fluctuations exist, including those which are shorter than the correlation length. The behavior of the scintillation index at very short ranges in isotropic media characterized by one or two scales is examined, and its dependence on frequency (k) and range (z) is listed for several regimes. Propagation is also studied in a nonisotropic medium, where the refractivity fluctuations are governed by the Garrett-Munk internal-wave spectrum. Here, the frequency-range dependence of the scintillation index changes from $k^{3/2} z^{5/2}$ at very near ranges to kz^2 at more distant ones.

11:20

MM14. Calculated and measured fish-school echoes. Paul D. Ingalls (Applied Physics Laboratory, College of Ocean and Fishery Sciences, University of Washington, 1013 N.E. 40th Street, Seattle, WA 98105)

A simulation model that generates the waveform of a high-frequency acoustic echo from a model fish school has been developed. The echo model generates the waveform by coherent addition of echoes from a collection of model point scatterers that have position, scattering amplitude, and velocity parameters chosen to reproduce some of the observable properties of echoes from real fish schools. Sample echo waveforms, spectra, and split-beam phase difference will be presented. This model has been used to show the effects of partial ensonification on apparent size and scattering parameters of fish schools. [Work supported by U.S. Navy.]

11:35

MM15. Determination of the ocean wave directional spectrum from acoustic backscatter. Steven F. Clifford and Richard J. Lataitis (NOAA/ERL/WPL-R/E/WP1, 325 Broadway, Boulder, CO 80303)

We describe a technique for extracting the ocean wave height directional spectrum (OWHDS) from underwater acoustic backscatter measurements. Our technique requires a bottom-mounted acoustic transceiver consisting of a quasi-isotropic source of sound and a receiver array designed to measure the mutual coherence function (MCF) of the surface scattered and reflected fields. The MCF is shown to be directly related to the OWHDS which can then be extracted using a simple inversion scheme. Our results are applicable for all relative values of the rms surface wave height to acoustic wavelength provided the rms surface wave slope s < 1.

THURSDAY MORNING, 10 MAY 1984

MONTPELIER ROOM, 8:30 TO 11:50 A.M.

Session NN. Engineering Acoustics IV: Pattern Recognition

Robert D. Finch, Chairman

Department of Mechanical Engineering, University of Houston, University Park, Houston, Texas 77004

Chairman's Introduction-8:30

Invited Papers

8:35

NN1. An overview of pattern recognition and its application in acoustics. K. S. Fu (School of Electrical Engineering, Purdue University, West Lafayette, IN 47907)

The problem of pattern recognition is introduced and its major approaches briefly reviewed. In the decision-theoretic approach, both parametric and nonparametric classification techniques are described. In the syntactic approach, pattern description languages and their recognition algorithms are discussed. Application examples are presented. VLSI implementations of some of the techniques are discussed. A unified syntacticsemantic approach is then proposed. Problems for further study are suggested. [Work supported by NSF under Grant ECS 81-19886.]

9:05

NN2. Pattern recognition applications in underwater acoustics. C. H. Chen (Department of Electrical and Computer Engineering, Southeastern Massachusetts University, North Dartmouth, MA 02747)

Pattern recognition application to underwater acoustics is a relatively less explored area, even though much study has been made of sonar signal detection. Recently, significant effort has been made of submarine transient signal analysis and classification. Various spectral and time domain features are considered for detection and event classification. Effective recognition requires signal segmentation. The use of entropy distance measure for waveform segmentation is then examined. The next pattern recognition application is the target motion analysis by using pattern matching idea in the estimation of target range, velocity, and bearing. Another application is in multipath ranging. An image processing technique is used to extract the significant tracks from the correlograms to provide a continuous estimate of time delay or range under a multipath environment. Major computer results reported earlier [C. H. Chen, Pattern Recog. J. 16 (6) (1983)] along with further results on transient signal analysis are presented. Other applications such as sonar recognition in fisheries are also examined. While the trend continues to be digital processing and system integration, the basic recognition issue remains to be the extraction of effective features from the preprocessed underwater acoustical data. [Work partially supported by NUSC at Newport, RI.]

٠ï٠

٠Ŭ

-

÷

÷

-1-

NN3. Textural feature extraction in seismic images. I. E. Stephanou and S. Y. Lu (Long Range Research Division, Exxon Production Research Company, P. O. Box 2189, Houston, TX 77001)

This lecture introduces a set of second-order statistical features that can be used to discriminate among several textural classes associated with seismic reflection configuration patterns. It is well known in the petroleum geology community that some of these patterns are characteristic of certain types of rock formations. The textural features that we use here are based on an extension of the co-occurrence matrix approach originally proposed by Haralick et al., in 1973. The feature extraction technique has been applied to a seismic image from offshore West Africa. The results indicate that the method is useful for the local discrimination of rock types deposited during the same geological period. Considerably more elaborate scene analysis techniques are however needed for image understanding purposes. They are not discussed in this talk.

10:05

NN4. Acoustic emission analysis using pattern recognition. P. G. Doctor and D. S. Daly (Battelle Northwest Laboratories, Box 999, Richland, WA 99352)

The purpose of the work is to design a fifethod of differentiating events, caused by a growing crack in a critical structure from innocuous noise sources, from the waveform in order to improve the accuracy of acoustic emission monitoring systems for metal structures. The development approach is to generate acoustic emissions from known (crack, fretting, electrical transient) sources in the laboratory, compute certain quantities (features) from the recorded signal, and design discriminant functions to differentiate among the sources. The selection of the features for the discriminant function is crucial. They are selected on the basis of physical as well as empirical grounds. The acoustic signal is influenced by subtle engronment effects as well as the instrument system, the geometry of the structure being monitored and its interaction with the changing ∉ geometry of the growing crack. The challenge of the work is finding features that are applicable to a range of

monitoring situations and are reasonably stable over time. [Work supported by NRC Office of Nuclear Regulatory Research and Defense Advanced Research Project Agency.]

10:35

NN5. Speech recognition at IBM research. Frederick Jelinek (IBM Corporation, T. J. Watson Research Center, P. O. Box 218, York Im Heights, NY 10598)

Continuous speech recomption is an attempt to develop a "voice-actuated typewriter" that automatically transcribes naturally spoken utterances into correct orthography. A reliable speech recognizer would facilitate the most economical speech compaction and transmission. The current IBM objective is to accomplish realtime transcription of office correspondence using an experimental system consisting of a minicomputer, several array processors, and an editing workstation with a display, keyboard, and printer. To make real-time performance possible, the vocabulary is restricted to 5000 words that must be spoken with short pauses between them. The lecture will describe the current state of the project, outline its methods, and discuss future prospects. •

Į.

11:05

NN6. Pattern recognition in speech processing. Jonathan Allen (Department of Electrical Engineering and Computer Science and Research Laboratory of Electronics, Massachusetts Institute of Technology, Cambridge, MA 02139)

The determination of linguistic structure from surface patterns in text and speech requires the integration of cues from multiple constraint domains including phonetic features, syllable and morpheme structure, syntax, and semantics together with pragmatics. Utilization of these constraints shows that the factors contributing to the integration metric vary along the utterance, and that principled surface variation can be accounted for in terms of these structures, thus reducing the apparent noise. Given the large number of factors that influences the pattern classification decision, it is important to defer commitment to structural hypotheses as long as possible, so that neither "bottom up" nor "top down" search strategies are appropriate models for the recognition of natural language patterns. Instead, observance of cooccurrence relations among the parameters of a model can be exploited in efficient training procedures that extract the maximum amount of information from The experimental corpus. These techniques naturally lead to formulations of constraint domain structures that are mathematically explicit, minimizing the use of heuristics except where dictated by complexity considerations. Experience from contemporary research in speech synthesis and recognition is used to illustrate these principles, characterize current capability, and indicate directions for future research.

-

≯

Contributed Paper

Æ

11:35

NN7. Pattern recognition in acoustic signature inspection of railroad wheels. Shivan Haran and R. D. Finch (Department of Mechanical Engineering, University of Houston, Houston, TX 77004)

There is a need for an automatic testing system for railroad wheels in service. Earlier work established the feasibility of using acoustic signatures for this purpose, to the extent that such a system has now been installed and is under test. An important conclusion from previous work was that the best detection method was a comparison of sounds from the two members of a wheel set. Pattern recognition techniques were used to detect the difference in the sounds of these two wheels. Preliminary results indicate that these techniques are adequate to discriminate good wheels from flawed ones. Various comparison schemes can be used depending on the features selected. Among features considered are spectral cross correlation, and the number of resonances common to the signals of both wheels. Linear decision functions and a least-squares procedure are used in the classification. The results obtained are encouraging. [Work supported by the Association of American Railroads.]

THURSDAY MORNING, 10 MAY 1984

GREENWAY ROOM, 8:30 TO 11:20 A.M.

Session OO. Physical Acoustics V: Waveguides and Propagation

Lawrence Flax, Chairman Naval Coastal Systems Center, Panama City, Florida 32407

Chairman's Introduction-8:30

Contributed Papers

8:35

OO4. Low-frequency vibrational modes of fluid-loaded thin spherical shells. L. H. Green, Roger H. Hackman, D. H. Trivett, and L. Flax

(Naval Coastal Systems Center, Panama City, FL 32407)

The low-frequency form function for plane-wave scattering by a fluidloaded thin spherical shell is characterized by the high Q monopole or "bubble" resonance. As the shell thickness is increased, the monopole resonance is observed to shift to higher frequency and broaden (i.e., the Qof the resonance decreases). With a further increase in thickness, high Qresonances appear on top of the spectrum of the monopole resonance. These low-frequency, high Q resonances, first reported by Diercks and Hickling [J. Acoust. Soc. Am. 41, 380–393 (1967)] have never been satisfactorily explained. In this paper we present the results of our investigation, based upon the linear theory of elasticity, of these high Q resonances. The dependence of the resonances on frequency, and shell and fluid parameters are presented along with the elastic stresses and displacements in the shell. Dispersion curves are generated from numerical solutions and a physical explanation for the strong coupling to the fluid medium is obtained.

9:35

OO5. Acoustic surface wave measurements on live bottlenose dolphins. W. M. Madigosky, G. F. Lee (Naval Surface Weapons Center, White Oak, Silver Spring, MD 20910), F. Borkat, R. Kataoka, and J. Haun (Naval Ocean Systems Center, San Diego, CA 92152)

Measurements of the velocity and attenuation of acoustic surface waves propagating on the outer surface of live bottlenose dolphins (*Tursiops truncatus*) were made as a function of frequency and location on four different animals. Two miniature accelerometers were attached to the skin and a surface wave was launched using an electromagnetic shaker driven by a noise source. A dual channel FFT spectrum analyzer and computer analyzed and computed the data [see J. Acoust. Soc. Am. 73, 1374 (1983)]. Surface wave velocities varied from 4 to 14 m/s over the frequency range 100–1000 Hz. The attenuation appeared to follow the $\alpha = A f^{10}$ law, where, $A \simeq 1.5$ dB-s/m. Generally, the wave speed and attenuation were independent of the propagation direction (anterior, posterior, dorsal, or ventral) except near the dorsal fin. Additional measurements of the shear wave velocity were obtained on just the epidermis plus dermis section of the skin. These velocities were found to be two or three times higher and dependent on the direction of the propagation.

9:50

OO6. Transient Rayleigh wave transmission across periodic surfaces. Jacques R. Chamuel (Sonoquest/Advanced Ultrasonic Research, P. O. Box 584, Sudbury, MA 01776) and Gary H. Brooke (Defense Research Establishment Pacific, FMO Victoria, BC VOS 1B0, Canada)

107th Meeting: Acoustical Society of America \$77

THUR SDAY AM

9:20

OO1. Stability analysis of a Stokes boundary layer in a waveguide having slowly varying height. Charles Thompson (Department of Engineering Science and Mechanics, Virginia Polytechnic Institute and State University, Blacksburg, VA 24061)

The stability of an acoustic disturbance in a two-dimensional waveguide having slowly varying height will be investigated. The enclosed fluid is assumed to be both viscous and compressible. It is shown that the dynamic behavior of the enclosed fluid can be parameterized by three small parameters, ϵ , 1/R, and 1/S, where ϵ is the ratio of the typical duct height H_0 to the wall wavelength L_{0r} , 1/S is the ratio of the oscillatory particle displacement U_0/ω to the typical duct height H_0 , and 1/R is the ratio of the oscillatory boundary layer thickness I_v to the typical duct height H_0 . Special attention will be paid to waveguides with cross sections that are small compared to an acoustic and/or wall wavelengths. A stability analysis will be presented in the amplitude range where $\epsilon^2 R/S^2 = O(\sqrt{R})$.

8:50

OO2. Propagation of axisymmetric free waves in a circular cylindrical shell. D. H. Trivett (Naval Coastal Systems Center, Panama City, FL 32407)

This paper presents the results of an investigation of free wave propagation in a circular cylindrical shell in vacuum, using the linear theory of elasticity. The study has resulted in identifying a previously unreported low-phase velocity axisymmetric mode. This new mode is a low-frequency branch of the first mode in a cylindrical shell and exists below the cutoff frequency of the second axisymmetric mode. The physical properties of the two low-frequency branches are discussed and numerical results are presented along with preliminary data verifying the existence of the new mode. In addition, the results are used to demonstrate that present thin shell theory does not adequately describe the behavior of thin shells at low frequency.

9:05

OO3. Some interesting modes of propagation in a large elastic sample. M. Paul Hagelberg (Wittenberg University, P. O. Box 720, Springfield, OH 45501)

The availability of a large sample of high-quality steel with carefully finished surfaces has made possible time resolution of propagation modes that ordinarily overlap. The resolved echo trains clearly demonstrate several interesting modes of propagation. These observations serve not only to illustrate important features of wave propagation in an elastic medium but also to show the importance of recognizing these features when interpreting results from experiments performed in such media.

Sharp attenuation of 10-Hz Scholte wave components has been observed in a region of the Canadian Arctic. The presence of shallow nearly periodic bottom ridges and surface features is believed to be the cause of the sharp attenuation of these low-frequency components (G. H. Brooke). Experimental investigations using ultrasonic models (Chamuel) have been carried out to study the transmission of transient Rayleigh waves across periodic surface grooves. Attenuation, dispersion, and time delay effects have been measured and related to groove dimensions and spatial distribution. The energy of the first Bragg frequency component is partly transmitted over a wide time window. Strong low-frequency components with a wavelength equal to 4 times the spatial wavelength of the grooves are transmitted. The effects of the number of grooves, and the groove depth and spacing on filtering and delaying the transmitted Rayleigh wave pulse will be described. The propagation of broadband transient Scholte waves across periodic surface grooves and ridges is being investigated. [Work sponsored by DREP.]

10:05

OO7. Impedance formulation and clipping technique in the fast field program. R. F. Richards (Department of Electrical Engineering, University of Houston, Houston, TX 77004), S. W. Lee, N. Bong (Department of Electrical Engineering, University of Illinois, Urbana, IL 61801), and Richard Raspet (U.S. Army Construction Engineering Research Lab, Champaign, IL 61820)

The propagation of a sound wave in a layered media excited by a point pressure source can be formulated into a Fourier integral. A powerful method for evaluating this integral is to use the Fast Fourier Transform, resulting in the so-called "Fast Field Program (FFP)" [F. R. DiNapoli and R. L. Deavenport, J. Acoust. Soc. Am. 67, 92-105 (1980)]. In the existing scattering matrix formulation, the FFP requires the multiplication of matrices containing exponential factors exp $(+\gamma h)$ and exp $(-\gamma h)$, where γ is the attenuation constant along the vertical direction of a layer, and h is the layer's thickness. These factors often exceed the computer's capability in handling large/small numbers, thus resulting in erroneous FFP solutions. In the present paper, we describe a new formulation of the FFP that is inherently numerically stable and is completely free from the difficulty mentioned above. The central step in our formulation is to calculate the equivalent impedance for each layer in succession starting from the top/bottom layers toward the source. This technique results in terms containing (γh) rather than ($-\gamma h$), which goes to unity smoothly as $\gamma h \rightarrow \infty$. In addition, we introduce a "clipping technique." For a given horizontal wavenumber, it removes layers that are not physically significant by terminating the preceding layer at its characteristic impedance.

10:20

OO8. Interface wave mode propagation in clad rod acoustic waveguides. Susan J. Hanna and Richard O. Claus (Department of Electrical Engineering, Virginia Polytechnic Institute and State University, Blacksburg, VA 24061)

The propagation of acoustic waves on the cylindrical boundary between the core and cladding materials of a clad rod waveguide is described. Typically, axisymmetric torsional, axisymmetric radial-longitudinal, and core-guided shear modes may propagate within a rod of cylindrical cross section if the velocity of plane shear waves in the cladding material exceeds the velocity in the material of the core [R. N. Thurston, J. Acoust. Soc. Am. 64, 1 (1978)]. If instead the elastic constants of the core and cladding materials of the rod are reversed so the material with the slower shear wave speed is on the outside, no modes are supported within the core but an interface wave can exist on the core-cladding boundary. In this paper the transmission properties of an all glass clad rod with a suitable core-cladding elastic constant relationship to support nonattenuating interface waves are discussed. The resulting improved freedom from spurious responses allowed by this single mode operation is discussed. [Work supported by NASA.]

10:35

OO9. Tangential component of an acoustic surface pulse. Richard O. Claus (Department of Electrical Engineering, Virginia Polytechnic Institute and State University, Blacksburg, VA 24061)

Measurements of the in-plane components of the surface particle displacement caused by a simulated Heavyside step function load source on the same surface of a large glass block are described and compared with theory. These components were measured by attaching a small rectangular solid crystal with reflecting surfaces to the block and observing the tangential motions of the normal surfaces of the crystal using stabilized optical interferometry. Although the bandwidth of the detected signals is limited by the length of the crystal compared to an acoustic wavelength, and the observable motions are influenced by the mass loading of the surface by the crystal, good agreement between theory and measurements is obtained. These data combined with similar optical measurements of the normal component [F. R. Brekenridge, C. E. Tschiegg, and M. Greenspan, J. Acoust. Soc. Am. 57, 626 (1975)] yield full localized three-dimensional displacement information. [Work supported by NASA.]

10:50

OO10. Mode shapes and propagation characteristics for waves propagating in nonuniformly lined ducts. P. G. Vaidya (Mechanical Engineering Department, Washington State University, Pullman, WA 99163-2920)

It is well established that the sound propagation in a duct, lined in a nonuniform fashion, either in the circumferential or the axial direction, cannot be described by means of separable modes. However, under these circumstances nonseparable modes can be used. In this paper it is shown that for some specific nonuniform boundary conditions, closed form solutions can be obtained. The mode shapes of the nonseparable modes have been obtained. It has been shown that these modes can be used to convert energy from lower modes to higher modes, which are easier to attenuate.

11:05

OO11. The propagation of spinning modes through nearly choked inlets. P. G. Vaidya (Mechanical Engineering Department, Washington State University, Pullman, WA 99163-2920)

It is well known that sound cannot propagate upstream against a supersonic flow. However, even at subsonic speeds, in excess of the Mach number of 0.6, considerable attenuation has been observed in practice. To explain this, an equation, for the propagation of spinning modes in ducts carrying flow with axial and radial gradients, has been derived. The equation has been used to show that when a wave passes through a convergentdivergent nozzle, the net result is an attenuation of sound. Alternative mechanisms for the sound reduction in practical flows are also discussed.

Session PP. Noise VI: Aircraft Noise and Aeroacoustics

Donald L. Lansing, Chairman

Mail Stop 125A, NASA Langley Research Center, Hampton, Virginia 23665

Chairman's Introduction-8:55

Contributed Papers

9:00

PP1. An analytical investigation of synchrophasing as a means of reduction of aircraft interior noise. C. R. Fuller (Department of Mechanical Engineering, Virginia Polytechnic Institute and State University, Blacksburg, VA 24061)

In this paper the noise control characteristics of synchrophasing (i.e., varying the relative rotational phase of individual propellers) are investigated using a simplified model of an aircraft. For the analysis considered here the aircraft fuselage is approximated by an infinite cylindrical shell and the acoustic sources due to the propellers as dipoles. The acoustic response of the interior of the shell can then be obtained by utilizing the spectral form of the shell response with forcing functions due to the dipole sources expanded into cylindrical coordinates using a special form of the Bessel addition theorem. The variation in sound pressure levels at various locations inside the cylinder is then studied for a variation in phase between the dipole sources. Correspondingly, the shell response is evaluated and decomposed into individual circumferential modes of vibration in order to give an indication of the mechanism of transmission of sound into the shell.

9:15

PP2. Measurements of periodic blade pressures on a transonic propeller with nonuniform inflow. Laurence J. Heidelberg, Milo D. Dahl, and Edward J. Rice (NASA Lewis Research Center, 21000 Brookpark Road, Cleveland, OH 44135)

As part of an experimental program to determine the installation effects on noise of a transonic propeller in front of a wing, blade surface pressures were measured. This paper is a preliminary investigation of these measurements with the purpose of relating pressure to blade angle of attack changes. The ultimate purpose is to use blade pressure as a tool to measure the inflow distortions and relate the resulting unsteady loading to noise. Several miniature pressure transducers were mounted on a highly swept transonic propeller known as SR-3. This propeller was run in a wind tunnel over a range of Mach numbers from 0.5 to 0.85. The propeller axis was set at several angles to the flow in order to produce a known inflow distortion. A second set of tests were run with a wing installed behind the propeller and the effect of this inflow distortion on blade pressures was measured. The magnitude of the pressure changes is shown as a function of the periodic angle of attack change. A significant phase lag between pressure and angle was noticed for transducers even near the leading edge of the blade.

9:30

PP3. Coupled aerodynamic and acoustic predictions for turboprops. Bruce J. Clark and James R. Scott (NASA Lewis Research Center, 21000 Brookpark Road, Cleveland, OH 44135)

To predict the noise fields for proposed turboprop airplanes, an existing turboprop noise code by Farassat has been modified to accept blade pressure inputs from a 3-D aerodynamic code. A Euler-type code written by Denton can handle the nonlinear transonic flow of these high-speed, highly swept blades. This turbofan code of Denton was modified to allow the calculation mesh to extend to about twice the blade radius and to apply circumferential periodicity rather than solid-wall boundary conditions on the blade in the region between the blade tip and the outer shroud. Outputs were added for input to the noise prediction program and for color contour plots of various flow variables. The input subroutines were modified to read files of blade coordinates and predicted surface pressures. Aerodynamic and acoustic results are shown for the SR-3 model blade and are compared to various measured data.

9:45

PP4. Fan noise reduction achieved by removing tip flow irregularities behind the rotor. James H. Dittmar, Richard P. Woodward, and Michael J. MacKinnon (NASA Lewis Research Center, 21000 Brookpark Road, Cleveland, OH 44135)

One of the major noise producing mechanisms in a fan stage for a turbofan engine is the interaction of the rotor wakes with the downstream stator vanes. Previous work has indicated that the rotor tip flow irregularities (vortices and velocity defects) may be as large or larger a source of blade passage tone noise as the usually considered mean rotor wake. Flow was removed between the rotor and stator of an existing fan stage by an outer wall slot and noise measurements were made to investigate the rotor tip flow irregularity-stator interaction as a noise source. Farfield noise data taken in an inlet arc showed little tone noise reduction with flow removal, probably the result of rotor-stator interaction noise not propagating upstream through the rotor. In-duct measurements behind the fan stator did show noise reduction with flow removal and proportionally more reduction occurred with the first increment of flow removal than with subsequent amounts. Since the tip flow irregularities were assumedly removed with the first increment of flow, the duct measurements indicate that the tip flow irregularity-stator interaction is probably as large a noise producing mechanism as the normally considered rotor wake-stator interaction.

10:00

PP5. Surface aerosound from a model wing/flap in an anechoic room. S.-C. Liu and W. C. Meecham (School of Engineering and Applied Science, University of California, Los Angeles, CA 90024)

The aerodynamic sound generated by a small scale wing model interacting with a 4-in. jet has been investigated experimentally in NASA-AMES anechoic chamber. The investigation consists of two parts. The first part is concentrated on the jet shear layer/wing interaction noise. The second part is the study of noise associated with separated flow. Crosscorrelation techniques are used to discriminate against unwanted noise. The results of experiment I show that the sound generated by shear layer/ wing interaction is 10 dB higher than the free jet noise. A round guide attached to the jet exit reduced the farfield sound by 8 dB. The rms pressure in the nearfield is found to be inversely proportional to the third power of the distance from generating eddies. The typical Strouhal number of sound generated, based on the shear layer thickness and the mean flow speed, is 0.17. The results of the sound experiment show that on the separation side of the wing the generating eddies are located near the trailing edge, as expected. The noise generating eddies propagate downstream with the convection velocity and are not triggered until they reached the trailing edge. The convection speed is found to be 0.85 times the jet mean flow speed, as judged by signal time delays.

10:15

PP6. Jet noise: An overview of the self and shear noise theory. W. G. Richarz (Institute for Aerospace Studies, University Toronto, 4925 Dufferin Street, Downsview, Ontario, Canada M3H 5T6)

Lighthill's theory of aerodynamic sound furnishes an exact set of differential equations. In order to obtain reasonable estimates of sound generated by aerodynamic sources certain simplifications are introduced. One model that has been quite successful is Ribner's self and shear noise formalism. The equivalent source terms therein are proportional to the unsteady momentum flux directed at an observer. The theory has been extended to deal with forward flight affects, heated turbulent flows. In addition there are results for nearfield pressures as well as the farfield coherence. All this can be obtained without any alteration of the underlying formalism. The turbulent flow is described by a "locally homogeneous isotropic" correlation function with specified length and time scales. Despite its simplicity the model is capable of predicting many features of the sound field generated by subsonic jets. [Work supported by NSERC, Canada.]

10:30

PP7. Sound intensity techniques for identifying locations of scale model jet noise sources. David J. Roth (Douglas Aircraft Co., Mail Code 36-60, McDonnell Douglas Corporation, 3855 Lakewood Boulevard, Long Beach, CA 90846)

Experimental investigations were made to identify the physical source locations of a 6-in. equivalent diameter scale model coaxial jet using twomicrophone sound intensity measurement techniques. Near and farfield measurements were made within a large volume anechoic chamber in two directions from the jet centerline. The jet was operated under conditions of hot and cold flow at several nozzle pressure ratios. The data were recorded on magnetic tape and narrow-band analyzed to identify the direction of the intensity vector from the centerline of the jet to the location of measurement. The analysis method consisted of converting the value of imaginary cross spectrum to intensity vector along a microphone line. The resultant vector was then calculated and extrapolated back to an estimated jet axis flow boundary. The source locations identified for the model jet were verified by a loudspeaker source and were in good agreement with SAE jet noise prediction models. The measurement method used was subject to some error due to dropout of intensity vector perpendicular to the radial in the farfield. An alternate two-microphone probe technique is suggested that may overcome this problem.

10:45

PP8. Aircraft noise synthesis system: An introduction. David A. McCurdy (NASA Langley Research Center, Mail Stop 463, Hampton, VA 23665)

An aircraft noise synthesis system has been developed to provide test stimuli for studies of community response to aircraft flyover noise. The computer-based system generates realistic, time-varying audio simulations of aircraft flyover noise at a specified observer location on the ground. The synthesis takes into account the time-varying aircraft position relative to the observer; specified reference spectra consisting of broadband, narrow-band, and pure tone components; directivity patterns; Doppler shift; atmospheric effects and ground effects. These parameters can be specified and controlled in such a way as to generate stimuli in which certain noise characteristics such as duration or tonal content are independently varied while the remaining characteristics such as broadband content are held constant. The system can also generate simulations of the predicted noise characteristics of future aircraft such as the proposed advanced turboprop. The paper includes a brief description of the overall system, a user-oriented discussion of the input data and modeling methods, and recordings of synthesized flyover noise produced with the system.

11:00

PP9. Aircraft noise synthesis system: Computer algorithms and methods. Robert E. Grandle (Mail Stop 461, NASA Langley Research Center, Hampton, VA 23665)

This paper describes in some detail the algorithms and methods used in the aircraft noise synthesizer program now in use at the Aircraft Noise Reduction Laboratory. This program is intended to produce aircraftlike flyover noise from a series of pure tone, narrow-band, and third-octave spectrums. Because the acoustic output of this program is intended to be played to subjects for determination of the fundamental response of humans to aircraft noise, a great deal of care must be taken to reduce to a minimum any extraneous noise produced by the synthesis process. In general the method described in this paper makes use of the fast Fourier techniques to produce analog time histories from the narrow-band power spectrum which is its input. The basic problem of noise synthesis of nonperiodic noise with a semi-periodic component (turbine and compressor whine) is to produce a sound which is sufficiently random enough to sound natural while maintaining a tight control of the spectral levels. The major difficulty in this is that the input spectral levels lack sufficient information to produce a continuous analog time history.

11:15

PP10. The role of induced vibrations in helicopter noise annoyance. Paul D. Schomer (U.S. Army Construction Engineering Research Laboratory, Champaign, IL 61820)

Community reaction to helicopter noise remains only a partially answered question. While the A-weighting appears to work out of doors and at modest noise levels, and the community response in terms of percent of population highly annoyed can be correlated with respect to the DNL (day/night level) descriptor, questions remain as to the role of perceived building vibrations in the response of people to helicopter noise. Does hearing windows rattle, or ceiling tiles rattle, objects in the room rattle, or the general perception of building vibration increase the public's adverse response to helicopter noise? The purpose of this study was to examine the growth in human response to helicopter noise as the noise levels grow from modest levels to fairly high levels. At the higher levels the noise will excite vibrations in building elements and objects within the structure. The purpose of this study was to discover a shift in the growth in human response (if any) to increasing noise which can be related to these vibrations. This study used a UH-IH helicopter in conjunction with an old farm house, a new mobile home, and outdoors in a tent as a live "laboratory." This paper reports on the test execution and initial results. [This was a joint U.S. Army/FAA study.]

11:30

PP11. Reduction and discrimination of wind noise in outdoor blast noise measurement. Douglas R. Walker (U.S. Army Construction Engineering Research Laboratory, Champaign, IL 61820)

It is difficult to distinguish between wind-induced noise and blast noise under field conditions, since the spectral content of both is concentrated below 50 Hz. As one solution, an omnidirectional, low-frequency, outdoor microphone windscreening system was designed and tested. An empirical data base of approximately 600 measurements characterizing outdoor blast noise was collected with the system. It employed a layered, low-porosity foam, mechanical windscreen which was optimized for rejection of low-frequency wind noise. This windscreen attenuated the Aweighted wind noise by up to 26 dB overall. Additionally, a two-microphone array was used and it was found that blast events could be distinguished reliably from wind by comparison of selected features of the two signals.

11:45

PP12. The use of radiation efficiencies in the diagnosis of noise sources. Paul R. Donavan (Current Product Engineering, General Motors Current Engineering and Manufacturing Services Staff, Milford, MI 48042)

Using the recently developed two-microphone technique of acoustic intensity measurement, radiation efficiencies of a single panel and individual panels of a complete vehicle structure have been made under controlled, laboratory conditions. The data obtained from the single panel were used to develop measurement techniques and study the sound field near the panel. Radiation efficiencies of the vehicle structure were used

along with measured vibration response obtained under normal operation conditions to determine the sound power produced by each individual panel. Results describing the technique development and the application to the vehicle structure are presented in this paper.

THURSDAY MORNING, 10 MAY 1984

BRANDON ROOM, 9:00 TO 11:20 A.M.

Session QQ. Physiological Acoustics VIII: Evoked Potentials, Otoacoustic Emissions, and Biochemistry

Robert W. Peters, Chairman

Division of Speech and Hearing Sciences, Wing D, Medical School, University of North Carolina, Chapel Hill, North Carolina 27514

Chairman's Introduction-9:00

Contributed Papers

9:05

QQ1. Brainstem evoked responses to vibratory stimuli in terrestrial and marine turtles. M. L. Lenhardt (Bioacoustics Laboratory, Department of Otolaryngology, Virginia Commonwealth University, Richmond, VA 23298)

A startle to acoustic stimulation is a primitive indication of hearing in vertebrates. Turtles have not been shown to startle to airborne sounds but do exhibit this reflex when audio frequencies are applied directly to the shell. Evoked responses were recorded to airborne and vibratory clicks using needle electrodes. Both stimuli yielded similar waveforms, with the exception of a slight time delay due to propagation in bone. When equated for equal latencies the vibratory stimuli seemingly had a greater dynamic range. Simultaneous stimulation with white noise masking in the other modality further suggested preferential response of the ear to vibratory stimuli. Somatosensory input was controlled by anesthetic manipulation of the vertebral column at C1. The results indicate that the turtles are more sensitive to vibrations than airborne sound and bone conduction may be the preferred route to the ear.

9:20

QQ2. Characteristics of the FFP to linear tone glides. S. B. Resnick, J. M. Heinz, E. W. Bookstein, and R. V. Pagano (John F. Kennedy Institute, 707 North Broadway, Baltimore, MD 21205)

The FFP to rising and falling linear tone glides of 12.8-ms duration was measured over a 51.2-ms period using multichannel recording for six normal hearing adults. Averaged response waveforms based on 8192 trials were obtained to tone glides rising or falling in frequency between 312 and 625 Hz or between 468 and 781 Hz. The averaged waveforms then were subjected to various analyses including bandpass filtering (using digital filters centered at the extremes of the frequency range of the glides), spectral analyses for selected post-stimulus intervals, cross correlation (with the input stimulus), and covariance. Preliminary review of the data suggests that linear tone glides may be of particular value for estimation of response latency and that response latency is dependent on frequency range and direction of the tone glides. Results of more detailed analyses and comparison of the FFP with responses to pure tones described previously [S. Resnick, J. Heinz, E. Bookstein, and R. Pagano, J. Acoust. Soc. Am. Suppl. 1 74, S65 (1983)] will be presented.

9:35

QQ3. The relation between the human frequency following response and the low pitch of complex tones. Ron D. Chambers (University of Illinois, Psychology, 219C, Champaign, IL 61820), Lawrence L. Feth (University of Kansas, 290 Haworth Hall, Department of Speech-Language-Hearing: Sciences and Disorders, Lawrence, KS 66045), and Edward M. Burns (Purdue University, Heavilon Hall, Department of Audiology and Speech Sciences, West Lafayette, IN 47906)

The objective of this study was to examine the relation between the value of the low pitch of complex tones and the f_0 of the frequency following response (FFR). Mean pitch matches between a series of six-component complex tones and comparison pure tones were obtained for four normal hearing subjects with extensive musical training. FFRs were recorded in response to the complex stimuli which were most divergent in pitch for each subject and to pure tone signals of equal pitch. The FFR records were analyzed for frequency composition. The f_0 of the FFRs elicited by complex tones did not covary with frequency or pitch shift; the fundamental remained much closer to 200 Hz (the frequency with the period of the stimulus waveform). The f_0 of the FFR to pure tones with pitch equal to the complex tones also approximated the stimulus waveform. It was suggested that the output of the neural mechanisms reflected in the FFR does not vary in a manner consistent with shift in low pitch of complex stimuli. [Work supported by NIH.]

9:50

QQ4. Asymmetries in pitch perception of dichotic chords and middle latency evoked potentials. L. J. Hood, C. I. Berlin (Department of Otorhinolaryngology and Biocommunication, Kresge Hearing Research Laboratory, Louisiana State University Medical Center, 1100 Florida Avenue, New Orleans, LA 70119), and D. J. Baker (Department of Hearing and Speech Sciences, University of Maryland, College Park, MD 20742)

The dominance of one ear over the other in the perception of pitch of dichotic chords has been reported by Efron and Yund [J. Acoust. Soc. Am. 59, 889-898 (1976)] and in subsequent studies by that group. The present investigation addressed the existence of correlations between psychophysical and electrophysiological asymmetries. Specifically, the relation between ear dominance measured psychophysically using the Efron THURSDAY AM

paradigm and right-left asymmetries in middle latency auditory evoked potentials was examined in ten normal-hearing adult subjects. Absolute and interwave latencies were obtained for middle latency responses to right and left monaural, binaural, and dichotic presentation conditions using tonal stimuli. Rank order correlation coefficients were used to compare right-left ear and hemifield evoked potential latency differences to measures of ear dominance. Results indicated that latency measures, particularly for components involving wave P_b of the middle latency response, correlated with the direction of ear dominance. The characteristics of these correlations will be discussed. [Supported by NINCDS #NS 11647, the Louisiana Lions Eye Foundation, and the Eye and Ear Foundation.]

10:05

QQ5. Adaptation of the acoustically emitted $2f_1-f_2$ combination tone. Thomas G. Dolan (Department of Otolaryngology, Medical University of South Carolina, 171 Ashley Avenue, Charleston, SC 29425) and Paul J. Abbas (Department of Speech Pathology and Audiology, The University of Iowa, Iowa City, IA 52242)

Recent studies suggest that the $2f_1-f_2$ ear-canal distortion product is produced by nonlinearities in the motion of the cochlear partition. Given its cochlear origin, we attempted to use the acoustically emitted combination tone (ACT) to indirectly examine changes in cochlear mechanics that may be associated with long-term adaptation (i.e., adaptation lasting several seconds) of eighth-nerve responses. We examined the effects of 1-min tonal exposures the amplitude of the $2f_1-f_2$ ACT in the ear canals of cats. These effects were compared with post-exposure changes in the wholenerve action potential (AP) responses to tone bursts that resulted from similar exposures. Both the distortion product and N_1 amplitudes were reduced for several seconds following exposure. The reduction in ACT amplitude suggests that 1-min exposures can alter cochlear mechanics. The fact that the same exposure tones cause reductions in N_1 amplitude further suggests that neurally measured long-term adaptation is linked to changes in the mechanics of transduction. The time courses of ACT and AP recovery were similar, and the post-exposure effects depended in similar ways upon the frequency and intensity of the exposure tone. These results suggest that both the ACT and AP post-exposure effects are reflections of the same underlying cochlear process.

10:20

QQ6. Long-term stability and familial aspects of spontaneous otoacoustic emissions (SOAEs). E. Strickland, E. M. Burns, A. Tubis, and K. Jones (Purdue University, West Lafayette, IN 47907)

The frequencies and levels of SOAEs in six subjects were monitored several times weekly (in some cases daily) over a period of several months. One additional subject was monitored over a period of about two years. The stability of individual emissions varies widely both within and between subjects (e.g., the standard deviation of repeated measures of frequency varies from about 0.1% to over 1.0%), and appears to be unrelated to either the frequency or the level of the emission. The frequency and level shifts of individual emissions in an ear with multiple emissions appear to be independent with one exception, the case when an emission is apparently a distortion product resulting from the interaction of two other emissions. In this case the frequency of the "distortion" emission depends on the frequencies of the "primary" emissions. A survey of emissions in children was also' undertaken. The incidence of SOAEs in children is fairly common and in all cases to date in which multiple emissions were found in a child, at least one of the parents also had multiple emissions. We have also identified at least one family of the type described by Glanville et al. [J. Oto. Laryngol. 85, 1-10 (1971)] in which several siblings all have very high level (40 dB SPL) high-frequency emissions. [Work supported by NINCDS.]

10:35

÷

QQ7. The relationship of threshold fine structure to spontaneous and evoked otoacoustic emissions. E. M. Burns, E. Strickland, K. Jones, and A. Tubis (Purdue University, West Lafayette, IN 47907)

Puge-tone thresholds at intervals of 10 Hz were obtained in a number of subjects with single or multiple spontaneous otoacoustic emissions (SOAEs). In all cases the SOAE frequencies corresponded to frequencies at which threshold minima occurred, and the subjective impressions of the listeners for frequencies in the region of SOAEs corresponded to known aspects of the interaction of external tones with SOAEs; i.e., distortion products, beats, and frequency locking. However there were always more threshold minima than SOAEs. In some cases these minima corresponded to the frequencies of distortion products, resulting from the interaction of two SOAEs, which were apparently below the noise floor of the measurement system. In other cases the minima corresponded to frequencies at which evoked otoacoustic emissions (EOAEs) occurred. However there were usually minima which were not "explained" by any of these correspondences. The results will be discussed in light of current cochlear models. [Work supported by NINCDS.]

10:50

QQ8. Potassium-induced release of glutamate and taurine into perilymph is calcium-dependent. G. L. Jenison, R. P. Bobbin (Kresge Hearing Research Laboratory, Louisiana State University Medical Center, New Orleans, LA 70119), and R. Thalmann (Department of Otolaryngology, Washington University School of Medicine, St. Louis, MO 63110)

Perfusion of the choclea with artificial perilymph containing high concentrations of potassium chloride selectively induces the release of several different endogenous amino acids [Neurosci. Abstr. 16.1 (1983)]. This study examines whether such augmentations reflect the liberation of neurotransmitter(s) from depolarized hair cells by comparing potassium-induced changes in amino acid levels evoked under normal divalent ion conditions (2.0 mM Ca+2-1.0 mM Mg+2) to the effects of potassium elicited under conditions known to antagonize evoked transmitter release (0.1 mM Ca⁺²-20.0 mM Mg⁺²). For each condition, high performance liquid chromatographic analyses were conducted on artificial perilymph samples collected before, during, and after the perfusion (scala tympani >scala vestibuli) of 50-mM potassium perilymph. Analysis of variance and subsequent Newman-Keuls multiple range tests were conducted on mean sample concentration values (N = 5/condition) for each of 17 endogenous amino acids. Exposure to 0.1 mM Ca+2-20 mM Mg+2 resulted in attenuations of evoked release only for amines identified as glutamate (-39.6%, p = 0.005) and taurine (-48.2%, p = 0.003). These data support the candidacy of glutamate and taurine as auditory receptoneuronal neurotransmitters or transmitter metabolites. [Supported by NIH Grants NS-06575, NS-16080, NS-07058, and NSF Grant BNS-8118772.]

11:05

QQ9. Otosclerosis: A generalized disorder of glycosaminoglycan (CAG) metabolism? Isolde Thalmann, Gertraud Thallinger, and Ruediger Thalmann (Department of Otolaryngology, Washington University, St. Louis, MO 63110)

There are numerous indications that otosclerosis represents a local manifestation of a generalized disorder of GAG and/or collagen metabolism, a contention supported by the heritable nature of the disease. Zechner and Manolidis reported a pronounced increase of total GAGs in urine of patients with active otosclerosis [Arch. Klin. Exp. Ohren Nasen Kehlkopfheilkd. 202, 634 (1972)]. We were not able to confirm their reported increase in total urinary GAGs. Therefore we searched for more subtle indicators of aberrant GAG metabolism, such as changes in ratios of individual GAGs. For this purpose it was necessary to develop a highly sensitive technique to quantitate individual GAGs; however, again no significant differences were found: dermatan sulfate (0.48 \pm 0.06 and 0.32 ± 0.04), heparan sulfate (0.43 \pm 0.06 and 0.40 \pm 0.04), chondroitin-4-sulfate (0.60 ± 0.07) and 0.71 ± 0.08 , and chondroitin-6-sulfate $(1.25 \pm 0.14 \text{ and} 1.41 \pm 0.16)$ in controls (N = 22) and active otosclerosis (N = 20), respectively $(\bar{X} \pm \text{SEM} \ \mu \text{g}$ hexuronic acid/mg creatinine). These negative data by no means rule out a possible error in GAG metabolism. More definitive conclusions should emerge from radiotracer (³⁵SO₄) studies for the detection of errors in GAG synthesis and/or degradation in skin fibroblast cultures. [Supported by Research Fund of American Otological Society and NIH Grant NS-06575.]

Session RR. Speech Communication VIII: Speech Acoustics and Intelligibility

John C. Webster, Chairman

Communications Research Department, National Technical Institute for the Deaf, Rochester, New York 14623

Chairman's Introduction-9:00

Contributed Papers

9:05

RR1. Pulsation threshold patterns of synthetic vowels: Study of the second formant emergence and the center of gravity effects. Pierre Escudier and Jean-Luc Schwartz (Institut de la Communication Parlée, Laboratoire Associé au CNRS, ENSERG, 23 rue des Martyrs, 38031 Grenoble Cedex, France)

Very small spectral irregularities are detected by the auditory system, thus suggesting the existence of a derivation-like mechanism. We have already shown this fact by the estimation of formant detection thresholds in relation to the spectral pattern of a given reference [Lublinskaya *et al.*, J. Acoust. Soc. Am. Suppl. 1 **67**, S102 (1980)]. On the other hand, the center of gravity phenomenon suggests the existence of an integrationlike mechanism [Lublinskaya *et al.*, Acts of the "Symposium Franco-Soviétique de Grenoble," 19–20 (1981)]. These two facts have been studied by means of pulsation threshold techniques. We have obtained psychophysical estimations of the internal representation of vowel-like spectra, to see how these two opposite spectral mechanisms are combined, and at what level of the auditory system they are susceptible to appear. This kind of information is necessary for the elaboration of auditory perception models.

9:20

RR2. Perceptual segregation of simultaneous vowels presented as steady states and as parallel and crossing glides. Magdalene H. Halikia and Albert S. Bregman (Department of Psychology, McGill University, 1205 Dr. Penfield Avenue, Montreal, Quebec, Canada H3A 1B1)

Recent research with synthesized pairs of simultaneous vowels, that had similar or different FOs and steady-state inflections has shown that the F0s must differ by more than 1-2 semitones in order for the vowels to be heard separately [M.T.M. Scheffers, IPO Ann. Prog. Rep. 17, 41-45 (1982)]. The present study investigated the combined effects of F0 differences and steady state or gliding (with the glides parallel or crossing) inflections on the perceptual segregation of simultaneous vowels. The stimuli were four vowel sounds synthesized using a serial three-formant method. Six basic pairs were the result of all possible combinations of these vowels, taken two at a time. Further pairs were created by altering the F0 of each vowel (so that the two F0s differed by $\frac{1}{2}$, $\frac{3}{2}$, $\frac{6}{12}$ semitones) and by keeping the F0 at a fixed frequency level (in the steady state case) or by making it glide between two different frequency values (in the glide case). Subjects had to identify the two vowels in each pair. It was expected that we would get better results with the glides since their formants are better defined because the harmonics will shift through the spectral envelope. We were also interested to see whether the direction of the glide is important in the perceptual segregation. The results confirmed our hypothesis and also showed that a minimum F0 separation is necessary before the use of glides can have an effect. The crossing glides gave significantly superior results over the parallel glides at the octave frequency separation of their F0s.

9:35

RR3. A comparison of spectra of loud and whispered speech. Igor V. Nábělek and Sumalai Maroonroge (Department of Audiology and Speech Pathology, University of Tennessee, Knoxville, TN 37996-0740)

Spectra of running speech of eight female subjects were determined for two conditions: loud reading and reading of the same text in whispered mode. The subjects were seated in a sound isolated booth. A 1-in. measuring microphone was 10 cm from the lips of the reader. The spectrum analyzer Nicolet UA 500 A was employed. The average spectrum of the eight subjects had a pronounced maximum at 300 Hz when the speech was loud. Between 500 and 1200 Hz the slope was around -17 dB/oct, and between 1.8 and 14 kHz the slope was -3.7 dB/oct. The whispered speech had very similar spectrum in the upper frequency range mentioned above. The spectrum had the same average slope. Below 1000 Hz the average whispered speech spectrum was rather flat. The differences between whispered and loud spectral levels in this range reached around 20-dB values.

9:50

RR4. Enhancing spectral contrast in the auditory representation of speech. Andrew Sidwell and Quentin Summerfield (MRC Institute of Hearing Research, University Park, Nottingham NG7 2RD, United Kingdom)

The intelligibility of many classes of speech sounds requires the preservation of spectral amplitude patterning in the auditory representation of the signal. In hearing impairment of cochlear origin contrast in spectral amplitude may be reduced: first, suppression may be less effective; second, auditory filters may be more broadly tuned. It is possible in principle to compensate for a reduction of contrast in the auditory spectrum by increasing contrast in the physical spectrum, e.g., by processing the signal to reduce formant bandwidths. Two steady-state noise-excited vowel sounds were synthesized, one similar to a naturally produced whispered vowel, the other with formant bandwidth reduced to 50 Hz. The auditory spectra of both sounds were measured using simultaneous and forward masking, to assess the enhancement due to suppression, in three normal-hearing and three sensorineurally impaired listeners. Little structure was preserved in the auditory spectrum of the vowel with conventional bandwidths above 2.5 kHz. Reducing formant bandwidths increased spectral contrast in both groups of listeners. Where contrast was preserved, it was enhanced by suppression, again in both groups. The ability to enhance the auditory spectrum in the impaired group may have implications for the design of signal-processing hearing aids.

10:05

RR5. Abstract withdrawn.

RR6. Speech reception thresholds in noise for native and non-native listeners. Mary Florentine, Søren Buus, Bertram Scharf, and Georges Canevet (Communication Research Laboratory (133FR) and Auditory Perception Laboratory, Northeastern University, Boston, MA 02115, and Laboratoire de Mecanique et d'Acoustique, CNRS, Marseille, France)

The noise level at which native and non-native listeners could repeat about 50% of very simple English sentences was measured with an adaptive procedure. The 14 non-native listeners were primarily native French speaking and were 19 to 53 years old. Four native listeners were 16 to 53 years old. On each trial the listener repeated one sentence presented at 70 dB SPL via loudspeakers in an anechoic chamber. If the entire sentence was correct, the noise level was increased; otherwise it was decreased. the step size was 5 dB until the first reversal and 2 dB thereafter. The speech reception threshold, SRT, as defined as the average noise level of ten trials following the first reversal. Three SRTs were measured for each listener. All listeners could repeat eight practice sentences presented in the quiet with 100% accuracy. The average SRTs were 57 dB SPL for listeners with minimal experience in English, 62 dB SPL for listeners with moderate experience, and 68 dB SPL for listeners with extensive experience. Native listeners had an average SRT of 72 dB SPL. (Work supports ed by the French Scientific Mission.]

10:35

4.

RR7. A multispeaker analysis of duration in read French paragraphs. Douglas O'Shaughnessy (INRS Telecommunications, Bell-Northern Research, 3 Commerce Place, Verdun, Quebec, Canada H3E 1H6)

An understanding of natural language durations will lead to more intelligible synthetic speech, and to improved automatic recognition. Toward this goal, a 111-word paragraph was read by 29 native French speakers. A pitch-extractor device plotted the speech amplitude waveform, at an average rate of 55 mm/s. Durations were measured to the nearest 5 ms, with a measurement error of about 10 ms (1/2 mm). Phoneme durations were found to be significantly shorter than those in stressed words from sentences pronounced in isolation [D. O'Shaughnessy, J. Phon. 9, 385-406 (1981)]. Previous trends (short schwa vowels and grammatical words, long unvoiced fricatives, nasal vowels, and prepausal syllables) were confirmed. Vowels lengthened preceding voiced fricatives (but not prior to / r/, and lengthened more at sentence-internal pauses than at the end of a sentence. Standard deviations of phoneme durations (at a fixed position in the paragraph) across speakers averaged about 20% for consonants and 25% for vowels. A generative model of French durations will be presented. [Supported by NSERC and the France-Quebec exchange.]

10:50

RR8. Word-frequency effects in modified rhyme test responses. J. C. Webster (Communications Research Department, NTID, Rochester Institute of Technology, Rochester, NY 14623)

Four (of six) lists of a recorded six-choice MRT made up of 10 numeral, 10 yowel (V), 15 initial consonant (IC), and 15 final consonant (FC) items were administered to 15 groups of 20 severely/profoundly deaf young adults. Analyses were made of the 960 non-numeral-item responses (4 lists \times 6 foils \times 40 items). The percentage of subjects choosing the correct response dropped from 47.98 for the Vs to 42.16 for ICs to 38.36 for FCs. Of the remaining 800 responses (errors), 89 were choller by over 20% of the students. Confusions of voicing (V), manner (M), and particularly place (P) would be expected to explain the majority of the 70 greater-than-chance (GTC) errors among the 600 IC and FC responses. Place confusion did account for the majority of the 39 FC GTC errors. However for the 31 GTC IC errors, and the 19 GTC V errors, the relative word -

familiarity interacted with VMP explanations. Twenty-eight of the 89 GTC errors could not be accounted for by either VMP confusions or word familiarity. Of these, six were confusions among /w,l, and r/.

×

11:05

RR9. Quantifying lexical redundancy effects in word recognition. Arthur Boothroyd and Susan Nittrouer (Speech and Hearing Sciences Program, City University Graduate Center, 33 West 42nd Street, New York, NY 10036)

The goals were to test two equations reflecting the effects of lexical redundancy on recognition probability, and to derive typical values for inf these constants appearing as parameters equations. $p_c = 1 - (1 - p_i)^k$, where p_c and p_w are recognition probabilities with and without lexical redundancy, and $p_w = p_p^2$, where p_w and p_p are the recognition probabilities for whole words and phonemes within words, respectively. Using phonemically balanced lists, word and phoneme recognition was measured, in normally hearing subjects, at four S/N levels and five word-frequency levels. Analysis of variance confirmed that j and * were relatively independent of S/N ratio, but highly dependent on word frequency. Values of j ranged from 3.1 for nonsense words to 2.3 for highfrequency words. Values of k were 1.3 for phoneme scores and 2.3 for word scores. These data confirm earlier findings indicating that phoneme scores are less influenced by lexical redundancy than are word scores. They also support the model underlying the theoretical equations and provide a means of predicting one type of score from another. [Work supported by PSC. CUNY Award #6-63137.]

11:20

RR10. An analysis of articulation index theory as applied to different speech material. Chaslav V. Pavlovic (Department of Communicative Disorders, University of Mississippi, University, MS 38677) and Gerald A. Studebaker (Department of Audiology and Speech Pathology, Memphis State University, Memphis, TN 38152)

We have reported earlier [J. Acoust. Soc. Am. Suppl. 1 73, S102–103 (1983)] the details of an articulation index (AI) scheme that was found satisfactory for the nonsense syllable material we use. We now explore the ways of extending the scheme to include speech material of different redundancy level and different phonemic composition. Using our own data, as well as that of early AI investigators, we examine the basic assumptions of the AI theory for various speech materials. These include the properties of additivity, band independency and monotonicity, as well as the importance function, and the intelligibility-articulation transfer function. The validity of the resulting AI scheme is discussed in terms of the magnitude of the error in speech intelligibility predictions for various speech materials. [Work supported by NINCDS.]

11:35

÷

RR11. Comparison of objective and subjective measures of communication difficulty. David C. Hodge and Georges R. Garinther (U.S. Army Human Engineering Laboratory DRXHE-BR, Aberdeen Proving Ground, MD 21005)

Speech intelligibility was determined for subjects wearing the M25 gas mask at various distances using the PB Monosyllabic Word Intelligibility Test. The subjects also rated communication difficulty at each distance, and specified the maximum distance at which short commands could easily be given and understood. The intelligibility tests were conducted outdoors at distances ranging from 1 to 32 m, using nine subjects serving as both talkers and listeners. The talkers were instructed to use that voice level which they felt was appropriate for each distance. Mean intelligibility ranged from 70% at 1 m, to 20% at 32 m. Voice level measured at 1 m increased from 66 to 74 dB(A) as communication distance increased. Subjects' ranging of communication difficulty were highly correlated with the intelligibility data. The subjects indicated an average maximum comfortable communication distance of 8.5 m, corresponding to about 49% PB intelligibility. An upward shift in voice spectrum was found as the subjects spoke at greater distances.

11:50

RR12. Using DECtalk as an aid for the handicapped. Dennis H. Klatt, Julie Tiao (Room 36-523, Massachusetts Institute of Technology, Cambridge, MA 02139), and Walt Tetschner (3-3/ U8, Digital Equipment Corporation, 146 Main Street, Maynard, MA 01754)

DECtalk is a commercial test-to-speech system with general interface capabilities to any of a number of terminals and computers. As an aid for the vocally handicapped, it has advantages over devices used previously in that any of several different voices, simulating men, women, and children, can be selected and modified to create a personal voice. Preliminary attempts to provide DECtalk to selected users have met with enthusiastic responses, particularly in women and children, who have had to use a male voice in the past. As an aid for the blind, DECtalk can replace the voice in presently available reading machines for the blind. While DECtalk is currently undergoing formal intelligibility testing by D. Pisoni, it is clear from side-to-side comparisons that such a switch improves both intelligibility and the naturalness of the voice. In addition, J. Tiao has been developing a talking text editor for blind computer professionals and others who may now become more productive in the workplace. The program uses DECtalk and a Rainbow personal computer to create and modify text files. [Work supported in part by an NIH grant.]

THURSDAY MORNING, 10 MAY 1984

YORK HALL, 9:25 A.M. TO 12:00 NOON

Session SS. Speech Communication IX: Vowel Perception

D. H. Whalen, Chairman

Haskins Laboratories, 270 Crown Street, New Haven, Connecticut 06511

Chairman's Introduction-9:25

Contributed Papers

9:30

SS1. Perception of vowel quality in the presence of other sound sources. Christopher J. Darwin (Laboratory of Experimental Psychology, University of Sussex, Brighton BN1 9QG, England)

If the energy of a harmonic (500 Hz) near the first formant of a vowel is increased, the vowel quality changes. But if the tone corresponding to this increase in energy starts or stops at a different time from the original vowel, then listeners can perceive the original vowel quality [Darwin, Attention and Performance, Vol. X (Erlbaum, 1983)] even though the spectrum present during the vowel is inappropriate. Listeners apparently partition the total sound present into separate percepts on the basis of onset- and offset-time differences. The present experiments show that the same partitioning still occurs when the "original" vowel has reduced energy at 500 Hz. Now adding extra energy to it restores a normal vowel spectrum. Listeners report a vowel quality corresponding to the "original" depleted vowel when the additional energy starts or stops at a different time from the rest of the vowel, even though the spectrum present during the vowel is appropriate to a vowel with a normal spectral envelope. The partitioning of sound sources observed here cannot be explained by a tendency to perceive vowels with conventional spectral envelopes. [Work supported by SERC.]

9:45

SS2. Multidimensional scaling and perceptual features: Reflections of stimulus processing or long-term memory prototypes? Robert Allen Fox (Speech and Hearing Science, 324 Derby Hall, The Ohio State University, Columbus, OH 43210)

Many researchers have obtained information on phonetic perception by using various multidimensional scaling (MDS) procedures to discover underlying perceptual dimensions. Such dimensions are usually characterized in terms of the acoustic characteristics of the stimuli and have been interpreted as representing factors used to identify vowel (or consonant) quality in phonetic perception. However, several studies suggest that such dimensions may reflect properties of the vowel's long-term memory prototype rather than the actual acoustic nature of the stimuli. For example, MDS studies commonly find no features reflecting dynamic acoustic information [e.g., R. Fox, Lang. Speech 26, 21–60 (1983)] and one study [B. Rakerd, J. Acout. Soc. Am. Suppl. 1 73, S54 (1983)] found that similar perceptual features were extracted when Ss either heard or imagined (remembered) stimulus tokens. To investigate this issue an experiment was designed to determine the extent to which slight acoustic variation in a subset of the synthetic vowels presented to Ss for scaling would produce differences in perceived perceptual distance estimates. Results suggest that Ss are sensitive to relatively small acoustic differences while making dyadic comparisons even when there is no concomitant phonemic quality variation or specific instructions expect such variations. It will be argued that such results suggest that MDS procedures *do* tap lower-level perceptual processes and do not merely reflect long-term memory prototypes.

10:00

SS3. The influence of postvocalic consonants on the duration of Spanish vowels. María Ignacia Massone and Ana María Borzone de Manrique (Laboratorio de Fonética Experimental, Universidad Católica Argentina, Bartolomé Mitre 1869, 1039 Buenos Aires, Argentina)

THURSDAY AM

The present work was undertaken in order to provide further evidence about the role played by the physiological and phonological factors in vowel lengthening before voiced consonants. Previous experiments compared cross-linguistically different consonantal contexts and syllabic types, but, with respect to Spanish disregarded neutralization in final syllable position. Two male adults recorded nonsense bisyllabic words and two other speakers recorded meaningful frequent words where the opposition voiced/voiceless was spontaneously neutralized. Results showed that in open and closed syllables of nonsense utterances (average ratios: 1.4 and 1.23, respectively) vowels are shorter before voiceless consonants than before voiced. In meaningful words, vowels presented longer duration before voiced realizations (20%) of lengthening. However, for nonsense utterances, higher values were obtained and we can assume that this difference is indicating some phonological effect. The lengthening value observed in meaningful words seems to represent more closely the physiological effect.

10:15

SS4. Vowel information is integrated across intervening nonlinguistic sounds. D. H. Whalen (Haskins Laboratories, 270 Crown Street, New Haven, CT 06511) and Arthur G. Samuel (Department of Psychology, Yale University, New Haven, CT 06520)

When the fricative noise of a fricative-vowel syllable is replaced by a noise from a different vocalic context, listeners experience delays in identi-

fying both the fricative and the vowel (D. H. Whalen, *Perception & Psychophysics*, 1984). Listeners (unconsciously) detect a mismatch between the vowel information in the fricative noise and in the vocalic segment. In the current experiment, noises and vowels were again cross-spliced, but, in addition, the first 60 ms of the vocalic segment either had a nonlinguistic noise added to it or was replaced by that noise. The fricative noise and the majority of the vocalic segment were left intact, and both were quite identifiable. Mismatches of vowel information caused delays for all stimuli, both originals and ones with the noise. Additionally, syllables with a portion replaced by noise took longer to identify than those that had the noise added to them. The results indicate that listeners integrate all relevant information even across a nonlinguistic noise. Similarly, having the signal present along with the noise delayed identifications less than replacing the signal completely. [Work supported by NIH.]

10:30

SS5. On reconciling monophthongal vowel percepts and continuously varying F patterns. Leigh Lisker (Haskins Laboratories, 270 Crown Street, New Haven, CT 06510 and University of Pennsylvania, Philadelphia, PA 19104)

When a sequence of pictures is presented in rapid succession the illusion of continuous movement can be created. A continuously varying acoustic signal may, contrariwise, be perceived as a sequence of "still" sounds. Not only is speech perceived as discrete sounds in sequence, but speakers will oblige, especially in the case of stressed vowels, by "citing" them in the form of steady state phonations judged to match auditorily the vowels in their natural contexts. These steady state imitations are adequately characterized by just two numbers, the frequencies of the two lowest vocal-tract resonances. Acoustic analyses of a number of tokens of the English nonsense forms [beb ded geg bæb dæd gæg] produced by a single talker indicate that, if each token is represented by a single pair of formant frequencies, there is a pattern of variation rather different from the crosstalker variations reported by Peterson and Barney in 1951. Moreover the variation patterns are different within syllable types, for the same vowel across contexts, for the same contexts across vowels, and for the two formants. It is, moreover, not that simple to apply the target-plus-undershoot model to explain the patterns of variation observed. [The support of the NICHHD is gratefully acknowledged.]

10:45

SS6. Vowel recognition in the absence of formant cues: Dynamic contributions to perception. H. Timothy Bunnell (Sensory Communication Research Laboratory, Gallaudet College, Washington, DC 20002)

The primary acoustic cue to vowel identity has typically been related to the center frequencies of the first two or three vowel formants. In experiments using specially degraded stimuli, results consistent with this assumption were obtained for stationary synthetic vowels, but not for vowels presented in syllabic contexts (e.g., /VwV/ and /orVd/). For these experiments, vowel stimuli (both stationary and in context) were synthesized with high-frequency square waves substituted for the standard synthesizer voicing source (Klatt, 1980 cascade synthesizer). Spectra associated with these stimuli have peaks, due to the source harmonics, located at odd multiples of the fundamental frequency. In identification studies using the vowels $\{/i/, /i/, /\epsilon/, /a/\}$, listeners tended to identify stationary vowels on the basis of the frequencies of their largest-magnitude spectral peaks. Since such peaks were invariably coincident with source harmonics, identification errors were frequent. Errors were, however, restricted almost entirely to the vowels $\{/1/, /\epsilon/, /ac/\}$. By contrast, vowels in syllabic context were reliably more resistent to identification errors, despite nearly identical acoustic structure throughout the medial portion of the vowel. Results are interpreted to suggest that listeners are well attuned to the contrast between source and vocal tract contributions to the signal. In order to separate these two contributions, however, listeners appeared to need information about changes over time in at least one function (the vocal tract function for these stimuli). [Work supported by NINCDS and the University of Maryland.]

11:00

SS7. Dynamic specification of vowels in CVC syllables spoken in sentence context. Winifred Strange (Department of Communicology, University of South Florida, Tampa, FL 33620)

In previous studies of citation-form /b/-V-/b/ syllables, vowel identification accuracy of "silent-center" syllables (in which steady states were attentuated to silence) was not significantly worse than for unmodified control syllables [W. Strange et al., J. Acoust. Soc. Am. 74, 695-705 (1983)]. New studies were performed in which vowels were produced in /b/-/b/, /d/-/d/, and /d/-/t/ syllables, spoken in a carrier sentence, "Say the word- - - - again." Silent-center syllables, in which all but the first three and last four pitch periods were attenuated to silence, were identified with 85% accuracy, as compared to 97% for control syllables. However, vowel identification was still much more accurate than when either the initial transitions or final transitions were presented alone (54% and 37% accuracy, respectively). Performance on silent-center syllables was not significantly better when subjects were presented the stimuli blocked according to consonantal context (87%). Neutralizing syllable duration differences decreased accuracy somewhat (78%), especially for short vowels. Additional identification studies are underway in which portions of syllables containing different consonants were interchanged, in order to test hypotheses about trajectories specified by initial and final transitions. [Work supported by NIMH.]

11:15

SS8. Vowel perception in reverberation. Anna K. Nabelek and Tomasz Letowski (Department of Audiology and Speech Pathology, University of Tennessee, Knoxville, TN 37996-0740)

Because identification of vowels was not affected by reverberation, possible changes in perception were assessed in a paired comparison paradigm. Fifteen English vowels and diphthongs recorded with and without reverberation (T = 1.2 s) were paired with each other. Ten normal-hearing subjects made similarity judgments using a scale from 1 to 7. Response matrices for the two conditions were analyzed using multidimensional scaling procedures. A three-dimensional solution was sought for the data on the basis of the experimental conditions and results of previous studies. Three- and two-way analyses were performed using a ALSCAL subroutine. Both with and without reverberation, the first two dimensions were identified as back-front and low-high, confirming the results of previous studies. The third dimension was identified as long-short while others interpreted it as tensness, openness, or left it unidentified. In both threeand two-way analyses, the shifts in stimulus configuration between test and retest and between reverberant and nonreverberant solutions were of the same order. Therefore, we concluded that reverberation did not contribute significantly to the perceptual distances among vowels and diphtongs. [Supported by NIH.]

11:30

SS9. The "center of gravity" and perceived vowel height. Patrice Speeter Beddor and Sarah Hawkins (Haskins Laboratories, 270 Crown Street, New Haven, CT 06510)

In oral vowels, perceived height is determined by the "center of gravity" of the spectral prominence in the vicinity of F1 rather than by F1peak frequency [Chistovich and Lublinskaya, Hear. Res. 1, 185–95 (1979)]. The present study of nasal vowels assessed the generality of the center of gravity effect. Five nasal vowels, $\sqrt{1} \in \bar{x} = \bar{a} \bar{o}/$, were synthesized. For each nasal vowel, a continuum of corresponding oral vowels was synthesized by manipulating the frequency of F1. Each continuum included one stimulus whose F1 frequency matched that of the nasal vowel and one whose centroid (a measure of center of gravity) matched. The five vowel sets consisted of oral-nasal vowel pairs; 20 listeners selected the "best-match" pair for each set. Subjects chose the F1 match for /i/ only; for nonhigh vowels, choices fell between F1 and centroid matches, but significantly closer to the centroid. Apparently center of gravity influences perception of nasal vowel height, but the centroid as a measure of this needs refinement. Whether the centroid is an appropriate measure of perceived oral vowel height, or whether another metric applicable to both oral and nasal vowels can be found, is currently under investigation. [Work supported by NIH.]

11:45

SS10. The role of nasalization in the perception of synthesized speech. John C. Thomas, Jonas N. A. Nartey, Mary Beth Rosson, and Judy Klavans (Remote Information Access Systems Group, IBM Watson Research Center, Yorktown Heights, NY 10598) Thus far synthesized speech has been reported by phonetically naive listeners as sounding "metallic" or "as if the speaker had a cold." One of the explanations for the above is that the simulation of nasal coupling is not close enough to natural speech. We report on research on diphone synthesized utterances (Dixon and Maxey, 1968). In order to simulate a better set of nasalized vowels in synthesized speech, a new set of diphones was created to replace the original ones in those cases in which there is a nasal consonant in the immediate vicinity. These new diphones were the result of hand-painting single nasal formants in addition to the regular formant frequencies found in the original diphones. Utterances made of both the new and old sets of diphones were played to phonetically naive listeners. Results on naturalness judgments and on intelligibility will be presented.

Session TT. Physiological Acoustics IX and Psychological Acoustics VII: Localization, Vibro-Tactile and Medical

Constantine E. Trahiotis, Chairman

Department of Speech and Hearing Science, University of Illinois, 901 S. Sixth Street, Champaign, Illinois 61820

Chairman's Introduction-1:00

Contributed Papers

1:05

TT1. Acoustic wave motion in the human pinna at high frequencies. George F. Kuhn (Vibrasound Research Corporation, 10957 E. Bethany Drive, Suite J, Aurora, CO 80014)

Localization studies have shown that spectral peaks as well as spectral nulls formed by the pinna are significant localization cues. Experimental results from real and from model pinnas as well as theoretical predictions, using the uniform theory of diffraction, show that the first null is formed via a single reflection within the pinna. This first null rotates with increasing frequency from an angle in the lower frontal quadrant to an angle in the upper frontal quadrant starting at as low a frequency as 4.5 kHz, depending on the size and geometry of the pinna and the particular location of the earcanal. As the frequency is increased, additional nulls and peaks are formed which rotate from the lower rear quadrant to the upper rear quadrant. These nulls and peaks are formed by the interference of edge-diffracted waves with multiply reflected waves within the pinna cavities. Both the measured and predicted pressure patterns in the pinna correlate well with psychoacoustic studies of vertical, median plane localization. [Work supported by NIH.]

1:20

TT2. The combination of interaural information across frequencies: Lateralization on the basis of interaural differences of time. Raymond H. Dye and Joseph N. Baumann (Parmly Hearing Institute, Loyola University, 6525 N. Sheridan Road, Chicago, IL 60626)

The basic question addressed here is how the binaural auditory system combines interaural differences of time (IDTs) arriving over multiple bands of frequencies. An initial study was undertaken to measure threshold IDTs for three-component stimuli with the middle component at 750 Hz. The frequency difference between components was 20, 50, 100, 250, or 450 Hz. After measuring thresholds for the individual components presented alone, measures were taken for the three-component complexes when only the lower, middle, or upper component was delayed; when the lower two components, the upper two components, or the sidebands were delayed; and when all three components were delayed. Best performance was obtained when all three components were delayed, regardless of Δf_{i} although the differences between Δ IDTs obtained when all three components were delayed and when the "best" (i.e., smallest thresholds) frequency of the complex was presented alone were small. When only two of the three components are delayed, thresholds approach those obtained when all three components are delayed, as long as one of the delayed components was the best frequency of the complex. When only one component of the complex was delayed, thresholds were 2-5 times higher than when the same component was presented alone. The data will be discussed in terms of a binaural mechanism which lateralizes acoustic images by taking a weighted average of information arriving from different frequency channels. [Work supported by NSF.]

1:35

TT3. Model of human sound localization based on spectral pattern L. Wightman (Auditory Research Laboratory (Audiology), Northwestern University, Evanston, IL 60201)

2:05

recognition. Mark E. Perkins, Doris J. Kistler, and Frederic

S88 J. Acoust. Soc. Am. Suppl. 1, Vol. 75, Spring 1984

1. Annalation

In the course of our research on sound localization we have measured direction-dependent pinna transfer functions of eight observers. The magnitudes of these functions have peaks and valleys that vary in spectral locus across subject and across source location. We addressed the question of whether these spectral patterns contain sufficient information for accurate localization of sounds in space. We used standard multivariate statistical techniques to develop a model of sound localization based on pattern recognition principles. A Bayesian classification procedure is employed to make a decision as to the most probable source location. The errors made by this procedure are compared to the errors made by subjects when judging source location in free-field listening conditions. Preliminary results are extremely encouraging. The source positions for which the model makes errors match quite well those for which the subjects make errors. [Work supported by NSF and NIH.]

1:50

TT4. Azimuthal localization of sounds with a single early reflection. Brad Rakerd (Department of Psychology, Michigan State University, East Lansing, MI 48824) and W. M. Hartmann (Department of Physics, Michigan State University, East Lansing, MI 48824)

When localizing sounds in a room, listeners must overcome interference from numerous echoes. We created a simple limiting case of this situation by conducting experiments in an anechoic chamber in which a heavy 4×8 ft panel provided a single early reflection. The panel alternatively served as a left wall, right wall, floor, or ceiling. Localization accuracy was assessed with the source identification method [W. M. Hartmann, J. Acoust. Soc. Am. 74, 1380-1391 (1983)] for eight loudspeakers separated in azimuth by three degrees of arc. The stimuli were 500-Hz tones which were either pulsed for 50 ms or turned on with a slow (7 s) envelope and left on to deprive the listener of any transient information. For pulses, performance was significantly poorer with side wall reflections than with reflections from the floor or ceiling, or with no reflections at all. There was no evidence that responses systematically deviated to the left or right of targets in any condition. Together, these findings indicate that the precedence effect [H. Wallach et al., Am. J. Psychol. 62, 315-336 (1949)] can break down over short intervals and that when it does so the result is simply increased uncertainty in localization. For tones with no transients, performance was very much poorer for side walls and ceiling than for the floor and no-wall conditions. Physical measurements indicate that these judgments were determined jointly by the binaural time and intensity differences that resulted from interference between the source and its reflection. [Work partially supported by NIH and the Department of Audiology and Speech Sciences, Michigan State University.]

TT5. Accuracy of sound localization by the frog Hyperolius marmoratus. R. R. Capranica (Section of Neurobiology and Behavior, Cornell University, Ithaca, NY 14853), N. I. Passmore, S. R. Telford, and P. J. Bishop (Department of Zoology, University of Witwatersrand, Johannesburg 2001, South Africa)

The sound localization ability of female painted reed frogs was studied by phonotactic approaches via a three-dimensional grid to an elevated loudspeaker (through which male mating calls were broadcast). Females readily resolved the sound source elevation with a mean jump error angle of 37° (26 trials, 17 females), compared to a mean jump error angle of 19° (33 trials, 13 females) for a more conventional two-dimensional ground approach. Lateral head scanning, often accompanied by vertical changes in head orientation, frequently preceded successive jumps. The ability of such small frogs to accurately localize a sound source in both the horizontal and vertical plane, given the absence of a pinna or external canal, is remarkable. [This study was supported by the South African Council for Scientific and Industrial Research, and the Animal Research Program, University of the Witwatersrand.]

2:20

TT6. Acoustic coding by the ear of the sunfish (Lepomis gibbosis): Sensitivity, tuning, and directionality of 8th nerve units. Sheryl Coombs and Richard R. Ray (Parmly Hearing Institute, Loyola University of Chicago, Chicago, IL 60626)

The auditory system of the sunfish is characteristic of many teleosts, and is unspecialized for sound pressure reception. It is likely that its otolithic ear responds primarily to acoustic particle motion in the manner of an accelerometer. Single units of the lagenar and saccular eighth nerve branches were characterized in response to whole-body acceleration. Using a three-dimensional vibration system [Fay et al., J. Acoust. Soc. Am. Suppl. 1 74, S7 (1983)], the directionality of single units were measured in three orthogonal planes, and the cell's best sensitivity axis determined in spherical coordinates. Acceleration tuning curves obtained along a nearly optimal axis were essentially low pass with cutoff frequencies ranging from below 100 to 250 Hz. Best sensitivity varied from - 30 to - 90 dB re: 1 g (rms). Lagenar units showed a wide range of "best directions," all roughly in a para-saggital plane. Saccular units fell into two or more directional groups. Directional patterns for both organs reflect aspects of the organs' orientation in the head, and the orientations of hair cells on the maculae. All cells reponded as if their input (most likely a group of hair cells) were equivalent to a single hair cell of a given three-dimensional orientation.

2:35

TT7. Physiological noise and the determination of vibro-tactile perception thresholds. J. E. Piercy, A. J. Brammer, and W. Taylor (Division of Physics, National Research Council, Ottawa, Ontario, Canada K1A 0R6)

Several physically different configurations are frequently used to couple sinusoidal vibration to the finger or palm for the determination of vibro-tactile perception thresholds (viz: exciter diameter and contact surface curvature, contact force and skin indentation, and the presence or absence of a surround). Vibration of physiological origin (physiological noise) has been studied in the frequency range 0.025–1000 Hz for several common configurations. The acceleration spectrum consists of a broad plateau between 0.1 and 10 Hz, with peak amplitude ~0.01 to 0.1 m/s² (with reference to 1-Hz bandwidth) depending on the configuration and subject. The spectrum falls rapidly with increasing frequency above 10 Hz. Substantial contributions to the physiological noise can be identified from blood circulation (1–10 Hz) and respiration (0.2–1 Hz). Preliminary psychophysical results from three subjects, when combined with current

knowledge of the masking of vibrotactile signals, suggest that vibrotactile thresholds at frequencies well above 10 Hz may be masked by this physiological noise under some conditions of flesh stimulation.

2:50

TT8. Effects of skin temperature and body site on psychophysical characteristics of cutaneous mechanoreceptor subsystems. Ronald T. Verrillo (Institute for Sensory Research, Syracuse University, Syracuse, NY 13210) and Stanley J. Bolanowski, Jr. (Center for Brain Research, University of Rochester School of Medicine, Rochester, NY 14642)

Psychophysical detection thresholds were obtained at the thenar eminence and volar forearm using 16 sinusoidal frequencies between 15 and 700 Hz. A small (0.008 cm²) contactor was used, which preferentially excites non-Pacinian (NP) subsystems. Measurements were made using carefully controlled (\pm 0.5 °C) skin surface temperatures of 15°, 20°, 25°, 30°, 35°, and 40 °C to enhance or degrade the subsystem responses. The results show several frequency characteristics that cannot be ascribed to activity in the Pacinian system, but do conform to electrophysiological measurements of Rufini capsules, Meissner corpuscies, and Merkel cells. When threshold values are averaged across temperatures, the resultant curve is approximately flat. The results suggest that the NP system is probably composed of more than a single receptor type and that well-controlled skin temperature is necessary for the precise measurement of vibrotactile sensation.

3:05

TT9. Evaluation of impulsive wave transmission through total knee joint prothesis. M. L. Chu, S. Yazdani, and I. A. Gradisar (Department of Mechanical Engineering, University of Akron, Akron, OH 44325)

The most significant advancement in orthopaedics in the last 50 years has been the evolution of practical total knee joint replacement. However, in the presence of all these successes, there is a note of "gloom" to a small percentage of patients in which loosening of the prosthesis occur, with the attendant pain and restricted mobility. At present, attempts to reduce the incidence of failure have been directed primarily at redesigning hip and knee implants, and research towards understanding the mechanics of impact force transmission across normal and prosthetic joints is practically nonexistent. The present study is an attempt to evaluate the differences between "normal" and prosthetic joint mode of impact wave transmission. Using cadaveric skeletal remains, an abbreviated (cut at the lower tibia and upper femur ends) lower extremity specimen is suspended vertically by long steel wires. The upper (femur) end is subjected to a 150-lb load (to simulate body weight) and the lower tibia end rests on a 100-lb shaker. The skeletal system is subjected to a 3-g impulsive load at a frequency range of 1-3 Hz to simulate brisk walking and jogging. The procedure is repeated twice; first with the original knee joint intact, and again with the knee joint portion replaced with a prosthesis. Preliminary results reveal that there are significant differences in the mode of impulsive wave transmission across the "normal" and prosthetic knee joints. Prosthetic joints appear to reduce impulsive peaks along both the tibia and femur as compared with "normal" joints. The effects of viscoelastic shoe inserts in the propagation of impact waves across the two types of joints (normal and prosthetic) is also being investigated.

Session UU. Architectural Acoustics IV: Recent Advances in HVAC System Noise Control

Howard F. Kingsbury, Chairman

Architectural Engineering Department, Pennsylvania State University, University Park, Pennsylvania 16802

Chairman's Introduction-2:00

Invited Papers

2:05

UU1. Current developments in heating, ventilating, and air conditioning system noise control. Howard R. Kingsbury (Architectural Engineering Department, The Pennsylvania State University, University Park, PA 16802)

Proper understanding of the sound generating and sound absorbing characteristics of the numerous elements in a typical ducted building air conditioning system has been an elusive goal. In some cases the data base is very thin, in others nonexistent. In addition, the technology of air conditions system design has been advancing faster than our understanding of the acoustical implications of such technology advances. This paper will review our current understanding of the acoustics of system elements and point out some of the areas where additional information is needed.

2:30

UU2. Revised noise criteria for design and rating of HVAC systems. Warren E. Blazier, Jr. (Warren Blazier Associates, Inc., Four Embarcadero Center-Suite 2840, San Francisco, CA 94111)

This paper reviews current methods of rating the noise produced by HVAC systems and explains why these ratings fail to be correlated with subjective opinion in many cases. An entirely new method of assigning noise ratings is proposed which is expected to provide a significantly better correlation between objective measurements and subjective response. The proposed new rating method makes use of a revised set of noise criterion eurves (RC curves) which appeared for the first time in Chap. 35 of the 1980 Systems Volume of the ASHRAE Handbook. This paper also discusses the technical considerations leading to the development of the RC curves as a replacement for the NC curves which have been used in the past.

2:55

UU3. Recent advances in the understanding of acoustic transmission through the walls of air conditioning ductwork. Alan Cummings (Department of Mechanical and Aerospace Engineering, University of Missouri-Rolla, Rolla, MO 65401)

Acoustic noise transmission through the walls of air conditioning ductwork has long been a neglected aspect of HVAC acoustics, but two recent ASHRAE-sponsored research projects have done much to rectify the situation. The results of this work are described here, and include both experimental data and prediction methods concerning interior/exterior noise transmission ("breakout") through the walls of plain, unlined rectangular, flat-oval, and circular ducts; the measured and predicted breakout insertion loss (IL) of external acoustic wall lagging on ducts of these three geometries is also discussed. Noise transmission *into* ducts (termed "breakin") is of importance too, and a simple theoretical treatment is available, enabling the breakin transmission loss (TL) of the duct walls to be found from the breakout TL. In addition, the calculation of sound pressure levels in rooms, from duct wall radiation, is discussed here. The prediction methods of the wall TL of rectangular and flat-oval ducts are simple to use and are fairly reliable; circular ducts are, however, difficult to cope with at present. The prediction of the IL of lagging on all duct geometries is straightforward and reasonably accurate. The "state of the art" in duct wall radiation is also discussed here.

3:20

UU4. Predicting sound pressure levels in furnished dwellings and offices. Theodore John Schultz (Theodore J. Schultz Associates, 7 Rutland Square, Boston, MA 02118)

The Diffuse Field Theory of sound propagation indoors, embodied in the formula, $[L_{\rho} = L_{w} + 10 \log(Q/4\pi r^{2} + 4/A)]$, does not work well for typical furnished rooms in dwellings and offices. An alternative simple empirical relationship has been found that predicts with considerable accuracy the sound pressure level in such rooms, based on the sound power level of the source, the room volume, the frequency, and the distance from the source: $L_{\rho} = L_{w} - 10 \log r_{(ft)} - 5 \log V_{(cu ft)} - 3 \log f_{(Hz)} + 25$ (dB). If this new relationship is accepted, there are serious implications for our current standard test procedures for field measure-

S90

ments in occupied buildings. Since the room absorption A does not appear explicitly in the formula, the customary normalization with terms like 10 log A in transmission loss and impact noise field tests is probably incorrect. In addition, since no uniform reverberant sound field occurs in normally furnished dwelling and office spaces, it is not clear what one ought to measure for the receiving-room sound pressure level in field tests of transmission loss, noise reduction, and impact noise. [Work supported by ASHRAE.]

Contributed Paper

3:45

UU5. An experimental investigation of active noise control in ducts. C. D. Smith (Kentron International, Hampton, VA 23665) and R. J. Silcox (NASA Langley Research Center, Hampton, VA 23665)

This study was directed to gaining an understanding of the physical mechanism of active noise suppression in ducts for both plane waves and higher order modes. Previous work has indicated large suppressions are attainable using active control concepts for plane progressive wave propagation. However, there is little evidence suggesting the mechanism of suppression. Furthermore, it was of interest to determine whether this concept could be applied to sound càrried by higher order modes in ducts. This work utilized NASA Langley's Spinning Mode Synthesizer duct facility to provide the number of control points necessary for higher order mode propagation. Pressure measurement probes were installed between the noise source and control point to provide data to define the suppression mechanism. Results indicated that for all modes suppressions of 25 dB or greater were attainable over a broad frequency range. The mechanism of suppression appeared to be a pressure minimum being forced at the control plane which caused a near perfect reflection to occur. This was actually developed.

THURSDAY AFTERNOON, 10 MAY 1984

GREENWAY ROOM, 2:00 TO 3:50 P. M.

Session VV. Physical Acoustics VI: Nonlinear Acoustics

John H. Cantrell, Jr., Chairman

Mail Stop 499, NASA Langley Research Center, Hampton, Virginia 23665

Chairman's Introduction-2:00

Contributed Papers

2:05

VV1. Bispectral analysis of parametric and nonlinear phenomena. D. Choi, E. J. Powers, J-H. Chang, and R. O. Stearman (College of Engineering, The University of Texas at Austin, Austin TX 78712)

A parametrically excited system at a frequency f_p near the sum of two natural frequencies of the system usually exhibits the so-called combination resonances at frequencies f_a and f_b which are close to the corresponding natural frequencies. This interesting phenomenon in which a single spectral component of the excitation induces two spectral components in the response cannot be identified by conventional spectral analysis. In the case of the combination resonances, a phase coherence exists between the two resonance modes and the excitation. This coherence can be detected by a triple correlation in the frequency domain between the spectral components at f_a , f_b , and f_p . This triple correlation known as bicoherence is effective in studying the combination resonances. It is also useful in detecting nonlinear interactions that occur among various resonance modes as the amplitude of the excitation is increased. The applicability of digital bispectral analysis in studies of the parametric and nonlinear phenomena is demonstrated by analyzing vibration data from a parametrically excited cantilever beam. Results for both sinusoidal and random excitations are presented. [The authors' work on bispectral analysis is supported in part by the DoD Joint Services Electronics Program.]

2:20

VV2. Boltzmann-Ehrenfest principle of adiabatic invariance and acoustic nonlinearity. John H. Cantrell, Jr. (NASA-Langley Research Center, Mail Stop 231, Hampton, VA 23665)

The Boltzmann-Ehrenfest principle of adiabatic invariance is applied to a nonlinear system consisting of a self-constrained finite amplitude acoustic wave propagating in a solid. The results predict the existence of an acoustic radiation stress having two source components. One component is associated with the stress nonlinearity of the solid and is obtained from the adiabatic variation in a parametrized natural wave velocity. The second component results from the variation in the first-order nonlinear term in the virial theorem expansion and gives rise to an acoustic radiation-induced static strain. Both components depend directly on the energy density of the propagating wave but are opposite in sign. The coefficient which couples the radiation-induced static strain to the energy density is the acoustic nonlinearity parameter which characterizes the nonlinearity of the wave equation.

2:35

VV3. Elastic waves, radiation stress, and static strains in solids: An experimental study of acoustic nonlinearity. William T. Yost and John H. Cantrell, Jr. (NASA-Langley Research Center, Mail Stop 231, Hampton, VA 23665)

The application of the Boltzmann-Ehrenfest principle of adiabatic invariance to a system consisting of a finite amplitude acoustic wave propagating in a nonlinear solid predicts the existence of an acoustic radiationinduced static strain. The static strain depends directly on the product of the energy density of the propagating wave and the acoustic nonlinearity parameter of the solid β . For propagating ultrasonic pulses or tonebursts theory predicts that the acoustic radiation stress generates a static displacement pulse having the shape of a right-angled triangle. The polarity and slope of the displacement pulse depend on the magnitude and sign of the nonlinearity parameter. We present measurements on single crystal silicon (positive β) and vitreous silica (negative β) which provide the first experimental confirmation of the theoretical predictions. Absolute measurements of the nonlinearity parameter determined from the static displacement pulses are in good agreement with those obtained from ultrasonic harmonic generation measurements.

2:50

VV4. Analysis of nonlinear harmonic generation for arbitrary dual frequency transducer excitation. Mosaad A. Foda and Jerry H. Ginsberg (School of Mechanical Engineering, Georgia Institute of Technology, Atlanta, GA 30332)

An earlier study of finite amplitude axisymmetric sound beams [J. H. Ginsberg, J. Acoust. Soc. Am. Suppl. 173, S83 (1983)] considered the case of monochromatic excitation. That work featured a singular perturbation analysis combining asymptotic integration and the renormalization version of the method of strained coordinates. The present paper initiates an extension of those techniques to the case of a dual frequency source. The parametric array, in which the primary beams are at closely spaced frequencies, has already received much attention. The system discussed here permits disparate frequencies. Aside from a restriction to axisymmetry, the excitation at each frequency is arbitrary. The analysis thus far has obtained the first two orders of approximation for the velocity potential. This expression describes the manner in which nonlinear effects accumulate for the various sum and difference frequencies. It is the foundation for a future derivation of an expression for the pressure that is descriptive of the entire field. In addition, the trend for harmonic generation indicated by the analysis suggests that conversion efficiency in the parametric array might be improved by altering the transverse vibration pattern of the individual primary beams. [Work supported by ONR, code 425-UA.]

3:05

VV5. Dissipative, nonlinear acoustics in fluids having positive and negative nonlinearity. M. S. Cramer (Department of Engineering Science and Mechanics, Virginia Polytechnic Institute and State University, Blacksburg, VA 24061), L. T. Watson, W. Pelz (Department of Computer Science, Virginia Polytechnic Institute and State University, Blacksburg, VA 24061), and A. Kluwick (Institute fuer Stroemungslehre und Waermeuebertragung, Technisch Universitaet, Wiew, A-1040, Vienna, Austria)

Recent studies by the first and last authors have shown that the nonlinear acoustics of fluids in which the nonlinearity parameter 1 + B/2Achanges sign is governed by a cubic Burger equation. Numerical solutions to this equation have been obtained by combining a collocation scheme in space and backward differencing in time. These will be presented and compared to exact solutions of the inviscid equations. New results include the viscous structure of the collision between expansion and compression shocks. Conditions under which flows are self-similar will also be presented.

3:20

VV6. Time domain observations of finite amplitude random noise. Joseph P. Welz (Applied Research Laboratory, The Pennsylvania State University, P. O. Box 30, State College, PA 16801) and Oliver McDaniel (Department of Mechanical Engineering, The Pennsylvania State University, PA 16801)

A research program has been conducted to study nonlinear effects in noise propagation from supersonic jets. Two microphones were used to measure spherically diverging finite amplitude noise from a 10-kW acoustic source. One microphone was located at a fixed position near the source and the second microphone was moveable by remote control. Observations of finite amplitude distortion of individual wave trains were made using two digital signal processing techniques. First, the time delay between the two microphones was determined by computing the crosscorrelation function. This procedure proved to be considerably more accurate than determination of time delay from measurement of microphone spacing and computation of sound speed using chamber temperature. The instrumentation system was then programmed to capture the same wave train sample from both microphones utilizing the time delay information. The experimental results were in good agreement with a numerical time domain solution to Burger's equation. Spectra obtained by Fourier transform of the theoretical and experimental results also agree well. [Work supported by NASA Langley Research Center.]

3:35

VV7. The bubble pulse on deep fired/long-range underwater explosion records. David Epstein (Science Department, SUNY Maritime College, Ft. Schuyler, Bronx, NY 10465)

Many years ago, the author analyzed a representative deep-fired/ long-range underwater explosion record [J. Acoust. Soc. Am. **35**, 800 (1963)]. The most striking feature was the so-called "double shock" formation, e.g., a strong resemblance between the shock wave and bubble pulse in both amplitude and shape. The phenomenon is attributed to the combined effects of detonation depth and waveform propagation. Recently [Proc. 11th Intern. Congress Acoust., Paris, 1983, Vol. 1, pp. 345–348] the characteristics of an explosion waveform at the source, as a function of firing depth was established. Here, weak shock theory is used to study the nonlinear distortion of the bubble pulse as it propagates. The criterion for shock wave formation depends *inter alia* on the strength and duration of the pulse. Pulse amplitude increases slowly, but its duration decreases rapidly, with charge depth. It is found that the shot depth plays the crucial role and that consequently the deep fired shots suffer the greatest distortion, tending towards shock wave formation at long range.

Session WW. Speech Communication X: Speech Recognition

J. G. Wilpon, Chairman

Acoustics Research Department, AT&T Bell Laboratories, Murray Hill, New Jersey 07974

Chairman's Introduction-2:00

Contributed Papers

2:05

WW1. On the performance of isolated word speech recognizers using vector quantization and temporal energy contours. L. R. Rabiner, K. C. Pan, and F. K. Soong (AT&T Bell Laboratories, Acoustics Research Department, Murray Hill, NJ 07974)

The technique of vector quantization has been widely applied in the area of speech coding and has recently been introduced into the area of speech recognition. For the conventional statistical pattern recognition word recognizer using LPC feature sets as the analysis frames, the use of vector quantization leads to a large reduction in computation for the dynamic time warping pattern matching, and a concomittant small increase in average word error rate. A second technique that has been recommended for improving the performance of isolated word recognizers is the addition of temporal energy information into the distance metric for comparing frames of speech. It has been shown that the information in the prosodic energy contour complements the segmental information of the LPC spectrum, thereby providing small but consistent improvements in performance for small word vocabularies. In this talk we present results of a series of speaker independent, isolated word recognition tests using a 10word digits vocabulary and a 129-word airlines vocabulary. We show the effects, on recognition accuracy, of adding both vector quantization and temporal energy in various combinations, to the recognition paradigm.

2:20

WW2. Global spectrum vowel recognition and human performance. Maxine Eskanazi (LIMSI-CNRS, BP30, 91406 Orsay, Cedex, France)

We have shown [Eskenazi and Lienard, J. Acoust. Soc. Am. Suppl. 1 73, S87 (1983)] that global characterizations of the French oral and nasal vowels in a speaker-independent automatic recognition task give generally better recognition results than formant-based methods. In particular, a very rough representation in the frequency domain, characterizing the curvature of the spectrum gave good results using very little reference information for each vowel. By now, changing the analysis that the curvature characterization is based on from an FFT to an LPC has significantly improved global results. This is very close to human intelligibility of the same databases used, in terms of distance between confusion matrices. We shall compare results of human and automatic recognition in order to better evaluate machine performance. There follows a comparison between the FFT and LPC results in order to estimate the pertinence of the information furnished by each in view of vowel recognition and in the light of the problems inherent in a speaker-independent task as well as in specific vowel properties.

2:35

WW3. A modified K-means clustering algorithm for use in speakerindependent isolated word recognition. J. G. Wilpon and L. R. Rabiner (Acoustics Research Department, AT&T Bell Laboratories, Murray Hill, NJ 07974)

Recent studies of isolated word recognition systems have shown that a set of carefully chosen templates can be used to bring the performance of speaker-independent systems up to that of systems trained to the individual speaker. The earliest work in this area used a sophisticated set of pattern recognition algorithms in a human-interactive mode to create the set of templates (multiple patterns) for each word in the vocabulary. Not only was this procedure time consuming but it was impossible to reproduce exactly, because it was highly dependent on decisions made by the experimenter. Subsequent work led to an automatic clustering procedure which, given only a set of clustering parameters, clustered tokens with the same performance as the previously developed supervised algorithms. The one drawback of the automatic procedure was that the specification of the input parameter set was found to be somewhat dependent on the vocabulary type and size of population to be clustered. Since the user of such a statistical clustering algorithm could not be expected, in general, to know how to choose the word clustering parameters, even this automatic clustering algorithm was not appropriate for a completely general word recognition system. It is the purpose of this paper to present a new clustering algorithm based on a K-means approach which requires no user parameter specification. Experimental data show that this new algorithm performs as well or better than the previously used clustering techniques when tested as part of a speaker independent isolated word recognition system.

2:50

WW4. Use of synthetic speech parameters to estimate success of word recognition. John J. Ohala, Mariscela Amador, Lynn Araujo, Steve Pearson, and Margot Peet (Phonology Laboratory, Department of Linguistics, University of California, Berkeley, CA 94720)

In an automatic speech recognition task, it would be good to estimate beforehand how recognizable the target vocabulary will be. Tests which involve numbers of human speakers using the ASR device are expensive and time consuming. Using stimuli synthesized by rule, although not without some drawbacks, would be cheaper and quicker. As a first step towards this latter goal we attempted to find out whether measures derived from rule-synthesized words would predict *human* listeners' performance in recognizing target words in continuous speech embedded in noise. Even a very simple measure of word detectability (essentially the length of the word's trajectory through the space whose dimensions are normalized F 1, F 2, F 3, and rms amplitude) correlated significantly with listener's performance (r = 0.53). The results of refined measures of detectability and the results of word confusability will be reported.

3:05

WW5. A speaker-independent isolated word recognition board. S. Kabasawa (Matsushita Electric Industrial Co., Ltd. Central Research Lab., Moriguchi Osaka 570, Japan), M. S. Hsieh, S. M. Chang, and C. H. Lin (Matsushita Electric Institute of Technology (Taipei) Co., Ltd., Republic of China)

A one-boarded, out-performance speech recognition system for speaker-independent isolated words has been developed. This board consists mainly of the 4-bit, 1-chip microcomputer and newly developed speech recognition LSI [Ohga et al., IEEE Trans. Consumer Electron. CE-28, 263–270 (1982)]. The board takes multiple templates and the KNN rules to cover various tokens of many persons. A new clustering method CLS (clustering with shared group) is based on the conception of the SNN method and the K-means iteration procedure [Rabiner et al., IEEE Trans. Acoust. Speech Signal Process. ASSP-27, 336–349 (1979)]. The experimental results showed more than 95% recognition accuracy not only for ten Japanese city names but ten Chinese city names. CLS can be easily implemented on the 16-bit microcomputer system and it takes less than 20 min to make seven templates with the microcomputer system.